Synthesis and Control of Reconfigurable mechanisms

Marie Fidèle Aimedee

N° Ordre : 2641
EDSPIC : 731

Université BLAISE PASCAL – Clermont II
Ecole Doctorale
Sciences pour l'Ingénieur de Clermont Ferrand

Thèse de Doctorat

Présentée
pour obtenir le grade de :

Docteur d'université

Spécialité : Génie Mécanique

Par

Marie Fidèle AIMEDEE

Synthesis and Control of Reconfigurable Mechanisms

Soutenue publiquement le 10 décembre 2015 devant le jury :

M. Jian S DAI	Professeur des Universités, King's Collège London	Président
M. Saïd ZEGHLOUL	Professeur des Universités, PPRIME, Université de Poitiers	Rapporteur
M. Stephane CARO	Charge de recherché CNRS, HDR, IRCCyN	Rapporteur
M. Grigore GOGU	Professeur des Universités, IFMA, Institut Pascal	Directeur de thèse
M. Chedli BOUZGARROU	Maitre de conférences, IFMA, Institut Pascal	Co-Encadrant
M. Nicolas BOUTON	Maitre de conférences, IFMA, Institut Pascal	Co-Encadrant

Institut Pascal
Institut Français de Mécanique Avancée et Université Blaise Pascal

Acknowledgements

I would like to express my special appreciation and thanks to my director Professor Grigore GOGU, for being a tremendous mentor for me. I am extremely thankful and indebted to him for sharing expertise, sincere and valuable guidance and encouragement extended to me. I also place on record, my sense of gratitude to my co-supervisors Dr. Chedli BOUZGARROU and Dr. Nicolas BOUTON who gave me a number of ways to improve the presented techniques and played important role in the successful completion of my doctorate degree.

I would also like to thank my committee members, professor Jian DAI, professor Said ZEGHLOUL and Dr. Stephane CARO for serving as committee members. I also want to thank you for letting my defense be an enjoyable moment, and for your brilliant comments and suggestions, thanks to you.

I thank the funders of this thesis. This work has been sponsored by the French government research program "*Investissements d'avenir"* through the IMobS^3 Laboratory of Excellence (ANR-10-LABX-16-01) and the RobotEx Equipment of Excellence (ANR-10-EQPX-44), by the European Union through the Regional program competitiveness and employment 2007-2013 (ERDF – Auvergne region), by the Auvergne region and by French Institute for Advanced Mechanics.

A special thanks to my family. Words cannot express how grateful I am to my mother and father for all of the sacrifices that you've made on my behalf. Your prayer for me was what sustained me so far. I thank my mother-in law and father-in-law for all the support throughout my thesis.

I would also like to thank all of my colleagues and friends who supported me in writing and incented me to strive towards my goal. A special mention to my best friend Mohamed Mohaideen, Ashok, Hemaanand, Karthik, Nadege, Lazher, Adel, Khaled, Jun, Said, Djily, Lam, Anh-Vu, Oleksii, Bassem, Seifeddine and to name a few whose support was priceless on many occasions. I would like to thank Montassar for the perfect design of the robot with which we were able to realize a real robot and perform experimentations on it.

Above all, I would like to express appreciation and heartfelt thanks to my beloved husband Raghunath RAJAVELU who spent sleepless nights with me and was always my support and strength in the moments when there was no one.

I dedicate my thesis to Raghu, my mom and to my dad.

Table of contents

Table of figures:

Tables:

Introduction

Motivation

Modern robotic world is seeking for robots which are able to adapt and reconfigure according to the environment and the task that has to be performed. With the development of science and technology and especially the progress of deep space and undersea exploration, the traditional mechanisms with limited adaptability and flexibility are facing challenges. Reconfigurable and deployable mechanical systems, being capable of adapting themselves to variable tasks, have been attracting great attentions in both academia and industry. Reconfigurable mechanisms are well suited for applications in domestic, hazardous, deep space, deep sea, and complex manufacturing environments. Deployable structures are also widely used in a variety of spacecrafts and planetary detectors, with increasing requirements upon transformation, dexterity, modularization, reconfigurability, and reliability. Research and development of reconfigurable and deployable mechanisms face a series of challenges both in theoretical and technical aspects. These robots are high in demand because of their beneficiary property of performing multiple tasks instead of multiple robots that perform only one particular task [Aimedee et al., 2016].

In this thesis, I take into account a strict constraint criterion for systematizing the reconfigurable mechanisms, i.e. we only consider mechanisms in which reconfigurability is achieved without assembling and disassembling of the parts. Henceforth, mechanisms presented in the following sections are those which are able to reconfigure itself by self-locking, changing relative position of joint axes, superposing or aligning two or more links, superposing the axis of two or more joints and so on.

Thesis goals

This thesis mainly addresses three major parts each of which are discussed in the following subsections. Also for the conceptual and methodological developments, we consider the following scientific issues as listed below:

Systematization and structural analysis

This part of the thesis is dedicated to the development of a systematization approach for reconfigurable mechanisms with respect to their structural parameters such as mobility, connectivity, redundancy and number of overconstraints. IFToMM terminology defines the mobility or degree of freedom as the number of independent coordinates required to define the configuration of a kinematic chain or mechanism [Ionescu, 2003]. The connectivity between two links of a mechanism represents the number of independent finite and/or infinitesimal displacements allowed by the mechanism between the two links. In free-of-singularity branches, full-branch connectivity is defined by the number of finite displacements [Gogu, 2009], [Dai, 2012]. In singular configurations, instantaneous connectivity can be

defined by the number of finite and/or infinitesimal displacements. The various types of motions associated with the connectivity are defined in terms of translational or rotational velocities. In this way, both finite and infinitesimal motion derivatives with respect to time could be integrated using a linear transformation method. The number of over constraints of a mechanism is given by the difference between the maximum number of joint parameters that could lose their independence in the closed loops, and the number of joint parameters that actually lose their independence in the closed loops [Gogu, 2008a]. The redundancy is given by the difference between the mobility of the parallel mechanism and the connectivity between the moving platform and the fixed base. Redundancy introduces internal mobilities in the limbs [Gogu, 2008a].

The mechanisms are analyzed structurally using the formulae of structural parameters proposed by Gogu [Gogu, 2008a]. These parameters help us to understand the mechanism and to systematize it according to type of mechanism, whether the mechanism is overconstraint or non-overconstraint, redundant or non-redundant, with/without internal mobilites, etc.

Geometric and kinematic formulation

To resolve the practical problems of modeling, control, simulation and development of the robot, the structural parameters are required. Various types of singularities are also systematized and analyzed by taking into account the structural parameters. Further to know the location of the robot links relative to each other, we need to compute the geometric model. We use Travel Coordinate System [Gogu and Coiffet 1996], [Gogu et al. 1997] to determine the position and orientation of the joint axes at each instant. To find out the linear and angular velocities of each joint variable, we need to formulate the kinematic equations for the robot under consideration.

Control strategies

This part is dedicated to the development of trajectory generation and control strategy, based on actuation redundancy. The challenging task in this control part is to develop an advanced control law in order to synchronize several actuators to have a smooth transition from one assembly mode to another without causing wear and tear to the robot. Choice of actuated joints also plays a vital role in ensuring high performance and controllability of the mechanism.

In this research we focus on the 8-bar single loop mechanism to illustrate the developments achieved in the three parts mentioned above. As it will be shown, this mechanism exhibits an interesting capacity to reconfigure. It has two degrees of mobility in a general configuration but needs at least five motors to be fully controlled in all singular configurations.

Thesis Structure

The present thesis is divided into four chapters. Chapter 1 discusses the related literature review in detail while chapter 2 discusses the structural analysis and geometric modelling of an eight- bar linkage. The singular configurations and their bifurcated branches are discussed

in chapter 3. Control strategies of the reconfigurable eight bar mechanism, tested by simulation on a prototype with five actuated motors, are presented in chapter 4.

- In chapter 1, a bibliographic review has been done, taking into consideration most of the reconfigurable mechanisms studied in the literature. Mechanisms are reconsidered and studied in detail by taking into account the way these mechanisms achieve reconfigurability. Furthermore we systematized them according to their types of morphing, types of motions and their applications. The proposed systemization is useful for the upcoming researches and helps to have a clear idea on the concept of reconfigurable mechanisms.

- In chapter 2, we take into account a particular design of the reconfigurable mechanism namely the spatial eight-bar single loop linkage. The structural parameters of this mechanism are analyzed for a general configuration. Structural analysis has shown that the eight bar linkage have two degrees of freedom in a general non-singular configuration. Further various assembly modes of the eight bar linkage were identified. The singular configurations of this particular mechanism have been identified and classified according to the types of singularities (constraint singularity, redundant singularity and constraint-redundant singularity). The properties of redundant and constraint-redundant singularities are defined for the first time in connection with the four main structural parameters: mobility, connectivity, number of overconstraints and structural redundancy. Therefore, we have defined and identified the different branches of the mechanism which can be singular or not. We found out that this mechanism has an interesting property of continuously transiting from one type of singularity to another by always remaining in a singular configuration. This property enhances the reconfiguration capability of the mechanism.

- The chapter 3 of thesis is dedicated to the analysis of singular configurations of the 8-bar reconfigurable mechanism. The mechanism has a large number of branches and can switch from one to another by crossing a singular configuration. The geometric models corresponding to each branch have been derived. They give all possible relations between joint variables and imposed by joint kinematic constraints. These models are useful for mechanism control, especially for configuration changes at singular positions where the actuation redundancy is used.

- In chapter 4, the dynamic model of the mechanism is built in ADAMS software with complete parameterization of length and angle between each joint. The challenge is to control the eight bar linkage by synchronizing all the five motors in such a way to avoid the lock of the robot. This is done by using the geometric model relations to control the mechanism for a planned trajectory. The implementation of the numerical results and simulated results on a real prototype has been carried out. The performance of the robot is monitored.

1 Chapter 1: Types of morphing and systematization of reconfigurable mechanisms

1.1 Metamorphic mechanisms

The development in the second part of 1990s raised much interest in reconfigurable mechanisms with researchers generating numerous types of such mechanisms. The change of states, configurations and/or functional modes is the transformation process that we called morphing in the sense of image processing or metamorphosis in the sense of biology. In the time of rigorous development of science and technology, the cross-disciplinary concept brings thriving progress of the technology and thus results in development of reconfigurable mechanisms characterized by a certain ability of morphing [Aimedee et al., 2016]. Metamorphic mechanisms originated by metamorphosis involving change in form, topology and configuration of a mechanism [Gan et al., 2010], [Zhang et al., 2010] is an extension of the context of biology to mechanism topology change [Zhang et al., 2008 (b)] characterized by change of main structure parameters of a mechanism (mobility, connectivity, overconstrained and redundancy) in a number of topological configurations.

The initial concept of "metamorphic mechanisms" was originated by metamorphosis, which depicts the change in form, topology, and configuration. Metamorphic robots were presented as a class of serial reconfigurable manipulators allowing the creation of structures presenting a large number of different anatomies each, many of which are outside the current line of design practice for robots [Charalampos et al., 2012].

1.2 Kinematotropic mechanisms

In the 1990s, two new types of mechanisms were identified as kinematotropic linkages [Wohlhart, 1996] and metamorphic mechanisms [Dai, 1996], [Dai et al., 1999] and [Zhang et al., 2008 (a)]. Kinematotropic mechanisms use the bifurcation phenomenon and extend it to involving mobility change with change of relative orientations of joint axes [Galletti et al., 2001 and [Qin et al., 2014].

We can see that both kinematotropic mechanisms and metamorphic mechanisms are complementary towards using mobility change.

1.3 Reconfigurable mechanisms

In the first decade of the 21st century, much interest has been raised with a broad search for reconfigurable mechanisms. In 2000, Yan and Liu [Yan et al., 2000] investigated mechanisms and chains with variable topologies by using the finite-state-machine representation and in 2003 the work was extended to joint-code representation [Yan et al., 2003]. Variable kinematic joints were further investigated by Yan and Kuo [Yan et al., 2006] and [Yan et al.,

2007]. With the variable prismatic joint [Yan et al., 2006], a number of mechanisms with variable topologies were presented by Yan and Kang [Yan et al., 2009].

In the same period, Lee and Hervé [Lee et al., 2002] revealed discontinuously movable mechanisms in 2002 by fully exploring the branching characteristics of mechanisms where one particular motion ends and switches to a different motion with a changed mobility. This resulted in a number of reconfigurable mechanisms with mobility change [Lee et al., 2005], [Lee et al., 2007] in 2005 and 2007. The branching characteristics entail much exploration and were investigated by Kong and Gosselin in developing multimode parallel mechanisms in 2007 [Kong et al., 2007].

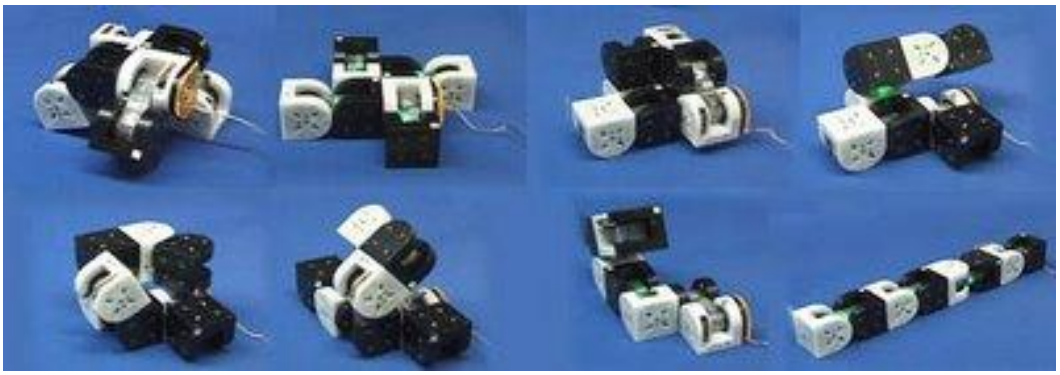

(a.)

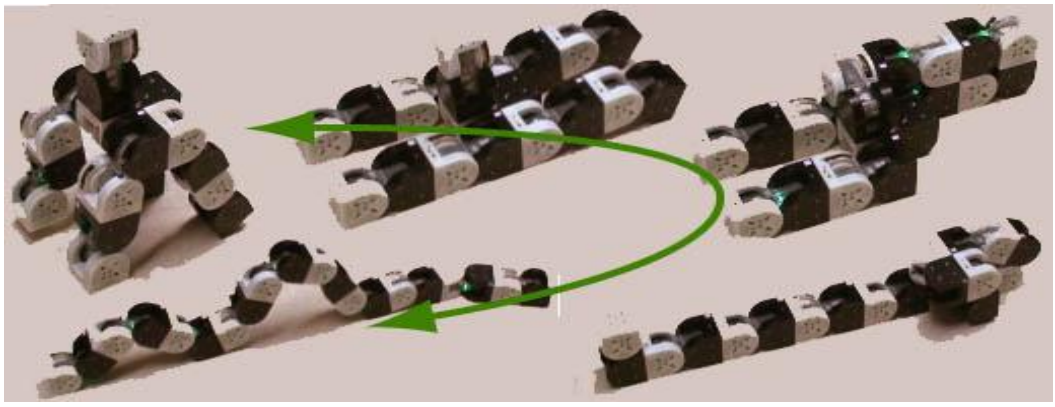

(b.)

Figure 1.1 (a.) M-TRAN III self-reconfigurable robot (b.) Metamorphosis of M-TRAN III [Kurokawa et al., 2006]

Modular self-reconfigurable (MSR) robots are robots composed of a large number of repeated modules that can rearrange their connectedness to form a large variety of structures. An MSR system can change its shape to suit the task, whether it is climbing through a hole, rolling like a hoop, or assembling a complex structure with many arms. These systems have three promises namely,

- **Versatility**: The ability to reconfigure allows a robot to form morphologies that are well-suited for a variety of given tasks.
- **Robustness**: Since the system is composed of many repeated parts which can be rearranged during operation, faulty parts can be discarded and replaced with an identical module on-the-fly, leading to self-repair.
- **Low cost**: MSR systems lower the module costs since mass production of identical unit modules has an economic advantage that scales favorably. Also, a range of complex machines can be made from a set of modules saving the cost versus having multiple single-function machines for doing different tasks.

Figure 1.1 illustrates one of the leading robots in the area of self-reconfigurable modular robotics, the M-TRAN III (Modular Transformer). These robots can change shape to walk, slither or crawl and climb over various obstacles on the way.

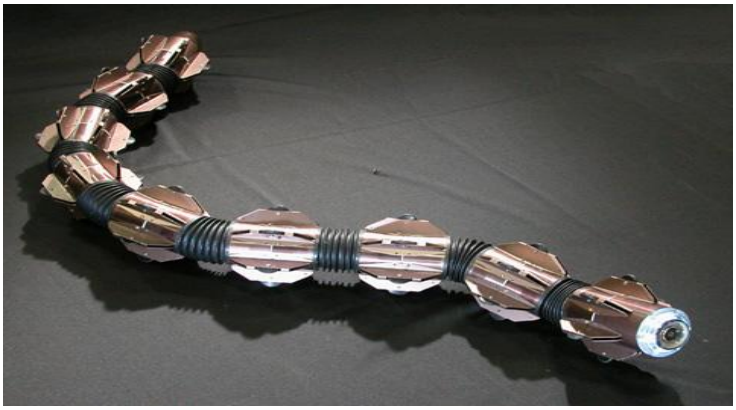

Figure 1.2 ACM-R5 amphibious robot [Shumeiu et al., 2011]

Figure 1.2 illustrates ACM-R5 amphibious robot created by Hirose Fukushima Robotics Lab. The acm-r5 is based on the mechanics behind snakes. Powered by a lithium-ion battery, the ACM-R5 is a radio-controlled amphibious robot designed to move like its real world counterpart. It can slither or swim underwater for 30 minutes on a full charge. An intricate sensor system (attitude/torque), small-sized camera, and a 32bit micro controller are placed inside the robot. While this robot seems more like a single object based robot it is made up of self-similar parts that work together to accomplish changing geometrical demands.

In the development of reconfigurable mechanisms, various ways to achieve reconfiguration were investigated and developed. In the study of reconfigurable packaging in late 1990s and in 2000s, metamorphic mechanisms were associated with ability to change their geometrical structures [Dai, 1996], [Dai et al., 2002]. Other approaches for reconfigurability and metamorphosis include change of number of links by link coincidence and self-locking [Zhang et al., 2008(a)], [Leonesio et al., 2007] and change of geometrical constraint to links and joints [Gan et al., 2010], [Zhang et al., 2010], [Zhang et al., 2014], [Zhang et al., 2011 (b)], [Zhang et al., 2013], [Gan et al., 2009]. In this way, a metamorphic mechanism was considered as a mechanism set composed by multiple kinematic chains which have the ability to be transformed sequentially from one to another following specific rules in order to meet

different requirements of tasks. In the paper presented by Charalampos et al [Charalampos et al., 2012], metamorphic manipulators were presented as a class of serial reconfigurable mechanisms allowing creation of a large number of different topologies.

1.4 Types of Morphing

In this section we will review various reconfigurable mechanisms in their essence in morphing or metamorphosis to present a systematic classification of morphing in their use to reconfigure a mechanism. Therefore, three types of morphing are classified as topological morphing, geometrical morphing and multi-furcating morphing and further classifications are made in terms of their intrinsic characteristics. These morphing types are then related to types of mechanisms and motion to demonstrate the morphing process in reconfigurable mechanisms [Aimedee et al., 2016]

1.4.1 Topological morphing

From a mathematical point of view, "topology" refers to continuous deformations including stretching and bending. This includes such properties as connectedness, continuity and boundary. In the field of mechanism and machine science, the concept of "topology" has been employed and extended to studying structural characteristics of mechanisms and machines. In general terms, "topology" is defined as a way that parts of a system are organized or connected. Topological morphing is defined by changing between the physical topology to an equivalent topology with fewer number of joints and links without assembly and disassembly. This change to the equivalent topology could be achieved by joint-motion range limits and by internal forces as shown in figure 1.3. The equivalent topology is associated with a reduced number of joints and links with respect to the initial topology. The way to interconnect links and joints could also change. This interconnection could be represented by the topological graph [Gogu, 2008a] and connectivity matrix [Zhang et al., 2010], [Dai et al., 2005]. The mechanism state matrices were discussed by Brain and Philip [Brain et al., 2011]. It deals with the state matrices which enable to represent the topological characteristics of planar reconfigurable mechanisms. These matrices also help calculating the degrees of freedom of the planar mechanisms with one DOF joints. The state matrices of the spatial reconfigurable mechanisms were also discussed by Philip et al [Philip et al., 2012].

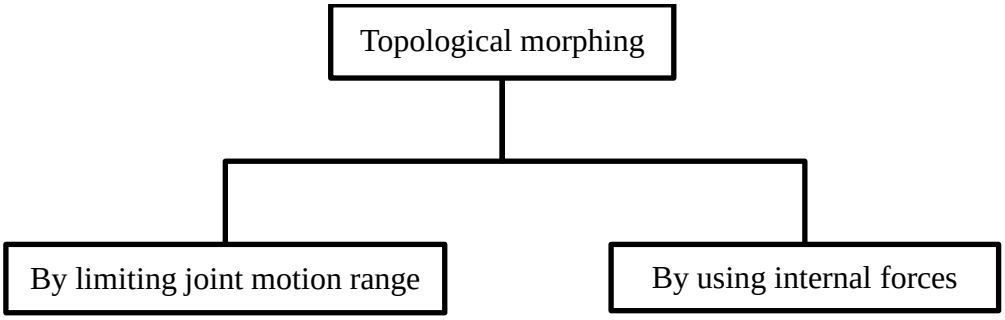

Figure 1.3 Classification of topological morphing

1.4.1.1 Morphing by limiting joint motion range

Joint-motion range limit is used in some of the mechanisms presented by Zhang and Dai [Zhang et al., 2008(a)]. Different working phases were generated from a source metamorphic mechanism by using a range limit with an orientation restriction. A spherical joint in this approach is degenerated into a revolute joint and a cylindrical joint is degenerated into a prismatic joint to achieve reconfigurability while a mechanism falls into a motion range that has a range limit. Therefore a physical topology can be reconfigured to an equivalent topology with various states and phases during the process of metamorphosis. The motion limit of the variable prismatic joint was used by Yan and Kang [Yan et al., 2009] to construct mechanisms with variable topologies.

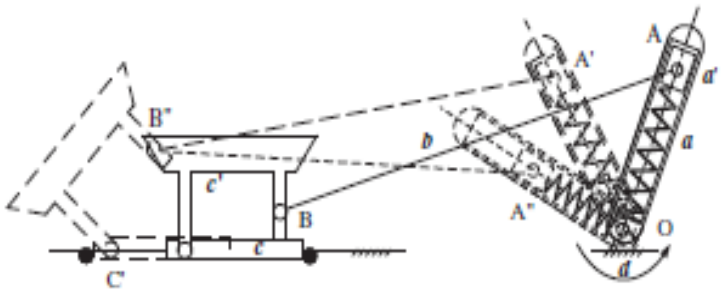

Figure 1.4 Workflow chart of the metamorphic mechanism in all configurations [Zhang et al., 2011(b)]

A motion range limit was further used in a mechanism presented by Zhang et al [Zhang et al., 2011(b)] on changing joint-motion direction when a joint reaches a certain geometry that guides the joint to rotate in a different direction. In figure 1.4, OABC, O$A'B'$C and O$A''B''$C represent the corresponding mechanism motion states such as translation, oscillating and ceasing, respectively. With this approach, these operations such as translating, oscillating and ceasing can be achieved by morphing.

1.4.1.2 Morphing by using internal forces

Using an internal force while limiting joint motion, a mechanism could change its configuration under this morphing. An example in figure 1.5 could be illustrated in a mechanism proposed by Zhang et al [Zhang et al., 2011(b)] and by Li and Dai [Li et al., 2012] whose reconfiguration is achieved by using a potential force from a spring with the joint motion range limit to create branching configurations. In this morphing, a metamorphic mechanism converts into a lower mobility mechanism by self-locking [Leonesio et al., 2007] a joint using the geometric limit together with a potential force that creates branching configurations where a slider acts as a mechanical element sprung back by a spring, leading to a different configuration.

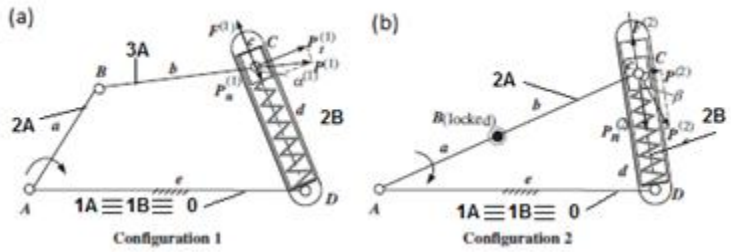

Figure 1.5 (a) and (b) Schematic graphs of a planar five bar force limit metamorphic mechanism [Zhang et al.,2011(b)]

The mechanisms with variable structure and geometry were presented by Sarkissyan et al [Sarkissyan et al., 2009] illustrating three types of reconfigurable mechanisms. Reconfiguration is implemented by locking joints and also by combining one or two subchains with axes of the kinematic pairs. It is ensured that the mechanisms chosen have the minimum degrees of freedom to obtain optimal solutions to the given tasks.

A new class of reconfigurable mechanism from a 3-CPS mechanism was discussed by Carbonari et al [Carbonari et al., 2014]. The mechanism is composed of 3 legs in which each leg is composed by a cylindrical, prismatic and a spherical joint. Reconfiguration is achieved by instantaneously locking one at a time, the revolute joints in the spherical joint. By doing this we obtain pure rotation and pure translation in the mechanism.

Further to this, a class of mechanisms called as parallel robot with enhanced stiffness (PRES) has been studied in Moosavian and Xi [Moosavian et al., 2014], to enhance the static and stiffness characteristics by varying their topology without a need of actuation redundancy. This was completed by locking passive joints which are used in reconfiguring the mechanisms.

According to Finistauri et al., group morphing is a combination of geometric and topological reconfiguration and is seen in advanced systems such as variable geometry truss mechanisms (VGTM). One such example is the modular wing truss capable of multiple level of reconfiguration to achieve unique wing shapes [Finistauri et al., 2009]. The topological morphing is also coupled with other morphing as introduced by Xi and Finistauri [Xi et al., 2012] in group morphing.

1.4.2 Geometrical morphing

After a critical review, we define geometrical morphing as the transformation of a particular geometrical position and orientation of relative joint axes and links achieved by geometrical constraints. This morphing can be achieved in different ways as represented in figure 1.6 and is discussed in the following subsections.

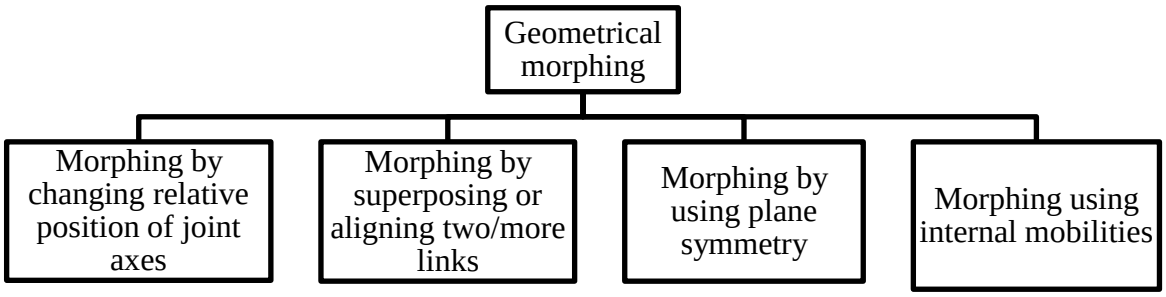

Figure 1.6 Classification of geometrical morphing

1.4.2.1 Morphing by changing relative position of joint axes

In changing of relative positions and orientations of joint axes without superposition or additional means, kinematotropic mechanisms proposed in 1996 entail a mobility change. Particular cases can be seen in Wunderlich mechanism, and Wren platform illustrated and the Queer-square linkage proposed by Wohlhart [Wohlhart, 1996], and the derivative Queer-square mechanism presented by Qin et al [Qin et al., 2014]. Using special joint property and link superposition to change relative positions and orientations of joint axes with superposition, multi-loop metamorphic mechanisms entail the mobility change as shown in figure 1.7 [Dai et al., 1999]. Both mechanisms complement the mobility change through change of relative positions of axes using different ways.

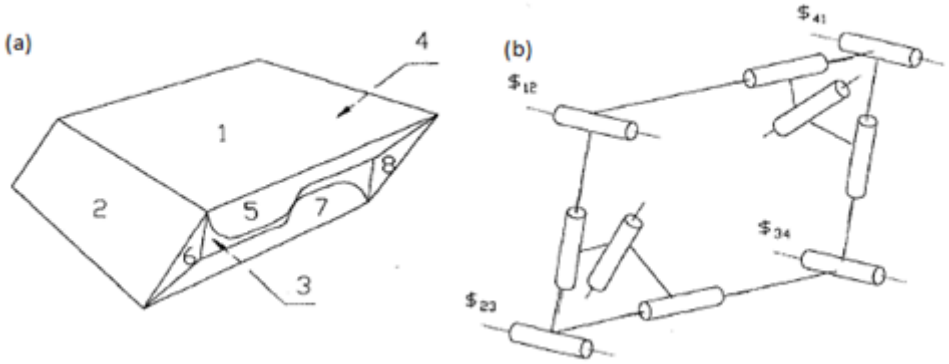

Figure 1.7 (a) A card box with a crash-lock base and (b) A special mechanism equivalent to the box [Dai et al., 1999]

In these mechanisms, a joint axis changes its relative position with respect to other joint axes following particular reconfigurations. These changes subsequently produce a change in the geometrical structure of a mechanism. By this way, kinematotropic mechanisms and a particular type of metamorphic mechanisms can be characterized under geometrical morphing.

1.4.2.1.1 Superposing joint axes

Superposing joint axes is a way of morphing. This was implemented by the vA joint. A vA joint is the variable-axis joint which decomposes the spherical motion of a conventional

spherical joint [Zhang et al., 2013]. Different rotation phases about three intersecting axes are produced by the vA joint. The three stable working phases are derived from the kinematic joint and the constraints supplied by this kinematic joint are changeable following the variation of the rotational axis.

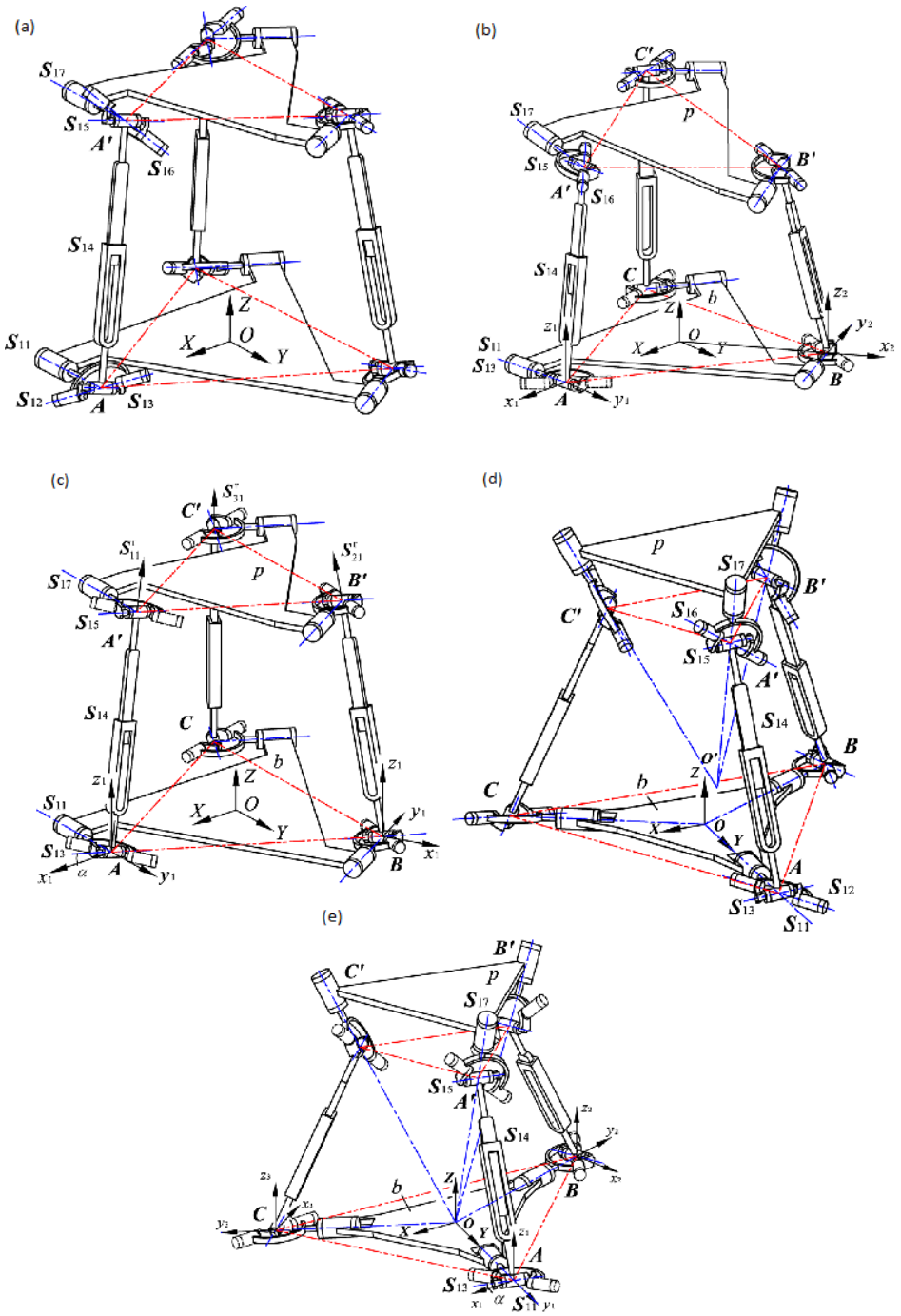

Figure 1.8 (a) The 3SvPSv-I (b) Phase 3RvPSv of the metamorphic parallel mechanism 3SvPSv-I (c) Phase 3UvPUv of the metamorphic parallel mechanism 3SvPSv-I (d) The SvPSv-II metamorphic parallel mechanism (e) Phase 3UvPUv of the metamorphic parallel mechanism 3SvPS [Zhang et al., 2013]

The vA joint is formed by three individual joints with their axes intersecting each other. The second-joint axis is the reconfigurable axis that intersects the first joint axis in 45 degree. This joint rotates the third joint axis either out of or into the plane formed by the first and the second joint axes. The former, while the third joint axis is out of the plane constitutes a spherical joint, the latter, while the third joint axis is in the plane forms a precondition for constituting both U-joint and R-joint. In the latter case when all joint axes are coplanar, there are two subcases. The first subcase occurs when the third joint axis is perpendicular to the first joint axis; this constitutes a U-joint circumstance. The second case occurs when the third-joint axes is in line with the first joint axis, this forms a R-joint circumstance. The transition from the U-joint case to the R-joint case is completed by the reconfigurable joint that rotates the third-joint axis out of the plane by 180 degree about the reconfigurable joint axis and to be back to the plane in alignment with the first-joint axis. This gives the R-joint case.

Therefore the vA joint is a variable-axis joint where the relative orientations of three intersecting axes are changing to achieve three different working phases of joint configurations.

This superposition of joint axes results in change of joint mobility and change of structural parameters of a parallel mechanism as in the mechanism presented by Zhang et al [Zhang et al., 2010], [Zhang et al., 2013]. Using this joint property to change the relative positions of joint axes is a type of metamorphic mechanisms. In this process, the source metamorphic phase makes a transition to various phases as shown in figure 1.8.

1.4.2.1.2 Enabling joint axes to be coplanar

Enabling joint axes to be coplanar is a way of morphing. While doing this enabling, various geometrical properties such as co-linearity, parallelism and perpendicularity of joint axes can be achieved. This creates a set of metamorphic parallel mechanisms with reconfigurability in geometric morphing.

This can be demonstrated in the vA joint whose joint axes are made to lie on a plane from their initial state of spatial arrangement [Zhang et al., 2010] to enable the vA joint to change to a Hooke joint from its initial spherical joint state.

In the mechanism presented by Zhang et al [Zhang et al., 2009], a metamorphic mechanism with articulated links is illustrated. By aligning links, a union of two links can be obtained acting as a single link. By doing so, axes of two revolute joints become collinear. Assembling four L-shaped flat cards inspired chains, a new metamorphic mechanism was obtained to change relative positions of joint axes. This mechanism performs circular translational motions.

1.4.2.1.3 Superposing a joint axis with a link

This morphing can be executed by the rT (Fig. 1.9) joint where one axis of the joint could be aligned with a limb of a parallel mechanism to initiate an idle mobility and subsequently

reduce the mobility of the platform as presented by Gan et al [Gan et al., 2009]. The examples presented in the paper are multi-loop mechanisms.

The rT joint is a reconfigurable Hooke joint in which an axis of a traditional T joint could rotate and change the initial orientation with respect to a link it connects. Usually a Hooke joint consists of two revolute joints with axes intersecting at the right angle to form a T-shaped connector of mobility two. Based on metamorphosis, it is expected that the direction of a rotation axis be altered to enable change of axis orientations. This leads to a new design that varies [Gan et al., 2010] the rotation axis to realize the reconfiguration of the joint. This ability of changing the rotation axis is initiated by rotating one axis along the groove of a ring. This subsequently creates the rT joint, where T is commonly used for a Hooke joint and 'r' stands for reconfigurable with the added revolute joint.

In the metamorphic parallel mechanism, two prominent phases of the rT joint [Gan et al., 2010] are used. With the relative position between the radial axis in the grooved ring and the limb it installs, two phases are presented. Phase 1 is achieved by fixing the radial axis perpendicular to a limb that the limb has two rotations in pitch motion about the radial axis and yaw motion about the other axis. Phase 2 is achieved by fixing the radial axis in line with the limb where the radial axis rotation becomes an internal mobility and the limb it installs will have only one rotation being exerted. These two phases stemming from change of the reconfigurable Hooke joint exert an alterable number of rotations to a mechanism.

Subsequently, a family of metamorphic parallel mechanisms were created by Gan et al [Gan et al., 2009] with a way of installing the reconfigurable Hooke joint rT as shown in figure 1.9. In these parallel mechanisms, three rT joints are installed between limbs and the platform, and other three rT joints are installed between limbs and a basis, together with three prismatic joints on limbs. All axes of the rT joints intersect at a single point to create the pure rotation. With the change of the rT joints by superposing one axis aligned with a limb, the platform mobility is changing.

With a combination of rT joints installed in a mechanism, more metamorphic parallel mechanisms can be identified.

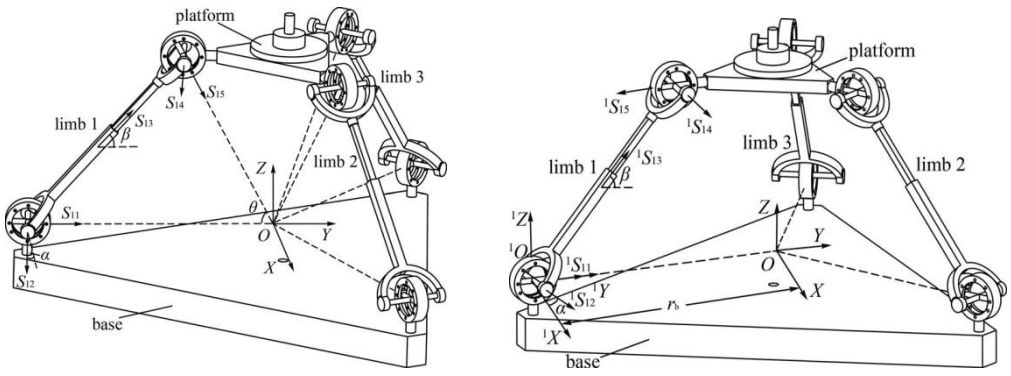

Figure 1.9 (a) 3(rT)g1P(rT)g3-pure rotation (b) 3(rT)g1P(rT)g2-pure translation [Gan et al., 2009]

1.4.2.1.4 Changing joint axes with respect to a base

Changing the arrangement of joint axes of the rT joints enables change of a motion type of a parallel mechanism. By making all rT joint axes in the metamorphic parallel mechanisms [Gan et al., 2009] in parallel to a base, the mechanism generates the translation-only mode to achieve the morphing from a pure rotation to a pure translation.

1.4.2.1.5 Using the joint-motion switch

Switching joint-motion direction proposed by Yan and Kuo [Yan et al.,2007] using a joint coined as the sA joint which is the switch-axis joint, a mechanism can reconfigure itself to achieve various mobility and connectivity. This shift axis of rotation to redirect the joint axis to a different orientation and to change the link orientation is used in a mechanism presented by Zhang et al [Zhang et al., 2012(d)] as shown in figure 1.10. To achieve the reconfiguration, the mechanism has four sA joints together with four conventional joints. By changing the orientation of joint axes, reconfigurability in geometrical morphing is elegantly achieved.

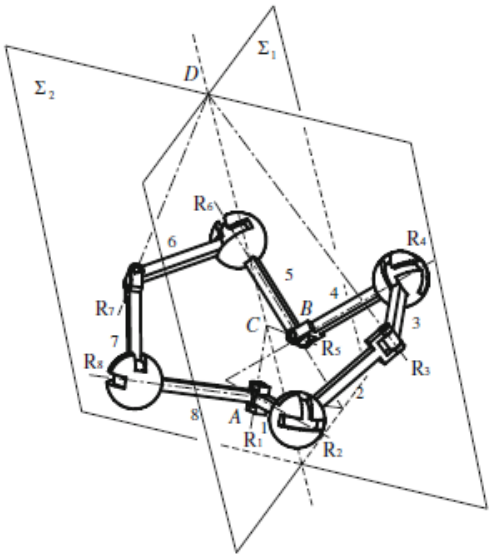

Figure 1.10 A reconfigurable eight-bar linkage [Zhang et al., 2012(d)]

A further single loop mechanism example proposed by Zhang and Ding [Zhang et al., 2012(b)] achieves morphing by utilizing a motion-type switch to change a mechanism from a planar mechanism to a spatial one as illustrated in figure 1.11 [Li et al., 2011]. With change of the axis orientation based on a metamorphosis process, Li et al [Li et al., 2013] proposed a mechanism of a multiple look that can be reconfigured from the planar motion to the spatial motion. In the study, a joint-axis matrix and an augmented adjacent matrix of kinematic chains were proposed to model the metamorphosis process.

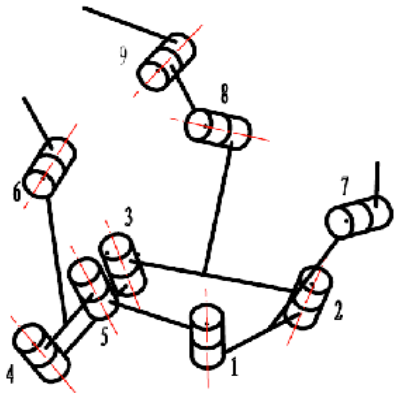

Figure 1.11 Spatial hybrid mechanism when link 4 and link 5 have been annexed [Zhang et al., 2012(b)]

Military domains require more manpower which seems to be risky. This manpower can be replaced by reconfigurable robots. One such robot which can be used for this application having three uniform modules, each forming a reconfigurable mechanism, was studied by Wang et al [Wang et al., 2006]. This JL-I robot achieves highly adaptive locomotion to drive serial and parallel mechanisms to form an active joint. This generation of active joint helps change shape and enhance motion on rough terrains. The yaw and pitch motions are achieved by the parallel mechanisms whereas the third rotation is achieved by a serial mechanism. Therefore by switching between motions, reconfigurability is achieved.

1.4.2.2 Morphing by superposing or aligning two or more links

The metamorphic palm of a novel multi-fingered robotic hand presented by Dai and Wang [Dai et al., 2007], [Dai et al., 2009 (b)] as illustrated in figure 1.12 and by Cui and Dai [Cui et al., 2011] is a spherical five-bar linkage having a characteristic of metamorphosis. There are two drivers on the palm which adjusts the position and orientation of the palm mechanism. When one of the drivers is fixed and the crank link of the palm overlaps the base link, two links are aligned, resulting in the palm to operate as a reconfigurable spherical four-bar linkage with one degree of freedom.

This mechanism was used in the creation of a novel multi-fingered hand as a metamorphic palm done by Dai et al [Dai et al., 2007], [Dai et al., 2009], [Cui et al., 2011] and by Wei et al [Wei et al., 2011] as shown in figure 1.12.

The mechanism in an anthropomorphic hand presented by Wei et al [Wei et al., 2011] illustrates a folding palm of the metamorphic hand where each finger consists of three revolute joints. Various tasks can be completed using the metamorphic hand as illustrated in figure 1.13. By aligning two links at one occasion, various palm configurations achieve, resulting in stretching and folding the palm with an in-hand manipulation. The process of aligning links leads to systematizing this mechanism under geometrical morphing.

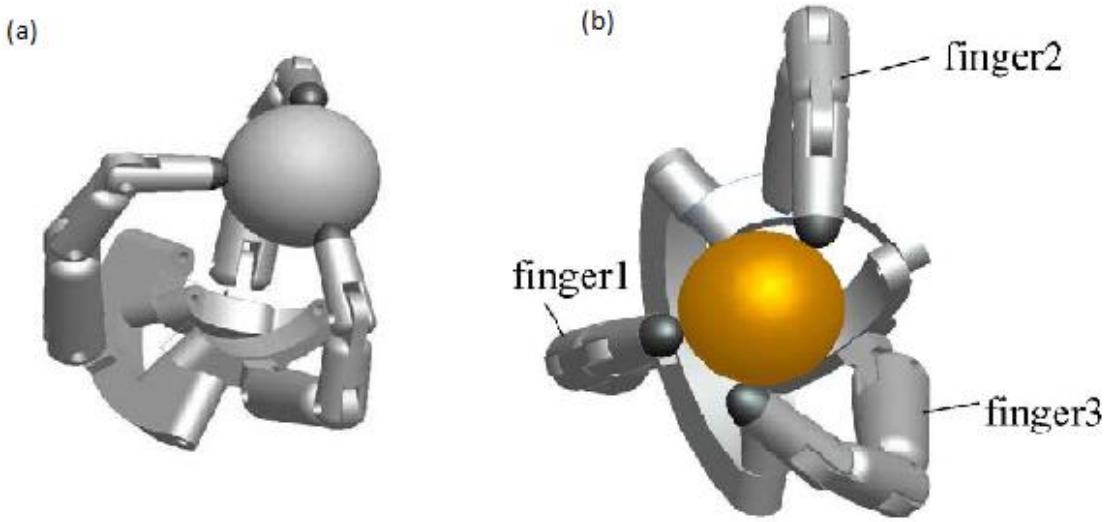

Figure 1.12 (a) Palm workspace and the corresponding hand poses with minimum palm workspace (b) The twisting motion [Dai et al., 2009]

Further example on aligning links can be seen in a spatial 10-bar mechanism derived from the augmented Assur group proposed by Li and Dai [Li et al., 2012], [Li et al., 2011].

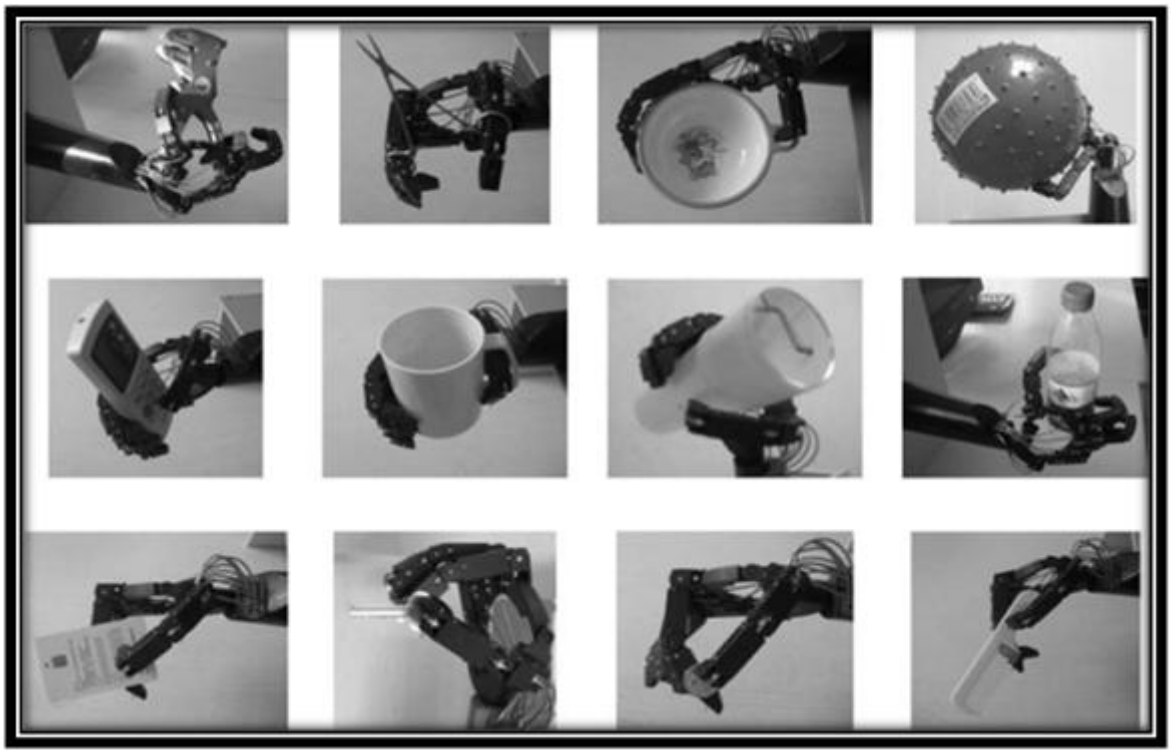

Figure 1.13 Prehensile tests of the metamorphic anthropomorphic hand [Wei et al., 2011]

Design of a metamorphic mechanism with three configurations was presented by Zhang et al [Zhang et al., 2011(b)]. This mechanism has a transformation sequence from one configuration to another by aligning two links using the force or geometrical limits. The mechanism was used in a door-opening structure of a space shuttle as a crank-slider

metamorphic mechanism via stiffness variation. This mechanism presents as an example of geometrical morphing.

A planar lift mechanism with a number of revolute joints was proposed by Zhao et al [Zhao et al., 2012]. This is an interesting mechanism portable by means of the zigzag arrangement of joints and by forming a triangular closed loop to operate as a lift. The lift mechanism is constructed from scissor-like linkages as a deployable unit. During the operation, the links of the mechanism get aligned in a single line and are hence compacted to complete the lift mechanism.

1.4.2.3 Morphing using plane symmetry

For a reconfigurable mechanism with a feature of plane symmetry and metamorphosis, its plane symmetry is used. This is in particular presented by kinematotropic mechanisms [Wohlhart, 1996], [Galletti et al., 2001], [Qin et al., 2014], [Fanghella, 2009].

The case can also be seen in a reconfigurable mechanism proposed by Zhang et al [Zhang et al., 2012 (d)]. Eight links are connected by four sA joints and four revolute joints. At a particular instant of plane symmetry, changing relative positions of two joints with respect to each other, reconfigurability using geometric morphing is achieved.

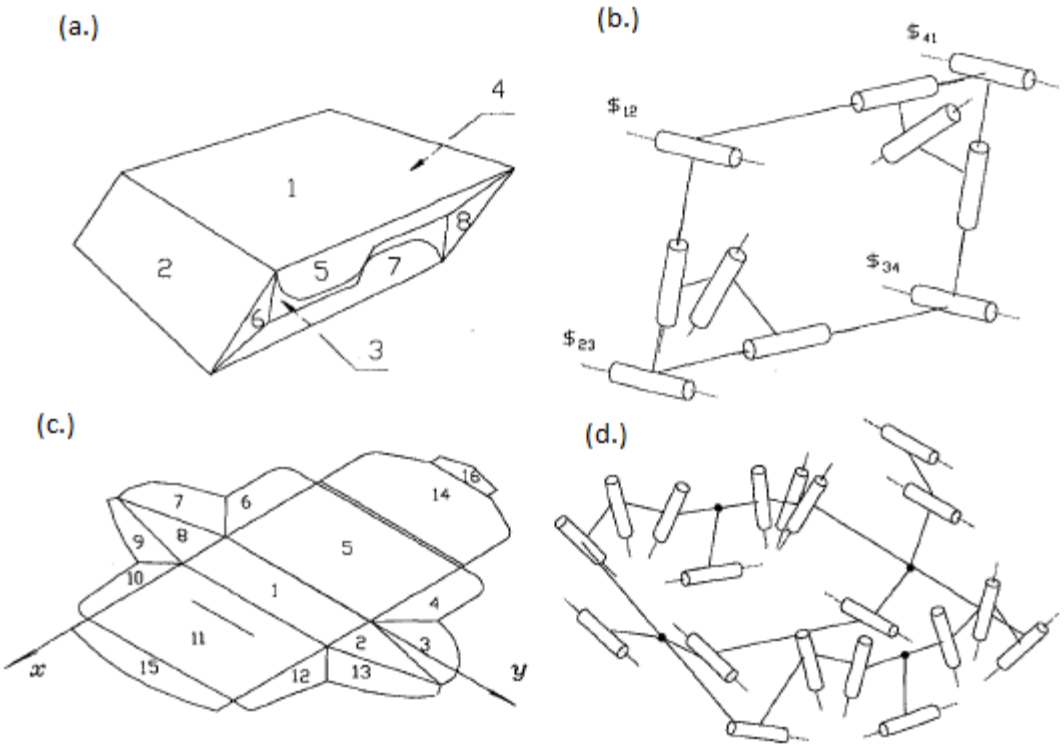

Figure 1.14 (a) A card box with a crash-lock base (b) A special mechanism equivalent to the box (c) A flattened configuration of a card box (d) Equivalent mechanism of a whole box [Dai and Rees Jones, 1999]

A mechanism of an origami presented in figure 1.14 by Dai and Rees Jones [Dai et al., 1999], [Dai et al., 2002], demonstrates a commonly found metamorphic mechanism. Taking panel sections and creases as links and revolute joints respectively, an origami mechanism with ten revolute joints was illustrated and reconfigurability was achieved by using the plane symmetry with five revolute joints in one side and other five revolute joints in the other side.

This reconfigurable mechanism is used in the industry for origami folding in the confectionary industry to adapt to various shapes of origami [Dai et al., 1999, Yao et al., 2011]. A further example of carton erection is dealt by Dai et al [Dai et al., 2009 (a)], [Dubey et al., 2007], where various motions in erecting origami-cartons are used to reconfigure the machine to adapt for different origami-carton sizes and styles.

1.4.2.4 Morphing using internal mobilities

This type of morphing can be achieved when internal mobilities are produced while replacing an existing joint with a reconfigurable joint. This is mostly done by using the rT joint or vA joint. Morphing of this type can be illustrated in examples presented by Gan et al [Gan et al., 2009]. In a 3-UPU mechanism, replacing all U joints by rT joints, a mechanism with variable mobility changes motion from a pure rotation to a pure translation. In this transition, the mechanism generates internal mobilities and forms a reconfigured mechanism.

A further example of geometrical morphing was demonstrated in figure 1.15 by Gan et al [Gan et al., 2010]. By altering the rT joint one by one in all three limbs of a metamorphic parallel mechanism, resulting in switching a global mobility to a local mobility gradually, the mobility changes from 6 to 1 consecutively. Therefore, by changing the internal mobilities, reconfigurability is achieved through alteration of the rT joints. The mechanisms presented are double loop mechanisms.

A type-changeable kinematic pair with various phases has been discussed by Zhang et al [Zhang et al., 2012 (c)]. The platform of a reconfigurable parallel mechanism has the ability to change the phases of the kinematic pair, leading to mobility change from 6 DOFs to 3DOFs. The type-changeable kinematic pair changes its topological configuration, resorting to link annex. By annexing links, reconfiguration is achieved in this parallel mechanism.

A systematic way of synthesizing metamorphic parallel mechanisms, using screw theory based on the internal mobility principle in co-line, co-plane and co-sphere with internal mobilities, was proposed by Gan et al [Gan et al., 2011] and some new metamorphic parallel mechanisms were constructed. The co-line principle was then extended for a new family of metamorphic parallel mechanisms based on point-plan geometric constraint in [Gan et al., 2014].

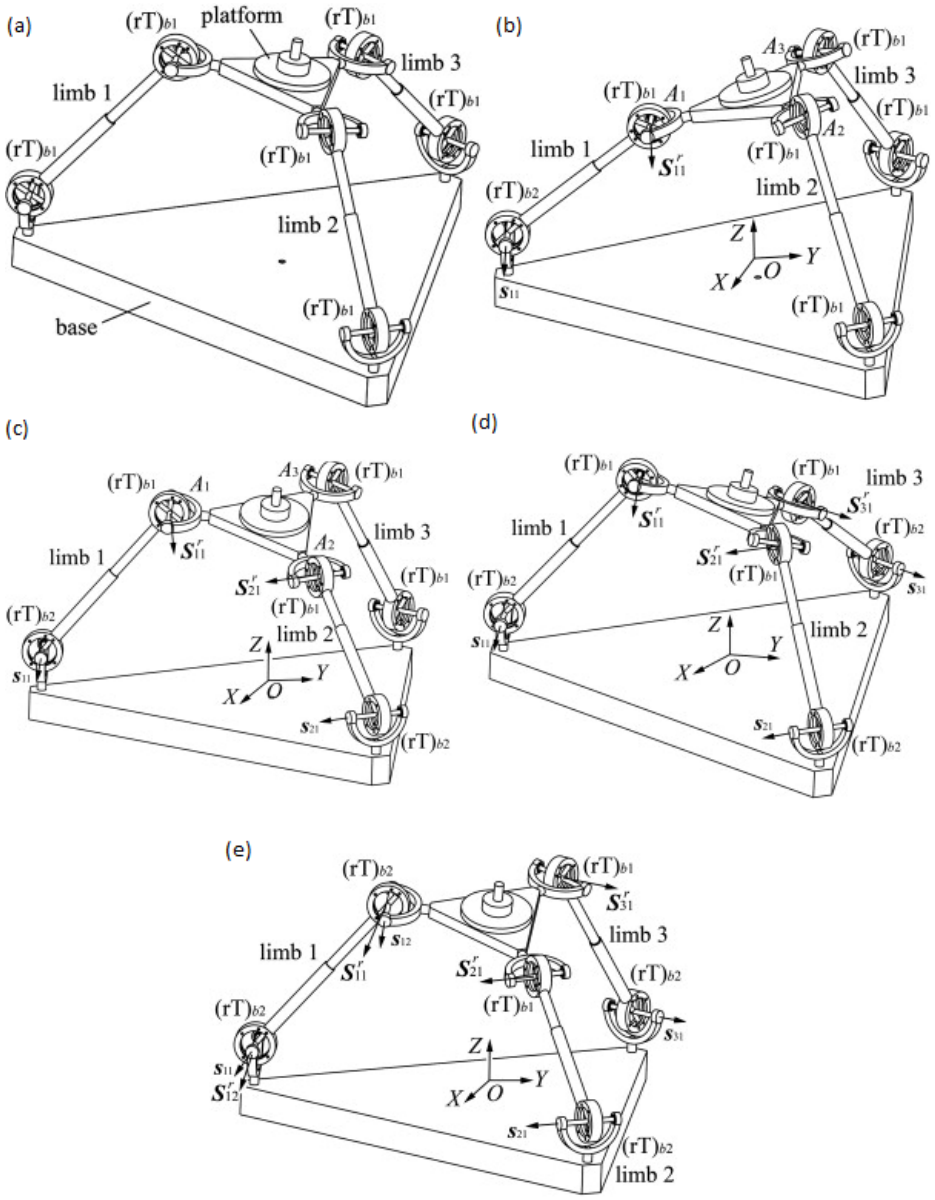

Figure 1.15 (a) The 3(rT)b1C(rT)b1 (b) The 2(rT)b1C(rT)b1–1(rT)b2C(rT)b1 (c) The 1(rT)b1C(rT)b1–2(rT)b2C(rT)b1 (d) The 3(rT)b2C(rT)b1 (e) The 2(rT)b2C(rT)b1–1(rT)b2C(rT)b2 [Gan et al.,2010]

1.4.3 Connectivity and Mobility change in furcating morphing

Furcating morphing can in general result in connectivity change and mobility change. While the former indicates not only mobility number change but also connectivity change that relates to change of motion types, the latter gives mobility variation with a typical representation of kinematotropic mechanisms.

The connectivity morphing covers several morphing branches where the degree of mobility is constant but connectivity changes. The mechanism provided by Galletti and Fanghella [Galletti et al., 2001] is a single loop planar four-bar linkage with one degree of freedom. At an initial stage, the mechanism has two prismatic joints with parallel axis and at this point, the

mobility is one and the connectivity of the prismatic pair is equal to one with a zero-mobility revolute joint. The mechanism then makes a transition and moves to a singular position and finally comes out of this position with coincident revolute joint axes as illustrated in figure 1.16. At this instant the mobility remains the same but the connectivity changes with the connectivity of the revolute pair as one and that of the prismatic as zero. This is an example in which morphing can be achieved.

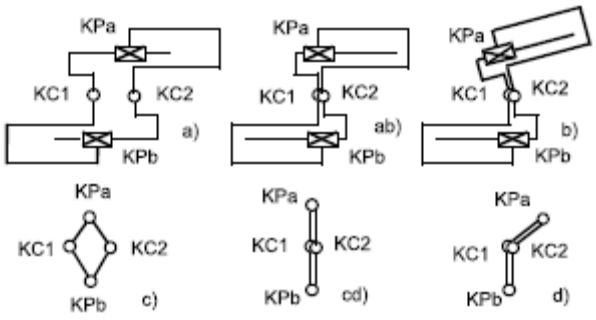

Figure 1.16 A planar four-bar linkage R-P-R-P (and R-R-R-R) [Galletti et al., 2001]

Mobility morphing mostly occurs in bifurcation in kinematotropic mechanisms [Wohlhart, 1996], [Qin et al., 2014], [Fanghella, 2009] that results in change of mobility. In 2013, a novel spatial-spherical metamorphic mechanism with bifurcated motion was presented by Gan and Dai [Gan et al., 2013 (a)]. This presents a class of 3-PUP double loop mechanisms with various configurations. When the mechanism is in a constraint singular configuration, it bifurcates hence the mobility changes from 3 to 2 with one translation and one rotation and the connectivity in the sense of motion type changes. Plitea et al also illustrated a robot with 6 degrees of freedom which enable its reconfiguration to achieve mechanism variation from 6 to 2 degrees of freedom [Plitea et al., 2013]

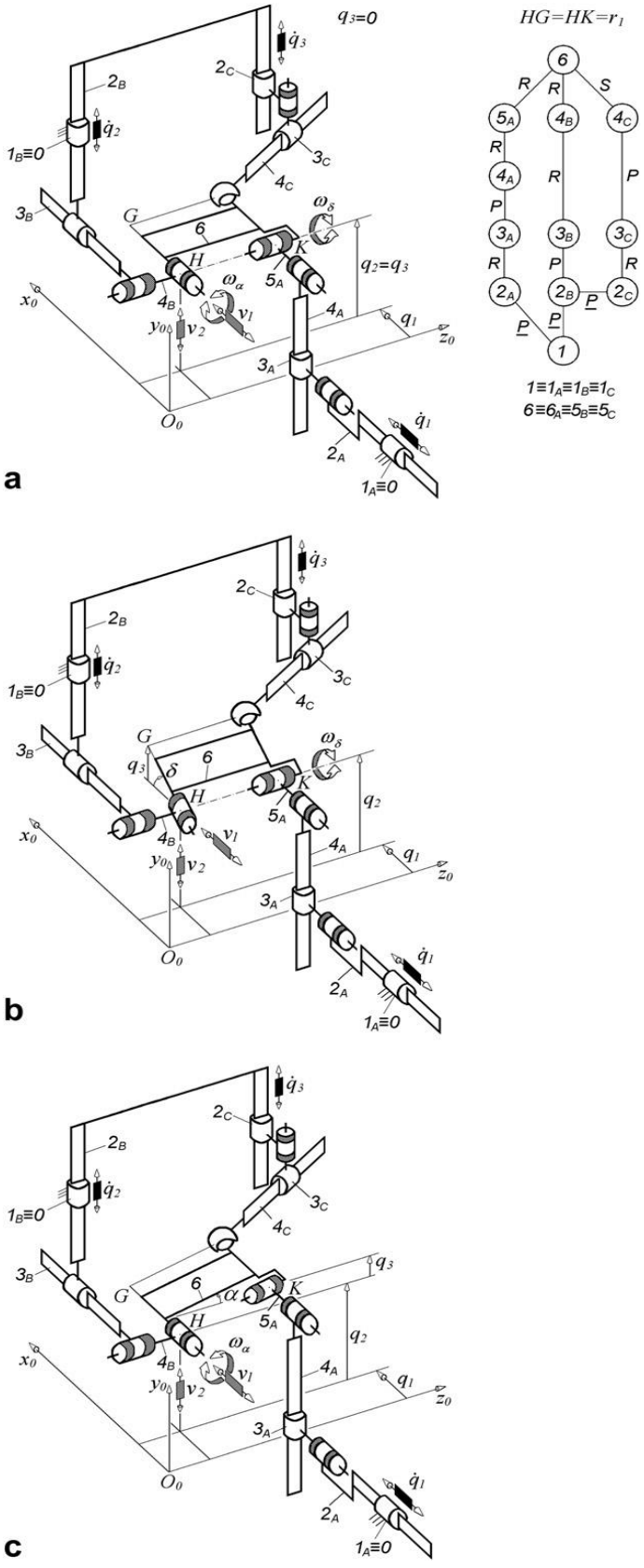

Figure 1.17 T2R1-type parallel manipulator with uncoupled and bifurcated planar-spatial motion of the moving platform: constraint singularity (a) branch with planar motion (b) branch with spatial motion (c) limb topology [Gogu, 2012]

Furcating morphing generates different branches in mechanism reconfiguration leading to classification of various numbers of branches in morphing. Bifurcation takes place in a constraint singularity position in which connectivity between moving and fixed platforms increases instantaneously with no change in limb connectivity. When branching occurs in a constraint singularity, a mechanism reaches different configurations as branches as shown in figure 1.17 and can have different independent motions of a moving platform [Gogu, 2012] leading to change in connectivity and/or mobility.

Several investigations have been made for bifurcation by Gan et al [Gan et al., 2010]; Gan and Dai [Gan et al., 2013 (a)]; Zhang et al [Zhang et al., 2013], [Zhang et al., 2012 (a)]; Lee and Hervé [Lee et al., 2012]; Gogu [Gogu, 2012]; and multi-furcating morphing by Qin et al [Qin et al., 2014]. When a metamorphic mechanism or a kinematotropic mechanism passes through a constraint singularity then bifurcates by influence of geometrical constraints such as parallelism or perpendicularity, morphing is achieved.

1.4.3.1 Branching in constraint singularities

In the example presented by Gogu [Gogu, 2009] four types of branching singularities are identified as type A (BS-A), type B (BS-B), type C (BS-C) and type D (BS-D) leading to furcating morphing. Each of them has their own properties of structural parameters.

A typical bifurcating morphing occurs in the parallel mechanisms with multiple modes proposed by Kong and Gosselin [Kong et al., 2007], [Kong, 2014].

In 2009, a group of kinematotropic mechanisms with bifurcated motion for each type of branching in constraint singularities has been presented by Gogu [Gogu, 2009]. During the process of bifurcation, axes of the last revolute joint of the first limb and the first revolute pair of the second limb overlap leading to a morphing process. A family of mechanisms presented by Gogu [Gogu, 2011] also illustrates bifurcation morphing.

The multi-loop mechanism presented in the paper by Zhang et al [Zhang et al., 2009] is an example of bifurcating morphing where one instantaneous rotation and a translation are exchanged during the motion.

A metamorphosis that results in reconfiguring a mechanism from generating the pure translation to the pure rotation can be illustrated in a metamorphic mechanism proposed by Zhang et al in figure 1.18 [Zhang et al., 2010] where the platform implements a translational motion from the transitory position, passing through a constraint singularity position. This produces a bifurcated motion branch with one translation. When the platform implements a rotation motion and passes to the transitory position, the second motion branch can be realized. Therefore, two bifurcating motions i.e. a twisting motion between the platform and the base and a curvilinear motion are implemented. Hence reconfigurability is achieved using the bifurcating morphing.

The 3-PUP parallel mechanism presented by Gan and Dai [Gan et al., 2013 (a)] consists of three identical PUP limbs, in which axes of three U joints are parallel correspondingly to each other and the P joints on the base are perpendicular to the base plane. When three limbs have the same length, the home position configuration is when the platform is parallel to the base, acting as the constraint singularity configuration. The bifurcation is trigged at this position enabling the mechanism to possess furcating morphing.

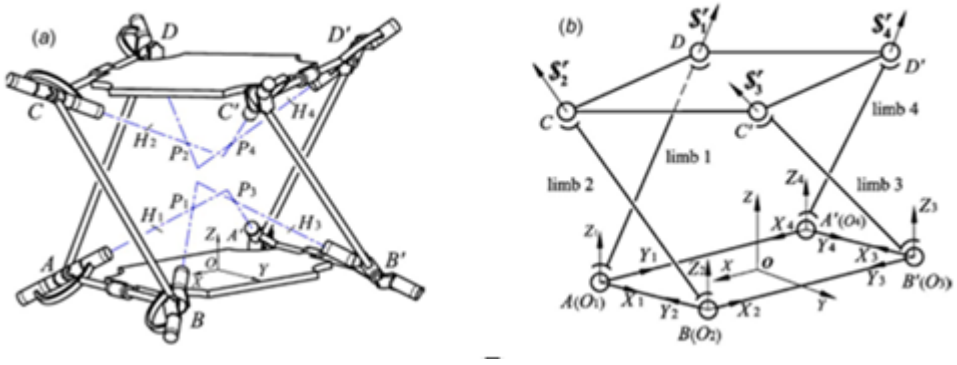

Figure 1.18 (a) Kinematic structure of the metamorphic mechanism (b) equivalent model with bifacial constraint forces [Zhang et al., 2010]

1.4.3.2 Instantaneous locking bifurcation

By instantaneous locking of joints, a mechanism can branch into a non-singular configuration. This is called as the instantaneous locking bifurcation.

This type of bifurcation occurs in double loop mechanisms dealt by Gogu [Gogu, 2012]. These mechanisms require two independent planar translations and one independent rotation of the mobile platform around an axis perpendicular to the plane of translations or parallel to this plane. In the first case, the moving platform has a planar motion, and in the second case, it has a spatial motion. By instantaneously locking a revolute joint, two bifurcating motions occur switching from planar to spatial motion.

1.4.4 Types of furcating morphing

The following types of furcating morphing are identified in figure 1.19 as: (a) kinematotropic bifurcating morphing (b) furcating morphing in metamorphic parallel mechanisms (c) bifurcation in the discontinuously movable parallel mechanisms (d) multifurcating morphing and (e) actuation morphing. Detailed explanations with its corresponding examples are described in the following sub-sections.

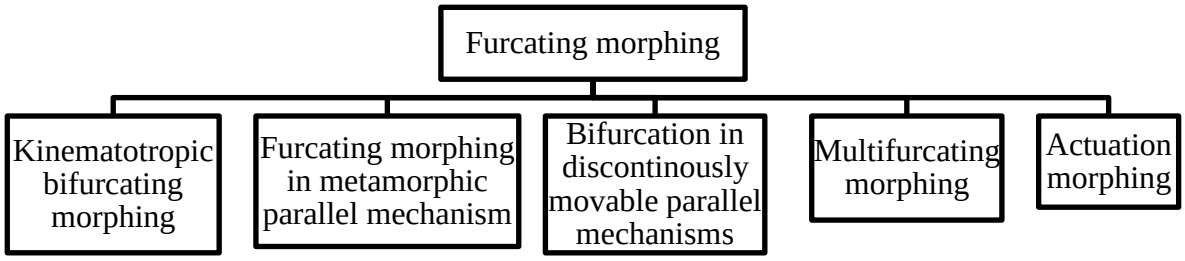

Figure 1.19 Classification of furcating morphing

1.4.4.1 Kinematotropic bifurcation morphing

Kinematotropic bifurcating morphing is to change the mechanism mobility by using bifurcation without changing any of joint property or link connectivity. A mechanism proposed by Galleti and Fanghella illustrated in figure 1.20 [Galleti et al., 2001] has eight links and eight revolute pairs with two set of joints having parallel axes and two revolute joints normal to these sets. The mechanism gets into a singular configuration when two revolute joints which are placed in the intermediate position get aligned and also when other six revolute joints become parallel to each other. The mechanism gets out of the singular position and bifurcates into two other configurations. One configuration has the coincident axes of the normal revolute joints but with a displacement of 3 revolute joints contributing 2 degrees of freedom.

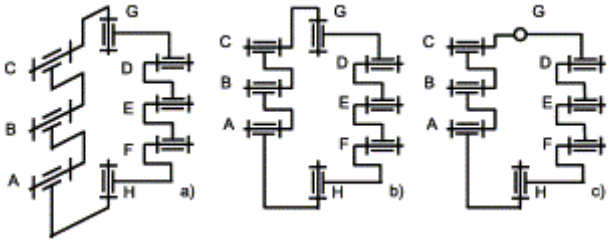

Figure 1.20 A kinematotropic chain (from 2 to 3 degrees of freedom) [Galletti et al., 2001]

Another configuration is obtained by rotating pairs of two planar sets with non-coincident axes of the normal revolute joints hence making this pair as locked revolute joints. At this configuration the mechanism has 3 degrees of freedom. The mechanism uses the kinematotropic bifurcation morphing.

1.4.4.2 Furcating morphing in metamorphic parallel mechanisms

Furcating morphing in metamorphic parallel mechanisms entails mobility change by using furcation with change of joint property. They perform bifurcation and hence possess the property of furcating morphing.

At the home position configuration, mobility changes from 6 to 1 by altering the rT joints from one phase to another in an example proposed by Gan et al [Gan et al., 2010]. It is found

that the 3 (rT)C(rT) metamorphic parallel mechanisms has the bifurcation point at the home position when it is evolved into a configuration with mobility fewer than 3. The home position presents the bifurcation point with two branch motions each of which has mobility one. In the last topological configuration, two branches have neither the same mobility nor the same motion. Hence this mechanism can be characterized under furcating morphing.

In the mobility 2 phase of the 4rT*PS* metamorphic parallel mechanism, two rotation branches bifurcate at the home position along two perpendicular directions while a common translation exists all the time as shown by Gan et al [Gan et al., 2013 (b)]. A further example with the reconfigurable Hooke joint is used in the mechanism presented by Gan et al [Gan et al., 2012], where the main characteristic is the mobility change from full mobility to lower mobility with constraint forces. This mechanism exhibits the property of reconfigurability by changing the phases of the rTPS limbs.

1.4.4.3 Bifurcation in discontinuous movable mechanisms

Discontinuously movable mechanisms proposed by Lee and Hervé shown in figure 1.21 [Lee et al., 2012] uses the bifurcation principle in generating different mobility in different motion branches where a motion would be ended at the constraint singularity discontinuously and switched to a different motion with different mobility. This reflects particular characteristics of this type of mechanisms by fully utilizing their branching behaviors. Subsequently, a number of these types of mechanisms [Lee et al., 2002], [Lee et al., 2005], [Lee et al., 2007], [Lee et al., 2009] were generated with their various branch behaviors.

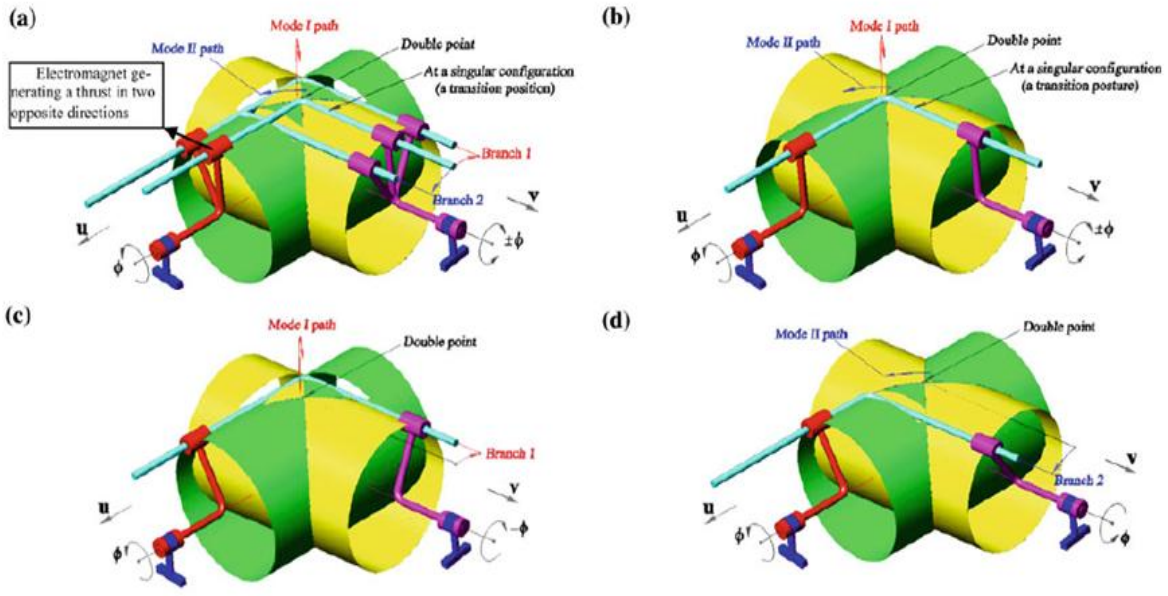

Figure 1.21 One bifurcation configuration of DM RC -//- Rc CVSC. (a) A bifurcation at double point of top surface; (b) at a transition posture; (c) symmetric motion at a mode I ; (d) motion at a mode II [Lee and Herve,2012]

1.4.4.4 Multifurcating morphing

Multifurcating morphing is the extent of furcating morphing. The feature of it can be illustrated by parallel mechanisms with multiple operating modes.

Kong et al [Kong et al., 2007] presented a family of parallel mechanisms with multiple operating modes. These mechanisms are of 3 degrees of freedom and produce both spherical motion and spatial translational motion systematically. By entailing the characteristics of branches as modes, multiple modes with both spherical and translational motions are generated. The main particularity of these modes is that they have the same mobility but generate different motions; we call this reconfiguration as multifurcating morphing.

Figure 1.22 is the derivative queer-square mechanism presented by Qin et al [Qin et al., 2014]. It clearly gives the process of multifurcation morphing where two phenomenon and fourteen states were discussed. Phenomenon one takes place when the mechanism passes through a constraint singular position leading to mobility changes. The mechanism changes its motion permanently during this phenomenon. Whereas, in phenomenon two, mobility change occurs as a result of change of orientations of the joint axes by passing through a constraint singularity. With the help of this phenomenon, multifurcation is achieved with different motions in four categories and fourteen states in the derivative queer-square mechanism.

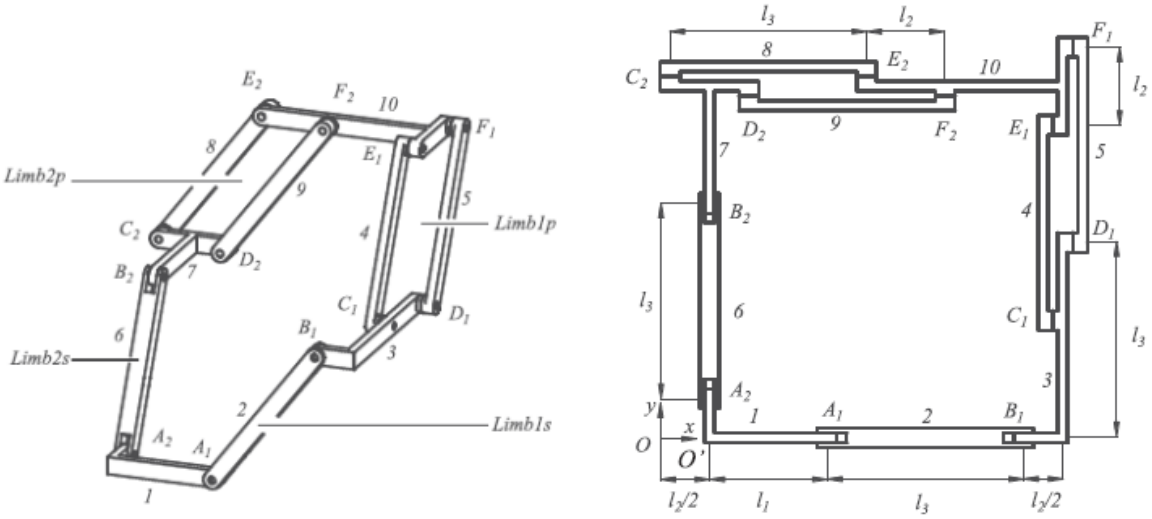

Figure 1.22 (a) General structure and (b) Singular posture of the derivative queer-square mechanism [Qin et al., 2014]

A family of reconfigurable parallel mechanisms with three identical kinematic reconfigurable limbs connecting the platform with the base is dealt by Ye et al [Ye et al., 2014]. This reconfigurable mechanism uses a four-bar linkage with equal dimensions making it as a diamond shaped kinematotropic mechanism. By applying a constraint force or couple on the reconfigurable limb, the mechanism is able to switch from one branch to another and also come out of the singular configuration allowing the mechanism to perform different kinds of motion. Due to its ability to generate different motions, we systematize this mechanism under multifurcating morphing.

1.4.4.5 Actuation morphing

By using different combinations of actuations, mechanism morphing can be achieved in different branches with different operating modes.

The mechanism presented by Kong et al [Kong et al., 2007], uses different numbers of actuators for different modes. In parallel mechanisms, reduced number of actuators can be used to generate different motion patterns. In this, initially six actuators are used to perform spherical motions and the number of actuators is reduced to four to switch to various modes.

1.4.5 Joint-Motion morphing

The joint-motion morphing occurs when a mechanism generates an idle mobility or when the mechanism switches between active and idle mobility. This type of morphing can be achieved by various ways as illustrated in figure 1.23 and is discussed in the following.

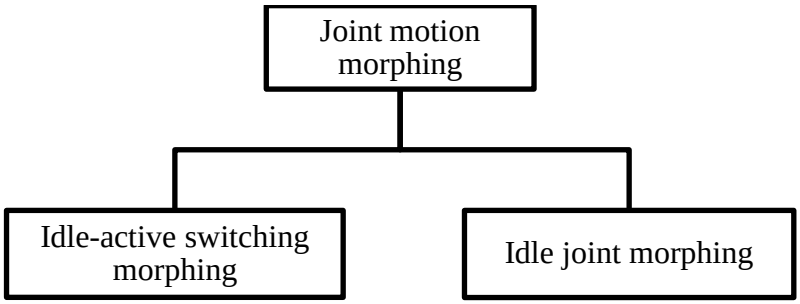

Figure 1.23 Classification of Joint motion morphing

1.4.5.1 Idle-active switch morphing

Switching between idle and active joints to achieve morphing can be illustrated in a metamorphic mechanism [Gan et al., 2010]. With presence of a source generator and by operation of metamorphosis, pure rotation and pure translation are achieved respectively in subphases 1 and 2. From this, by reconfiguring the axis of rotation of the rT joint, the joint motion switch between idle and active joints is achieved.

Further example with idle-active switch morphing is the pin-in-slot joint presented by Yan and Kuo [Yan et al., 2006]. At the initial configuration, the mechanism performs both rotation and translation with 2 degrees of freedom. During this motion, when the pin reaches the end of the slot, a mobility produced by translation is restricted whereas it continues to rotate. This changes the property of a joint and leads to changing the number of degrees of freedom from 2 to 1.

Figure 1.24 is an application of a metamorphic mechanism to a steel-ingot cutting machine proposed by Li and Dai [Li et al., 2012] which illustrates two working stages of the machine. In the first working stage the movement of the lower cutter is blocked by a spring and the upper cutter moves downwards. By this, one movement and hence one mobility produced by

the lower cutter becomes idle. When the mechanism reaches the second working stage, the upper cutter remains static and the lower cutter moves upward. By this operation, the mobility of the upper cutter becomes idle and that of the lower cutter becomes active. This single loop mechanism clearly illustrates switching between idle-active morphing.

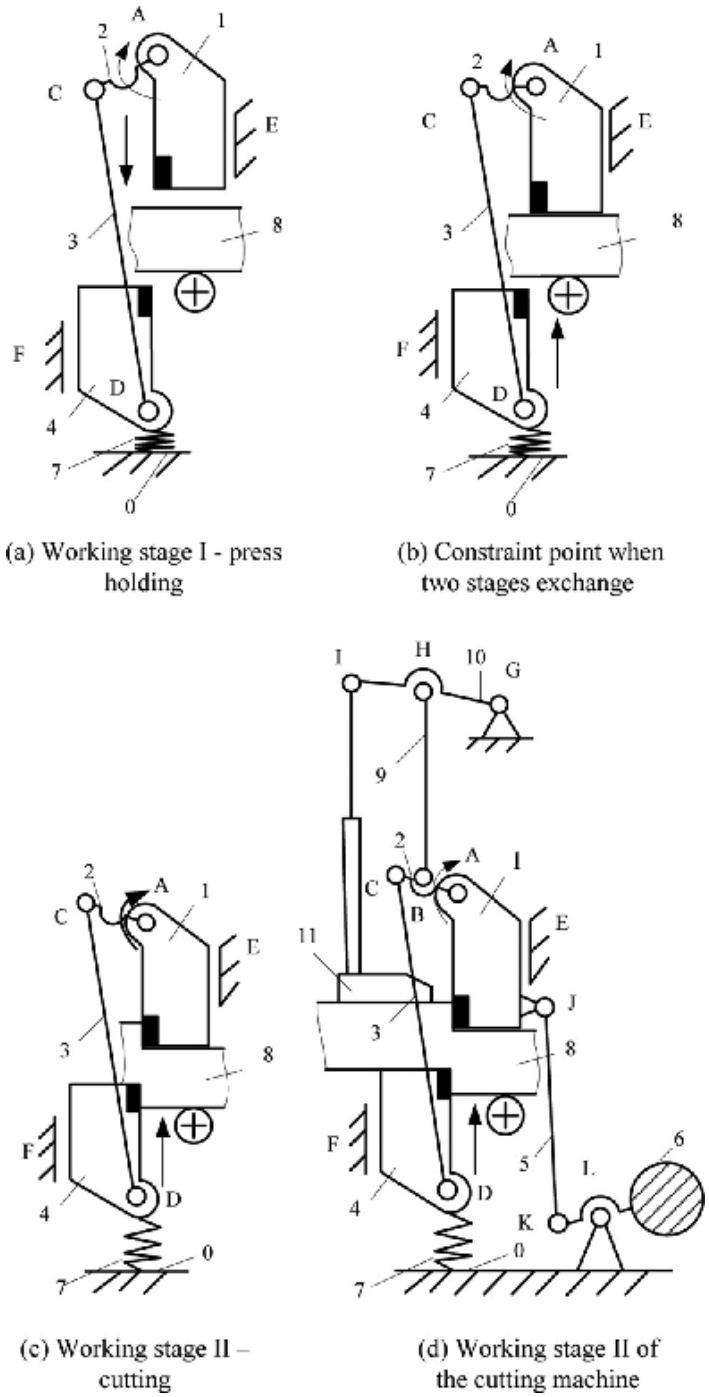

Figure 1.24 The working stages of the metamorphic mechanism extracted from a steel-ingot cutting machine [Li and Dai, 2012]

1.4.5.2 Idle-joint morphing

Changing an active joint to an idle joint is the idle-joint morphing. In 2009, Zhang et al [Zhang et al., 2009] presents a mechanism where two panels are folded together and made as a single link. By doing this with the mechanism equivalence principle [Dai et al., 1999], two revolute joints become perpendicular and two independent rotational degrees of freedom are produced. Hence by annexing, an idle revolute joint is generated leading to idle-joint motion morphing.

In the metamorphic robotic hand [Dai et al., 2007] shown in figure 1.25, [Dai et al., 2009 (b)] and a spatial hybrid mechanism [Li et al., 2012], an idle joint was generated, by superposing and by annexing two links respectively. The morphing in these mechanisms is also coupled with the geometrical morphing.

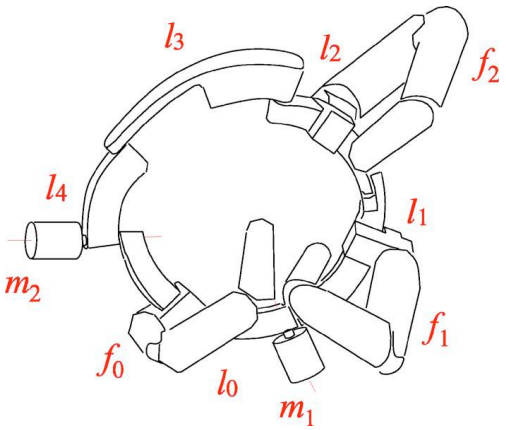

Figure 1.25 A metamorphic robotic hand with a spherical five-bar [Dai et al., 2007]

By superposing two revolute joints in a 5R spherical metamorphic mechanism presented by Li and Dai [Li et al., 2012] a degree of freedom is lost and hence an idle joint is generated. Reconfigurability is achieved in this mechanism by using the idle-joint morphing which is implemented in the steel ingot cutting machine. These steel ingots were used in a number of rail-craft systems including steel tools, rails, bore heads and indirectly in the tunnel bore via the production of steel blocks.

In each of the double loop mechanisms presented in the paper by Zhang et al [Zhang et al., 2013], an idle mobility was generated by using the principle of metamorphosis of the vA joints. This spatial-spherical metamorphic parallel mechanism evolves themselves into different mobility configurations.

Note:

Some metamorphic mechanisms can be grouped under two or more types of morphing. For instance the mechanisms proposed by Dai and Wang [Dai et al., 2007] and Li and Dai [Li et al., 2012] possess both geometrical as well as idle-joint morphing. Also, the crank-slider mechanism presented by Zhang et al [Zhang et al., 2011(b)] uses both the motion range limit (topological morphing) as well as aligning two links using force or geometrical limits (geometrical morphing). Hence there is a common property between these two morphing types.

1.5 Applications

The reconfigurable eight-bar linkage has various interesting applications in the day to day life and in industrial fields. One of the brainstorming applications of the eight-bar linkage is the reconfigurable cube mechanism which is commonly called as RCM [Kuo et al., 2014]. It is equivalent to a single-loop 8R spatial linkage possessing eight different topological configurations during reconfiguration. The reconfigurable cube mechanism is a foldable puzzle mechanism that has the ability to manipulate, alter its topological configurations followed by changes in mobility. This RCM can be viewed as a reconfigurable mechanism, variable topology mechanism, kinematotropic linkage or discontinuous mobility mechanism.

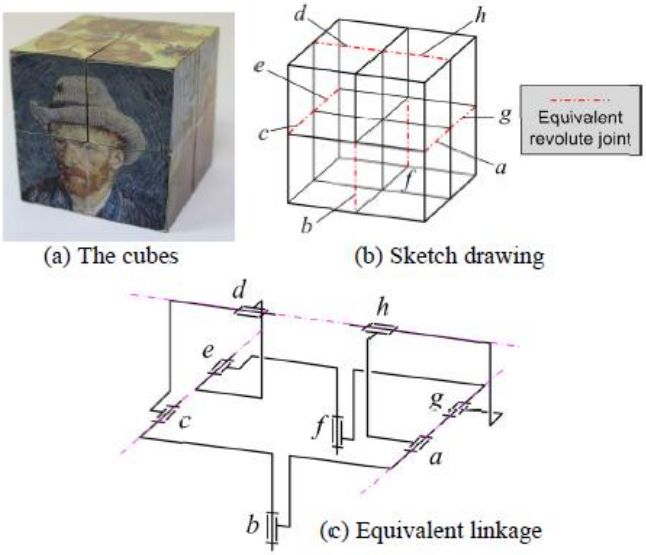

Figure 1.26 The reconfigurable cube mechanism (RCM) [Kuo et al., 2014]

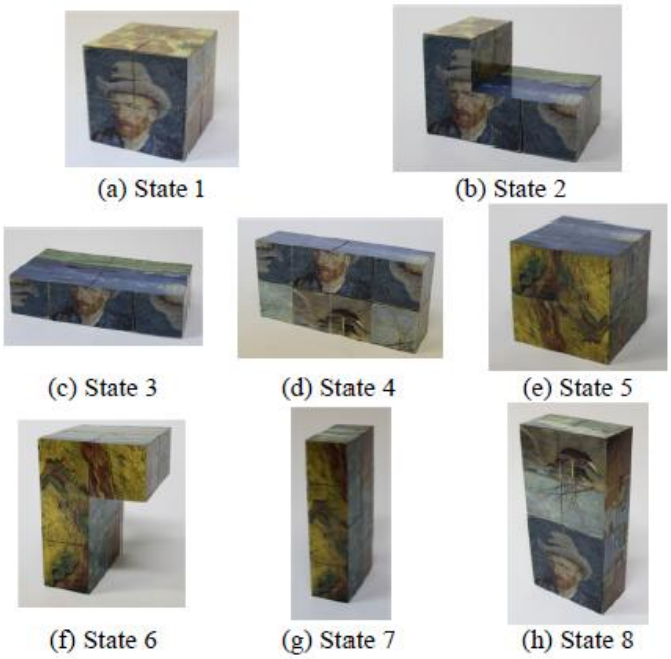

Figure 1.27 The eight configurations of the RCM [Kuo et al., 2014]

The RCM is made up of eight connecting cubes folded together as an integrated bigger cube as shown in figure 1.26. The RCM can be manipulated to demonstrate eight different configurations as in figure 1.27.

Other applications of reconfigurable mechanisms used in industrial fields are as follows,

- Origami folding: The Origami folding shown in figure 1.14 and figure 1.28 is an art of paper folding. The principles of origami are used in stents, packaging and other engineering applications.

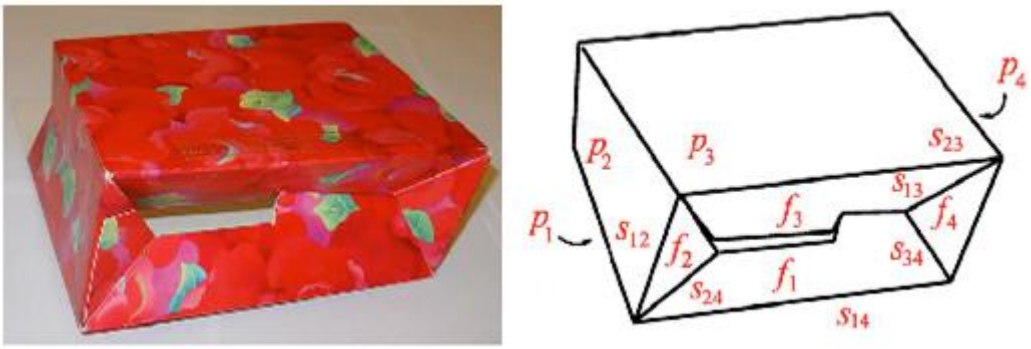

Figure 1.28 A carton fold [Dai et al.,2008]

- Metamorphic palm illustrated in figure 1.12 is capable of generating reconfigurable motions with the help of its foldable and flexible palm.

- The Metamorphic hand presented in figure 1.29 plays an important role in industrial automation and space technology.

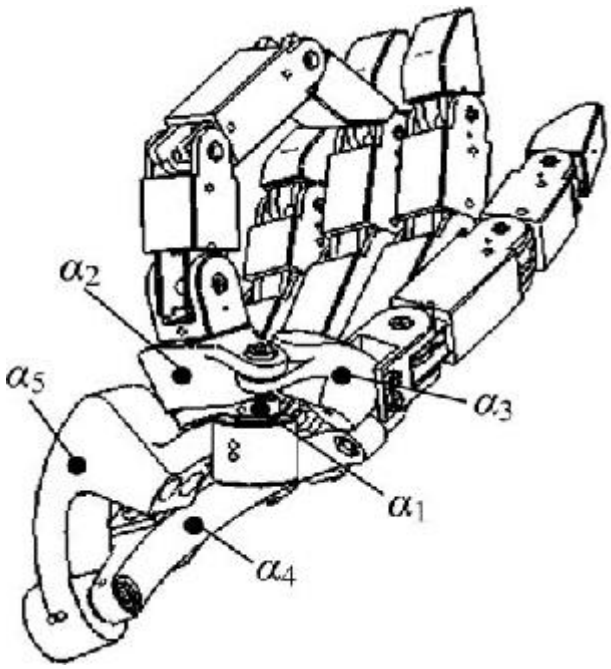

Figure 1.29 Metamorphic hand with its palm in a reconfigured position [Wei et al.,2011]

Figure 1.13 illustrates the prehension of metamorphic hand to our daily life objects of different geometric features. These prehensile tests are performed to change of position and orientation of the fingers for various objects and environment by changing the configurations of the reconfigurable palm.

- Door opening mechanism for space shuttle: The mechanism shown in figure 1.32 and figure 1.33 can be used in the door opening of a space shuttle.

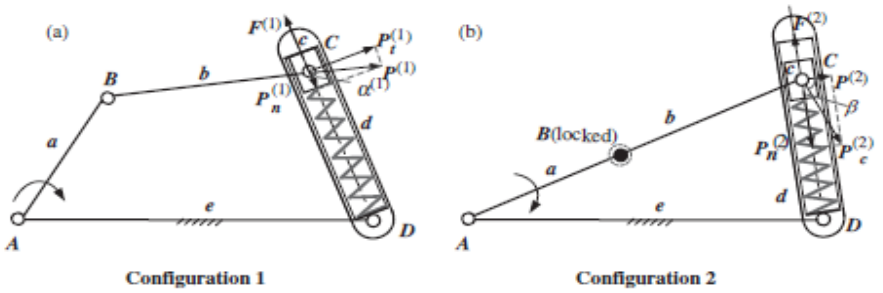

Figure 1.30 Schematic graph of a planar five bar force limit metamorphic mechanism [Zhang et al.,2011a]

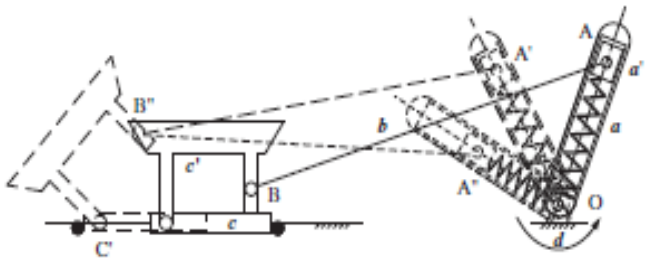

Figure 1.31 Workflow chart of the metamorphic mechanism in all configurations [Zhang et al., 2011b]

- Steel ingot cutting machine: The machine presented in figure 1.24 is used for industrial purposes for cutting steel ingots. There steel ingots are produced by the blast furnace and the industrial blast furnace as well as through various crafting recipes. They are used in a number of rail craft recipes including steel tools, rails, bore heads, etc.

➢ Paper and board packaging:

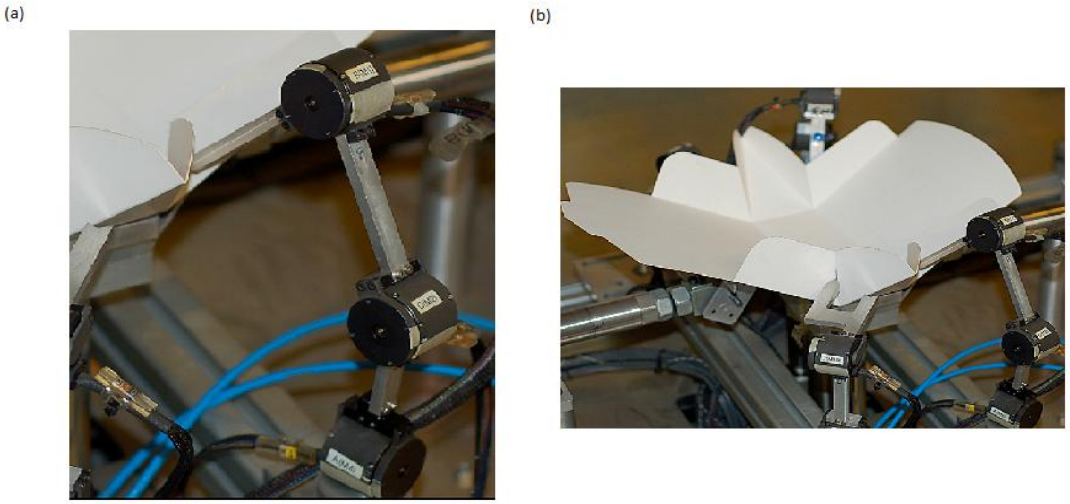

Figure 1.32 (a) Robotic finger for packaging (b) A demonstration [Dai and Caldwell, 2010]

The applications presented above are largely used in the robotic industry due to its versatile reconfiguration motions and configurations.

1.6 Conclusion

This chapter has presented a comprehensive review of morphing techniques in reconfigurable mechanisms and has examined their relationship and existence in the mechanisms to help achieve reconfiguration. Based on mobility and connectivity, the morphing process has been analyzed in terms of topological, geometrical and furcating morphing, each of which has been revealed through literature in its broadness in the field of reconfigurable mechanisms and robots. These morphing techniques have been further related to mechanism type and motion type, and their applications have been identified. Typical reconfigurable joints such as vA joints and rT joints have been illustrated through the review in achieving mechanism reconfiguration. This chapter on bibliographic review has presented a foundation for the study of morphing techniques and metamorphosis in reconfigurable mechanisms.

In this thesis, we focus on furcation morphing. Furcation morphing does not require joint activation or locking. Nevertheless, we show in the following chapters that actuation redundancy is used to control the mechanism to perform multifurcation and switch between several branches.

2 Chapter 2: Structural analysis and geometric modeling of reconfigurable robots: Application to the single-loop eight bar linkage

This second chapter is devoted to the structural synthesis and modeling of reconfigurable robots. The first section presents the objectives and the general perspectives of structural analysis and synthesis. We then recall the formulation and parameters based on TCS method [Gogu, 1996] in order to obtain an expression of the geometric models. The rest of the chapter deals with the application of these methods to a single-loop eight-bar mechanism for its general non-singular configurations.

2.1 Structural analysis of parallel manipulators

Recent advances in research on parallel robots have contributed mainly to expand their potential use to both terrestrial and space applications including areas such as high speed manipulation, material handling, motion platforms, machine tools, medical fields, planetary and underwater exploration [Gogu, 2008a]. Therefore, the need for methodologies devoted to the systematic design of highly performing parallel robots is continually increasing. Structural synthesis is directly related to the preliminary phase of robot design, and represents one of the highly challenging subjects in recent robotics research. [Patel et al., 2012], [Kong and Gosselin, 2007], [Gogu, 2008a], [Gogu, 2009], [Gogu, 2010], [Gogu, 2012], [Gogu, 2014].

2.1.1 Introduction

Mobility is the main structural parameter of a mechanism and also one of the most fundamental concepts in the kinematic and the dynamic modelling of mechanisms. Mobility is used to verify the existence of a mechanism, to indicate the number of independent parameters in the both kinematic and the dynamic models and to determine the number of inputs needed to drive the mechanism. The state of the art in the development of mobility formulae was largely discussed in [Gogu, 2005a]. Earlier works on the mobility of mechanisms go back to the second half of the XIX century to Chebychev [Chebychev, 1869], Sylvester [Sylvester ,1874], Grübler [Grübler 1883,1885], Somov [Somov ,1887] and Hochman [Hochman 1890]. During the XX century, sustained efforts were made to find general methods for the determination of the mobility of any rigid body mechanism. Various formulas and approaches were derived and presented in the literature by Koenigs [Koenigs, 1905], Grübler [Grübler 1916, 1917], Malytsheff [Malytsheff, 1923], Kutzbach [Kutzbach, 1929], Dobrovolski [Dobrovolski 1949,1951], Artobolevski [Artobolevski , 1953], Moroskine [Moroskine 1954,1958] Voinea and Atanasiu [Voinea et al., 1960], Kolchin [Kolchin , 1960], Rossner [Rossner , 1961], Boden [Boden, 1962], Manolescu and Manafu [Manolescu et al., 1963], Ozol [Ozol , 1963], Hunt and Phillips [Hunt et al., 1965], Waldron [Waldron, 1966], Manolescu [Manolescu, 1968], Bagci [Bagci, 1971], Antonescu [Antonescu 1973,1999], Freudenstein and Alizade [Freudenstein et al.,1975], Hunt [Hunt, 1978], Hervé [Hervé 1978a, 1978b], Baker [Baker 1980,1981], Gronowicz [1981] , Davies [Davies 1983a, 1983b, 1983c], Agrawal and Rao [Agrawal et al., 1987a, 1987b, 1987c], Angeles and Gosselin [Angeles et

al., 1988], Dudita and Diaconescu [Dudita et al., 1987], Fanghella and Galletti [Fanghella et al., 1988,1994], Fayet [Fayet 1995a, 1995b, 1995c] Tsai [Tsai, 1999], McCarthy [2000]. Contributions have continued to emerge in the last years: Huang et al. [Huang et al., 2003], Rico and Ravani [Rico et al., 2003a], Rico, Gallardo and Ravani [Rico et al., 2003b].

The major drawback of these approaches is that the mobility cannot be determined quickly without setting up the kinematic model of the mechanism. For this reason, the real and practical value of these approaches is very limited in spite of their valuable theoretical foundations. The challenging and difficult objective of structural synthesis is to find a method to set up the mechanical architecture achieving the required structural parameters. The mechanical architecture is defined by number, type and relative position of the joint axes in the parallel robot. The structural parameters are mobility, connectivity, redundancy and degrees of freedom and the motion-type of the moving platform. Formula for a quick calculation of mobility and structural parameters was proposed by Gogu in 2005 [Gogu, 2005b]. Usually, these structural parameters are easily determined by inspection without need to develop the set of kinematic constraint equations.

In general, parallel manipulators performances are highly dependent on their mechanical architecture, so that structural synthesis becomes the central problem in the preliminary design phase. To synthesize new reconfigurable robots, it is necessary to investigate structural properties of particular mechanisms. Indeed, the mechanism reconfigurability can be highlighted by the changes of its structural parameters. These parameters are determined by using recently developed methods and formulae [Gogu, 2008a].

2.1.2 Structural parameters of a mechanism

A parallel mechanism is a mechanism in which an end-effector is connected to a reference link by $k \geq 2$ structurally independent kinematic chains called limbs or arms [Gogu, 2008a]. In a parallel mechanism, the end-effector and the reference link are usually called moving and reference platforms. They represent the distal links of the parallel mechanism and of each limb as well. The limb can be simple or complex kinematic chain. In a simple limb just monary and binary links exist. They are connected in the kinematic chain by one or two joints. At least one polinary link is combined with monary and binary links in a complex limb in which at least one closed loop exists.

The main structural parameters of a parallel mechanism are associated with mobility, connectivity, redundancy and overconstraint. We recall briefly the meaning of these parameters. More details can be found in [Gogu, 2008a].

IFToMM terminology defines the **mobility or the degree of freedom** as the number of independent coordinates required to define the configuration of a kinematic chain or mechanism. We note that the classical formulae for a quick calculation of mobility, known as Chebychev-Grübler-Kutzbach formulae do not fit many classical mechanisms, recent parallel robots and kinematotropic mechanisms. These formulae have been recently reviewed and their limits have been set up [Gogu, 2005a]. New formulae for quick calculation of the

mobility have been proposed and demonstrated recently via the theory of linear transformations [Gogu 2005b, 2008a].

The **connectivity** between two links of a mechanism represents the number of independent finite and/or infinitesimal displacements allowed by the mechanism between the two links. Limb connectivity is given by the connectivity between the distal links of the limb. The connectivity of a parallel mechanism is given by the connectivity between the characteristic link (end-effector) and the fixed base.

The **number of overconstraints** of a mechanism is given by the difference between the maximum number of joint parameters that could lose their independence in the closed loops, and the number of joint parameters that actually lose their independence in the closed loops.

The structural **redundancy** is given by the difference between the mobility of the parallel mechanism and the connectivity of the end-effector. Redundancy introduces internal mobilities in the limbs. The internal mobilities in a limb are given by the difference between limb mobility and connectivity.

The following formulae have been proposed in [Gogu, 2008a] for the calculation of the structural parameters of a parallel mechanism $F \leftarrow G_1\text{-}G_2\text{-}...\text{-}G_k$ in which the mobile platform $n \equiv n_{Gj}$ is connected to the reference platform $1 \equiv 1_{Gj}$ by k simple and/or complex limbs G_j (1_{Gj}-2_{Gj}-…-n_{Gj}), $j=1,2,…,k$.:

$$M_F = \sum_{j=1}^{p} f_j - r_F \,, \tag{2.1}$$

$$N_F = 6q - r_F \,, \tag{2.2}$$

$$T_F = M_F - S_F \,, \tag{2.3}$$

where,

$$S_{Gj} = dim(R_{Gj}) \,, \tag{2.4}$$

$$S_F = dim(R_F) = dim(R_{G1} \cap R_{G2} \cap ... \cap R_{Gk}) \,, \tag{2.5}$$

$$r_F = \sum_{j=1}^{k} S_{Gj} - S_F + r_l \,, \tag{2.6}$$

$$p = \sum_{j=1}^{k} p_{Gj} \,, \tag{2.7}$$

$$q = p - m + 1, \tag{2.8}$$

and

$$r_l = \sum_{j=1}^{k} r_{Gj} \ . \tag{2.9}$$

The following notations are used in these formulae:
M_F – the mobility (or degree of mobility) of the parallel mechanism F,
N_F - number of overconstraints (degree of overconstraint) of the parallel mechanism F,
T_F – number of structural redundancies (degree of redundancy) of parallel mechanism F,
T_{Gj} – number of structural redundancies (degree of redundancy) of the kinematic chain G_j disconnected from the parallel mechanism F,
R_{Gj} - vector space of relative velocities between the mobile and the reference platforms, n_{Gj} and 1_{Gj}, in the kinematic chain G_j disconnected from the parallel mechanism F,
R_F - vector space of relative velocities between the mobile and the reference platforms, $n \equiv n_{Gj}$ and $1 \equiv 1_{Gj}$, in the parallel mechanism $F \leftarrow G_1\text{-}G_2\text{-}...\text{-}G_k$,
S_{Gj} - connectivity between the mobile and the reference platforms, n_{Gj} and 1_{Gj}, in the kinematic chain G_j disconnected from the parallel mechanism F,
S_F - connectivity between the mobile and the reference platforms $n \equiv n_{Gj}$ and $1 \equiv 1_{Gj}$, in the parallel mechanism $F \leftarrow G_1\text{-}G_2\text{-}...\text{-}G_k$,
p_{Gj} – number of joints of G_j-limb,
p - total number of joints of parallel mechanism F,
m - total number of links in mechanism F including the moving and reference platforms,
q - total number of independent closed loops in the sense of graph theory,
f_j - mobility of the jth joint,
$r_F = r_p + r_l$ - total number of joint parameters that lose their independence in the closed loops of mechanism F,
r_p - total number of joint parameters that lose their independence in the closed loops formed between the limbs of mechanism F.
r_l - number of joint parameters that lose their independence in the closed loops that may exist in the limbs of mechanism F.
r_{Gj} - number of joint parameters that lose their independence in the closed loops that may exist in the loops of limb G_j,
$k = k_1 + k_2$ - total number of limbs of the mechanism F,
k_1 - number of simple limbs of mechanism F,
k_2 - number of complex limbs of mechanisms F.
$Dim(R_{Gi})$ - dimension of the basis of the vector space R_{Gi}.

The key parameters used in Eqs. (2.1)-(2.6) are the basis and the dimension of R_{Gj}. They can be easily obtained by inspection for each limb by identifying the independent motions between the distal link n_{Gj} and 1_{Gj} in the kinematic chain G_j disconnected from the parallel mechanism. An analytical method to compute these parameters has been developed in [Gogu, 2008a] just for verification and for a better understanding of the meaning of these parameters. In this method, the dimension of R_{Gj} is given by the rank of the forward velocity Jacobian J_{Gj} of G_j-limb disconnected from the parallel mechanism, that is $S_{Gj} = dim(R_{Gj}) = rank(J_{Gj})$.

Note 1. Equations (2.1)-(2.9) are valid for any parallel mechanism with structurally independent limbs. Equation (2.7) gives the condition of existence of structurally independent limbs. It indicates that the limbs of the parallel mechanism $F \leftarrow G_1\text{-}G_2\text{-}\ldots G_k$ must be defined in such a way that each joint belongs to just one limb.

Note 2. The intersection in Eq. (2.5) is consistent if vector spaces R_{Gi} are defined by the translational and rotational velocities of the same point belonging to the moving platform with respect to the same reference frame. This point, denoted by H, is called the characteristic point. It must be the point with the most restrictive motions of the moving platform.

Note 3. The connectivity S_F of the moving platform $n \equiv n_{Gj}$ with respect to the reference platform $1 \equiv 1_{Gj}$ in the mechanism $F \leftarrow G_1\text{-}G_2\text{-}\ldots G_k$ is less than or equal to the mobility M_F of mechanism F. In the same way, the connectivity S_{Gj} of the moving platform n_{Gj} with respect to the reference platform 1_{Gj} in limb G_j disconnected from the mechanism F is less than or equal to the mobility M_{Gj} of limb G_j.

Note 4. The basis (R_F) of the vector space R_F of relative velocities between the moving and reference platforms in the mechanism $F \leftarrow G_1\text{-}G_2\text{-}\ldots G_k$ must be valid for any point of the moving platform $n \equiv n_{Gj}$.

Note 5. When there are various ways to choose the bases of the vector spaces R_{Gj} in Eq. (2.4), the bases (R_{Gj}) are selected such that the minimum value of S_F is obtained by Eq. (2.5). By this choice, the result of Eq. (2.1) fits in with the definition of general mobility as the minimum value of the instantaneous mobility. The various bases of the vector spaces R_{Gj} have the same dimension.

We note that the bases of vector spaces R_{Gj} and R_F may contain up to 6 independent velocity vectors $\boldsymbol{v}_x$, $\boldsymbol{v}_y$, $\boldsymbol{v}_z$, $\boldsymbol{\omega}_x$, $\boldsymbol{\omega}_y$, and $\boldsymbol{\omega}_z$. By $\boldsymbol{v}_x$, $\boldsymbol{v}_y$, $\boldsymbol{v}_z$ we denote the independent linear velocities of the characteristic point H of the moving platform and by $\boldsymbol{\omega}_x$, $\boldsymbol{\omega}_y$, $\boldsymbol{\omega}_z$ the independent angular velocities of the moving platform.

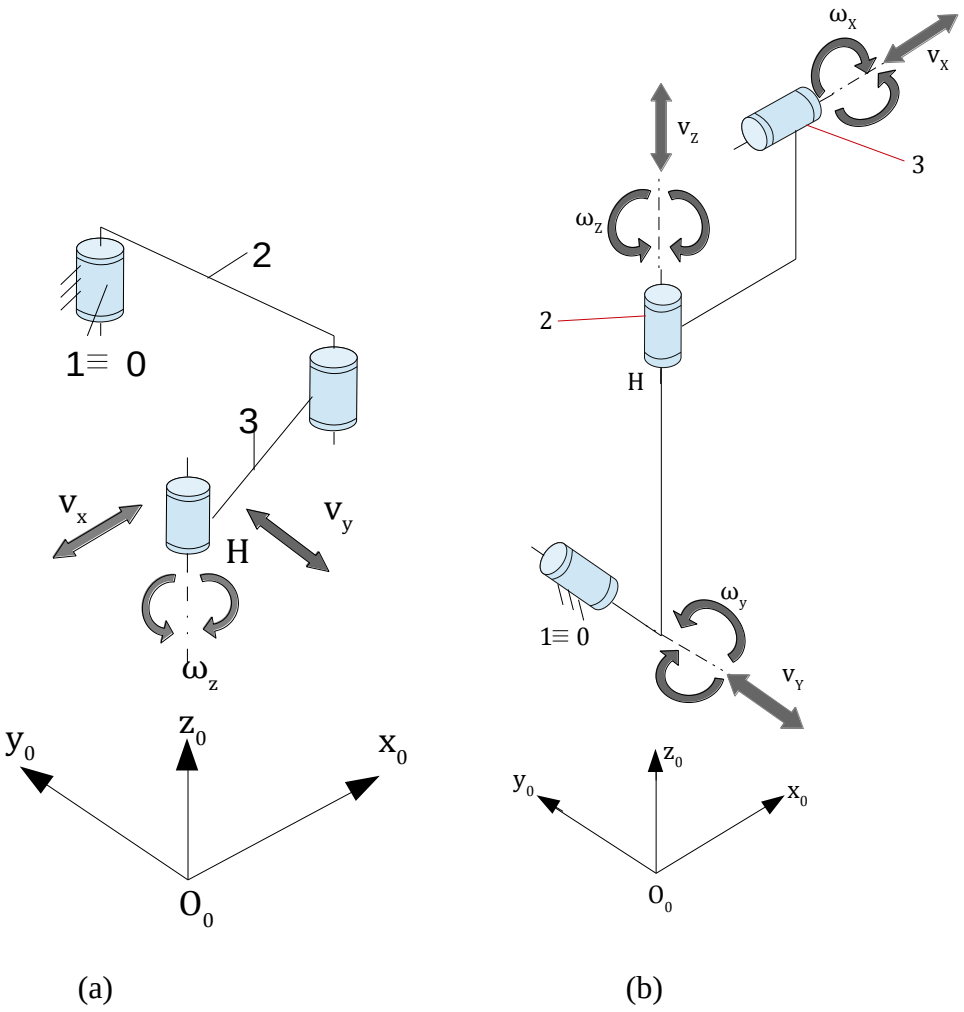

Figure 2.1 Simple open kinematic chain with 3R joints (a) three joint axes are parallel to z-axis (b) three revolute joints with orthogonal axes

For example the basis of vector space R_{Gj} of a planar limb with three revolute joint is always $(R_{Gj})=(\boldsymbol{v}_x,\boldsymbol{v}_y,\boldsymbol{\omega}_z)$ if the three joint axes are parallel to *z*-axis. This is illustrated in figure 2.1 (a) with three simple revolute joints (3R).

For the same dimension S_{Gj}, the basis of vector space R_{Gj} of certain kinematic chains may be defined by different combinations of velocity vectors $\boldsymbol{v}_x$, $\boldsymbol{v}_y$, $\boldsymbol{v}_z$, $\boldsymbol{\omega}_x$, $\boldsymbol{\omega}_y$, and $\boldsymbol{\omega}_z$. For example, in a spatial limb with three revolute joints with orthogonal axes and non zero distance between the joint axes adjacent to the same link, vector space R_{Gj} has always three dimensions, but the basis can be defined by various combination of three out of six vectors $\boldsymbol{v}_x$, $\boldsymbol{v}_y$, $\boldsymbol{v}_z$, $\boldsymbol{\omega}_x$, $\boldsymbol{\omega}_y$, and $\boldsymbol{\omega}_z$. The rotational joint axes of three orthogonal revolute joints are illustrated in figure 2.1 (b).

In these cases, the bases of R_{Gj} in Eq. (2.5) are selected such as the minimum value of S_F is obtained. By this choice, the result of Eq. (2.5) fits in with general mobility definition as the minimum value of the instantaneous mobility in a free of singularity branch. The bases of R_{Gj} giving larger values of S_F are associated with robot singularities.

2.1.3 Conclusion

In this section, we have presented the formulae (2.1) - (2.9) to calculate the main structural parameters of parallel mechanisms. The structural parameters such as mobility, connectivity, structural redundancy, degrees of freedom and motion-type of the moving platform help in setting up the mechanical architecture defined by the number, the type and the relative position of joint axes in the parallel manipulator.

2.2 Geometric modelling of an open loop kinematic chain

This section is devoted to the geometric modeling of robotic open/closed loop kinematic chains. The geometric model helps to represent the configuration of the robot based on joint variables. This section presents a general geometric model for serial robots along with the open loop and closed loop geometric models.

2.2.1 Introduction

The principal methods proposed in the literature for geometric model parameterization and formulations of a robot are presented in [Gogu et al. 1997]. They are Denavit-Hartenberg, Paul, Khalil-Kleifinger, Yih, Sheth-Uicker, Litvin, Megahed and Gogu-Coiffet-Barraco methods. In the context of the geometric modeling, the method of Denavit-Hartenberg [Hartenberg et al. 1964] and its adaptations were most commonly used. However this method includes more number of operations which complicates the calculations. Hence, we have chosen the formalization of Gogu-Coiffet-Barraco which is commonly called as Travelling Coordinate System (TCS method) as its use allows simplification of the calculations and provides more flexible notation [Gogu et al. 1997]. It is considered that initially the type of kinematic pairs (axis of rotation or translation) and the relative position of the different axes (perpendicular or parallel) are known.

We will first recall the Travelling Coordinate System method [Gogu et al. 1997] and the notations used in the definition of the geometric and kinematic models.

2.2.2 Travelling Coordinate System

The objective of this method is to express at each moment, the relative positions and orientations of the links of an open kinematic chain according to joint variables. A coordinate system which travels over the kinematic chain of the robot starting from the reference link to the final link is considered. The coordinate systems attached to the links of the robot are the intermediate positions of the coordinate system travelling from the reference frame to the end-effector frame. The TCS glides over the links of the kinematic chain of the robot and carries out the relative displacement of rotation and of translation. For TCS method, a hypothesis is made i.e. the axes of the kinematic pairs of rotation or of translation are supposed to be orthogonal or parallel to each other. We fix on to this hypothesis which is valid for a majority of robots and most commonly for parallel robots. These are various criterions in the formulation of the travelling coordinate system. A detailed description with examples illustrating these criterions has been dealt in [Gogu and Coiffet, 1996] and [Gogu et al., 1997].

The two dimensional parameters which are considered for each kinematic chain *i* are:

- a_i called as eccentricity which is the distance defined on the axes of the joint (*i*-1, *i*)
- b_i called as the length of the element *i*, is the distance defined on the direction of the common normal to the axes of joints (*i*-1, *i*) and (*i*, *i*+1).

These parameters are illustrated with two revolute joints in figure 2.2 as shown below.

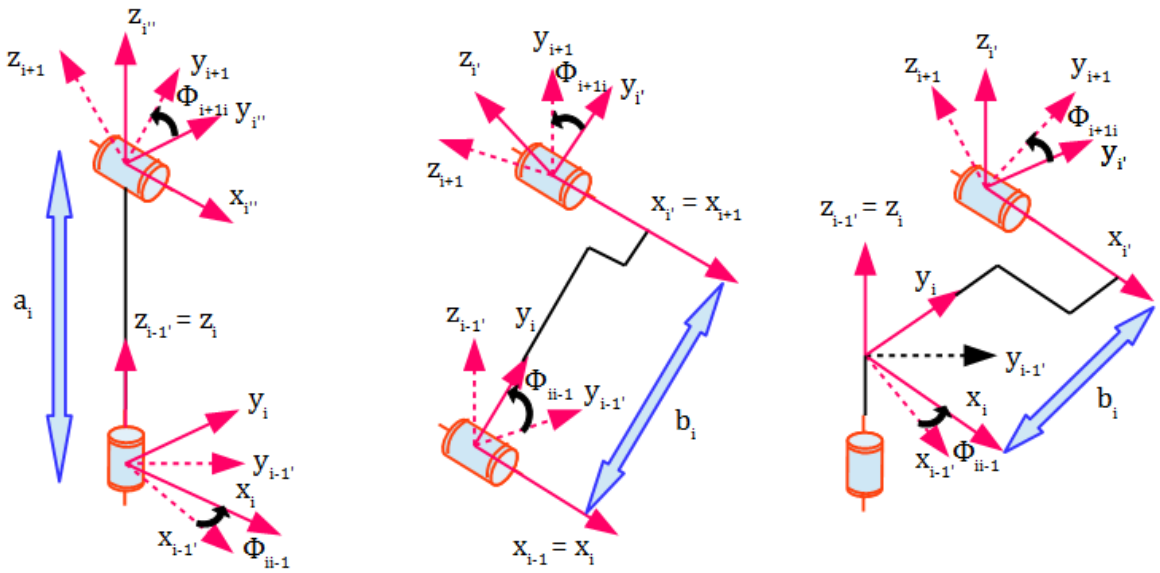

Figure 2.2 Example of modeling associated with TCS method illustrating the lengths a_i and b_i

To explain the angle of rotation between the frames, let us consider the passage of TCS of two elements '*m*' and '*n*' with a kinematic pair. These elements undergo a finite displacement of rotation/translation around the axes of the TCS superposed by the axes of the pair . The finite displacement of rotation is represented by $\emptyset_{nm}$ and the finite displacement of translation is denoted by d_{nm}.

Note:

The indices *nm*, in this order, indicates the relative displacement of element *n* with respect to element m, produced by the kinematic pair (*m*-*n*).

The circular permutation rule helps us to define the joint axis. By making a product of the translational and rotation homogeneous matrices, we obtain the matrix describing the configuration of each characteristic frame of the mechanism relatively to the previous joint.

If the axes of the adjacent joints of the element *i* are parallel, then the two joints (*i*-1, *i*) and (*i*, *i*+1) will have the same axis such as x, y or z axis of TCS. We follow the circular permutation rule to denote the direction of the common normal to the joints as in figure 2.3.

Link axis (*i-1*, *i*)	Link axis (*i*, *i+1*)	Common normal
x	*x*	*y*
y	*y*	*z*
z	*z*	*x*

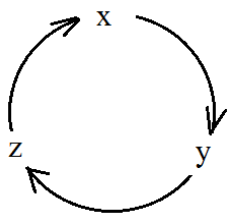

Figure 2.3 Joint axes (i-1, i) and (i, i+1) are parallel

If the axes of the adjacent joints are perpendicular, the axes of TCS carried out by the joint (*i*, *i*+1) is obtained by the circular permutation with respect to the axes of TCS carried out by (*i*-1, *i*). This rule is illustrated in figure 2.4 along with the direction of the common normal.

Link axis (*i-1*, *i*)	Link axis (*i*, *i+1*)	Common normal
x	*y*	*z*
y	*z*	*x*
z	*x*	*y*

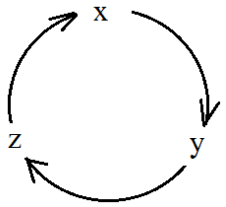

Figure 2.4 Joint axes (i-1, i) and (i, i+1) are perpendicular

2.2.3 Geometric modelling of a robot using TCS method

In the direct geometric model, the finite displacements of the joints are independent variables, the position and orientation of the robot elements are the dependent parameters. We need also to compute the geometric model to know the location of the robot links relative to each other. The solution of the direct geometric model is obtained by the multiplication of the homogeneous operators which modelize the elements and the finite displacements in the joints.

We can obtain the position and orientation of the final frame with respect to the reference frame, by the matrix product,

$$A_{0n} = \prod_{i=1}^{n} A_{i-1,i} \tag{2.10}$$

where,

$A_{i-1,i}$ is a 4x4 matrix which express the position and orientation of the frame *i* with respect to frame *i*-1. Each operator $A_{i-1,i}$ $(i + 1,2, \dots, n)$ in its structure must have one and just one independent variable defining the relative displacement in the joint $(i - 1, i)$.

$$A_{i-1,i} = \begin{bmatrix} 1 & 0 & 0 & 0 \\ x_{TCS} & a_{11} & a_{12} & a_{13} \\ y_{TCS} & a_{21} & a_{22} & a_{23} \\ z_{TCS} & a_{31} & a_{32} & a_{33} \end{bmatrix}$$

The solution for the inverse geometric model expresses the final displacements in the kinematic pairs in function of the position and the orientation of the final element of the robot. The mechanical architecture defined by number, type and relative position of joint axes of the robot and the geometrical dimensions of the kinematic elements are the inputs.

The solutions of the direct and inverse geometric model involving the angle of rotation of each joint and the dimensional parameters of each link will be implemented in the reconfigurable eight-bar mechanism. This application is followed in section 2.3.

2.2.4 Calculation of the forward velocity Jacobian of the open kinematic chains associated to simple limbs

Jacobian matrices are a useful tool, and commonly used throughout robotics and control theory. Basically, a Jacobian defines the kinematic relationship between two different representations of a system. For example, if we have a 2-link robotic arm, there are two obvious ways to describe its current position: 1.) the end-effector position and orientation, and 2.) as the set of joint angles (which we will denote q). The Jacobian for this system relates how movement of the elements of q causes movement of the elements of $v_x, v_y, v_z, \omega_x, \omega_y, \omega_z$.

Formally, a Jacobian is given by:

$$\begin{bmatrix} v_x \\ v_y \\ v_z \\ \omega_x \\ \omega_y \\ \omega_z \end{bmatrix} = J\,\dot{\boldsymbol{q}}$$

This tells us that the end-effector velocity is equal to the Jacobian, J, multiplied by the joint angle velocity.

Mathematically, the forward geometric equations define a function between the cartesian positions and orientations and joint positions. The velocity relationships are then determined by the Jacobian of this function. The Jacobian is a matrix-valued function and can be thought of as the vector version of the ordinary derivative of a scalar function. This Jacobian or Jacobian matrix is one of the most important quantities in the analysis of the possible velocity bases(R_G), connectivity (S_G) and also for the control of robot motion. Also Jacobian matrices are used in every aspect of robotic manipulation: in the planning and execution of smooth trajectories, in the determination of singular configurations, in the derivation of the dynamic equations of motion, and in the transformation of forces and torques from the end-effector to the manipulator joints.

The kinematic model is formulated for the limbs associated with the eight bar reconfigurable single loop parallel mechanism using the joint angles and the homogeneous matrix. For the associated open chain, the relationship between the operational velocity, Jacobian matrix and joint velocities are as follows:

$$\begin{bmatrix} v_x \\ v_y \\ v_z \\ \omega_x \\ \omega_y \\ \omega_z \end{bmatrix} = \begin{bmatrix} {}^{p}J_h \end{bmatrix} \begin{bmatrix} \dot{\phi}_{10} \\ \dot{\phi}_{21} \\ \dot{\phi}_{32} \\ \dot{\phi}_{43} \\ \dot{\phi}_{87} \\ \dot{\phi}_{76} \\ \dot{\phi}_{65} \\ \dot{\phi}_{54} \end{bmatrix}$$

The calculation of Jacobian is done using the formulation proposed by Gogu [Gogu, 1996, 1997]. We use the formulation of TCS and the homogeneous matrix A_{0n} to calculate the Jacobian. We can express the Jacobian matrix in the system of coordinates *e* situated in any point of any element of the robot. This method implies symbolic calculation of the Jacobian matrix by using the components of the homogeneous matrix from the direct geometric model. One of the advantages of using this method is that the number of mathematical operators necessary for the symbolic calculation of the Jacobian matrix is much diminished when compared to the other existing methods in the literature.

The eight bar reconfigurable mechanism comprises two simple limbs. Using this method, the 6x4 Jacobian matrix is calculated for each limb and hence the rank of this matrix is calculated. For the general configuration of the mechanism, a rank of 4 for each calculated Jacobian is necessary. Henceforth, we select all the 4x4 Jacobian submatrices of rank 4 and systematize the operational vector bases corresponding to their velocities. We then calculate (R_F) which is the intersection between vector spaces of each limb. The choice of the vector space should respect a criterion presented previously in Note 5. While there are various ways to choose the basis for the operational spaces, the bases of R_{Gi} are selected such as the minimum value of S_F is obtained. By this choice, the calculation of mobility sets up a general mobility as the minimum value of the instantaneous mobility. Respecting this criterion, (R_F) is valid for a general eight-bar reconfigurable mechanism. From Table 2.1, we can see the various possible combinations of the vector spaces giving $S_F=2$.

Table 2.1 Various bases of vector space R_F

$(\boldsymbol{R_{G1}})$	$(\boldsymbol{R_{G2}})$	$(\boldsymbol{R_F})$	$\boldsymbol{S_F}$
$(v_z, \omega_x, \omega_y, \omega_z)$	$(v_x, v_y, \omega_y, \omega_z)$	(ω_y, ω_z)	2
$(v_z, \omega_x, \omega_y, \omega_z)$	$(v_x, v_y, \omega_x, \omega_z)$	(ω_x, ω_z)	2
$(v_z, \omega_x, \omega_y, \omega_z)$	$(v_x, v_y, \omega_x, \omega_y)$	(ω_x, ω_y)	2

$(v_z, \omega_x, \omega_y, \omega_z)$	$(v_x, v_y, v_z, \omega_z)$	(v_z, ω_z)	2
$(v_z, \omega_x, \omega_y, \omega_z)$	$(v_x, v_y, v_z, \omega_y)$	(v_z, ω_y)	2
$(v_z, \omega_x, \omega_y, \omega_z)$	$(v_x, v_y, v_z, \omega_x)$	(v_z, ω_x)	2
$(v_y, \omega_x, \omega_y, \omega_z)$	$(v_x, v_z, \omega_y, \omega_z)$	(ω_y, ω_z)	2
$(v_y, \omega_x, \omega_y, \omega_z)$	$(v_x, v_z, \omega_x, \omega_z)$	(ω_x, ω_z)	2
$(v_y, \omega_x, \omega_y, \omega_z)$	$(v_x, v_z, \omega_x, \omega_y)$	(ω_x, ω_y)	2
$(v_y, \omega_x, \omega_y, \omega_z)$	$(v_x, v_y, v_z, \omega_z)$	(v_y, ω_z)	2
$(v_y, \omega_x, \omega_y, \omega_z)$	$(v_x, v_y, v_z, \omega_y)$	(v_y, ω_y)	2
$(v_y, \omega_x, \omega_y, \omega_z)$	$(v_x, v_y, v_z, \omega_x)$	(v_y, ω_x)	2
$(v_y, v_z, \omega_y, \omega_z)$	$(v_x, \omega_x, \omega_y, \omega_z)$	(ω_y, ω_z)	2
$(v_y, v_z, \omega_y, \omega_z)$	$(v_x, v_z, \omega_x, \omega_z)$	(v_z, ω_z)	2
$(v_y, v_z, \omega_y, \omega_z)$	$(v_x, v_z, \omega_x, \omega_y)$	(v_z, ω_y)	2
$(v_y, v_z, \omega_y, \omega_z)$	$(v_x, v_y, v_z, \omega_y)$	(v_y, ω_y)	2
$(v_y, v_z, \omega_y, \omega_z)$	$(v_x, v_y, v_z, \omega_x)$	(v_y, v_z)	2
$(v_y, v_z, \omega_x, \omega_z)$	$(v_x, \omega_x, \omega_y, \omega_z)$	(ω_x, ω_z)	2
$(v_y, v_z, \omega_x, \omega_z)$	$(v_x, v_z, \omega_y, \omega_z)$	(v_z, ω_z)	2
$(v_y, v_z, \omega_x, \omega_z)$	$(v_x, v_z, \omega_x, \omega_y)$	(v_z, ω_x)	2
$(v_y, v_z, \omega_x, \omega_z)$	$(v_x, v_y, \omega_y, \omega_z)$	(v_y, ω_z)	2
$(v_y, v_z, \omega_x, \omega_z)$	$(v_x, v_y, \omega_x, \omega_y)$	(v_y, ω_x)	2
$(v_y, v_z, \omega_x, \omega_z)$	$(v_x, v_y, v_z, \omega_y)$	(v_y, v_z)	2
$(v_y, v_z, \omega_x, \omega_y)$	$(v_x, \omega_x, \omega_y, \omega_z)$	(ω_x, ω_y)	2
$(v_y, v_z, \omega_x, \omega_y)$	$(v_x, v_z, \omega_y, \omega_z)$	(v_z, ω_y)	2
$(v_y, v_z, \omega_x, \omega_y)$	$(v_x, v_z, \omega_x, \omega_z)$	(v_z, ω_x)	2
$(v_y, v_z, \omega_x, \omega_y)$	$(v_x, v_y, \omega_y, \omega_z)$	(v_y, ω_y)	2
$(v_y, v_z, \omega_x, \omega_y)$	$(v_x, v_y, \omega_x, \omega_z)$	(v_y, ω_x)	2
$(v_y, v_z, \omega_x, \omega_y)$	$(v_x, v_y, v_z, \omega_z)$	(v_y, v_z)	2
$(v_x, \omega_x, \omega_y, \omega_z)$	$(v_y, v_z, \omega_y, \omega_z)$	(ω_y, ω_z)	2
$(v_x, \omega_x, \omega_y, \omega_z)$	$(v_y, v_z, \omega_x, \omega_z)$	(ω_x, ω_z)	2
$(v_x, \omega_x, \omega_y, \omega_z)$	$(v_y, v_z, \omega_x, \omega_y)$	(ω_x, ω_y)	2
$(v_x, \omega_x, \omega_y, \omega_z)$	$(v_x, v_y, v_z, \omega_z)$	(v_x, ω_z)	2
$(v_x, \omega_x, \omega_y, \omega_z)$	$(v_x, v_y, v_z, \omega_y)$	(v_x, ω_y)	2
$(v_x, \omega_x, \omega_y, \omega_z)$	$(v_x, v_y, v_z, \omega_x)$	(v_x, ω_x)	2
$(v_x, v_z, \omega_y, \omega_z)$	$(v_y, \omega_x, \omega_y, \omega_z)$	(ω_y, ω_z)	2
$(v_x, v_z, \omega_y, \omega_z)$	$(v_y, v_z, \omega_x, \omega_z)$	(v_z, ω_z)	2
$(v_x, v_z, \omega_y, \omega_z)$	$(v_y, v_z, \omega_x, \omega_y)$	(v_z, ω_y)	2
$(v_x, v_z, \omega_y, \omega_z)$	$(v_x, v_y, \omega_x, \omega_z)$	(v_x, ω_z)	2
$(v_x, v_z, \omega_y, \omega_z)$	$(v_x, v_y, \omega_x, \omega_y)$	(v_x, ω_y)	2
$(v_x, v_z, \omega_y, \omega_z)$	$(v_x, v_y, v_z, \omega_x)$	(v_x, v_z)	2
$(v_x, v_z, \omega_x, \omega_z)$	$(v_y, \omega_x, \omega_y, \omega_z)$	(ω_x, ω_z)	2
$(v_x, v_z, \omega_x, \omega_z)$	$(v_y, v_z, \omega_y, \omega_z)$	(v_z, ω_z)	2
$(v_x, v_z, \omega_x, \omega_z)$	$(v_y, v_z, \omega_x, \omega_y)$	(v_z, ω_x)	2

$(v_x, v_z, \omega_x, \omega_z)$	$(v_x, v_y, \omega_y, \omega_z)$	(v_x, ω_z)	2
$(v_x, v_z, \omega_x, \omega_z)$	$(v_x, v_y, \omega_x, \omega_y)$	(v_x, ω_x)	2
$(v_x, v_z, \omega_x, \omega_z)$	$(v_x, v_y, v_z, \omega_y)$	(v_x, v_z)	2
$(v_x, v_z, \omega_x, \omega_y)$	$(v_y, \omega_x, \omega_y, \omega_z)$	(ω_x, ω_y)	2
$(v_x, v_z, \omega_x, \omega_y)$	$(v_y, v_z, \omega_y, \omega_z)$	(v_z, ω_y)	2
$(v_x, v_z, \omega_x, \omega_y)$	$(v_y, v_z, \omega_x, \omega_z)$	(v_z, ω_x)	2
$(v_x, v_z, \omega_x, \omega_y)$	$(v_x, v_y, \omega_y, \omega_z)$	(v_x, ω_y)	2
$(v_x, v_z, \omega_x, \omega_y)$	$(v_x, v_y, \omega_x, \omega_z)$	(v_x, ω_x)	2
$(v_x, v_z, \omega_x, \omega_y)$	$(v_x, v_y, v_z, \omega_z)$	(v_x, v_z)	2
$(v_x, v_y, \omega_y, \omega_z)$	$(v_z, \omega_x, \omega_y, \omega_z)$	(ω_y, ω_z)	2
$(v_x, v_y, \omega_y, \omega_z)$	$(v_y, v_z, \omega_x, \omega_z)$	(v_y, ω_z)	2
$(v_x, v_y, \omega_y, \omega_z)$	$(v_y, v_z, \omega_x, \omega_y)$	(v_y, ω_y)	2
$(v_x, v_y, \omega_y, \omega_z)$	$(v_x, v_z, \omega_x, \omega_z)$	(v_x, ω_z)	2
$(v_x, v_y, \omega_y, \omega_z)$	$(v_x, v_z, \omega_x, \omega_y)$	(v_x, ω_y)	2
$(v_x, v_y, \omega_y, \omega_z)$	$(v_x, v_y, v_z, \omega_x)$	(v_x, v_y)	2
$(v_x, v_y, \omega_x, \omega_z)$	$(v_z, \omega_x, \omega_y, \omega_z)$	(ω_x, ω_z)	2
$(v_x, v_y, \omega_x, \omega_z)$	$(v_y, v_z, \omega_y, \omega_z)$	(v_y, ω_z)	2
$(v_x, v_y, \omega_x, \omega_z)$	$(v_y, v_z, \omega_x, \omega_y)$	(v_y, ω_x)	2
$(v_x, v_y, \omega_x, \omega_z)$	$(v_x, v_z, \omega_y, \omega_z)$	(v_x, ω_z)	2
$(v_x, v_y, \omega_x, \omega_z)$	$(v_x, v_z, \omega_x, \omega_y)$	(v_x, ω_x)	2
$(v_x, v_y, \omega_x, \omega_z)$	$(v_x, v_y, v_z, \omega_y)$	(v_x, v_y)	2
$(v_x, v_y, \omega_x, \omega_y)$	$(v_z, \omega_x, \omega_y, \omega_z)$	(ω_x, ω_y)	2
$(v_x, v_y, \omega_x, \omega_y)$	$(v_y, v_z, \omega_y, \omega_z)$	(v_y, ω_y)	2
$(v_x, v_y, \omega_x, \omega_y)$	$(v_y, v_z, \omega_x, \omega_z)$	(v_y, ω_x)	2
$(v_x, v_y, \omega_x, \omega_y)$	$(v_x, v_z, \omega_y, \omega_z)$	(v_x, ω_y)	2
$(v_x, v_y, \omega_x, \omega_y)$	$(v_x, v_z, \omega_x, \omega_z)$	(v_x, ω_x)	2
$(v_x, v_y, \omega_x, \omega_y)$	$(v_x, v_y, v_z, \omega_z)$	(v_x, v_y)	2
$(v_x, v_y, v_z, \omega_z)$	$(v_z, \omega_x, \omega_y, \omega_z)$	(v_z, ω_z)	2
$(v_x, v_y, v_z, \omega_z)$	$(v_y, \omega_x, \omega_y, \omega_z)$	(v_y, ω_z)	2
$(v_x, v_y, v_z, \omega_z)$	$(v_y, v_z, \omega_y, \omega_z)$	(v_y, ω_z)	2
$(v_x, v_y, v_z, \omega_z)$	$(v_y, v_z, \omega_x, \omega_y)$	(v_y, v_z)	2
$(v_x, v_y, v_z, \omega_z)$	$(v_x, \omega_x, \omega_y, \omega_z)$	(v_x, ω_z)	2
$(v_x, v_y, v_z, \omega_z)$	$(v_x, v_z, \omega_x, \omega_y)$	(v_x, ω_z)	2
$(v_x, v_y, v_z, \omega_z)$	$(v_x, v_y, \omega_x, \omega_y)$	(v_x, v_y)	2
$(v_x, v_y, v_z, \omega_y)$	$(v_z, \omega_x, \omega_y, \omega_z)$	(v_z, ω_y)	2
$(v_x, v_y, v_z, \omega_y)$	$(v_y, \omega_x, \omega_y, \omega_z)$	(v_y, ω_y)	2
$(v_x, v_y, v_z, \omega_y)$	$(v_y, v_z, \omega_y, \omega_z)$	(v_y, ω_y)	2
$(v_x, v_y, v_z, \omega_y)$	$(v_y, v_z, \omega_x, \omega_z)$	(v_y, v_z)	2
$(v_x, v_y, v_z, \omega_y)$	$(v_x, \omega_x, \omega_y, \omega_z)$	(v_x, ω_y)	2
$(v_x, v_y, v_z, \omega_y)$	$(v_x, v_z, \omega_x, \omega_z)$	(v_x, v_z)	2

$(v_x, v_y, v_z, \omega_y)$	$(v_x, v_y, \omega_x, \omega_z)$	(v_x, v_y)	2
$(v_x, v_y, v_z, \omega_x)$	$(v_z, \omega_x, \omega_y, \omega_z)$	(v_z, ω_x)	2
$(v_x, v_y, v_z, \omega_x)$	$(v_y, \omega_x, \omega_y, \omega_z)$	(v_y, ω_x)	2
$(v_x, v_y, v_z, \omega_x)$	$(v_y, v_z, \omega_y, \omega_z)$	(v_y, v_z)	2
$(v_x, v_y, v_z, \omega_x)$	$(v_x, \omega_x, \omega_y, \omega_z)$	(v_x, ω_x)	2
$(v_x, v_y, v_z, \omega_x)$	$(v_x, v_z, \omega_y, \omega_z)$	(v_x, v_z)	2
$(v_x, v_y, v_z, \omega_x)$	$(v_x, v_y, \omega_y, \omega_z)$	(v_x, v_y)	2

Table 2.2 Direct Kinematic model for each limb

The table below illustrates the direct kinematic model for one solution of the vector space for each limb.

Direct kinematic model of G_1	$(\boldsymbol{R_{G1}})$	**Direct kinematic model of G_2**	$(\boldsymbol{R_{G2}})$
$\begin{bmatrix} v_z \\ \omega_x \\ \omega_y \\ \omega_z \end{bmatrix} = [J_{G_1}]_{4x4} \begin{bmatrix} \dot{\phi}_{10} \\ \dot{\phi}_{21} \\ \dot{\phi}_{32} \\ \dot{\phi}_{43} \end{bmatrix}$	$(v_z, \omega_x, \omega_y, \omega_z)$	$\begin{bmatrix} v_x \\ v_y \\ \omega_y \\ \omega_z \end{bmatrix} = [J_{G_2}]_{4x4} \begin{bmatrix} \dot{\phi}_{87} \\ \dot{\phi}_{76} \\ \dot{\phi}_{65} \\ \dot{\phi}_{54} \end{bmatrix}$	$(v_x, v_y, \omega_y, \omega_z)$

2.3 Analysis of an eight-bar linkage in a general configuration

A bibliographic study was made on several reconfigurable mechanisms discussed in the literature in chapter 1. Out of all those, we have chosen to focus on the single-loop eight-bar linkage. In fact, for a special design we propose for this mechanism, we have detected numerous remarkable kinematic properties in relation with reconfigurability. In the forthcoming sections, we undertake a complete analysis of this mechanism in order to exhibit all these properties. Gogu's formulae and the TCS method have been used to carry out the structural analysis and the geometric modeling of this special eight-bar mechanism in its general configuration.

2.3.1 Introduction and description of the special eight-bar linkage

A single-loop eight bar linkage has two degrees of freedom in its general configuration. A particular design of this mechanism with alternate orthogonal and parallel joint axes and symmetric lengths exhibits remarkable properties of reconfiguration [Aimedee et al., 2015]. The mechanism has concurrent axis where two revolute joints intersect each other making the square shape with four common points of intersection. Hence we can coin this concurrency and say the eight-bar mechanism to be a quadric-symmetric mechanism. This mechanism is a modified version of the eight-bar mechanisms presented by Wei and Dai, 2014 [Wei and Dai, 2014] and Zhang et al., 2011[Zhang et al., 2011a].

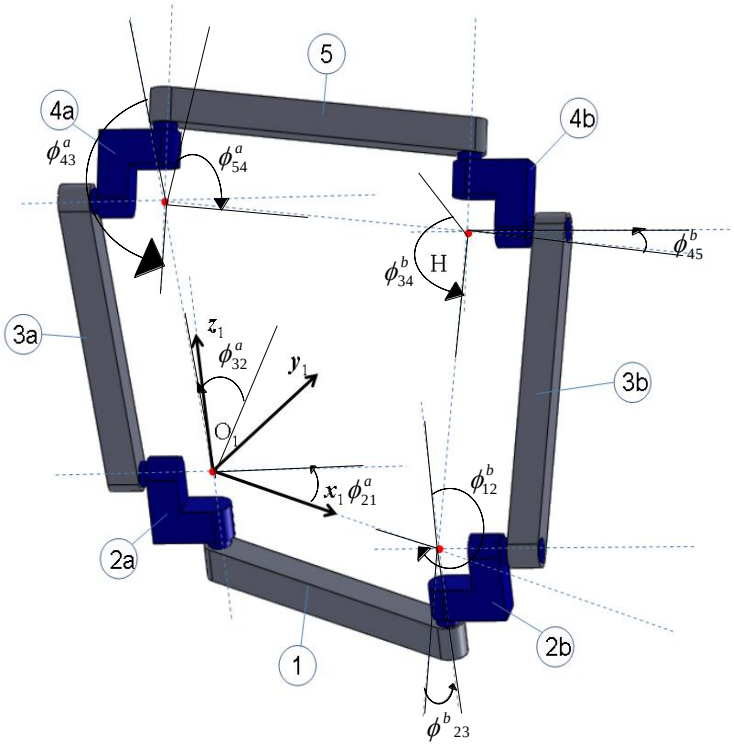

Figure 2.5 Single loop eight-bar mechanism with orthogonal/ parallel axes in a non-singular configuration

2.3.2 Structural analysis of the eight-bar linkage

In this section, we illustrate the application of the formulae (2.1)-(2.9) to calculate the global mobility in a non-singular configuration of the reconfigurable single-loop eight-bar mechanism presented in Figure 2.5. The revolute joints adjacent to the eight links of the mechanism have parallel or orthogonal axes. The mechanism can be considered as a parallel mechanism in which the distal link 5 is connected to the reference link 1 by two simple 4R limbs of type $R \perp R || R \perp R$, where R denotes the revolute joint, $\perp$ and $||$ the perpendicular and parallel position of joint axes. Links 1, 5, 3_a and 3_b have the same length. Links 2_a, 2_b, 4_a and 4_b have also the same geometric configuration and dimensions. The axes of the revolute joints adjacent to reference link 1 are parallel, and the axes of the revolute joints adjacent to the moving platform 5 are also parallel. No closed loops exist inside a limb, that is $r_l=0$. This linkage is called single-loop eight-bar mechanism with orthogonal/parallel axes. To simplify the notations of the links e_{Gj} ($j=1$, 2, and $e=1,2,...5$) by avoiding the double index in Figure 2.5 we have denoted by e_a the links belonging to limb G_1 ($e_a \equiv e_{G1}$) and by e_b, the links of limb G_2 ($e_b \equiv e_{G2}$). As we have mentioned, the distal links 1 and 5 belong to the two limbs ($1 \equiv 1_a \equiv 1_b$ and $5 \equiv 5_a \equiv 5_b$).

In a non-singular configuration the eight-bar mechanism has the following structural parameters:

Table 2.3 Structural parameters of the eight bar reconfigurable mechanism:

No.	Structural parameter	Notations	Solution
1	m	total number of links including the fixed base	8
2	p_1	number of joints in limb 1	4
3	p_2	number of joints in limb 2	4
4	p	total number of joints in the parallel mechanism	8
5	q	number of independent closed loops in the parallel mechanism	1
6	k_1	number of simple limbs of mechanism	2
7	k_2	number of complex limbs of mechanisms	0
8	k	total number of limbs of mechanism	2
9	(R_{G1})	vector space of relative velocities between the mobile and the reference platforms, n_{Ga} and 1_{Ga}, in the kinematic chain G_a disconnected from the parallel mechanism	See Table 2.1
10	(R_{G2})	vector space of relative velocities between the mobile and the reference platforms, n_{Gb} and 1_{Gb}, in the kinematic chain G_b disconnected from the parallel mechanism	See Table 2.1
11	$S_{G1}=S_{G2}$	connectivity between the mobile and the reference platforms, n_{Gj} and 1_{Gj}, in the kinematic chain G_j disconnected from the parallel mechanism F,	4
12	$r_{G1}=r_{G2}$	number of joint parameters that lose their independence in the closed loops that may exist in the loops of limb G_a and G_b	0
13	$M_{G1}=M_{G2}$	mobility of kinematic chains associated with G_a and G_b	4
14	(R_F)	vector space of relative velocities between the mobile and the reference platforms, $n \equiv n_{Gj}$ and $1 \equiv 1_{Gj}$,	See Table 2.1
15	S_F	connectivity between the mobile and the reference platforms $n \equiv n_{Gj}$ and $1 \equiv 1_{Gj}$, in the parallel mechanism in the parallel mechanism	2
16	r_l	number of joint parameters that lose their independence in the closed loops that may exist in the limbs of mechanism	0
17	r_F	total number of joint parameters that lose their independence in the closed loops of mechanism	6
18	M_F	mobility (or degree of mobility) of parallel mechanism	2
19	N_F	number of overconstraints (degree of overconstraint) of parallel mechanism	0
20	$T_{G1}=T_{G2}$	number of structural redundancies (degree of redundancy) of the kinematic chains G_a and G_b disconnected from the parallel mechanism	0

21	T_F	number of structural redundancies (degree of redundancy) of parallel mechanism	0
22	$\sum_{j=1}^{p1} f_j$	total degree of mobility of the joints in limb 1	4
23	$\sum_{j=1}^{p2} f_j$	total degree of mobility of the joints in limb 2	4
24	$\sum_{j=1}^{p} f_j$	total degree of mobility of the joints in the mechanism	8

The joint arrangement and structural parameters of the solutions presented in figure 2.5 are systematized in Table 2.2. From table 2.2, we can observe that the mechanism has only simple limbs (k_1=1) with one degrees of freedom revolute joints. The mechanism has eight revolute joints in two simple limbs consisting of four revolute joints in each limb. The eight bar reconfigurable mechanism has two degrees of freedom in a general non-singular configuration with six joint parameters that lose their independence in the closed loops of mechanism. Since there are no closed loops existing in the simple limbs of the mechanism, r_l =0. The basis of the vector space R_F can be defined by any combination of two independent translational velocities and/or two independent rotational velocities as presented in Table 2.1. The connectivity and the bases of the vector spaces presented in this table are determined by using the rank and the corresponding submatrices of the Jacobian matrices of the two open kinematic chains associated to the simple limbs of the parallel mechanism as presented in Annex II

2.3.3 Parameterization of the eight-bar linkage using Travelling Coordinate System

The schematic diagram of the eight-bar linkage with its origin and the length of the elements of each link are represented in figure 2.6. One of the main characteristic of this mechanism is that the lengths $b_2 = b_4 = b_6 = b_8$. For the eight-bar mechanism, we use the TCS parameters to determine the position and orientation of the characteristic frames attached to each link. The notation below shows the axis of rotation for each revolute joint with parallel and orthogonal axes in the associated open loop kinematic chain obtained by splitting the reference link.

$$R^z \perp R^x // R^x \perp R^y // R^y \perp R^z // R^z \perp R^x$$

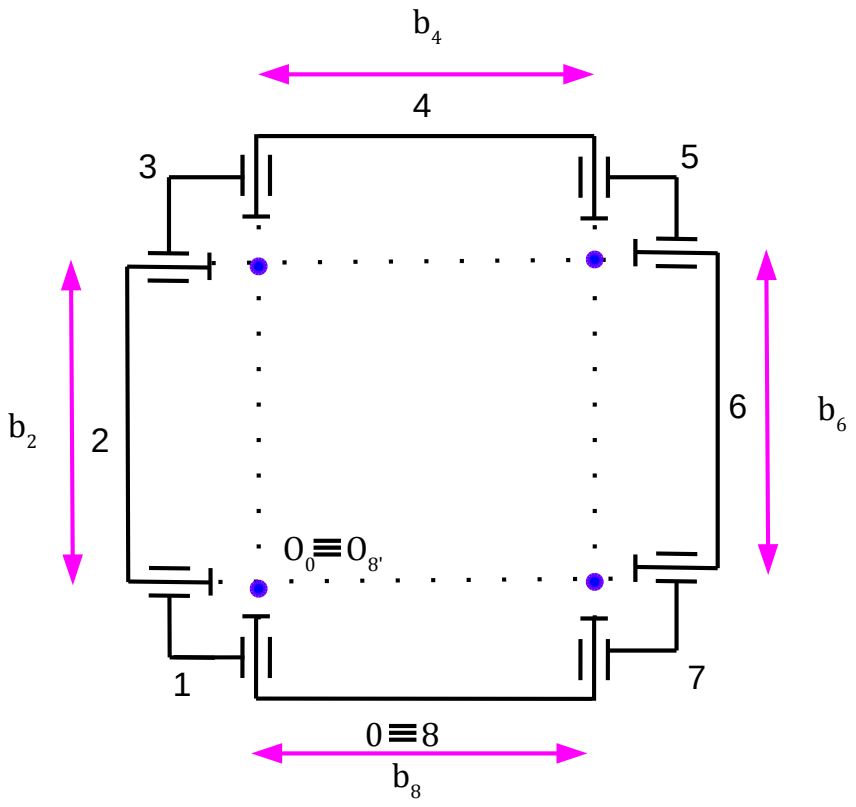

Figure 2.6 Schematic diagram of eight bar linkage

2.3.4 Geometric modeling of the eight-bar linkage

The solution of the direct geometric model of the associated open loop is obtained by the multiplication of the homogeneous operators such asA_{01}, A_{12}, A_{23}, A_{34}, A_{45}, A_{56}, A_{67}, A_{78} which modelize the elements and the finite displacements in the joints. The homogeneous operators are defined as follows:

$$A_{01} = \mathrm{R}^{z}_{01}$$

$$A_{12} = \mathrm{R}^{x}_{12}\,\mathrm{T}^{y}_{22'}$$

$$A_{23} = \mathrm{R}^{x}_{2',3}$$

$$A_{34} = \mathrm{R}^{y}_{34}\,\mathrm{T}^{z}_{44'}$$

$$A_{45} = \mathrm{R}^{y}_{4',5}$$

$$A_{56} = \mathrm{R}^{z}_{56}\,\mathrm{T}^{x}_{66'}$$

$$A_{67} = \mathrm{R}^{z}_{6',7}$$

$$A_{78} = \mathrm{R}^{x}_{78}\,\mathrm{T}^{y}_{88'}$$

We can obtain the position and orientation of the final frame with respect to the reference frame in the open kinematic chain, by the matrix product,

$$A_{08} = \prod_{i=1}^{8} A_{i-1,i}$$

$$A_{08} = A_{01}A_{12}A_{23}A_{34}A_{45}A_{56}A_{67}A_{78}$$

where,

$A_{i-1,i}$ is a 4x4 matrix which express the position and orientation of the frame *i* with respect to frame *i*-1. The direct geometric model of the open kinematic chain associated with the eight-bar reconfigurable mechanism can be expressed as,

$$A_{08} = \mathrm{R}_{01}^{z}(\emptyset_{10})\mathrm{R}_{12}^{x}(\emptyset_{21})\mathrm{T}_{22,}^{y}(b_2)\mathrm{R}_{2,3}^{x}(\emptyset_{32})\mathrm{R}_{34}^{y}(\emptyset_{43})$$

$$\mathrm{T}_{44,}^{z}(b_4)\mathrm{R}_{4,5}^{y}(\emptyset_{54})\mathrm{R}_{56}^{z}(\emptyset_{65})\mathrm{T}_{66,}^{x}(b_6)\mathrm{R}_{6,7}^{z}(\emptyset_{76})\mathrm{R}_{78}^{x}(\emptyset_{87})\mathrm{T}_{88,}^{y}(b_8)$$

$$A_{08} = A_{01}\overbrace{A_{12}\ A_{23}}^{A_{13}}\overbrace{A_{34}\ A_{45}}^{A_{35}}\overbrace{A_{56}\ A_{67}}^{A_{57}}\ A_{78}$$

$$A_{18} = A_{12}\ A_{23}\ A_{34}\ A_{45}\ A_{56}\ A_{67}\ A_{78}$$
$$A_{28} = A_{23}\ A_{34}\ A_{45}\ A_{56}\ A_{67}\ A_{78}$$
$$A_{38} = A_{34}\ A_{45}\ A_{56}\ A_{67}\ A_{78}$$
$$A_{48} = A_{45}\ A_{56}\ A_{67}\ A_{78}$$
$$A_{58} = A_{56}\ A_{67}\ A_{78}$$
$$A_{68} = A_{67}\ A_{78}$$
$$A_{78} = A_{78}$$

where,

$\emptyset_{10}$ = angle of rotation around Z_1
$\emptyset_{21}$ = angle of rotation around X_2
$\emptyset_{32}$ = angle of rotation around X_3
$\emptyset_{43}$ = angle of rotation around Y_4
$\emptyset_{54}$ = angle of rotation around Y_5
$\emptyset_{65}$ = angle of rotation around Z_6
$\emptyset_{76}$ = angle of rotation around Z_7
$\emptyset_{87}$ = angle of rotation around X_8

The detailed calculation using Maple software is illustrated in the Appendix I. In a general configuration, we calculate six joint angles with respect to two independent angles. By using the TCS method, we define the frames and the joint angles. Figure 2.7 illustrates the special single-loop 8-bar mechanism with the joint variables and associated frames.

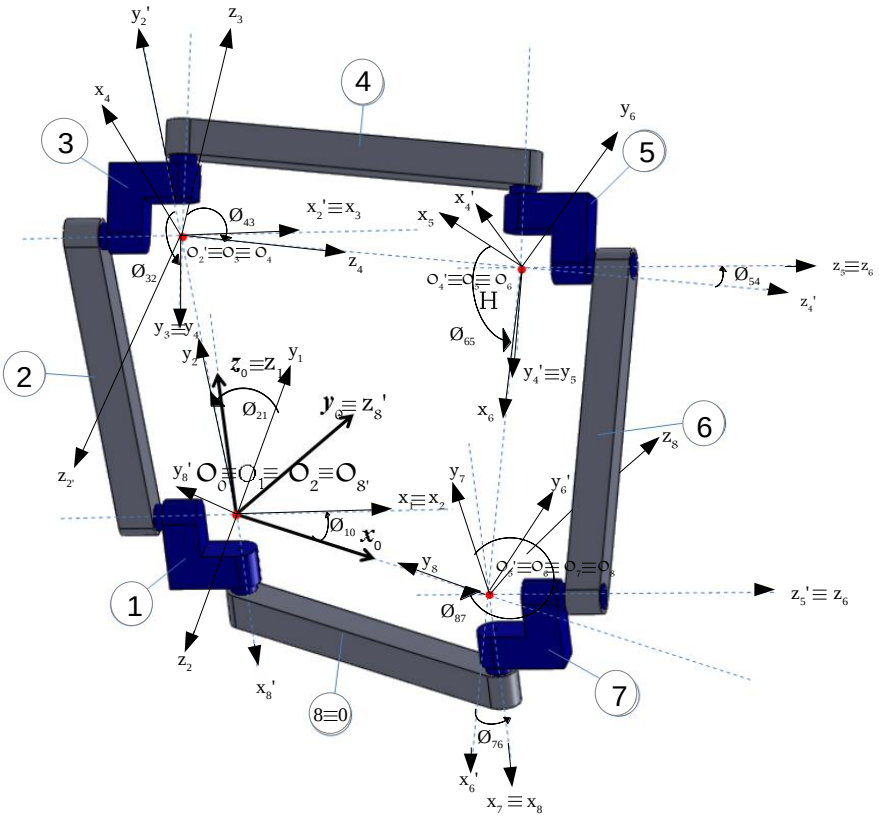

Figure 2.7 Modeling of the eight bar reconfigurable mechanism by TCS method

By taking the rules of the TCS method into account, we formulate the travelling coordinate system for the open kinematic chain associated with the eight-bar mechanism as follows:

$$O_0x_0y_0z_0 \xrightarrow{R_{01}^{z}(\phi_{10})} O_1x_1y_1z_1 \xrightarrow{R_{12}^{x}(\phi_{21})} O_2x_2y_2z_2 \xrightarrow{T_{22'}^{y}(b_2)}$$

$$O_{2'}x_{2'}y_{2'}z_{2'} \xrightarrow{R_{2'3}^{x}(\phi_{32})} O_3x_3y_3z_3 \xrightarrow{R_{34}^{y}(\phi_{43})} O_4x_4y_4z_4 \xrightarrow{T_{44'}^{z}(b_4)}$$

$$O_{4'}x_{4'}y_{4'}z_{4'} \xrightarrow{R_{4'5}^{y}(\phi_{54})} O_5x_5y_5z_5 \xrightarrow{R_{56}^{z}(\phi_{65})} O_6x_6y_6z_6 \xrightarrow{T_{66'}^{x}(b_6)}$$

$$O_{6'}x_{6'}y_{6'}z_{6'} \xrightarrow{R_{6'7}^{z}(\phi_{76})} O_7x_7y_7z_7 \xrightarrow{R_{78}^{x}(\phi_{87})} O_8x_8y_8z_8 \xrightarrow{T_{88'}^{y}(b_8)}$$

$$O_{8'}x_{8'}y_{8'}z_{8'}$$

In order to determine the mechanism configuration, the geometric model of mechanism has been solved. This has been performed by formulating the six loop closure constraint equations while considering two independent input joints. In our calculation, we consider $\emptyset_{10}$ and $\emptyset_{21}$ as the independent variables and $\emptyset_{32}, \emptyset_{43}, \emptyset_{54}, \emptyset_{65}, \emptyset_{76}$ and $\emptyset_{87}$ as the dependent variables.

In this chapter we will make use of these constraint equations to solve kinematic problems, namely, the initial position or assembly problem, the finite displacement problem, and the

velocity and acceleration analysis. The six kinematic equations are obtained by using the properties of perpendicularity and parallelism of the SSL8B mechanism.

Note:

SSL8B: special single-loop 8-bar

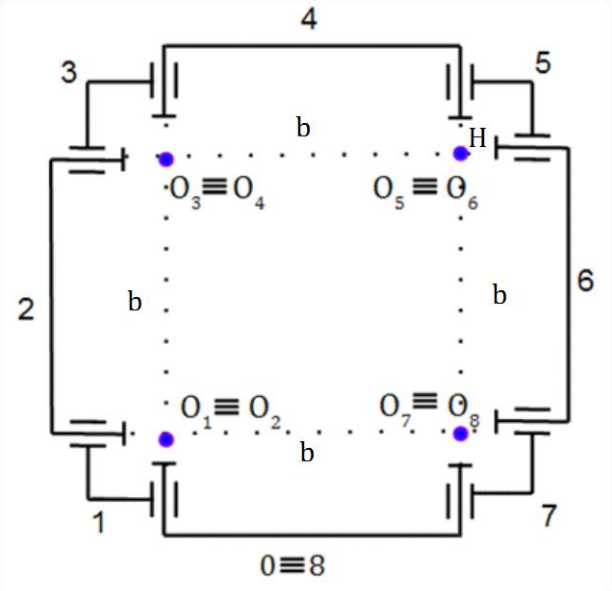

Figure 2.8 Schema of the eight bar mechanism with its natural coordinates

The detailed calculations of these kinematic constraint equations and their complete solution are presented in Appendix II.
To summarize, the six kinematic constraint equations are as follows:

$$\| \overrightarrow{\mathbf{O_5O_7}} \| = b$$

$$\overrightarrow{\mathbf{y_3}}.\left(\overrightarrow{\mathbf{O_8H}} \times \overrightarrow{\mathbf{z_1}}\right) = 0$$

$$\overrightarrow{\mathbf{z_1}}.\left(\overrightarrow{\mathbf{x_3}} \times \overrightarrow{\mathbf{z_6}}\right) = 0$$

$$\mathbf{z_7} = 0 \ \text{[where } \mathbf{z_7} \text{ is obtained from } A_{07}[4,1]]$$

$$\overrightarrow{\mathbf{z_5}}.\left(\overrightarrow{\mathbf{z_8}} \times \overrightarrow{\mathbf{x_1}}\right) = 0\ ,\quad \overrightarrow{\mathbf{x_8}}.\overrightarrow{\mathbf{x_1}} = 0$$

$$\overrightarrow{\mathbf{y_8}} = -\overrightarrow{\mathbf{x_0}}$$

By solving these six equations, six dependent joint variables are determined in terms of $\emptyset_{10}$ and $\emptyset_{21}$ in a particular configuration of the mechanism. Multiple solutions of the geometric model were found corresponding to several assembly modes.

After solving the loop-closure equations, we obtain the values of dependent angles for a particular configuration as follows:

$$\emptyset_{32} = \frac{\Pi}{2} - \emptyset_{21} \qquad (2.11)$$

$$\emptyset_{43} = \frac{\Pi}{2} - \emptyset_{10} \tag{2.12}$$

$$\emptyset_{54} = \frac{\Pi}{2} + \emptyset_{10} - \arccos\left(\frac{\sin\left(\frac{\Pi}{2} - \emptyset_{10}\right) - \cos(\emptyset_{10})}{\cos(\emptyset_{21} - \Pi)}\right) \tag{2.13}$$

$$\emptyset_{65} = \emptyset_{21} - \Pi \tag{2.14}$$

$$\emptyset_{76} = \frac{\Pi}{2} - \emptyset_{21} \tag{2.15}$$

$$\emptyset_{87} = \emptyset_{10} - \arccos\left(\frac{\sin\left(\frac{\Pi}{2} - \emptyset_{10}\right) - \cos(\emptyset_{10})}{\cos(\emptyset_{21} - \Pi)}\right) \tag{2.16}$$

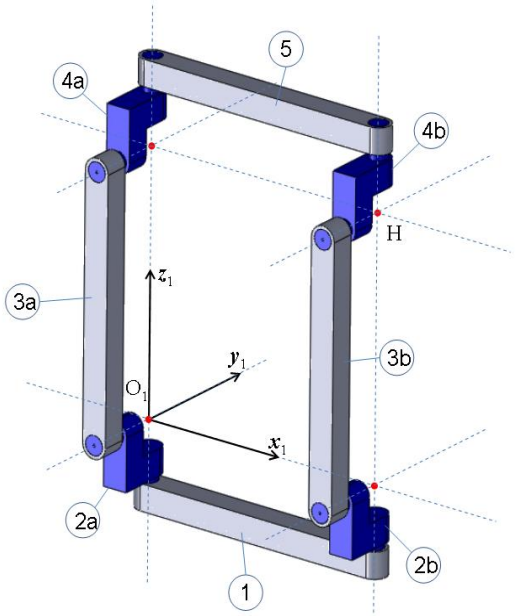

Figure 2.9 Single-loop eight-bar mechanism with orthogonal/ parallel axes

Figure 2.9 shows an assembly mode which validates and satisfies the above set of equations. This is one of the singular configurations of the SSL8B mechanism where the axes are parallel to the plane $O_i y_i z_i$. This mechanism has a continuous mobility change of two to five degrees of freedom without assembling/ disassembling of the mechanism. Also the mechanism exhibits different bifurcation modes to get out of singularity. This leads to an interesting property of continually transiting from one assembly mode to another. The angular values and its detailed description will be dealt in chapter 3.

2.3.5 Conclusion

We applied the formulae of structural parameters to a reconfigurable eight-bar linkage. The mechanism is parameterized using the TCS method followed by the formulation of the geometric model. The structural analysis and the geometric modeling are performed for a general configuration of the mechanism. Various assembly modes and singularities will be analyzed in detail in the next chapter.

2.4 Conclusion

In this chapter, we presented the structural analysis and the geometric modeling based on the TCS method applied to the proposed SSL8B mechanism. Initially we recalled the structural parameters such as mobility, connectivity, overconstraint and redundancy of the parallel robots, and their calculation formulae. A structural analysis has been performed for general configuration of the mechanism showing all possible motions of the end-effector with respect to the reference frame. Thereafter, the TCS method has been implemented for the geometric modeling of the SSL8B mechanism. The mechanism kinematic constraints have been formulated in order to determine the mechanism configuration with respect to two independent joint variables. This resolution is required for mechanism control. One of the possible solutions of the geometric model was given for a non-singular configuration. The other solutions of the geometric model as well as those in singularity will be discussed in the following chapter. Also, possible singular configurations of this mechanism and the nature of these singularities will be discussed in Chapter 3.

3 Chapter 3: Singularity analysis of the single-loop eight bar reconfigurable mechanism

A parallel manipulator is naturally associated with a set of constraint functions defined by its closure constraints. The differential forms arising from these constraint functions completely characterize the kinematic properties of the manipulator. In this chapter, we provide a thorough geometric study on the various types of singularities of a parallel manipulator and their relations with the structural parameters. The role that redundant actuation plays in reshaping the singularities and improving the performance of the manipulator.

3.1 Parallel manipulators and its singularities

The mechanical architecture of parallel robots is based on parallel mechanisms in which a member called a mobile platform is connected to a reference element by at least two limbs that can be simple or complex [Gogu, 2008a]. Perhaps, the best known parallel manipulator is formed from six linear actuators that support a movable base for devices such as flight simulators. This device is called a Stewart platform or the Gough-Stewart platform in recognition of the engineers who first designed and used them [Merlet, 2008].

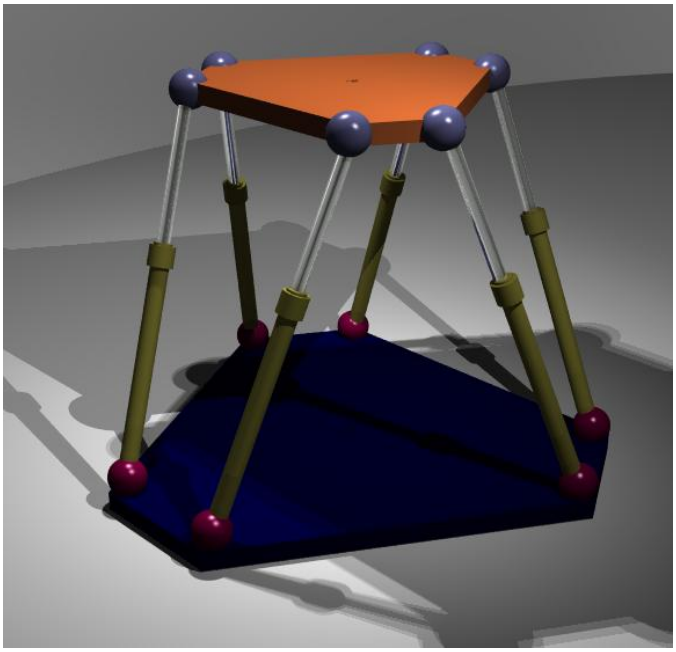

Figure 3.1 Structure of Steward Platform [Merlet, 2008]

A drawback of parallel manipulators, in comparison to serial manipulators, is their limited workspace. As for serial manipulators, the workspace is restricted by joint limits and self collisions. The workspace is also limited by the existence of *singularities*, which are positions where, the variation of the actuated joint variables is infinitely smaller than the variation of the displacement of the moving platform. Conversely, at a singular position, an external force applied on the end-effector induce infinitely larger force or torque in the actuated joint, which

may result in loss of control and a kind of "explosion" of the manipulator. The determination of the singular positions is difficult (for a general parallel manipulator, this is an open problem). This implies that it is dangerous to utilize the manipulator near singular configurations, which generally limits the effective workspace of the parallel manipulators to a small region where one knows that there is no singularity.

Another drawback of parallel manipulators is their nonlinear behavior: the command (or control) which is needed for getting a linear or a circular movement of the end-effector depends dramatically on the location in the workspace and does not vary linearly during the movement. The following sub-sections deals with the definitions of different types of singularities and the impacts of each on the parallel manipulator kinematics

3.1.1 Importance of singularities

Many research works have studied the singularities of serial and parallel manipulators. Compared with its serial counterparts, a parallel manipulator (or a closed-chain mechanism) has a much more complex structure in terms of its kinematics, dynamics, trajectory planning and control. In particular, the configuration space of a parallel manipulator is not even explicitly known; it is implicitly defined by a set of constraint functions introduced by the manipulator's closure constraints [Liu et al., 2003]. A parallel manipulator also has, in addition to the usual end-effector singularities, different types of singularities such as configuration space singularities and actuator singularities. Understanding the intrinsic nature of the various types of singularities and their relations with the kinematic parameters and the configuration spaces is of ultimate importance in design, trajectory or task planning and control of the system. In the upcoming sections we will discuss the major types of constraint and redundant singularities identified in the SSL8B mechanism.

3.1.2 Types of singularities

Unlike its serial counterparts, where there have been well established mathematical tools for their analysis, studies on singularities of parallel manipulators were confined to basic issues such as definition, classification and identification of singularities. Furthermore, the mathematical tools used in most studies were directly borrowed from that for serial manipulators and were applicable only to local analysis. The unique structures of parallel mechanisms were not fully explored. Gosselin and Angeles [Gosselin et al., 1990] were perhaps the first to define and study singularities of closed-loop kinematic chains. Based on some derived Jacobian relations, they introduced several notions of singularities which formed a basis of later research. Park and Kim [Park et al., 1999] used differential geometric tools to study singularities of parallel mechanisms and provided a finer classification of singularities. In their later works, they proposed the use of redundant actuation as a means of eliminating actuator singularities and improving manipulator performances. Merlet and others [Merlet, 1989], [Hunt, 1986], [Ma et al., 1991], [Kumar et al., 1990] studied extensively singularities of the Stewart–Gough platform and several of its variants.

The determination of singularities for parallel manipulator is indeed very complex. An interesting example is offered by that of the Seoul National University (SNU) manipulator, a 3-DOF translational manipulator with the joints of its three subchains arranged in the order of universal–prismatic–universal (UPU). Zlatanov et al. [Zlatanov et al., 2002] studied the rotational and translational singularity using screw theory and classified it as a constraint singularity. The same singularity was also identified by Joshi and Tsai [Joshi et al., 2002], Simaan and Shoham [Simaan et al., 2001], and Wolf et al. [Wolf et al., 2002] using an augmented Jacobian matrix which took the constraints into account.

In the following sections, we identify and describe all possible singular configurations of the SSL8B mechanism. We characterize the singular configurations using structural parameters. We investigate the intrinsic nature of the various singularities of a parallel mechanism, their relations with the kinematic parameters and classify them accordingly under different types of singularities.

We propose to use redundant actuation for the SSL8B mechanism, which translates into more actuation options than required to perform a particular task in its general configuration. The role of redundant actuation plays in reshaping the singularities and improving the manipulator's performance. We present a detailed classification of parameterization singularities and identify those which are potentially dangerous and should be avoided or eliminated through design.

3.2 Singularities in connection with structural parameters

The aim of this chapter is to identify and make an analysis on the nature of the singularity behavior with the associated structural parameters by using the new formulae recently proposed in [Gogu 2008a]. Singular configurations of parallel robots are particular configurations at which the robot loses its natural rigidity. When a parallel manipulator reaches its singular configuration, the platform becomes uncontrollable. Also, singularities can damage the robot; hence measures should be taken to avoid singularities in the reachable space during designing the robot. The singular configurations can be determined by analyzing the rank of the matrix J or J^{-1} (inverse of the Jacobian matrix).

In a singular configuration at least one of the structural parameters in Eq. 2.6 is instantaneously altered. We denote by an anterior superior index *i* the instantaneous values of the structural parameters defined above. We note that, in general, any structural parameter used in Eqs. (2.1)-(2.9) can be affected by singular configurations excepting f_j and q. Various singular configurations can be associated with the eight-bar mechanism analysed in this section. They can be defined by the following configurations of the rotation axes of the eight revolute joints: (1) coplanar, (2) intersecting a line, (3) parallel to a plane, and (4) parallel to a plane and in the same time intersecting a line. As we will illustrate in the next sections, the last configuration can be associated with a constraint singularity, the third configuration with a constraint or with a redundant singularity, the second with a redundant singularity and the first with a constraint-redundant singularity. In all singular or non-singular configurations of

the eight-bar mechanism, the following structural parameters are invariants: $m=8$, $p_1=p_2=4$, $p=8$, $q=1$, $k_1=2$, $k_2=0$, $k=2$, $r_{G1}=r_{G2}=0$,$M_{G1}=M_{G2}=4$, $r_l=0$.

3.2.1 Constraint Singularities

A constraint singularity is a configuration of the parallel manipulator in which both the connectivity of the moving platform with respect to the fixed base and the mobility of the parallel mechanism increase their instantaneous values with no change in limb connectivity and mobility. The following properties of the parallel mechanisms have been associated with the constraint singularities in [Gogu, 2008b].

Property 1: If the vector space of relative velocities between the distal links n_{Gj} and 1_{Gj} in the kinematic chain G_j disconnected from the mechanism F, accept various bases, the connectivity of the moving platform can increase instantaneously its value ${}^iS_F>S_F$, with no instantaneous change in limb connectivity (${}^iS_{Gj}=S_{Gj}$).

This property results directly from Eq. 2.5 and shows that a constraint singularity may occur when the vector space of relative velocities between the distal links n_{Gj} and 1_{Gj} in the kinematic chain G_j disconnected from the mechanism F, accept various bases at least for one of the limbs.

Property 2: An instantaneous increase of the connectivity of the moving platform (${}^iS_F$-S_F) is accompanied by an identical increase of the mobility of the parallel mechanism (${}^iM_F$-M_F) when no instantaneous changes occur in limb connectivity and the number of joint parameters that lose their independence in the closed loops that may exist in limb G_j

$$ {}^iM_F-M_F={}^iS_F-S_F \tag{3.1}$$

when ${}^iS_{Gj}=S_{Gj}$ and ${}^ir_l=r_l$. This property results directly from Eqs. 2.1 and 2.6.

Property 3: An instantaneous increase of the connectivity of the moving platform (${}^iS_F$-S_F) is accompanied by an identical increase of the degree of overconstraint of the parallel mechanism (${}^iN$-N) when no instantaneous changes occur in limb connectivity and the number of joint parameters that lose their independence in the closed loops that may exist in limb G_j

$$ {}^iN-N={}^iS_F-S_F \tag{3.2}$$

when ${}^iS_{Gj}=S_{Gj}$ and ${}^ir_l=r_l$. This property results directly from Eqs. 2.2 and 2.6.

Property 4: An instantaneous increase of the connectivity of the moving platform (${}^iS_F$-S_F) accompanied by an identical increase of the mobility of the parallel mechanism (${}^iM_F$-M_F) does not affect the redundancy of the parallel mechanism.

This property results directly from Eq. 2.3.

The four properties characterizing the constraint singularities are illustrated in this section with respect to the single-loop eight-bar mechanism with orthogonal/parallel axes. Two constraint singularities can be associated with this mechanism as presented in Figure 3.2.

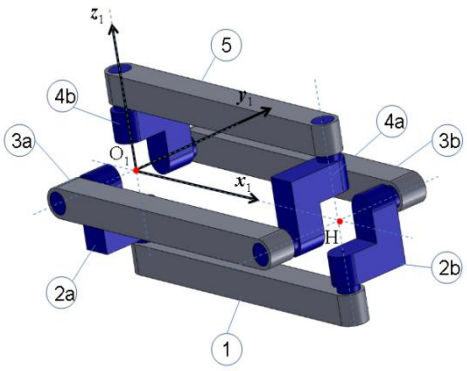

(a)

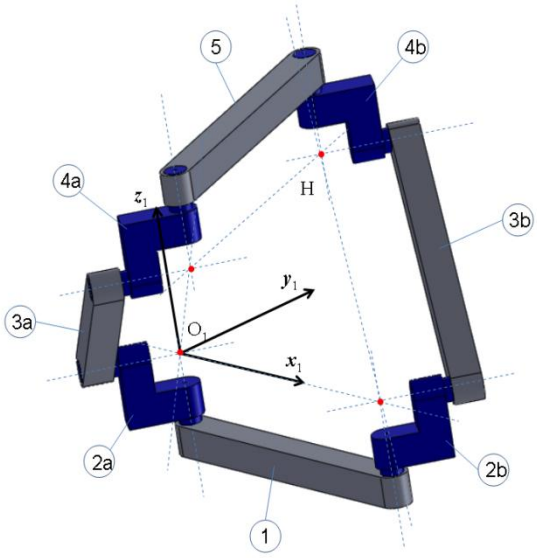

(b)

Figure 3.2 SSL8B mechanism two distinct constraint singularities

In the singular configuration in Figure 3.2a, the axes of the eight revolute joints are parallel to plane $O_1x_1y_1$ and in the same time intersect axis O_1x_1. The following values are associated with the joint rotation angles in the constraint singularity in Figure 3.2a: $\phi_{21}^a = 90^\circ, \phi_{32}^a = 180^\circ, \phi_{43}^a = 90^\circ, \phi_{54}^a = 0^\circ, \phi_{45}^b = 90^\circ, \phi_{34}^b = 0^\circ, \phi_{23}^b = 90^\circ, \ \phi_{12}^b = 0^\circ$. Each limb has $S_{Gi}=4$ and the same basis of the velocity vector space $({}^iR_{G1})=({}^iR_{G2})= (\boldsymbol{v}_y,\boldsymbol{v}_z,\boldsymbol{\omega}_y,\boldsymbol{\omega}_z)$. Each limb has $S_{Gi}=4$ and the same basis of the velocity vector space $({}^iR_{G1})=({}^iR_{G2})= (\boldsymbol{v}_y,\boldsymbol{v}_z,\boldsymbol{\omega}_y,\boldsymbol{\omega}_z)$. For this singular configuration, Eqs. (2.1)-(2.9) give the following values for the structural parameters: ${}^iM_{G1}={}^iM_{G2}=4$, ${}^ir_F=4$, ${}^iM_F=4$, ${}^iS_F=4$, ${}^iN_F=2$, ${}^iT_F=0$. The basis of the vector space ${}^iR_F$ is $({}^iR_F)= (\boldsymbol{v}_y,\boldsymbol{v}_z,\boldsymbol{\omega}_y,\boldsymbol{\omega}_z)$. The mechanism can get out of this constraint singularity in a non-singular branch with various bases of vector space R_F, as indicated in section 2.1.2, or in the constraint singularity configuration presented in Figure 3.2b. A non-singular branch defines the connexe set of non-singular configurations of the mechanism in which the structural parameters keep the same value. The transition from one branch to another without disassembling the mechanism is always done passing through a singular configuration.

The vector spaces associated with each limb of the mechanism presented in Figure 3.2a are illustrated below by means of calculating the Jacobian matrix of each limb.

$$J_{04}=\begin{bmatrix}0&0&0&0\\0&0&0&-b\\0&0&b&0\\0&0&0&0\\0&1&1&0\\1&0&0&1\end{bmatrix}, Rank(J_{04})=4$$

$$R_{G1}=(v_y,v_z,\omega_y,\omega_z)$$

$$J_{85}=\begin{bmatrix}0&0&0&0\\0&-b&0&0\\b&0&0&0\\0&0&0&0\\1&0&0&-1\\0&1&1&0\end{bmatrix}, Rank(J_{85})=4$$

$$R_{G2}=(v_y,v_z,\omega_y,\omega_z)$$

Table 3.1 Possible combinations of vector spaces with minimum S_F for the configuration in Fig. 3.2a

$(\boldsymbol{R_{G1}})$	$(\boldsymbol{R_{G2}})$	$(\boldsymbol{R_F})$	$\boldsymbol{S_F}$
$(v_y, v_z, \omega_y, \omega_z)$	$(v_y, v_z, \omega_y, \omega_z)$	$(v_y, v_z, \omega_y, \omega_z)$	4

In the singular configuration in Figure 3.2b, the axes of the eight revolute joints are parallel to the plane defined by the rotation axes of the two first revolute joints of limb G_1. The following values are associated with the joint rotation angles in the constraint singularity in Figure 2b: $\phi^a_{21}=50^\circ, \phi^a_{32}=130^\circ, \phi^a_{43}=320^\circ, \phi^a_{54}=70^\circ, \phi^b_{45}=230^\circ, \phi^b_{34}=-49^\circ, \phi^b_{23}=-40^\circ, \phi^b_{12}=40^\circ$. Each limb has $S_{Gi}=4$ and each vector space R_{Gi} ($i=1$ and 2) can have one of the following bases: $(\boldsymbol{v}_x,\boldsymbol{v}_z,\boldsymbol{\omega}_x,\boldsymbol{\omega}_z)$, $(\boldsymbol{v}_x,\boldsymbol{v}_z,\boldsymbol{\omega}_y,\boldsymbol{\omega}_z)$, $(\boldsymbol{v}_y,\boldsymbol{v}_z,\boldsymbol{\omega}_x,\boldsymbol{\omega}_z)$ or $(\boldsymbol{v}_y,\boldsymbol{v}_z,\boldsymbol{\omega}_y,\boldsymbol{\omega}_z)$. Two different values can be obtained for the connectivity between the moving platform and the base. The minimum value ${}^iS_F=3$ is associated with the mechanism in Figure 3 where the moving platform have just three independent motions. For example, if we consider $({}^iR_{G1})=(\boldsymbol{v}_x,\boldsymbol{v}_z,\boldsymbol{\omega}_x,\boldsymbol{\omega}_z)$ and $({}^iR_{G2})=(\boldsymbol{v}_y,\boldsymbol{v}_z,\boldsymbol{\omega}_x,\boldsymbol{\omega}_z)$ we get $({}^iR_F)=(\boldsymbol{v}_z,\boldsymbol{\omega}_x,\boldsymbol{\omega}_z)$ and if $({}^iR_{G1})=(\boldsymbol{v}_x,\boldsymbol{v}_z,\boldsymbol{\omega}_y,\boldsymbol{\omega}_z)$ and $({}^iR_{G2})=(\boldsymbol{v}_y,\boldsymbol{v}_z,\boldsymbol{\omega}_y,\boldsymbol{\omega}_z)$ we get $({}^iR_F)=(\boldsymbol{v}_z,\boldsymbol{\omega}_y,\boldsymbol{\omega}_z)$. Eqs. 1-9 give: ${}^iM_{G1}={}^iM_{G2}=4$, ${}^ir_F=5$, ${}^iM_F=3$, ${}^iS_F=3$, ${}^iN_F=1$, ${}^iT_F=0$, $T_{G1}=T_{G2}=0$.

The vector spaces associated with each limb of the mechanism presented in Figure 3.2b are illustrated below as:

$$J_{04}=\begin{bmatrix}0 & b & 0 & 0\\ b & 0 & 0 & -b\\ 0 & 0 & b & 0\\ 0 & -b & -b & 0\\ 0 & 1 & 1 & 0\\ 1 & 0 & 0 & 1\end{bmatrix}, Rank(J_{04})=4$$

$$R_{G1}=(v_x,v_z,\omega_x,\omega_z),(v_x,v_z,\omega_y,\omega_z),(v_y,v_z,\omega_x,\omega_z) or (v_y,v_z,\omega_y,\omega_z)$$

$$J_{85}=\begin{bmatrix}0 & b & 0 & 0\\ b & 0 & 0 & -b\\ 0 & 0 & b & 0\\ 0 & -b & -b & 0\\ 0 & 1 & 1 & 0\\ 1 & 0 & 0 & 1\end{bmatrix}, Rank(J_{85})=4$$

$$R_{G2}=(v_x,v_z,\omega_x,\omega_z),(v_x,v_z,\omega_y,\omega_z),(v_y,v_z,\omega_x,\omega_z) or (v_y,v_z,\omega_y,\omega_z)$$

Table 3.2 Possible combinations of vector spaces with minimum S_F for the configuration in Fig. 3.2b

$(\boldsymbol{R_{G1}})$	$(\boldsymbol{R_{G2}})$	$(\boldsymbol{R_F})$	$\boldsymbol{S_F}$
$(v_x, v_z, \omega_x, \omega_z)$	$(v_x, v_z, \omega_y, \omega_z)$	(v_x, v_z, ω_z)	3
$(v_x, v_z, \omega_x, \omega_z)$	$(v_y, v_z, \omega_x, \omega_z)$	$(v_z, \omega_x, \omega_z)$	3
$(v_x, v_z, \omega_y, \omega_z)$	$(v_y, v_z, \omega_y, \omega_z)$	$(v_z, \omega_y, \omega_z)$	3
$(v_y, v_z, \omega_x, \omega_z)$	$(v_y, v_z, \omega_y, \omega_z)$	(v_y, v_z, ω_z)	3

The mechanism can get out of this constraint singularity in a non-singular branch with various bases of vector space R_F, as indicated in section 2.1.2, or in a constraint-redundant singularity as will be present in the following section.

3.2.2 Constraint-redundant singularities

A constraint-redundant singularity is a configuration of the parallel mechanism in which the following structural parameters increase instantaneously their values with respect to a non-singular configuration [Aimedee et al. 2015]:

a) connectivity of the moving platform in the parallel mechanism, ${}^{i}S_F > S_F$
b) mobility of the parallel mechanism, ${}^{i}M_F > M_F$
c) redundancy of the parallel mechanism, ${}^{i}T_F > T_F$ with no change in limb mobility
(${}^{i}M_{Gj} = M_{Gj}$).

By analogy with the constraint singularity analysis, the following properties of parallel mechanisms can be associated with constraint-redundant singularities.

Property 5: Instantaneous mobility of the parallel mechanism is divided between the instantaneous mobility of the moving platform ${}^{i}S_F$ and the instantaneous internal mobilities in the limbs ${}^{i}T_F$

$$ {}^{i}M_F={}^{i}S_F+{}^{i}T_F. \tag{3.3}$$

This property results directly from Eq. (2.3).

Property 6: An instantaneous increase of mechanism redundancy (${}^{i}T_F$-T_F) is identical with the instantaneous increase of internal mobilities in the limbs disconnected from the parallel mechanism

$$ {}^{i}T_F - T_F = \sum_{j=1}^{k} {}^{i}T_{Gj} - \sum_{j=1}^{k} T_{Gj} \ . \tag{3.4}$$

This property results directly from the definition of internal mobilities in connection with mechanism redundancy.

Property 7: An instantaneous increase of limb redundancy (${}^{i}T_{Gj}$-T_{Gj}) is identical with the instantaneous decrease of the connectivity between the moving platform and the reference link (S_{Gj}-${}^{i}S_{Gj}$) in the limb disconnected from the parallel mechanism

$$ {}^{i}T_{Gj}\text{-}T_{Gj}= S_{Gj}\text{-}{}^{i}S_{Gj} \ . \tag{3.5}$$

This property results from Eq. (2.3) by taking into account that the mobility of the limb disconnected from the parallel mechanism is not affected by this singular configuration.

Property 8: An instantaneous increase of the mobility of the parallel mechanism (${}^{i}M_F$-M_F) is accompanied by an identical increase of the degree of overconstraint of the parallel mechanism (${}^{i}N_F$-N_F)

$$ {}^{i}N_F\text{-}N_F={}^{i}M_F\text{-}M_F \tag{3.6}$$

This property results directly from Eqs. 2.1 and 2.2.

The four properties characterizing the constraint- redundant singularities are illustrated in this section with respect to the configuration of the single-loop eight-bar mechanism with orthogonal/parallel axes presented in Figure 3.3. In this singular configuration, the axes of the eight revolute joints are coplanar and situated in plane $O_1x_1z_1$.

Each limb has $S_{Gi}=3$ and the same basis of the velocity vector space (${}^{i}R_{G1}$)=(${}^{i}R_{G2}$)=($\boldsymbol{v}_y$,$\boldsymbol{\omega}_x$,$\boldsymbol{\omega}_z$). For this singular configuration, Eqs. (2.1)-(2.9) give the following values for the main structural parameters: ${}^{i}M_{G1}={}^{i}M_{G2}=4$, ${}^{i}r_F=3$, ${}^{i}M_F=5$, ${}^{i}S_F=3$, ${}^{i}N_F=3$, ${}^{i}T_F=2$, $T_{G1}=T_{G2}=1$. The basis of the vector space ${}^{i}R_F$ is (${}^{i}R_F$)= ($\boldsymbol{v}_y$,$\boldsymbol{\omega}_x$,$\boldsymbol{\omega}_z$). Each limb has one internal mobility associated with an unlimited rotation of the sub chain 2-3-4 around the superposed rotational axis of the first and the last revolute joints of the limb.

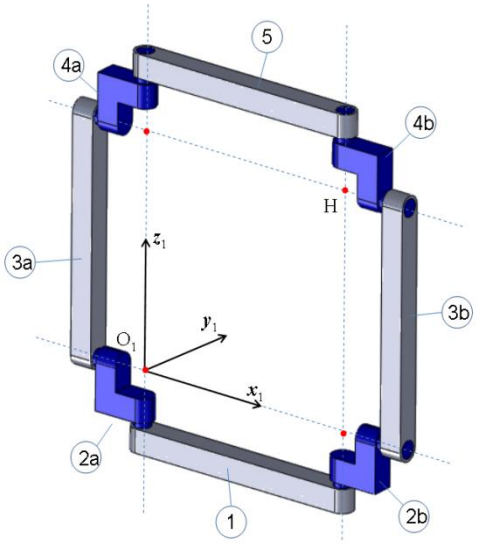

Figure 3.3 Single-loop eight-bar mechanism with orthogonal/ parallel axes in constraint-redundant singularity

The mechanism can get out of this constraint singularity in a non-singular branch with various bases of vector space R_F, as indicated in section 2.1.2, or in various redundant singularities as presented in the following section. The following values are associated with the joint rotation angles in the constraint-redundant singularity in Figure 3.3: $\phi^a_{21}=0^\circ, \phi^a_{32}=90^\circ, \phi^a_{43}=0^\circ, \phi^a_{54}=90^\circ, \phi^b_{45}=0^\circ, \phi^b_{34}=270^\circ, \phi^b{}_{23}=0^\circ,\ \phi^b_{12}=270^\circ$.

The vector spaces associated with each limb of the mechanism presented in Figure 3.3 are illustrated below as:

$$J_{04}=\begin{bmatrix}0&0&0&0\\ b&-b&0&b\\ 0&0&0&0\\ 0&1&1&0\\ 0&0&0&0\\ 1&0&0&1\end{bmatrix}, Rank(J_{04})=3$$

$$R_{G1}=(v_y,\omega_x,\omega_z)$$

$$J_{85}=\begin{bmatrix}0&0&0&0\\ -b&0&-b&b\\ 0&0&0&0\\ 0&1&1&0\\ 0&0&0&0\\ 1&0&0&-1\end{bmatrix}, Rank(J_{85})=3$$

$$R_{G2}=(v_y,\omega_x,\omega_z)$$

Table 3.3 Possible combinations of vector spaces with minimum S_F for the configuration in Fig. 3.3

$(\boldsymbol{R_{G1}})$	$(\boldsymbol{R_{G2}})$	$(\boldsymbol{R_F})$	$\boldsymbol{S_F}$
$(v_y, \omega_x, \omega_z)$	$(v_y, \omega_x, \omega_z)$	$(v_y, \omega_x, \omega_z)$	3

3.2.3 Redundant Singularities

A redundant singularity is a configuration of the parallel mechanism in which the following structural parameters change instantaneously their values with respect to a non-singular configuration [Aimedee et al. 2015]:

a) connectivity of the moving platform with respect to the fixed base in the parallel mechanism decreases, ${}^{i}S_F < S_F$

b) mobility of the parallel mechanism keep its value or increases, ${}^{i}M_F \geq M_F$

c) redundancy of the parallel mechanism, ${}^{i}T_F > T_F$ increases, with no change in limb mobility (${}^{i}M_{Gj} = M_{Gj}$).

The properties defined in the previous section for the constraint-redundant singularities are also applicable to the redundant singularities with a slight reformulation of property 8. A new specific property is also associated in this section to this type of singularities.

Property 8bis: A possible instantaneous increase of the mobility of the parallel mechanism (${}^{i}M_F$-M_F) is accompanied by an identical increase of the degree of overconstraint of the parallel mechanism (${}^{i}N_F$-N_F).

This property results directly from Eqs. 2.1 and 2.2.

Property 9: If the instantaneous value of mechanism mobility ${}^{i}M_F$ is equal to the instantaneous value of mechanism redundancy ${}^{i}T_F$, the moving platform of the parallel mechanism is instantaneously blocked and the parallel mechanism has just internal mobilities.

This property results from Eq. (3.3).

The properties characterizing the redundant singularities are illustrated in this section with respect to the configurations of the single-loop eight-bar mechanism with orthogonal/parallel axes presented in Figure 3.4.

In the singular configuration in Figure 3.4a the axes of the eight revolute joints intersect O_1z_1 axis and the configuration in Figure 3.4b they intersect a line passing by point H and parallel with O_1z_1. We recall that two parallel axes intersect at infinity. In the singular configuration in Figure 3.4c, the axes of the eight revolute joints are parallel to the plane $O_1y_1z_1$. We recall that two parallel axes intersect at infinity. In the singular configuration in Figure 4c, axes of the eight revolute joints are parallel to the plane $O_1y_1z_1$. The following values are associated with the joint rotation angles in the redundant singularity:

In Figure 3.4a : $\phi^a_{21} = 90^\circ, \phi^a_{32} = 90^\circ, \phi^a_{43} = 0^\circ, \phi^a_{54} = 0^\circ, \phi^b_{45} = 0^\circ, \phi^b_{34} = 270^\circ, \phi^b{}_{23} = 0^\circ,\ \phi^b_{12} = 270^\circ$.

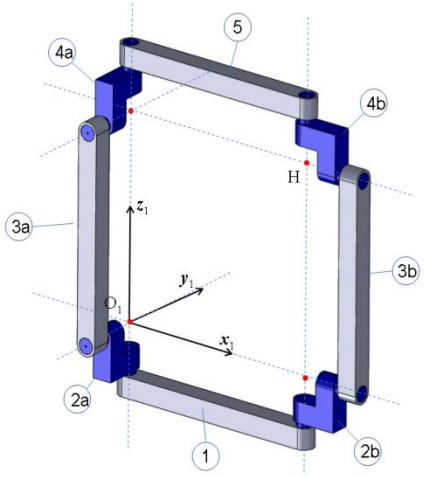

(a)

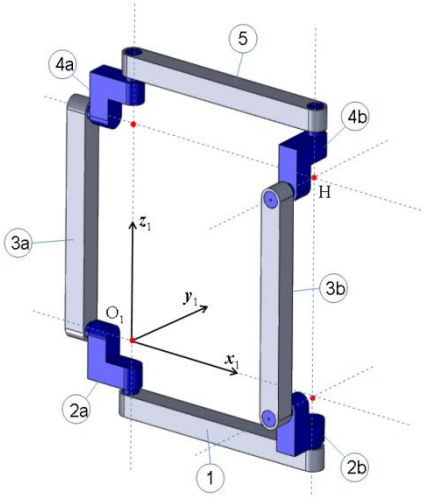

(b)

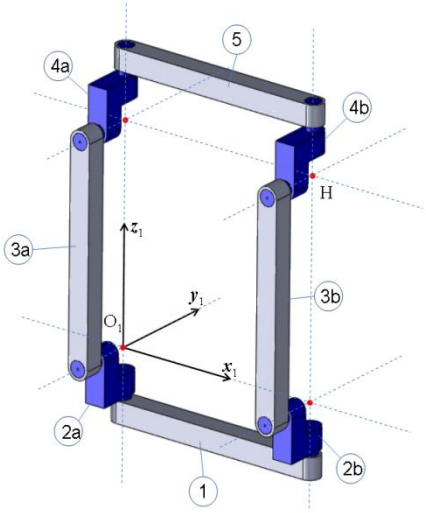

(c)

Figure 3.4 Single-loop eight-bar mechanism with orthogonal/ parallel axes in three different redundant singularities

The vector spaces associated with each limb of the mechanism presented in Figure 3.4a are illustrated below as:

$$J_{04}=\begin{bmatrix}0 & b & 0 & 0\\ b & 0 & 0 & b\\ 0 & -b & -b & 0\\ 0 & 0 & 0 & 0\\ 0 & 1 & 1 & 0\\ 1 & 0 & 0 & 1\end{bmatrix}, Rank(J_{04})=3$$

$$R_{G1}=(v_x,\omega_y,\omega_z),(v_z,\omega_y,\omega_z) or (v_x,v_z,\omega_z)$$

$$J_{85}=\begin{bmatrix}0 & 0 & 0 & 0\\ -b & 0 & -b & b\\ 0 & 0 & 0 & 0\\ 0 & 1 & 1 & 0\\ 0 & 0 & 0 & 0\\ 1 & 0 & 0 & -1\end{bmatrix}, Rank(J_{85})=3$$

$$R_{G2}=(v_y,\omega_x,\omega_z)$$

Table 3.4 Possible combinations of vector spaces with minimum S_F for the configuration in Fig. 3.4a

$(\boldsymbol{R_{G1}})$	$(\boldsymbol{R_{G2}})$	$(\boldsymbol{R_F})$	$\boldsymbol{S_F}$
(v_x, v_z, ω_z)	$(v_y, \omega_x, \omega_z)$	(ω_z)	1
$(v_x, \omega_y, \omega_z)$	$(v_y, \omega_x, \omega_z)$	(ω_z)	1
$(v_z, \omega_y, \omega_z)$	$(v_y, \omega_x, \omega_z)$	(ω_z)	1

In Figure 3.4b : $\phi^a_{21}=0^\circ, \phi^a_{32}=90^\circ, \phi^a_{43}=0^\circ, \phi^a_{54}=90^\circ, \phi^b_{45}=90^\circ, \phi^b_{34}=270^\circ, \phi^b_{23}=0^\circ,\ \phi^b_{12}=0^\circ$.

Table 3.5 Possible combinations of vector spaces with minimum S_F for the configuration in Fig. 3.4b

$(\boldsymbol{R_{G1}})$	$(\boldsymbol{R_{G2}})$	$(\boldsymbol{R_F})$	$\boldsymbol{S_F}$
$(v_y, \omega_x, \omega_z)$	(v_x, v_z, ω_z)	(ω_z)	1
$(v_y, \omega_x, \omega_z)$	$(v_x, \omega_y, \omega_z)$	(ω_z)	1
$(v_y, \omega_x, \omega_z)$	$(v_z, \omega_y, \omega_z)$	(ω_z)	1

$$J_{04}=\begin{bmatrix}0 & 0 & 0 & 0\\ b & -b & 0 & b\\ 0 & 0 & 0 & 0\\ 0 & 1 & 1 & 0\\ 0 & 0 & 0 & 0\\ 1 & 0 & 0 & 1\end{bmatrix}, Rank(J_{04})=3$$

$$R_{G1}=(v_y,\omega_x,\omega_z)$$

$$J_{85}=\begin{bmatrix}0 & 0 & -b & 0\\ 0 & -b & -b & 0\\ b & 0 & 0 & -b\\ 0 & 0 & 0 & 0\\ 1 & 0 & 0 & -1\\ 0 & 1 & 1 & 0\end{bmatrix}, Rank(J_{85})=3$$

$$R_{G2}=(v_x,v_z,\omega_z),(v_x,\omega_y,\omega_z),(v_z,\omega_y,\omega_z)$$

In Figure 3.4c : $\phi^a_{21}=90^\circ,\phi^a_{32}=90^\circ,\phi^a_{43}=0^\circ,\phi^a_{54}=0^\circ,\phi^b_{45}=90^\circ,\phi^b_{34}=270^\circ,\phi^b{}_{23}=0^\circ,\ \phi^b_{12}=0^\circ$.

$$J_{04}=\begin{bmatrix}0 & b & 0 & 0\\ b & 0 & 0 & b\\ 0 & -b & -b & 0\\ 0 & 0 & 0 & 0\\ 0 & 1 & 1 & 0\\ 1 & 0 & 0 & 1\end{bmatrix}, Rank(J_{04})=3$$

$$R_{G1}=(v_x,\omega_y,\omega_z),(v_x,v_y,v_z),(v_x,v_z,\omega) or (v_x,v_y,\omega_y)$$

$$J_{85}=\begin{bmatrix}0 & 0 & -b & 0\\ 0 & -b & -b & 0\\ b & 0 & 0 & -b\\ 0 & 0 & 0 & 0\\ 1 & 0 & 0 & -1\\ 0 & 1 & 1 & 0\end{bmatrix}, Rank(J_{85})=3$$

$$R_{G2}=(v_x,\omega_y,\omega_z),(v_x,v_y,\omega_z),(v_x,v_z,\omega_z),(v_x,v_z,\omega_y),(v_x,v_y,v_z) or (v_x,v_y,\omega_y)$$

Table 3.6 Possible combinations of vector spaces with minimum S_F for the configuration in Fig. 3.4a

$(\boldsymbol{R_{G1}})$	$(\boldsymbol{R_{G2}})$	$(\boldsymbol{R_F})$	$\boldsymbol{S_F}$
(v_x, v_y, v_z)	(v_x, v_y, ω_z)	(v_x)	1
(v_x, v_y, v_z)	(v_x, v_z, ω_y)	(v_x)	1
(v_x, v_y, v_z)	$(v_x, \omega_y, \omega_z)$	(v_x)	1
(v_x, v_y, ω_y)	(v_x, v_z, ω_z)	(v_x)	1
(v_x, v_y, ω_y)	(v_x, v_z, ω_z)	(v_x)	1
(v_x, v_z, ω_y)	(v_x, v_y, v_z)	(v_x)	1
(v_x, v_y, ω_y)	(v_x, v_z, ω_z)	(v_x)	1
(v_x, v_z, ω_z)	(v_x, v_y, ω_y)	(v_x)	1
$(v_x, \omega_y, \omega_z)$	(v_x, v_y, v_z)	(v_x)	1

The Jacobian matrix associated with each limb of the mechanism is presented in Annex III.

In the configurations presented in Figure 3.4, each limb has $S_{Gi}=3$. The velocity vector spaces have the following bases: $({}^iR_{G1})=(\boldsymbol{v}_x,\boldsymbol{\omega}_y,\boldsymbol{\omega}_z)$, $({}^iR_{G2})=(\boldsymbol{v}_y,\boldsymbol{\omega}_x,\boldsymbol{\omega}_z)$, $({}^iR_F)=(\boldsymbol{\omega}_z)$ for the configuration in Figure 3.4a, $({}^iR_{G1})=(\boldsymbol{v}_y,\boldsymbol{\omega}_x,\boldsymbol{\omega}_z)$, $({}^iR_{G2})=(\boldsymbol{v}_x,\boldsymbol{\omega}_y,\boldsymbol{\omega}_z)$, $({}^iR_F)=(\boldsymbol{\omega}_z)$ for the configuration in Figure 3.4b, and $({}^iR_{G1})=(\boldsymbol{v}_x,\boldsymbol{v}_y,\boldsymbol{v}_z)$, $({}^iR_{G2})=(\boldsymbol{v}_x,\boldsymbol{\omega}_y,\boldsymbol{\omega}_z)$, $({}^iR_F)=(\boldsymbol{v}_x)$ for the configuration in Figure 3.4c. For these singular configurations, Eqs. (2.1)-(2.9) give the following values for the main structural parameters: ${}^iM_{G1}={}^iM_{G2}=4$, ${}^ir_F=5$, ${}^iM_F=3$, ${}^iS_F=1$, ${}^iN_F=1$, ${}^iT_F=2$, $T_{G1}=T_{G2}=1$. As in the constraint-redundant singularity, each limb has one internal mobility associated with an unlimited rotation of the sub chain 2-3-4 around the superposed rotational axis of the first and the last revolute joints of the limb. The mechanism can get out of these constraint singularities in a non-singular branch with various bases of vector space R_F, as indicated in section 2.1.2, or back in the constraint-redundant singularity.

The mechanism can transit continuously from one type of singularity to another by remaining always in a singular configuration. This is an interesting property of this mechanism enhancing its reconfiguration capability. For example, by locking two, three or four revolute joints with superposed axes in Figure 3.4c, the eight-bar mechanism can be reconfigured in six, five or four-bar mechanisms. The three mechanisms have an equivalent kinematics with a planar four four-bar parallelogram mechanism and different degrees of overconstraint.

The six-bar mechanism can be obtained by locking the first revolute joint of each limb of the eight-bar mechanism in Figure 3.4c. The resulting six-bar mechanism has the following structural parameters: $m=6$, $p_1=p_2=3$, $p=6$, $q=1$, $k_1=2$, $k_2=0$, $k=2$, $r_l=0$, $S_{G1}=S_{G2}=3$, $r_{G1}=r_{G2}=0$, $(R_{G1})=(\boldsymbol{v}_x,\boldsymbol{v}_y,\boldsymbol{v}_z)$, $(R_{G2})=(\boldsymbol{v}_x,\boldsymbol{\omega}_y,\boldsymbol{\omega}_z)$, $(R_F)=(\boldsymbol{v}_x)$, $M_{G1}=M_{G2}=3$. Equations (2.1)-(2.6) give $r_F=5$, $M_F=1$, $S_F=1$, $N_F=1$, $T_F=0$. This six-bar mechanism has one degree of mobility and one degree of overconstraint.

Two five-bar mechanisms can be obtained by locking the first revolute joint of each limb and the last joint of just one limb in the eight-bar mechanism in Figure 3.4c. For example, if the

joints between links 1 and 2a, 1 and 2b, and 4a and 5 are locked in Figure 3.4c, the resulting five-bar mechanism has the following structural parameters: $m=5$, $p_1=2$, $p_2=3$, $p=5$, $q=1$, $k_1=2$, $k_2=0$, $k=2$, $r_l=0$, $S_{G1}=2$, $S_{G2}=3$, $r_{G1}=r_{G2}=0$, $(R_{G1})=(\boldsymbol{v}_x,\boldsymbol{v}_z)$, $(R_{G2})= (\boldsymbol{v}_x,\boldsymbol{\omega}_y,\boldsymbol{\omega}_z)$, $(R_F)=(\boldsymbol{v}_x)$, $M_{G1}=2$, $M_{G2}=3$. Equations (2.1)-(2.6) give $r_F=4$, $M_F=1$, $S_F=1$, $N_F=2$, $T_F=0$. This five-bar mechanism has one degree of mobility and two degrees of overconstraint.

The four-bar planar parallelogram mechanisms can be obtained by locking the first and the last revolute joints of each limb of the eight-bar mechanism in Figure 3.4c. The resulting four-bar mechanism has the following structural parameters: $m=4$, $p_1=2$, $p_2=2$, $p=4$, $q=1$, $k_1=2$, $k_2=0$, $k=2$, $r_l=0$, $S_{G1}=2$, $S_{G2}=2$, $r_{G1}=r_{G2}=0$, $(R_{G1})=(\boldsymbol{v}_x,\boldsymbol{v}_z)$, $(R_{G2})= (\boldsymbol{v}_x,\boldsymbol{\omega}_y)$, $(R_F)=(\boldsymbol{v}_x)$, $M_{G1}=2$, $M_{G2}=2$. Equations (2.1)-(2.6) gives $r_F=3$, $M_F=1$, $S_F=1$, $N_F=3$, $T_F=0$. The mechanism has one degree of mobility and three degrees of overconstraint.

3.3 Transition from one singularity to another

In the field of parallel manipulators, the possibility of changing assembly mode without passing through a singular configuration is well known. These kinds of transitions have been studied and it is a common issue [Pagis, 2014]. This section focuses on the SSL8M eight-bar reconfigurable mechanism for which we propose a continuously transiting from one singular assembly mode to another by using redundant actuation. In our work, we have identified six singularities as studied above from which the mechanism can bifurcate into several assembly modes.

This mechanism has an interesting property to continually transit from a constraint singularity to a constraint - redundant singularity by remaining always in a constraint singularity branch as shown in Figure 3.5. For example, the mechanism can pass from a constraint singularity as in Figure 3.2a to a constraint-redundant singularity as in Figure 3.3 by passing through various singular configurations of type Figure 3.2b.

The singular configurations in Figure 3.5 are defined by the following geometric features. The angles of rotation in the revolute joint between link 2a and link 1 denoted by (2a, 1) and between 2b and 1 denoted by (2b, 1) are identical and have opposite signs. The same is with the angles of rotation in the joint (5, 4a) and (5, 4b). In the constraint singularity branch, the rotational axis in the following joints (1, 2a), (5, 4a), (5, 4b) and (1,2b) are always parallel.

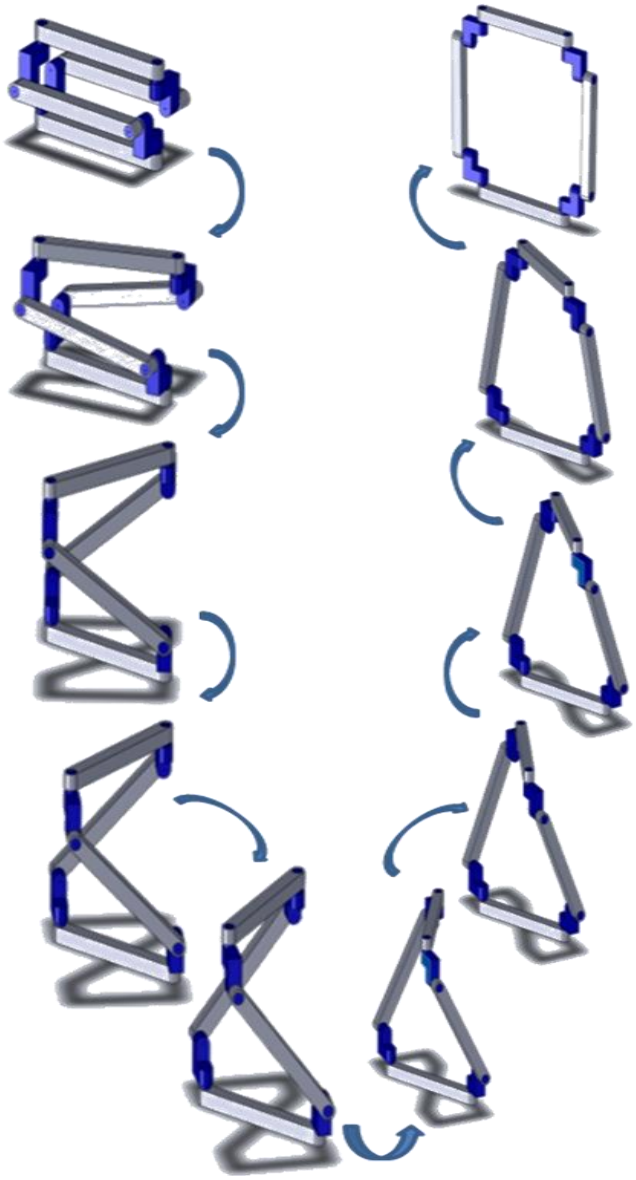

Figure 3.5 Transition between constraint singularity and constraint - redundant singularity of an eight-bar mechanism

3.4 Conclusion

In this chapter, constraint, redundant and constraint- redundant singularities have been comparatively defined and analysed. The natures of these singularities have been explained and their properties have been formalized using the novel formulae of mobility, connectivity, overconstraint and redundancy of parallel robots, recently proposed in the literature. The common property of the three types of singularities resides in the instantaneous change of connectivity between the moving platform and the base which takes place with no change in limb mobility. The common properties of constraint and constraint-redundant singularities consist in the instantaneous increase of mechanism mobility and connectivity between the moving platform and the base. The difference between these two types of singularities consists in the fact that mechanism redundancy is not affected in constraint singularity but increases in constraint-redundant singularity. The properties of the constraint-redundant

singularities are also applicable to redundant singularities. The main difference between these two types of singularities is associated with the fact that the connectivity of the moving platform with respect to the base in the parallel mechanism increases in a constraint-redundant singularity and it decreases in a redundant singularity. The analysis of these singularities associated with a reconfigurable eight-bar single loop mechanism with orthogonal/parallel axes has underlined the capacity of this mechanism to continually transit from one type of singularity to another by remaining always in a singular configuration. From these different singularities the mechanism can also get out at any time in a non-singular configuration. The singularity analysis presented in this chapter is useful for the study of reconfiguration capability of this mechanism which can take place in the various singular configurations illustrated in this chapter.

4 Chapter 4: Control strategies of the SSL8B mechanism reconfiguration: Simulation and experimental results

4.1 Introduction

Industrial robotics is booming and there are about 1.5 million industrial robots today active in the world [IFR, 2014]. Many of these robots are constituted by a serial architecture: the robot is characterized by an open kinematic chain, which implies that their links are mounted in series. These systems are relatively simple to model and feature a large workspace. However, their report on payload weight of the robot is very low. A parallel architecture is distinguished from a serial architecture where it has several kinematic chains connecting the base (fixed) to the mobile platform. These architectures have several advantages: each limb typically has a single motor which can significantly reduce the weight of the movable part of the robot. These architectures also allow improved stiffness and have a better dynamic behavior [Tlusty et al., 1999] (acceleration, report payload / total weight) as well as a better theoretical precision [Briot, 2007]. From a theoretical point of view, parallel kinematic machines allow better dynamic performances than serial ones, in terms of speed, accuracy and stiffness [Merlet, 2000]. Due to this, they seem perfectly suitable for industrial high-speed applications, such as pick and place or high speed machining. On the other hand, recent machines allow maximal acceleration, which is not achievable by the serial kinematic machines.

Despite all these advantages, the proportion of parallel robots in operation in the industry is widely lower than that of serial robots. This under-representation of parallel robots is due to two key points: parallel robots are more complex, which complicates their modeling and control. Moreover, workspace is, at equal size, lower than that of serial robots. We believe that the relative complexity of parallel robots is not a major obstacle to their industrial development. It is time being largely negligible compared to the operation time of the industrial machinery. It is mainly the small size of their workspace that now limits applications. This small size is generally due to the presence of singularities [Arakelian, 2008, Conconi et al., 2009, Gosselin et al., 1990].

The control problem for the parallel robotic platform was rigorously analyzed in the robotic community. A great variety of control approaches have been proposed. Generally, the classical control strategies from serial robotics can be used for parallel kinematic machines. By cons, even if the conventional control approaches of the serial robots can be used for parallel robots, they can induce larger errors because of the coupling between the axes of the parallel machines. Several issues with accuracy and stiffness of parallel kinematic machines were studied in the literature. One major issue is the presence of numerous joints which causes kinematic model errors because of clearance and assembly defects [Wang et al., 1993]. Another issue is that, the actuators of the parallel kinematic machine tool do not apply a torque along the end-effector motion axis, contrary to a serial one [Tlusty et al., 1999]. This results in a decrease of stiffness leading to a lack of accuracy during machining process. In the

following section, we are going to present all the control laws used in robotics that can be used to control parallel robots.

4.1.1 Control Schemes in Robotics

The knowledge on parallel robotics comes directly from the serial one. Therefore, parallel kinematic machines are mainly controlled with the same strategies as serial ones [Khalil et al., 2002]. Figure 4.1 illustrates the various control laws used for robotic manipulators. The most commonly used control law for industrial robots is a decentralized "proportional, integral, derivative" (PID) control which is also called as linear single-axis control. More sophisticated linear or nonlinear control schemes have been developed, such as computed torque control (also called as decoupling control) and passivity-based control. Others advanced control laws such as adaptive control and predictive controls are proposed in the literature to minimize large servo errors.

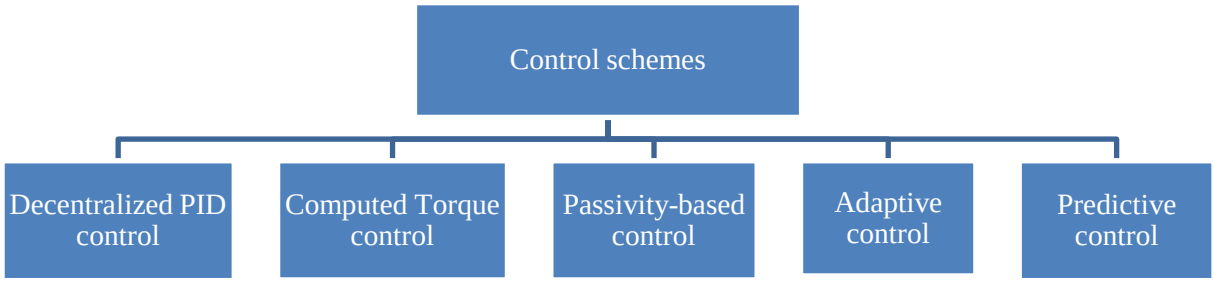

Figure 4.1 Control methods for Robotic manipulators

Figure 4.1 enumerates the control schemes presented in the literature. In the following sub-sections we analyze these control schemes and thereafter make a choice of control for the SSL8B mechanism described in section 4.1.2.

4.1.1.1 Proportional, Integral and Derivative control

The PID control is most popular solution for the control of serial robots and processes. For most of today's industrial robots, a local decentralized PID control with constant gains is implemented for each joint. The advantages of this control are simplicity of implementation and the low computational cost. Also, the choice of the gains can be achieved according to the first natural frequency of the robot [Khalil et al., 2004]. However, for this decentralized control law, it is assumed that each axis is independent of the others. We can see that this is not a publicity to make it simple and obtain slow movements but this assumption is quickly becoming invalid on parallel robots with high dynamics.

PID control in joint space is implemented to control the joints of the mechanism with constant gains without using any model of the robot. Therefore, this kind of control law can be quickly implemented on the robot controller. However, by using PID control in joint space, the end-effector motion is not controlled directly and it is then difficult to compensate pose errors due to geometric calibration uncertainties (obstacle avoidance is performed in trajectory planning

and / or active perception). As a consequence, if the motion of the end-effector has to be specified and controlled, PID control in task space will be preferred to PID control in joint space. However, since PID control in task space requires the knowledge of direct or / and inverse geometric model, PID control in task space is very difficult to implement for parallel robots.

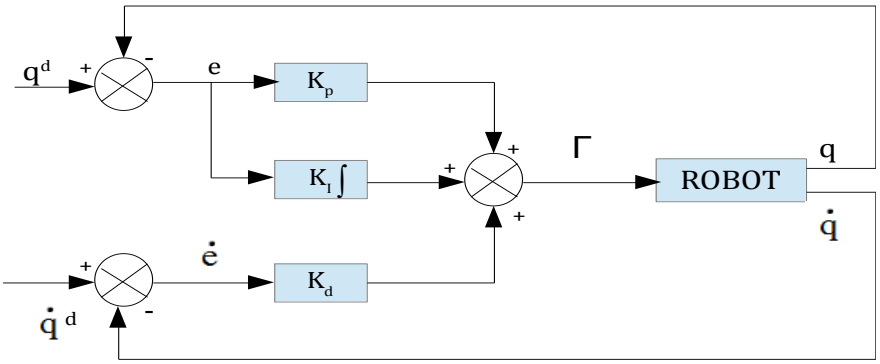

Figure 4.2 Block diagram of a PID control scheme in the joint space

The block diagram of such a control scheme in the joint space is shown in figure 4.2. The control law for the corresponding scheme is given by:

$$\Gamma = K_p(q^d - q) + K_d(\dot{q}^d - \dot{q}) + K_I \int_{t_0}^{t} (q^d - q) d\tau \tag{4.1}$$

where, $q^d(t)$ and $\dot{q}^d(t)$ denote the desired joint positions and velocities (computed by using trajectory generator as described in Sec.4.2.3), and K_p, K_d and K_I are positive definite diagonal matrices whose generic elements K_{pj}, K_{dj} and K_{Ij} are respectively the proportional, derivative and integral gains of each axis.

4.1.1.2 Computed torque control

Another most commonly used control strategy is the computed torque control. The control law is based on the formulation of inverse dynamic model of the robot:

$$\Gamma = A(q)\ddot{q} + H(q, \dot{q}) \tag{4.2}$$

Where, $A(q)$ is the inertia matrix of the robot and $H(q, \dot{q})$ is the vector of dynamic parameters such as inertial and frictional parameters.

By replacing $\ddot{q}$ in equation 4.2 by an adapted control signal u, an exact linearization of the dynamics is ensured. The following control signal is used:

$$u = \ddot{q}_d + K_v \dot{e} + K_d e \tag{4.3}$$

This control strategy can be improved with friction and backlash compensation, like that of the linear single-axis control. This control does not cope very well with modeling errors

[Khalil et al., 2002] and require the dynamic model of the robot. Modeling errors create perturbation on the tracking error behavior which may lead to a lack of stability and accuracy. Therefore this kind of control law can be coupled with an adaptive control algorithm (as described hereafter, see Fig.4.3) in order to reduce the tracking error. Then, the main advantage of computed torque control for parallel robots is the fact that coupling between axis are taken into account. On the contrary, the main inconvenient is the fact that the control law requires a good dynamic model of the robot which is difficult to obtain for parallel robots.

Further analysis of the different types of controls applied to parallel mechanisms are proposed in [Khalil et al., 2004, Spong et al., 2006, Paccot et al., 2009].

4.1.1.3 Passivity-based control

In this section, we investigate another approach that used the property of passivity of the robot. These control laws modifies the natural energy of the robot in order to satisfy the desired position control. Hamiltonian formulations are used to calculate the dynamics of the robot.

The Hamiltonian gives the total energy of the robot:

$$H = E + U \tag{4.4}$$

where, $E(q,\dot{q})$ is the kinematic energy of the robot equal to $\frac{1}{2}\dot{q}^T A(q)\dot{q}$

$U(q)$ is the potential energy of the robot

$A(q)$ is the inertia matrix of the robot

The passivity control can be classified as passivity-based position control, passivity-based tracking control and Lyapunov-based method.

Let us assume that we want to drive the robot to a desired position q^d. Intuitively, this can be achieved by shifting the open-loop energy minimum from $(\dot{q}=0, q=0)$ towards $(\dot{q}=0, e=0)$ for the closed-loop system, where $(e=q^d-q)$ is the position error. This shifting can be obtained by reshaping the potential energy of the system such that it attains the desired minimum at $(e=0)$. Let us define the control law as:

$$\Gamma = -\frac{\partial U^*(q)}{\partial q} + \frac{\partial U(q)}{\partial q} + v \tag{4.5}$$

where, v is the (nx1equation format) new input control vector and,

$$U^* = \frac{1}{2} e^T K_p e \tag{4.6}$$

After simplification, the control law in equation (4.5) becomes,

$$\Gamma = K_p e - K_d \dot{q} + Q(q^d) \qquad (4.7)$$

Equation 4.7 represents gravity compensation and a linear state-feedback loop where $Q(q)$ is the vector of gravity torques.

4.1.1.4 Adaptive control

This control method is used to estimate or adjust on-line the parameter values used in the control law. For example, this kind of algorithm is used to adapt on-line the robot model parameters since it (kinematic, dynamic …) is not often exactly known. The adaptive control is further classified into adaptive feedback linearizing control and adaptive passivity-based control. [Khalil et al., 2004]

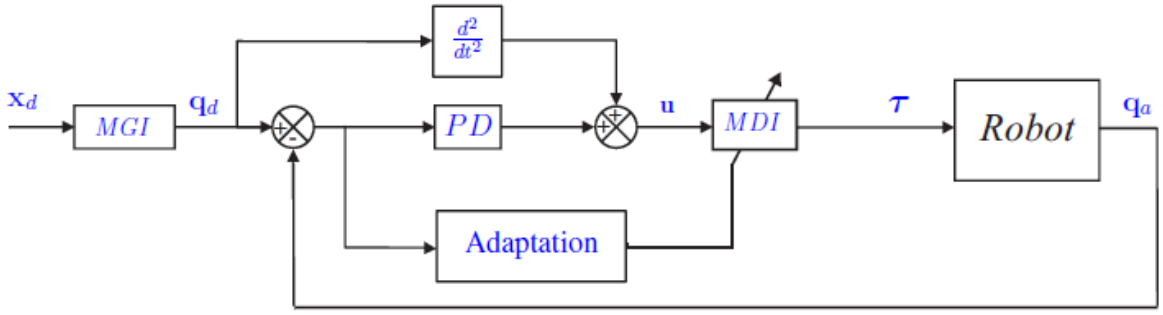

Figure 4.3 Principle of the adaptive control applied to computed torque control [Pagis, 2015]

Adaptive control differs from other types of control by the fact that the parameters of the model it uses varies over time. Figure 4.3 shows the block diagram of the adaptive control applied to the computed torque control law. Rather than calculating the control to be applied on a horizon prediction as done in predictive control, a law of adaptation modifying the parameters of the dynamic model is determined. This is particularly suitable for the control of systems whose parameters change over time.

4.1.1.5 Predictive control

Predictive control was proposed explicitly for the first time in 1960 [Propoï, 1963]. However, it was not discovered until 1987 that the first generalized predictive control has been formalized [Clarke et al., 1987]. The idea is to insert into the control algorithm a predictor of concerning the evolution of the process output from a model [Richalet 1993b]. The computer determines, at the present sampling instant, the control sequence to be applied over a period of prediction so that the output has the desired behavior over the horizon.

This type of control is particularly suitable for mobile robotics [Bouton, 2009, Lenain et al., 2004, Lenain, 2005] and in industry [Richalet 1993a], but is difficult to adapt to parallel mechanisms because of its models complexity. Indeed, predictive control algorithm requires a long computation time not very compatible with the parallel robot models.

Most applications in parallel robots with the predictive control robot are based on a principle similarly based on a compromise between modeling accuracy and performance of the order. This technique seems difficult to integrate to our robot.

4.1.2 Conclusion and choice of position control

The control laws presented in this section rely on the availability of joint positions and velocities. Out of all the methods presented above, we choose position control scheme to be implemented in the SSL8B mechanism. As with other control schemes like dynamic control, adaptive control, etc… it is difficult to control the motions of the 8-bar mechanism (since the model used to compute the control variable is too difficult to obtain), then the position control is desirable.

4.2 Control of the 8-bar mechanism

As discussed in section 4.1.1, there are many different control approaches for parallel manipulators. This section discusses the particular case of redundant actuation and the two position control strategies that are implemented on the 8-bar reconfigurable mechanism.

Parallel mechanisms frequently contain an unstable type of singularity that has no counterpart in serial mechanisms. The robot loses the ability to counteract external forces in certain directions, when the mechanism is at or near this type of singularity. The singularity can be modified or removed, by adding kinematic linkages which alters the mechanism. Another approach is to actuate certain unactuated degrees of freedom. The manipulability is guaranteed to improve over the original mechanism, but the mechanism is now over-actuated. The following section deals with the redundant actuation to overcome this problem.

4.2.1 Particular case of redundant actuation mechanism

By using 5 actuators, the 8-bar mechanism can be considered partially as a redundant actuated mechanism. These redundant robots are mechanisms with more actuators than required for doing the prescribed task in the task space. Redundant actuation is achieved by [Gogu, 2008a]:

- Actuating some of the passive joints within the existing limbs.
- Introducing additional actuated limbs beyond the minimum necessary to actuate the manipulator.
- Introducing some additional actuated joints within the limbs beyond the minimum necessary to actuate the manipulator.

Actuator redundancy does not affect the connectivity of the end-effector but only increases the number of actuators. In all case, only ‘M’ actuators can have independent motions. The other actuators have dependent motions. A selective choice of actuators with independent motion could have more advantages.

Redundancy in parallel manipulators is used to eliminate some singular configurations [Wang and Gosselin 2004; Kurtz and Hayward 1992; Merlet 1997; Firmani and Podhorodeski 2004, Alberich et al. 2006], to minimize the joint rates, to optimize the joint torques/forces [Dasgupta and Mruthyunjaya 1998; Bruckman et al 2006; Nokleby et al. 2005] to increase dexterity workspace [Marquet et al 2001a,b], stiffness [Chakarov 2004], eigen frequencies, kinematic and dynamic accuracy [Valasek et al. 2004], to improve velocity performances [Krut et al. 2004] and both kinematic and dynamic control algorithms [Liu et al. 2001; Cheng et al. 2003], to develop large forces in micro electro-mechanical systems [Mukherjee et al. 2001], decoupling the orientations and the translations [Jin et al. 2004, Gogu 2006], to obtain reconfigurable platforms (Mohamed and Gosselin 2005) and limbs [Fischer et al. 2004] or combined advantages [Nahon and Angeles 1991; Zanganach and Angeles 1994a,b; Kim 1997; Kock and Scumacher 1998, 2000; Mohamed 2003a,b].

New formulae for calculating the degree of structural redundancy of the parallel robots have been proposed by [Gogu, 2006, 2008a]. Actuation redundancy is achieved by introducing additional actuated joint within the limbs, beyond the minimum necessary to actuate the manipulator. In this way, motion coupling in parallel manipulators can be reduced.

For our mechanism we have a minimum of two degrees of freedom in a general configuration and five degrees of freedom for a planar constraint-redundant configuration. Hence we introduce five motors to cross from one type of singularity to another. Redundant robot control techniques cannot be used in all cases. Therefore, we prefer using more advanced techniques (multi-model control) [Pagis, 2015] coupled with PID controller to reflect the local actuation redundancy of the robot. The following sections explain the various control strategies used for the SSL8B mechanism.

4.2.2 General principle of position control dedicated to SSL8B reconfigurable mechanism

This part aims to detail the two position control approaches that are implemented for the SSL8B mechanism, namely the synchronization of the actuators and modification of the degrees of actuation. Synchronization of actuators can be achieved by two ways: namely the PID controller method (by tuning the values of the gain) and by the conventional control of generating trajectories respecting the geometric model. The modification of the degrees of actuation is attained by the multi-model control strategy. In the following subsection, we will discuss in details about these approaches with some simulated results. Figure 4.4 illustrates the classification of position control for the 8-bar mechanism.

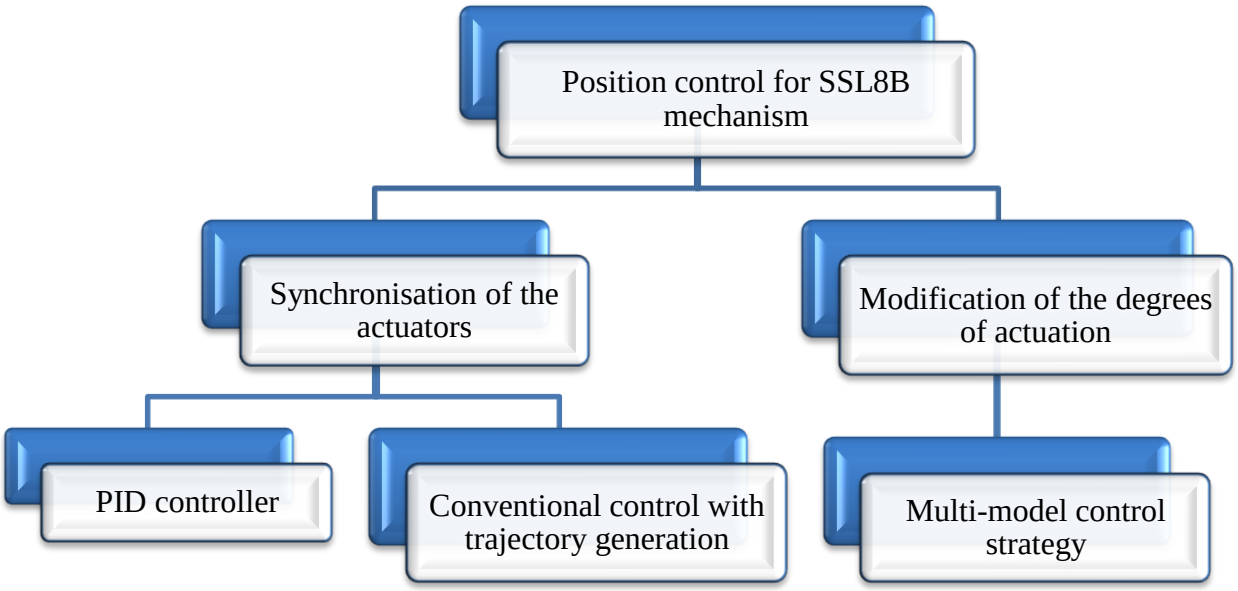

Figure 4.4 Control strategies for SSL8B mechanism

These position control techniques can follow a path in the joint space. This trajectory is generated using conventional approaches as discussed in the next section.

4.2.3 Trajectory generation

Trajectory generation is obtaining a desired motion of the parallel manipulator in the joint space. The basic concept of trajectory generation is to move the robot manipulator from an initial joint position to some desired final joint position by using interpolation functions as described in [Khalil et al., 2004].

Several interpolation functions (denoted $r(t)$ in the sequel) can provide a trajectory generation and are described below:

Table 4.1 Various interpolation functions

Interpolation functions	Equation
Linear Interpolation	$q(t) = q_i + \frac{t}{t_f} \times D$
Third degree polynomial	$q(t) = q_i + \frac{3}{{t_f}^2} \times D - \frac{2}{{t_f}^3} \times D$
Fifth degree polynomial	$q(t) = q_i + r(t) \times D \; with$ $r(t) = 10\left(\frac{t}{t_f}\right)^3 - 15\left(\frac{t}{t_f}\right)^4 + 6\left(\frac{t}{t_f}\right)^5$
Bang-bang profile	$q(t) = q_i + 2\left(\frac{t}{t_f}\right)^2 D \; for \; 0 \le t \le \frac{t_f}{2}$ $q(t) = q_i + [-1 + 4\left(\frac{t}{t_f}\right) - 2\left(\frac{t}{t_f}\right)^2 D \;\; \frac{t_f}{2} \le t \le t_f$

where,

q_i and q_f are the joint coordinate vectors corresponding to the initial and final configurations. t_f is the transfer time of the trajectory and *D* is the joint displacement corresponding to the difference between q_f and q_i

In our work, in order to ensure that we have continuity in acceleration as well as to avoid exciting the resonances in the mechanism, we use the fifth degree polynomial interpolation function with smooth position and velocity profiles. The general form of this polynomial is:

$$q(t) = a_0 + a_1 t + a_2 t^2 + a_3 t^3 + a_4 t^4 + a_5 t^5$$

By taking derivation of this equation, we get the joint velocity and acceleration as,

$$\dot{q}(t) = a_1 + 2a_2 t + 3a_3 t^2 + 4a_4 t^3 + 5a_5 t^4$$
$$\ddot{q}(t) = 2a_2 t + 6a_3 t + 12a_4 t^2 + 20a_5 t^3$$

Six constraints should be satisfied to obtain an interpolation of polynomial of fifth degree. These six constraints are as follows:

$$q(0) = q_i,\ q(t_f) = q_f,\ \dot{q}(0) = 0,\ \dot{q}(t_f) = 0,\ \ddot{q}(0) = 0,\ \ddot{q}(t_f) = 0.$$

These constraints are used to calculate the coefficients of a fifth degree polynomial which gives us the interpolation function as:

$$r(t) = 10\left(\frac{t}{t_f}\right)^3 - 15\left(\frac{t}{t_f}\right)^4 + 6\left(\frac{t}{t_f}\right)^5$$

The two approaches used for control of the 8-bar mechanism will be presented in detail in the following section and both of them uses the fifth degree polynomial for trajectory generation.

4.2.4 The first control strategy: Synchronization of the actuators

The robot has a property of transiting from one singular configuration to another. This is attained by synchronizing the actuators. Synchronization is achieved either by adjusting the values of the gains in the PID controller or by using the conventional control by generating a trajectory respecting the geometric model of the SSL8B mechanism.

4.2.4.1 PID control by adjusting the values of gains

Classical tuning of the gains K_p, K_d and K_i allows to have a limited positioning error. The integral gain K_i is generally increased to compensate for the dry frictions and gravity effects, while the derivative gain K_d is generally decreased to cope with measurements noise.

Additional features such as friction, gravity and backlash compensation in the industrial controllers improve accuracy. Therefore, a PID control ensures an efficient compensation of the small dynamics and the behaviors of the stiff mechanical structure ensure a good static accuracy.

4.2.4.2 *Conventional control with trajectory generation*

Having obtained the geometric model of the SSL8B mechanism (chapter 2: section 2.3.4), we describe in mathematical form the relationship between the joint variables, position and orientation of the robot. This mathematical representation is obtained from the travelling coordinate system which involves the link between the rotation and translation of the adjacent links. As a conclusion, by using the geometric model of the robot for dependent actuated joints coupled with a trajectory generator for independent actuated joints, it is possible to synchronize on-line all the actuated joints motions.

4.2.5 The second control strategy: Modification of the degrees of actuation using multi-model control strategy

In this control strategy, we use a selection matrix which helps us to modify the degrees of actuation with respect to time.

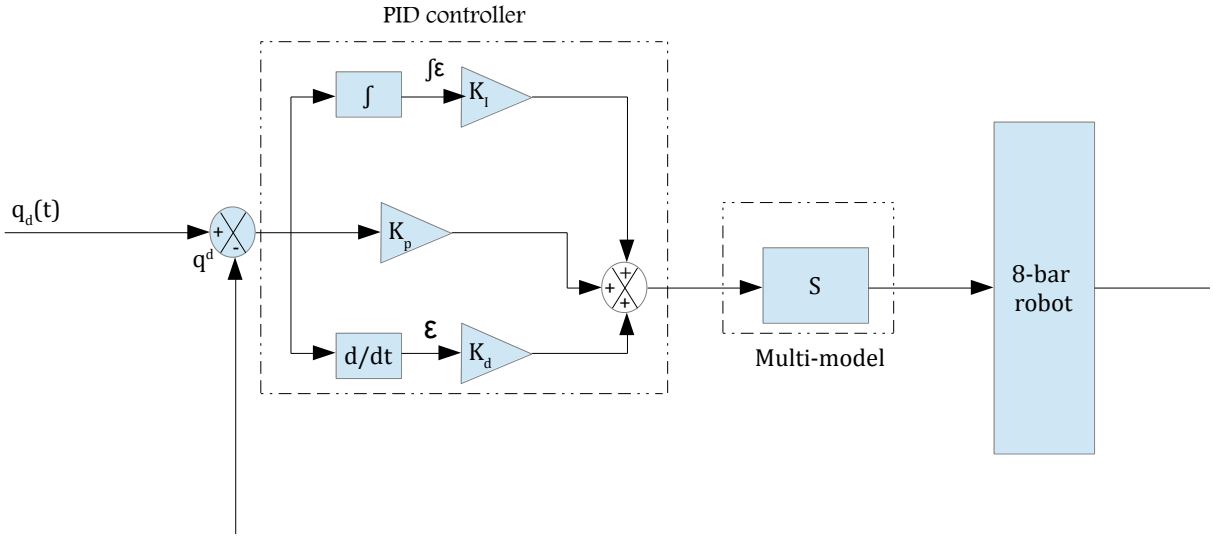

Figure 4.5 Schema of the principle of the multi-model control law

Figure 4.5 illustrates the control law of the multi-model control strategy. 'S' is a selection matrix which permits to activate or deactivate a motor in real time.

where,

$$S = \begin{pmatrix} 1 & \cdots & 0 \\ \vdots & \ddots & \vdots \\ 0 & \cdots & 1 \end{pmatrix} \forall\, t < \tau \text{ and } S = \begin{pmatrix} 1 & \ldots & 0 \\ \vdots & 0 & \vdots \\ 0 & \ldots & 1 \end{pmatrix} \forall\, t \geq \tau$$

where, τ is calculated in function of time from which the robot approaches a singular position. τ can be calculated with the conditioning of matrix J. The diagonal matrix 'S' can also be used with transition functions where the diagonal permits to deactivate one or more motors in a flexible manner to avoid the deterioration of the mechanism.

$$S = \begin{pmatrix} \sigma 1(t) & \cdots & 0 \\ \vdots & \ddots & \vdots \\ 0 & \cdots & \sigma 1(t) \end{pmatrix}$$

With, σ (t) = a_0+ a_1 t+ a_2 t^2+ a_3 t^3

σ (t= t_1) = 1

σ (t= t_2) = 0.

$\dot{\sigma}$ (t= t_1) = $\dot{\sigma}$ (t= t_2) = 0 (t_1 and t_2 are calculated in function of the conditioning of matrix J)

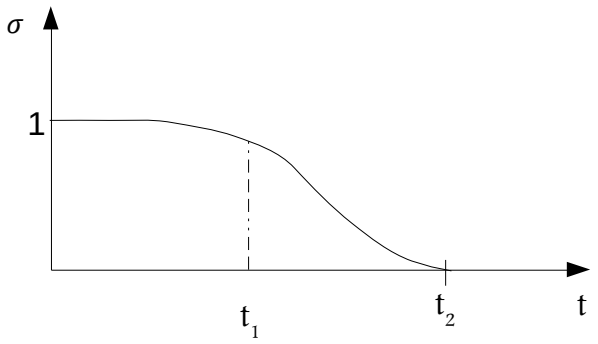

Figure 4.6 Graph of σ Vs t

$$\Longrightarrow \begin{cases} a_0 + a_1 t_1 + a_2 t_1^2 + a_3 t_1^3 = 1 \\ a_0 + a_1 t_2 + a_2 t_2^2 + a_3 t_2^3 = 1 \\ a_1 + 2 * a_2 t_1 + 3 * a_3 t_1^2 = 1 \\ a_1 + 2 * a_2 t_2 + 3 * a_3 t_2^2 = 1 \end{cases}$$

$$\Longrightarrow \underbrace{\begin{pmatrix} 1 & t_1 & t_1^2 & t_1^3 \\ 1 & t_2 & t_2^2 & t_2^3 \\ 0 & 1 & 2t_1 & 3t_1^2 \\ 0 & 1 & 2t_2 & 3t_2^2 \end{pmatrix}}_{A} \underbrace{\begin{pmatrix} a_0 \\ a_1 \\ a_2 \\ a_3 \end{pmatrix}}_{X} = \underbrace{\begin{pmatrix} 1 \\ 0 \\ 0 \\ 0 \end{pmatrix}}_{B}$$

This is of the form $AX = B \Rightarrow X = A^{-1}B$. Hence we calculate the transition matrix 'S'.

In the following section, we are going to test these control laws on the robot models carried out by ADAMS to perform advanced simulations using Adams / Simulink. Henceforth, we present firstly the virtual models/prototype of the SSL8B reconfigurable robot.

4.3 Advanced simulation results of the SSL8B control law

Now, we implement the control strategies presented in section 4.2.2 to our SSL8B reconfigurable mechanism. Before that, we will make a study on the prototype modeled using ADAMS. Section 4.3.1 details the development of the prototype.

4.3.1 Description of the prototype and development of the ADAMS model

The prototype consists of 8 parts as shown in the figure 4.7.

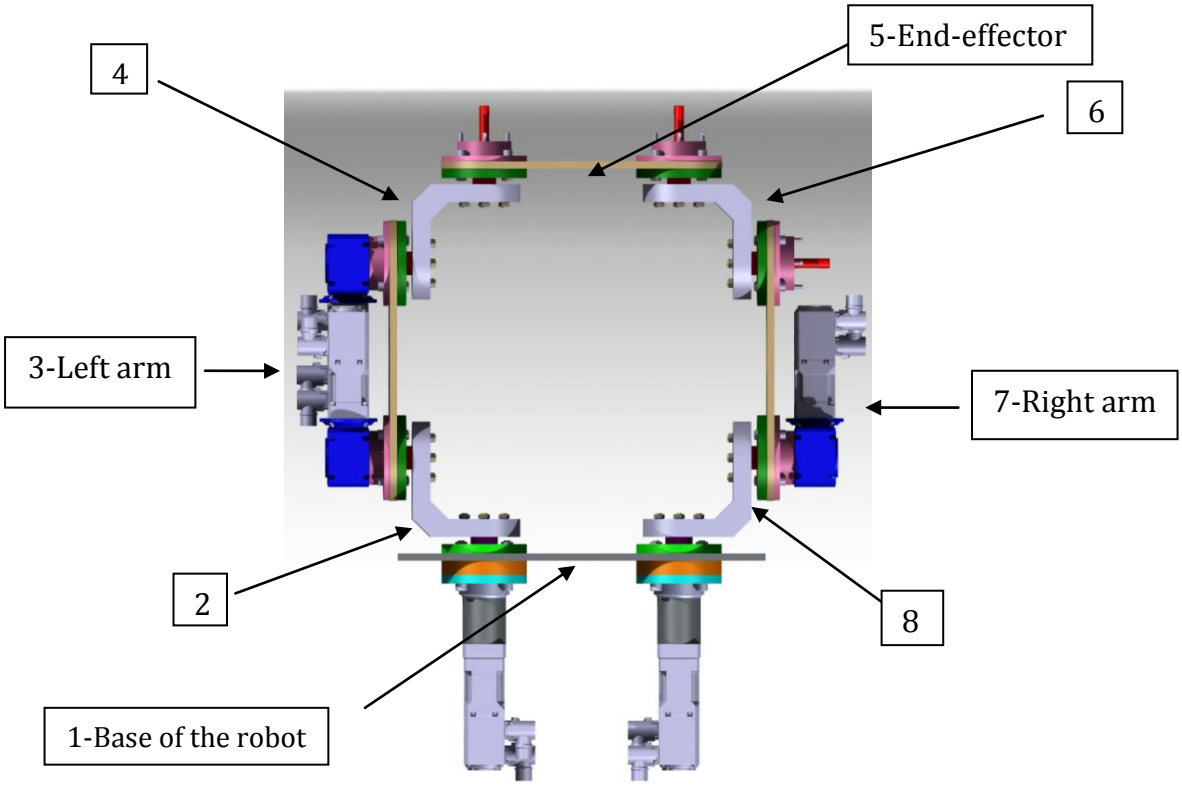

Figure 4.7 Front view of the 8 bar linkage

The base of the robot comprises an aluminium plate which serves to fix the robot on the support and to maintain the motors and other accessories. Two motors with their gearboxes are installed at the base of the robot. The four square shaped parts helps to rotate the side arms of the 8-bars about the axes of the base engine. The end-effector is composed of an aluminum plate with two revolute joints.

ADAMS helps us to estimate the dynamic parameters which can be directly used to control the SSL8B reconfigurable mechanism. The table 4.2 below shows the mass and the inertial parameters of all the parts shown in figure 4.7.

Table 4.2 Mass and Inertial parameters of the 8-bar mechanism

Part number of the prototype as shown in figure 4.7	Mass	Inertial parameters in $kg.mm^2$
1-Base of the robot	9.229kg	$I_{XX} = 9.5^{-002}$ $kg.mm^2$ $I_{YY} = 0.266$ $kg.mm^2$ $I_{ZZ} = 0.183$ $kg.mm^2$ $I_{XY} = I_{ZX} = I_{YZ} = 0$ $kg.mm^2$
2-Connector between 1 and 3	2.218kg	$I_{XX} = 9.0^{-003}$ $kg.mm^2$ $I_{YY} = 7.0^{-003}$ $kg.mm^2$ $I_{ZZ} = 6.0^{-003}$ $kg.mm^2$ $I_{XY} = I_{ZX} = I_{YZ} = 0$ $kg.mm^2$
3-Left arm	8.23kg	$I_{XX} = 0.102$ $kg.mm^2$ $I_{YY} = 0.101$ $kg.mm^2$ $I_{ZZ} = 1.7^{-002}$ $kg.mm^2$ $I_{XY} = I_{ZX} = I_{YZ} = 0$ $kg.mm^2$
4-Connector between 3 and 5	2.217kg	$I_{XX} = 1.0^{-002}$ $kg.mm^2$ $I_{YY} = 7.0^{-003}$ $kg.mm^2$ $I_{ZZ} = 6.0^{-003}$ $kg.mm^2$ $I_{XY} = I_{ZX} = I_{YZ} = 0$ $kg.mm^2$
5-End-effector	2.818kg	$I_{XX} = 4.4^{-002}$ $kg.mm^2$ $I_{YY} = 3.0^{-003}$ $kg.mm^2$ $I_{ZZ} = 4.6^{-002}$ $kg.mm^2$ $I_{XY} = I_{ZX} = I_{YZ} = 0$ $kg.mm^2$
6- Connector between 5 and 7	2.217kg	$I_{XX} = 1.0^{-002}$ $kg.mm^2$ $I_{YY} = 7.0^{-003}$ $kg.mm^2$ $I_{ZZ} = 6.0^{-003}$ $kg.mm^2$ $I_{XY} = I_{ZX} = I_{YZ} = 0$ $kg.mm^2$
7-Right arm	5.681kg	$I_{XX} = 7.0^{-002}$ $kg.mm^2$ $I_{YY} = 7.0^{-002}$ $kg.mm^2$ $I_{ZZ} = 1.2^{-002}$ $kg.mm^2$ $I_{XY} = I_{ZX} = I_{YZ} = 0$ $kg.mm^2$
8- Connector between 7 and 1	2.218kg	$I_{XX} = 9.0^{-003}$ $kg.mm^2$ $I_{YY} = 7.0^{-003}$ $kg.mm^2$ $I_{ZZ} = 6.0^{-003}$ $kg.mm^2$ $I_{XY} = I_{ZX} = I_{YZ} = 0$ $kg.mm^2$

Figures 4.8, 4.9 and 4.10 shows the different parts of the b-bar linkage illustrated in figure 4.7.

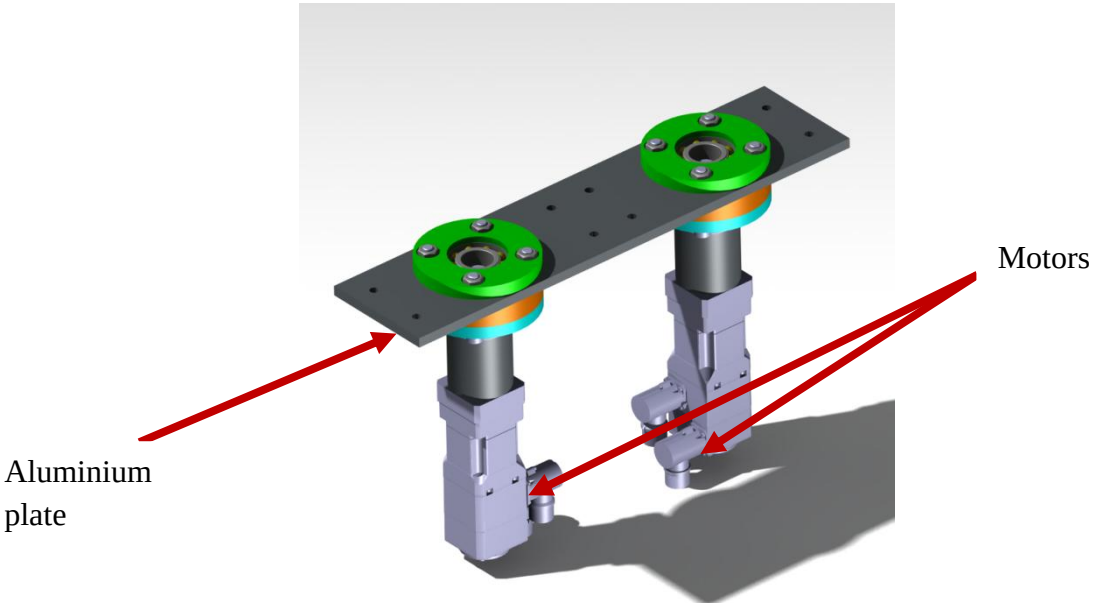

Figure 4.8 Base of the robot

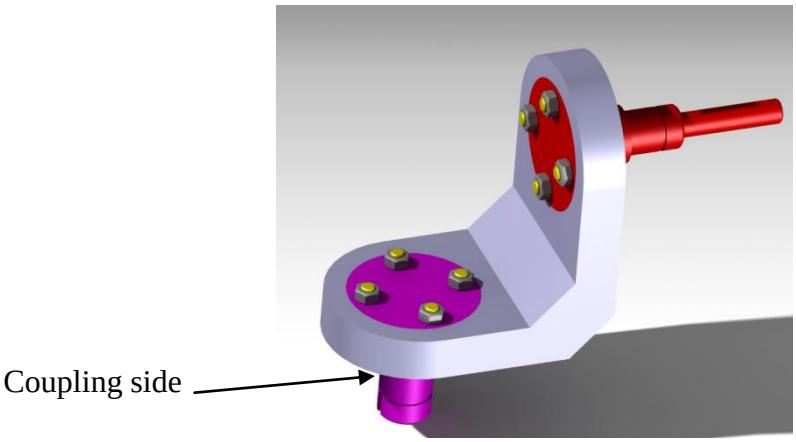

Figure 4.9 Square shaped parts of 2, 4, 6 and 8 in reference to figure 4.7

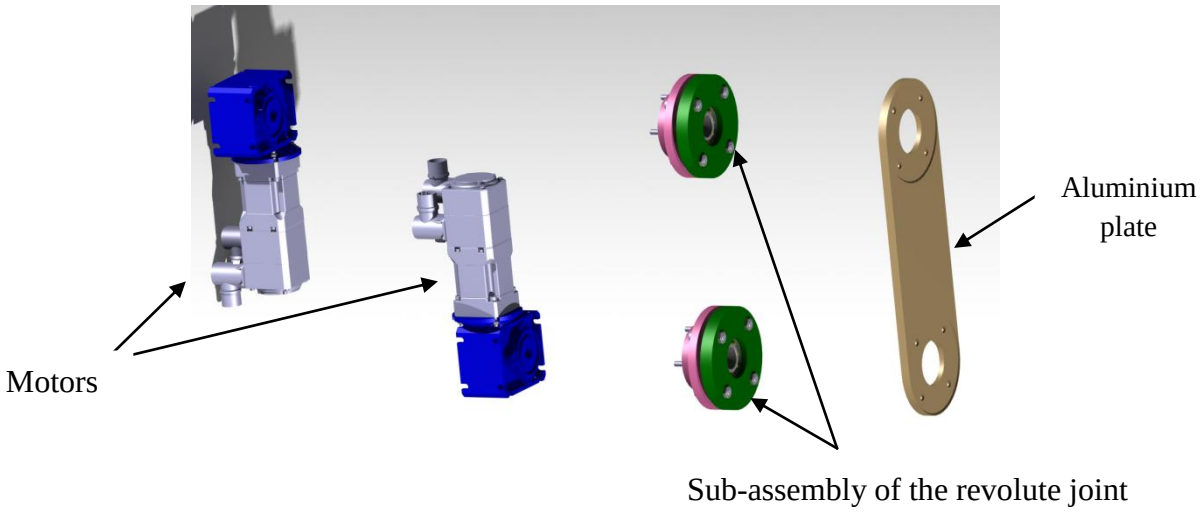

Figure 4.10 Accessories used in right and left arm

Figure 4.11 shows the real prototype of the SSL8B mechanism. Two motors are already mounted on the base. Three motors will be fixed on the robot arm. Once this is done, the robot is ready for experimentation.

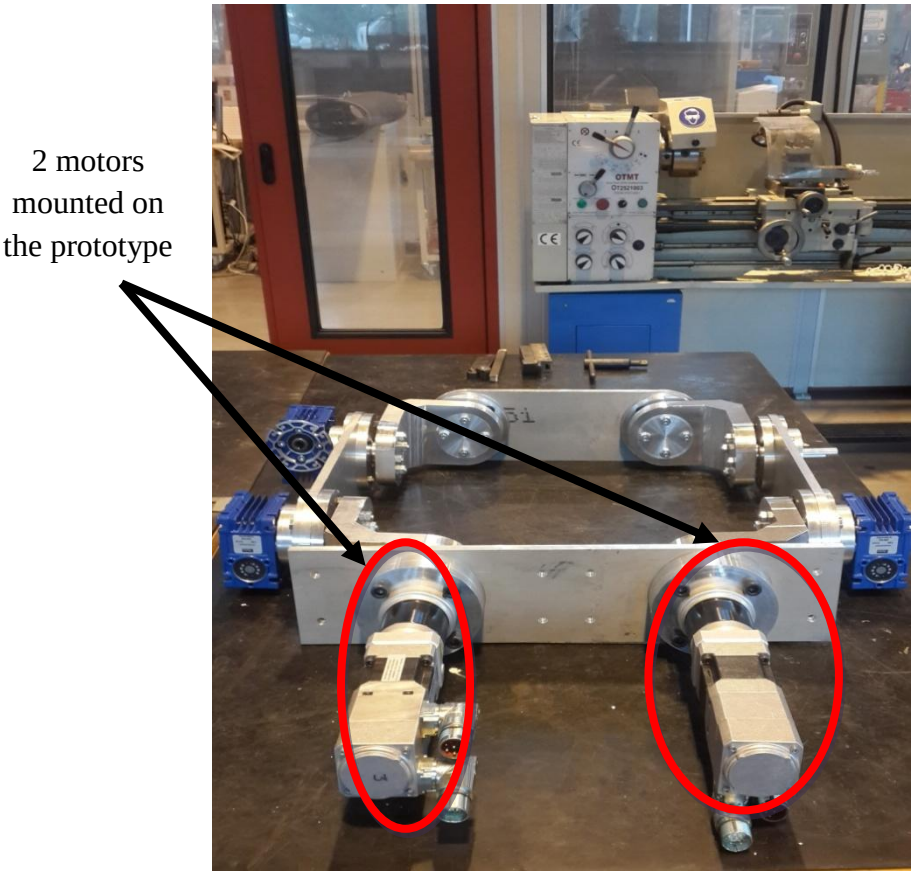

Figure 4.11 Real prototype of the SSL8B mechanism

Figure 4.12 shows the gearboxes which help to couple the prototype with the motors. They are used to transmit the rotational movement of the motors mounted on the arms (3 motors where two are on the left arm and one on the right arm) from the axis of rotation of these actuators. So these bevel gears will be coupled with three actuators. Coupling and transmission of rotational movement is by a wedge on the side as shown below in figure 4.12.

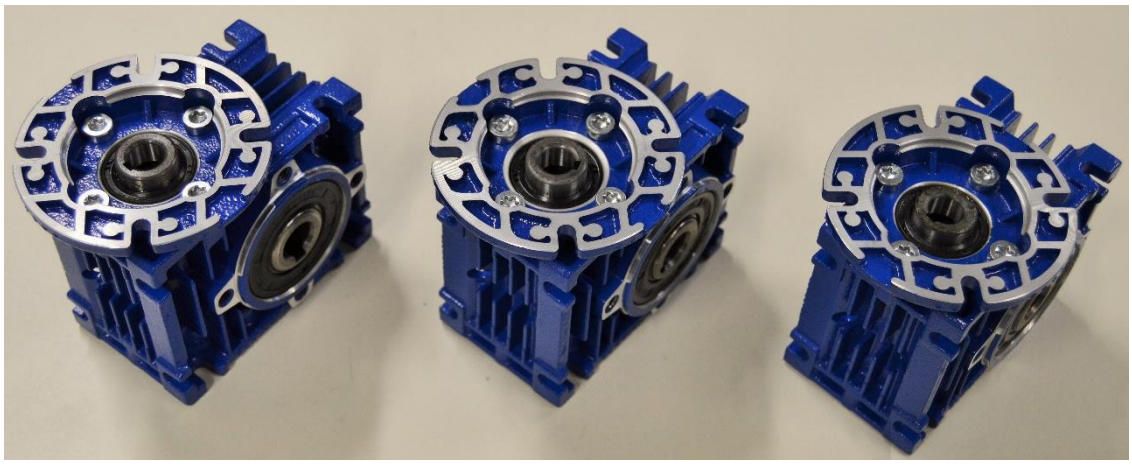

Figure 4.12 The three bevel gearboxes acquired

4.3.2 Dynamic model of the robot using Adams

The dynamic model represents the robot's motion equations and gives an idea about the robot's behavior when performing a specific task. This model allows establishing relationships between couples (forces) developed by the actuators and the positions, speeds and accelerations of the mechanism joints to control.

Parallel robots are single or multiple closed loop mechanisms. Complexity in the formulation of the dynamic model using the Lagrangian method increases with the number of joints and links as well as the loop-closer constraints. Developing the dynamic model for a parallel manipulator has been of great challenge. The ADAMS software helps to generate the dynamic model of a closed loop mechanism. Since obtaining the "dynamic model" of the 8-bar mechanism is complex, we use modeling robots with ADAMS/ Controls. This helps us to generate a robot block for the use in MATLAB/Simulink.

The mechanism can be controlled using ADAMS/Controls in connection with the MATLAB/Simulink environment. The ADAMS/Controls product is an add-on product to ADAMS. This product has been created for the ADAMS user to analyze the mechanism in either the control application environment or in the ADAMS environment. The model is used in the control scheme to predict the behavior of the system using a PID controller. The SSL8B is firstly modeled in ADAMS and is parameterized which facilitates model modification. The length of the bars and the orientation of the axes of rotation of each revolute join are parameterized. Figure 4.13 show the 5 actuators that are controlled for a planar 8-bar mechanism. $\gamma_1, \gamma_2, \gamma_3, \gamma_4$ and γ_5 shown in figure 4.13 are the joint torques corresponding to the five joints to be controlled.

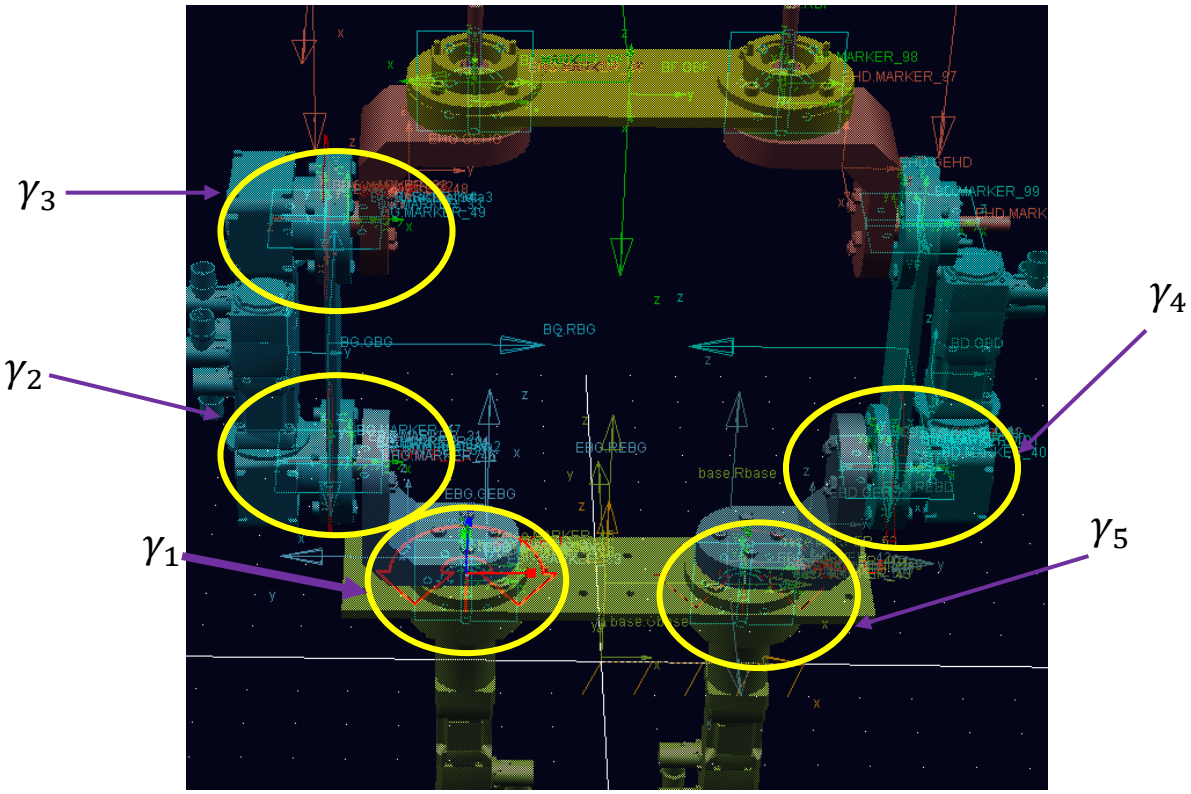

Figure 4.13 ADAMS model of the eight bar mechanism

4.3.3 Application of the two control strategies on the SSL8B reconfiguration mechanism

In section 4.2.2 we have discussed the theoretical aspects on the two control strategies. In the former part of this section, we will induce few motions in the joints in ADAMS to show the various configurations of the mechanism. In the latter part of this section, we are going to apply control algorithms on the prototype of the 8-bar reconfigurable mechanism and show some simulated results using ADAMS coupled with Simulink.

By actuating the two motors at the base and by imposing a rotational movement of 90 °, the robot arrives to the 4-bar mechanism configuration as shown below:

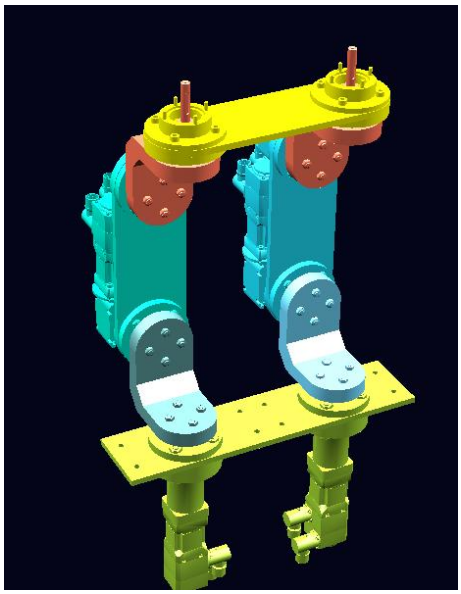

Figure 4.14 SSL8B mechanism at the 4-bar singular configuration

Other configurations can also be achieved. Those configurations are shown below:

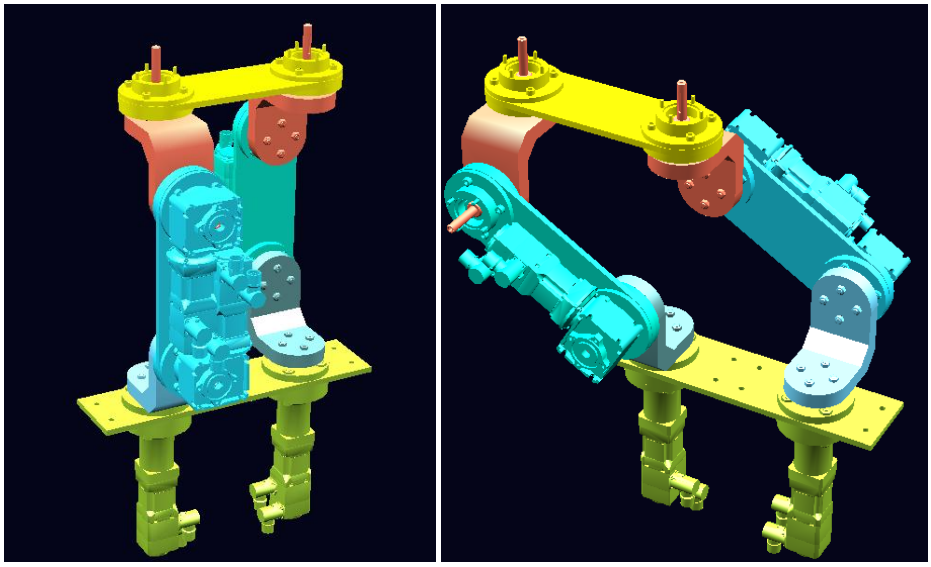

Figure 4.15 Other 4-bar configurations (opposed)

There are numerous assembly modes for this mechanism. We will consider some particular assembly modes to explain how the eight-bar linkage reconfigures.

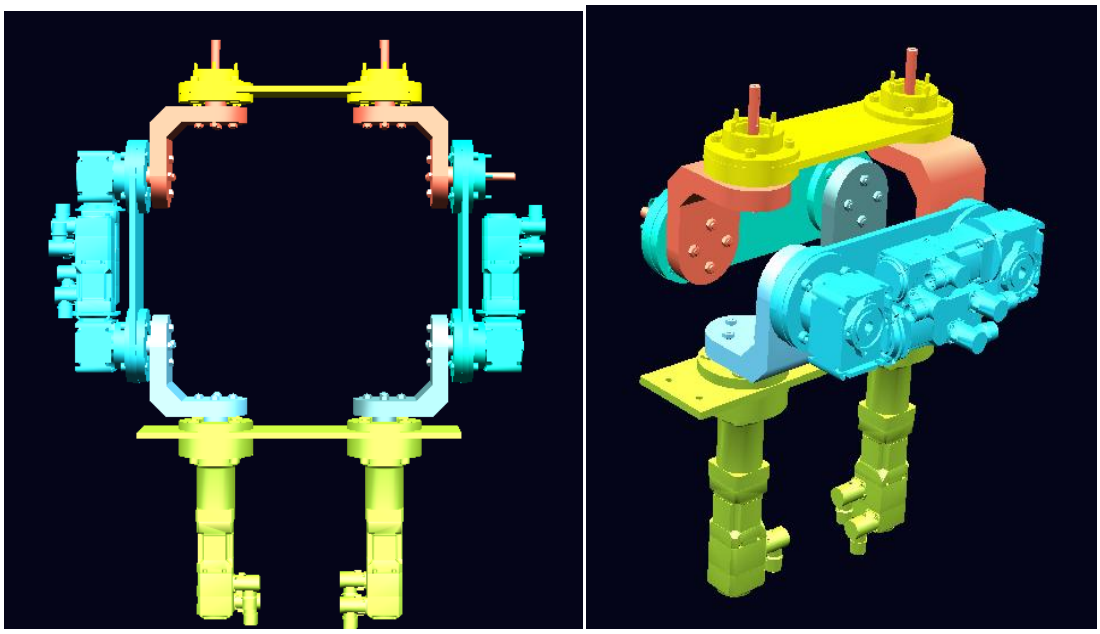

Figure 4.16 Two solutions after bifurcation (a.) Solution with constraint-redundant singularity (b.) Solution with constraint singularity

In figure 4.16, the SSL8B mechanism is able to bifurcate from a planar constraint-redundant singular configuration (figure 4.16a) to a constraint singular configuration (figure 4.16b). These configurations are identified as a constraint-redundant singularity and constraint singularity in Aimedee et al. [Aimedee et al., 2015]

After structural analysis, as we have presented in the previous sections, we find out that the mobilities are five and four for the mechanisms illustrated in figure 4.16a and figure 4.16b respectively.

The configuration shown in figure 4.16b is simulated from the initial position of the planar 8-bar mechanism to this folded configuration by actuating four motors (we actuate always 5 motors even if the motion is null: the applied torque maintain the joint in a fixed position), two motors at the base and two motors of the two arms with synchronized rotational movement.

From this configuration (figure 4.16b) and controlling one motor from the base we obtain the following configuration:

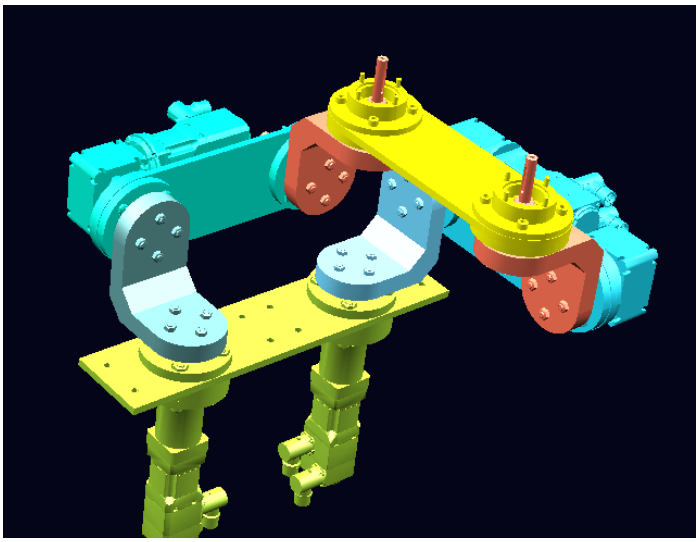

Figure 4.17 8-bar mechanism with folded and outstretched arm configuration

4.3.4 Advanced simulation results

In this section, we are going to shows some simulations results by implementing the control strategies on the SSL8B mechanism.

4.3.4.1 Principle of the advanced simulations using Adams/Simulink

The model should be completed and should include all necessary geometry, constraints, forces, and measures in order to be controlled by a simple PID controller. Any changes in the model under ADAMS are automatically taken into account in the dynamic model under Simulink. The successful interface between ADAMS and MATLAB/Simulink yields a powerful tool to model the mechanism and to analyze the dynamic behavior of the model.

The input torques, the output positions and velocities are defined as state variables and represent the different data exchange between Adams and Matlab as explained in the figure 4.18

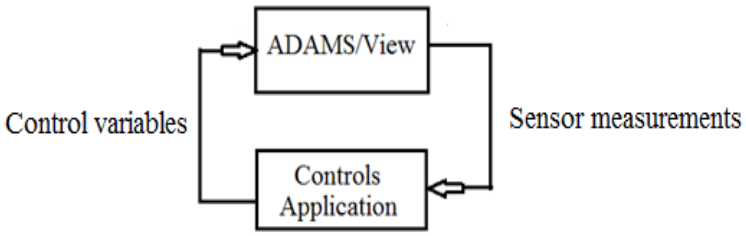

Figure 4.18 ADAMS/Controls step by step process

Once the Adams model block is obtained, the global dynamic model can be simulated with the control within the Simulink environment.

4.3.4.2 *Tuning of gains using PID controller*

The most common solution in robotics consists in adjusting the gains in order to obtain a negative real triple pole. This yields the fastest possible response without overshoot. Determining gains of PID controllers can be done with these three equations below from the inertia matrix 'A' obtained by the dynamic model [Khalil et al., 2004].

$$\begin{cases} K_{pj} = 3\ aj\ \omega_j^2 \\ K_{dj} + F_{vj} = 3\ aj\ \omega_j \\ KIj = aj\ \omega_j^3 \end{cases}$$

Where, ω_j is the frequency and a_j corresponds to the maximum magnitude of the inertia matrix of the robot.

However for mechanisms whose architecture is complex, including parallel robots, reconfigurable, redundant ... etc. control becomes increasingly difficult.

In order to obtain a 4-bar mechanism from the 8-bar, we must perform a movement of +/- 90 ° in the motors situated on the base of the robot. By doing this, we achieve the following 5 trajectories as shown in figure 4.19 using the fifth degree polynomial interpolation.

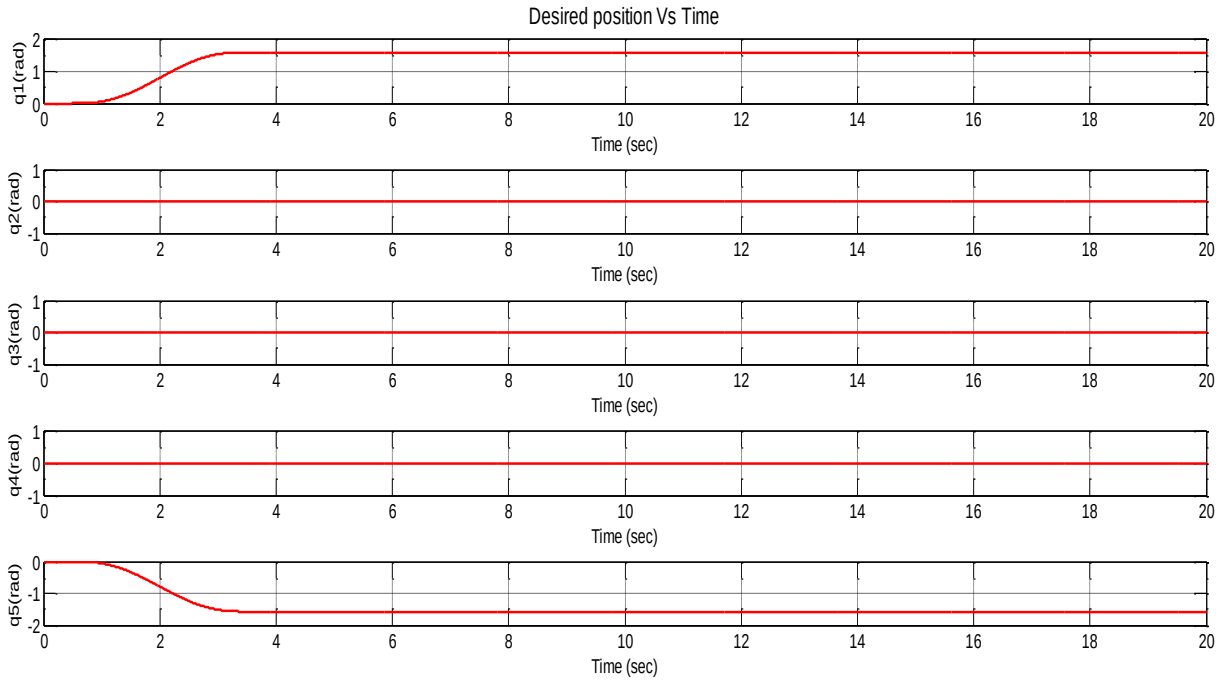

Figure 4.19 Desired trajectories of the five joints

The challenge now is to be able to adjust the gains of PID controllers. For the PID control scheme by gain tuning, we have found out the exact values of the gains at which the robot is able to go from the planar configuration to the four bar mechanism. The values we used are as follows:

For Torque 1: K_p = 0.0078, K_d =0.001s

For Torque 2: K_p = 100, K_d =0.1s

For Torque 3: K_p = 50, K_d =0.1s

For Torque 4: K_p = 100, K_d =0.1s

For Torque 5: K_p = 0.0048, K_d =0.001s

Tuning of the gains K_p, K_d and K_i plays a prominent role to stabilize and synchronize the actuators. The following graph shows the position errors of the 8-bar mechanism by tuning the gains in the PID controller.

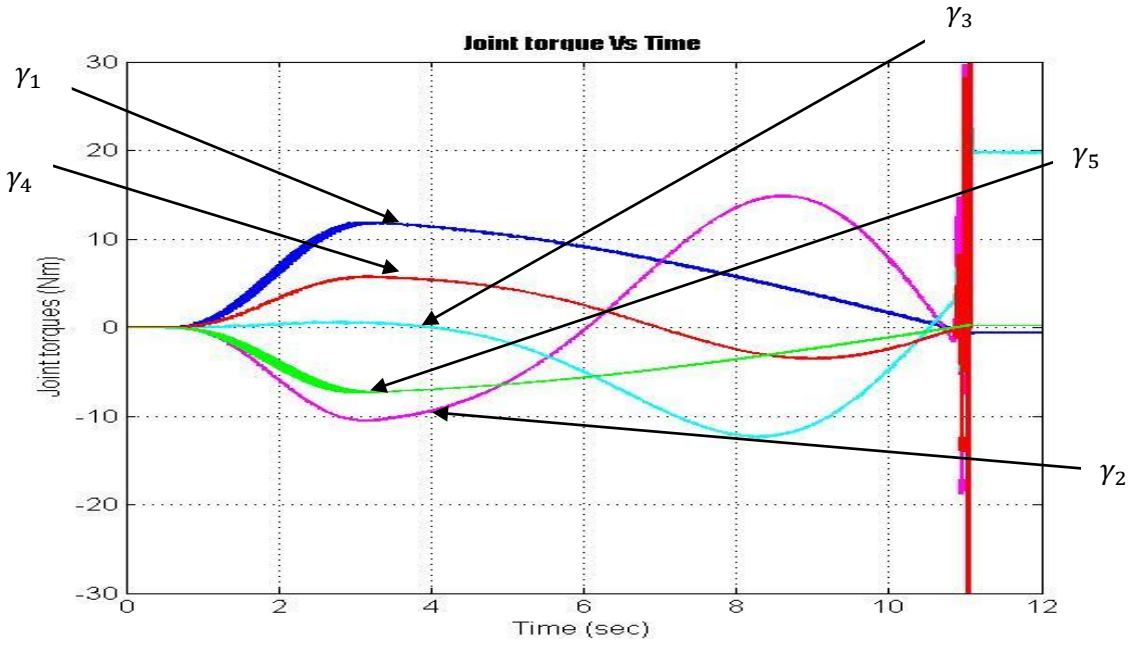

Figure 4.20Graph illustrating the input torques of the five joints

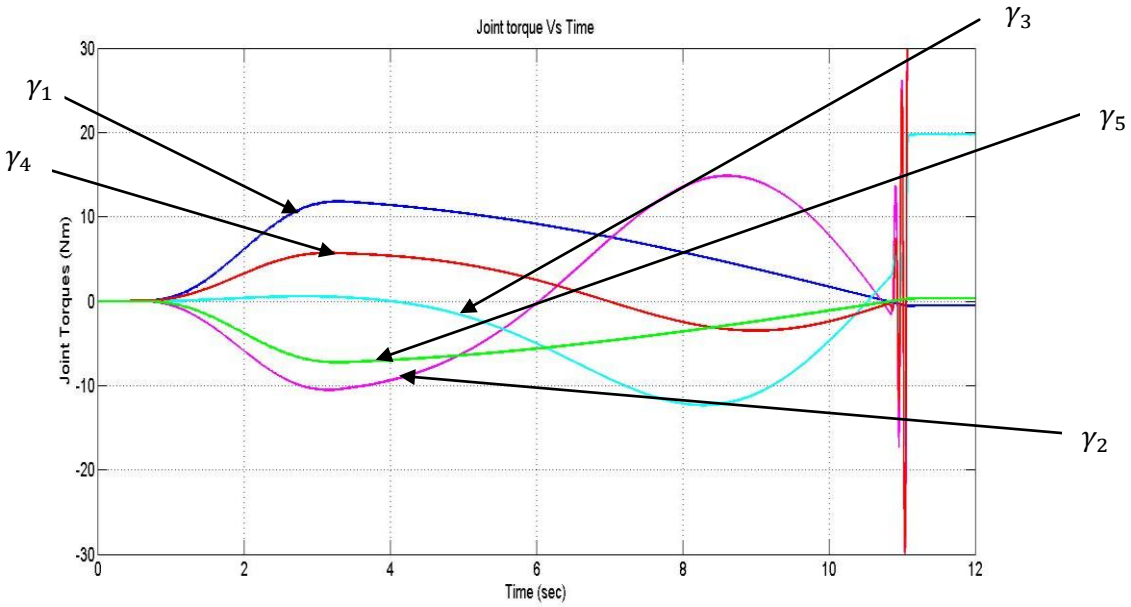

Figure 4.21 Graph illustrating the input torques of the five joints using filter

Figure 4.22 Measure position of the joints

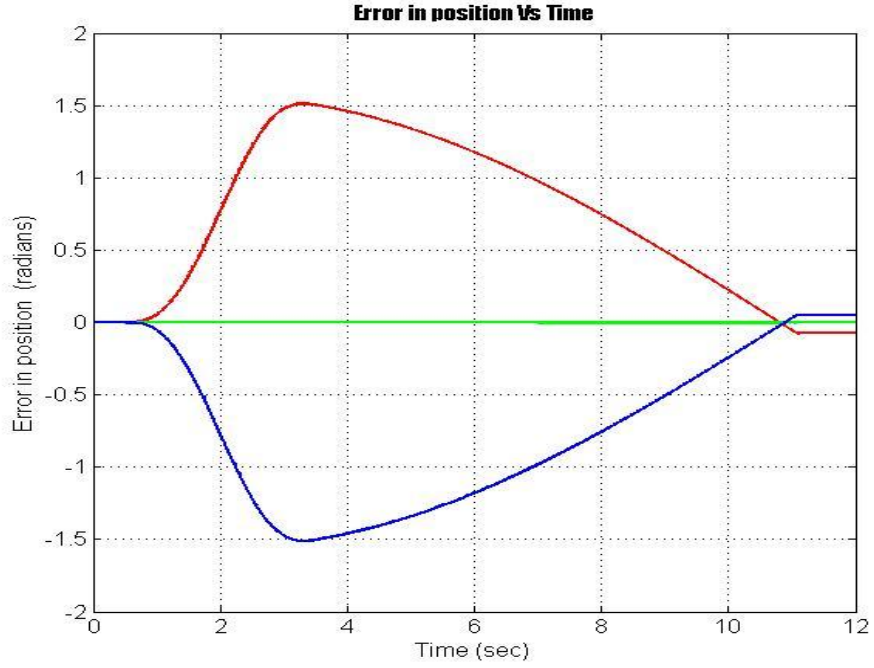

Figure 4.23 Position errors for each joint

Figure 4.20, figure 4.21 and figure 4.22 shows the evolutions of the input torques (with and without filter) and joint positions with respect to time. From the graph in figure 4.23, we can say that by tuning the gain using the PID control law, joint 1 and joint 2 are controlled at t = 11.1s with a negligible error whereas other joints are able to stabilize itself to reach the final configuration of 4-bar with zero error. The PID control strategy is used for passing from the planar 8-bar configuration to a 4-bar configuration. To pass through other singular configurations, the multi-model control strategy is better suited as presented in section 4.3.4.4.

4.3.4.3 Trajectory generator respecting the geometric model

Generating movement for the robot can be modeled by a mathematical equation of a trajectory. Joint or operational parameters depending on the type of control follow this trajectory path to reach a desired final position. In this control strategy, we develop a trajectory respecting the geometric model of the 8-bar mechanism and by using the 5^{th} polynomial interpolation (see Section 4.3) in order to compute the trajectory of the independent joint.

Figure 4.24 Measure position of the joints

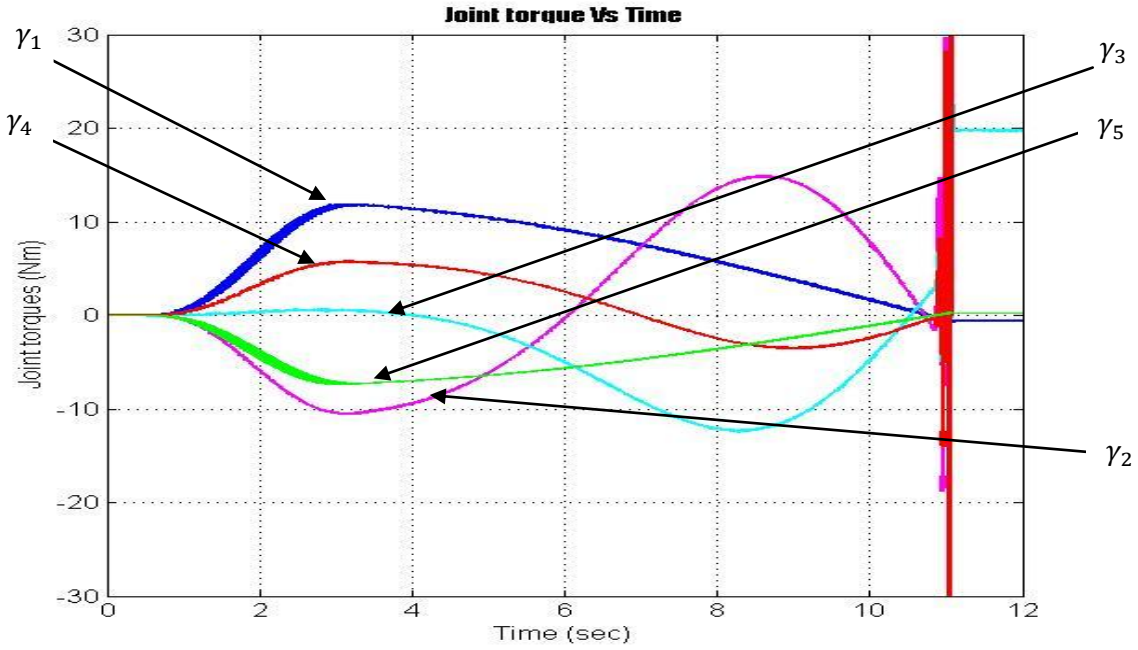

Figure 4.25 Graph illustrating the filtered input torques of the five joints

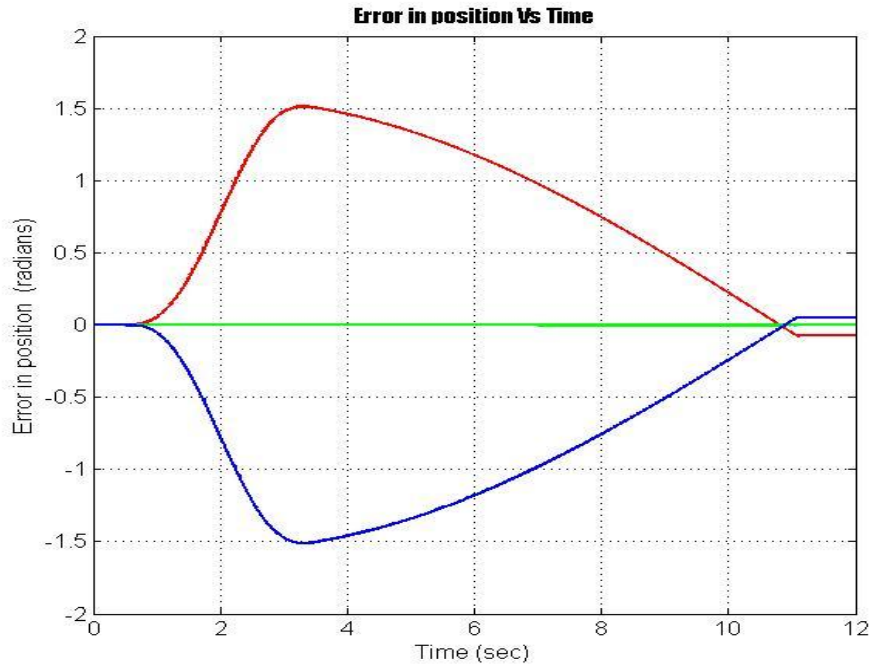

Figure 4.26 Position errors for each joint

In the trajectory generation part of the PID control (sec 4.3.4.2), we generate our trajectory respecting the geometric equations enumerated in chapter 2, section 2.3.4 (equations 2.11 to 2.16). We obtain the results as shown in figure 4.24, figure 4.25 and figure 4.26.

4.3.4.4 Multi-model control law

The second control scheme implemented for the SSL8B mechanism is the multi-model system. Using multi-model control (See section 4.2.5), we deactivate some actuators by setting a threshold period. Few seconds before the robot goes to the position of four bars, we make two of the motors passive. This is illustrated in figure 4.5.

At the singular configuration, the robot is difficult to control. These extra degrees of actuation help us to cross singular positions and branch to other positions with lesser degrees of freedom.

The values of the gains are tuned in such a way that the robot is able to stabilize at its desired final position with negligible error. Hence, by tuning, the gain values we used in the PID controller to stabilize the robot with multi-model control law are as follows:

For Torque 1: K_p=0.098, K_d = 0.098s
For Torque 2: K_p = 15, K_d =1s
For Torque 3: K_p = 15, K_d =1s
For Torque 4: K_p = 15, K_d =1s
For Torque 5: K_p=0.062, K_d = 0.062s

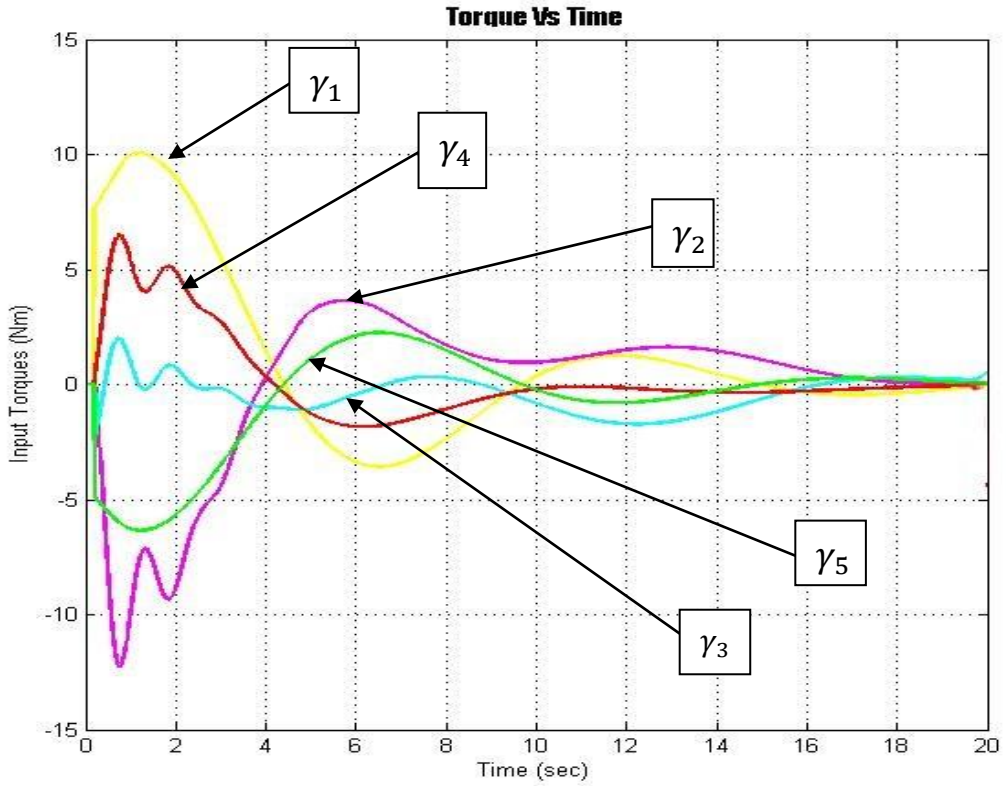

Figure 4.27 Graph illustrating the input torques of the five joints

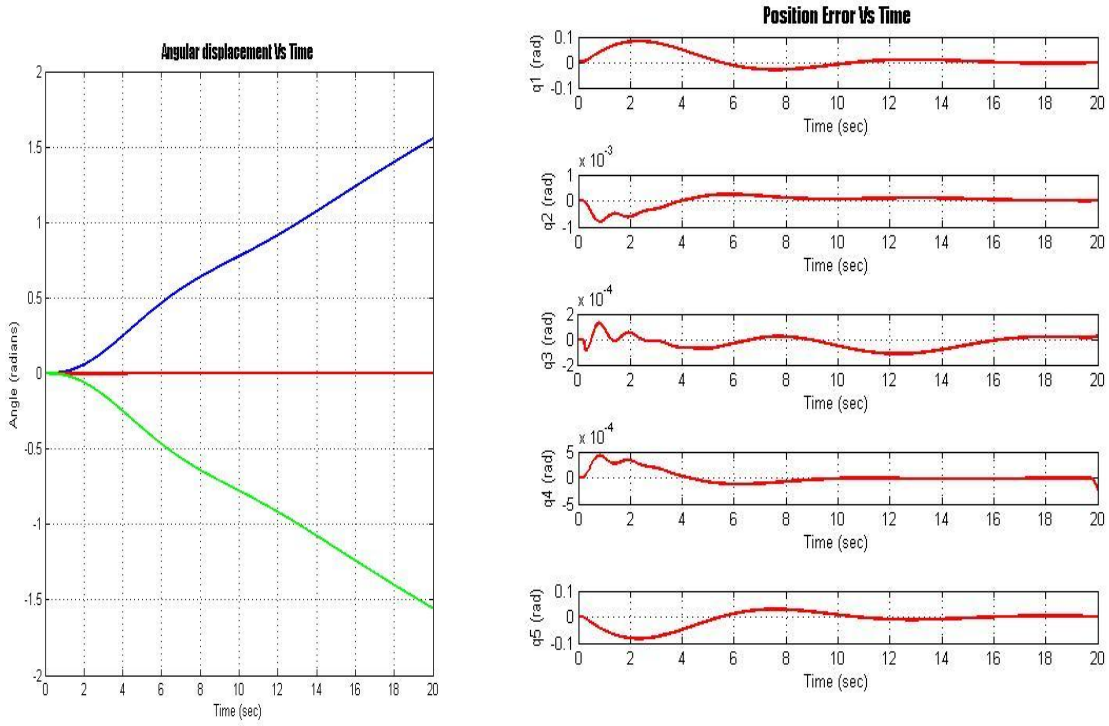

Figure 4.28 Graph illustrating (a) Measured position of the joints (b) Position error

The graphs in figure 4.27 show the stabilization of the torques after a threshold period of 19.7 seconds. The robot is able to move from the planar configuration with 5 degrees of mobility to a 4-bar mechanism and then it is able to stabilize in this configuration of 4 bars. The graphs shown in figure 4.28 (a) illustrates the output position of the five controlled joints with a movement of 90^o and -90^o. In figure 4.28 (b), we can see that the mechanism is able to reach the desired position with a negligible error.

Note that the evolution of the two joint variables is synchronized and the two curves converge towards the final value of $q_1 = 90^0$ and $q_2 = 90^0$. This is achieved by the synchronous movement of the two lateral arms of the 8-bar mechanism from the initial configuration to the 4-bar configuration.

4.4 Critical analysis of the control laws

From the above sections, we can summarize the control laws as follows:

Table 4.3 Pros and Cons of different control laws used for the SSL8B mechanism

Control Laws	Pros	Cons
PID control	• Simplicity of implementation and low computational cost	• Dynamic performance of the robot varies according to its configuration • Poor dynamic accuracy when tracking a high velocity trajectory
Conventional control using trajectory generation	• Simple way to describe the desired input positions • Possible to synchronize the joints so that they reach their final points simultaneously	• Use of interpolation is difficult to exploit with increasing the number of points • Increased number of points increases the computational burden of trajectory generation.
Multi-model control	• Stabilize the movement of the robot • Minimal error	• Difficult to be set.

Table 4.3 illustrates the pros and cons of the different control strategies used for the 8-bar reconfigurable mechanism. From this table we can conclude that the multi-model control strategy is preferable to be implemented on the SSL8B mechanism as the robot is able to go from the planar configuration to the 4-bar mechanism with negligible error. However, this kind of control law is difficult to be implemented since the time to switch between one actuation states to another depends on the joints trajectories and the singular position of the robot.

4.5 Conclusion

In this chapter we discussed the interesting property of reconfigurability of an eight-bar mechanism. Reconfigurability is achieved by crossing singularities without disassembling and assembling of the robot. In order to cross singularities without losing the control of mechanism, we have proposed few control schemes in this chapter. From the two control strategies presented in this chapter, we can conclude that the multi-model control law shows better performances with negligible errors and the robot is able to stabilize at the final configuration. In the case of the single-loop 8 bar mechanism, 5 joints have to be actuated while it has only 2 DOFs in its general configuration. The configuration control with bifurcation from one configuration to another is also explained in this chapter. Also the mechanical design, modeling and simulation in Adams are illustrated and permit us to show the relevance of the proposed control algorithms by using advanced simulations.

The SSL8B mechanism is under fabrication and these simulated results will be checked with the real 8-bar mechanism. A perspective of the thesis will be to develop advanced accurate and robust control laws.

5 Conclusion

5.1 Synthesis and contributions

The contribution of this thesis can be explained in four parts as detailed from chapters 1 to 4. This thesis mainly addresses three major parts namely the systematization and structural analysis, geometric and kinematic formulation followed by the control strategies of the 8-bar reconfigurable mechanism.

The first chapter proposes a complete systematization of the types of morphing in the reconfigurable mechanisms and details the systematization of the structural parameters such as mobility, connectivity, redundancy and number of over-constraints. These morphing techniques have been further related to mechanism type and motion type, and their applications have been identified. This chapter on bibliographic review has presented a foundation for the study of morphing techniques and metamorphosis in reconfigurable mechanisms. Hence this chapter presents a comprehensive review of morphing techniques in reconfigurable mechanisms and their relationship and existence in the mechanisms to help achieve reconfiguration has been examined.

The second chapter presents the structural analysis and the geometric modeling of the eight bar reconfigurable mechanisms. We used the travelling coordinate system for the geometric formulation of the robot. The mechanism kinematic constraints have been formulated in order to determine the mechanism configuration with respect to two independent joint variables. We need these constraint equations for the mechanism control. The geometric relationship between the joint variables for the general non-singular configuration has been determined with the frames of the travelling coordinate system.

The third chapter comprises singularity analysis of the SSL8B mechanism. The solutions of the geometric model for all the singular configurations identified have been formulated. Also, various singular configurations of this mechanism and the nature of these singularities are discussed in Chapter 3. This mechanism possesses an interesting property of reconfigurability. Different types of singularities such as constraint singularity, redundant singularity and constraint-redundant singularities are identified for the SSL8B reconfigurable mechanism. From these different singularities the mechanism can also get out at any time in a non-singular configuration. The singularity analysis presented in this chapter is useful for the study of reconfiguration capability of this mechanism which can take place in the various singular configurations illustrated in this chapter.

The fourth chapter addresses the control of the SSL8b especially for bifurcation from a singular configuration to different branches of the mechanism. In order to control the mechanism in any configuration, we proposed the use of redundant actuation. Indeed, five joints are actuated, which correspond to the maximal number of instantaneous mobilities that the mechanism can reach in a constraint singularity, while it has only two mobilities in its general configuration. Following this, we present two control schemes implemented for the SSL8B mechanism namely the synchronization of the actuators and modification of the

degrees of actuation. The robot is modeled using Adams software and the dynamic parameters are tabulated. The control schemes are applied for the 8-bar mechanism and the simulation results are illustrated. From the two control strategies presented in this chapter, we can conclude that the multi-model control law shows better performances with negligible error and the robot is able to stabilize at the final configuration. The chapter is concluded with a comparative analysis of the control strategies presented.

5.2 Perspectives

The future work of this thesis could concentrate on the following aspects: i) investigate the reconfigurability of other kind of reconfigurable mechanism to identify and characterize other types of singularities used during the reconfiguration phase, ii) formulate general rules for structural synthesis of reconfigurable mechanism starting from formalizing the singularity conditions; iii) control the real prototype to obtain optimized results by implementing the multi-model control law to obtain a negligible error; iv) generalize the multi-model control to be applicable to other types of reconfigurable mechanism; formulate general conditions for achieving reconfigurability of other mechanism with continuous transitions from one type of singularity to another.

Publications

Aimedee F., Gogu G., Dai J.S., Bouzgarrou C., Bouton N., Redundant versus constraint singularities in parallel mechanisms, In: Proceedings of the Imeche, Part C: Journal of Mechanical Engineering Science, in press, accepted on September 27, 2015.

Aimedee F., Dai J., Gogu G., Bouzgarrou B. C., Bouton N., Systematization of Morphing in Reconfigurable Mechanisms, Mechanism and Machine Theory 96 (2016) pp: 215-224, 2016.

Bibliographic References

Agrawal V.P., Rao J.S., Fractionated freedom kinematic chains and mechanisms, Mech. Mach. Theory 22, 125–130, 1987a.

Agrawal V.P., Rao J.S., Structural classification of kinematic chains and mechanisms, Mech. Mach. Theory 22, 489–496, 1987b.

Agrawal V.P., Rao J.S., The mobility properties of kinematic chains, Mech. Mach. Theory 22, 497–504, 1987c.

Aimedee F., Gogu G., Dai J.S., Bouzgarrou C., Bouton N., Redundant versus constraint singularities in parallel mechanisms, In: Proceedings of the Imeche, Part C: Journal of Mechanical Engineering Science, in press, accepted on September 27, 2015.

Aimedee F., Dai J., Gogu G., Bouzgarrou B. C., Bouton N., Systematization of Morphing in Reconfigurable Mechanisms, Mechanism and Machine Theory 96 (2016) pp: 215-224, 2016.

Alberich M., Thomas F., Torras C. On redundant flagged manipulators.In:Proc IEEE International conference on Robotics and Automation, Orlando, pp 783-789,2006.

Angeles J., Gosselin C., Détermination du degré de liberté des chaines cinématiques, Trans. CSME 12/4, 219–226, 1988.

Antonescu P., Extending of structural formula of Dobrovolski to the complex mechanisms with apparent family, in: Proceedings of the SYROM, Bucharest, 1973.

Antonescu P., General formula for the d.o.f. of complex structure manipulators and robots, Tenth World Congress on the Theory of Machines and Mechanisms, Oulu, 1999.

Arakelian V.H., Smith M.R., Design of planar 3-DOF 3-RRR reactionless parallel manipulators, Mechatronics 18(10): 601-606, 2008.

Artobolevskii I.I., Theory of mechanisms and machines (in Russian), Moscow, 1953.

Bagci C ., Degrees of freedom of motion in mechanisms, ASME J eng Industry 93B : pp.140-148, 1971.

Bagci C., Degrees of freedom of motion in mechanisms, ASME J. Eng. Industry 93B (1971) 140–148. 1094 G. Gogu / Mechanism and Machine Theory 40, 1068–1097, 2005.

Baker J.E., On relative freedom between links in kinematic chains with cross-jointing, Mech. Mach. Theory 15, 397–413, 1980.

Baker J.E., On mobility and relative freedoms in multiloop linkages and structures, Mech. Mach. Theory 16, 583–597 1981.

Boden H., Zum Zwanglauf gemischt ra¨umlich-ebener Getriebe, Maschinenbautechnik (Getriebetechnik) 11, 612–615, 1962.

Bouton N., Lenain R., An active anti-rollover device based on Predictive Functional Control : application to an All-Terrain Vehicle. IEEE International Conference on Robotics and Automation (ICRA), pp. 1309–1314, 2009.

Brain J.S., Philip A.V., Mechanism State Matrices for Planar Reconfigurable Mechanisms, J. Mech. Rob., Trans. ASME 3: 011012, 2011.

Briot S., Bonev I., Are parallel robots more accurate than serial robots? CSME Transactions 31 (4), 445-456, 2007.

Bruckmann T., Pott A., Hiller M., Calculating force distributions for redundantly Actuated tendon-based Stewart platforms. In: Lenarcic J, Roth B (eds) Advances in robot kinematics: Mechanisms and motion, Springer, Dordrecht, Pp 403-412, 2006.

Carbonari L., Callegari M., Palmieri G. Palmieri, Palpacelli M.C., A new class of reconfigurable parallel kinematic machines, Mech. Mach. Theory 74, pp.173-183, 2014

Chakarov D., Study of the antagonistic stiffness of parallel manipulators, With actuation redundancy. Mech Mach Theory 39:583-601,2004.

Charalampos V., Moulianitis V., Aspragathos N., Index based optimal anatomy of a metamorphic manipulator for a given task, ROBOT CIM-INT MANUF, Volume 28, Issue 4, pp. 517–529, 2012.

Chebychev P.A., Théorie des mécanismes connus sous le nom de parallélogrammes, 1ére partie, Mémoires présentés a` l'Académie impériale des sciences de Saint-Pétersbourg par divers savants, 1854.

Chebychev P.A., Théorie des mécanismes connus sous le nom de parallélogrammes, 2ème partie, Mémoires présentés a` l'Académie impériale des sciences de Saint-Pétersbourg par divers savants, 1869.

Cheng H., Yiu YK., Li Z., Dynamics and control of redundantly actuated parallel Manipulators. IEEE Trans Mechatronics 8(4):483-491, 2003.

Clarke D. W., Mohtadi C., Tuffs, P. S., Generalized predictive control. Chap I : The basic algorithm. Automatica, 23 :137–148, 1987.

Conconi M., Carricato M., A new assessment of singularities of parallel kinematic chains, IEEE Transactions on Robotics 25(4), pp. 757-770, August 2009.

Cui L., Dai J.S., Posture, workspace, and manipulability of the metamorphic multifingered hand with an articulated palm, J. Mech. Rob., Trans. ASME 3 (2) : 021001, 2011.

Dai J.S., Conceptual Design of the Dexterous Reconfigurable Assembly and Packaging System (D-RAPS), Science and Technology Report, Unilever Research, Port Sunlight, (No. PS960326), 1996.

Dai J.S., Jones J.R., Mobility in metamorphic mechanisms of foldable/erectable Kinds, J. Mech. Des. ASME 121 (3), pp. 375–382, 1999.

Dai J.S., Jones J.R., Kinematics and mobility analysis of origami-carton folds in packing manipulation based on the mechanism equivalent, J. Mechanical Engineering Science 216 (10), pp. 959-970, 2002.

Dai J.S., Jones J.R., Matrix representation of topological configuration transformation of metamorphic mechanisms, J. Mech. Des. ASME 127 (4), pp. 837-840, 2005.

Dai J.S., Huang Z., Lipkin H., Mobility of overconstrained parallel mechanisms, J. Mech. Des. Trans. ASME 128 (1), pp. 220-229, 2006.

Dai J.S., Wang D., Geometric Analysis and Synthesis of the Metamorphic Robotic Hand, J. Mech. Eng., Trans. ASME 129 (11), pp. 1191-1197, 2007.

Dai J.S., Cannella F., Stiffness Characteristics of Carton Folds for Packaging, *Transactions of the ASME: Journal of Mechanical Design*, 130(2): 022305_1-7, 2008.

Dai J.S., Medland A.J., Mullineux G., Carton erection using reconfigurable folder mechanisms, International Journal of Packaging Technology and Science, Volume 22, Issue 7, pp. 385–395, 2009a.

Dai J.S., Wang D., Cui L., Orientation and Workspace Analysis of the Multifingered Metamorphic Hand—Metahand, IEEE Trans. Robot. 25 (4), pp. 942-947, 2009b.

Dai J.S., Caldwell D.G, Origami-Based Robotic Paper-and-Board Packaging for Food Industry, Invited to submit to special issue of advances in food processing and packaging automation, *Trends in Food Science and Technology*, 21(3): 153-157, 2010.

Dai J.S., Finite displacement screw operators with embedded chasles motion, J. Mech. Robot. Trans. ASME 4(4) : 041002, 2012.

Dasgupta B., Mruthyunjaya TS., Force redundancy in parallel manipulators. Mech Mach Theory 33:727-742, 1998.

Davies T.H., Mechanical networks—I: Passivity and redundancy, Mech. Mach. Theory 18, 95–101, 1983a.

Davies T.H., Mechanical networks—II: Formulae for degrees of mobility and redundancy, Mech. Mach. Theory 18,103–106, 1983b.

Davies T.H., Mechanical networks—III: Wrenches on circuit screws, Mech. Mach. Theory 18, 107–112, 1983c.

Dobrovolski V.V., Dynamic analysis of statically constraint mechanisms, Akad. Nauk. SSSR, Trudy Sem. Teorii Masin i Mekhanizmov 30 (8) ,1949 (in Russian).

Dobrovolski V.V., Theory of mechanisms (in Russian), Moscow, 1951.

Dubey V.N., Dai J.S., Complex Carton Packaging with Dexterous Robot Hands, in Industrial Robotics: Programming, Simulation and Applications, Huat, L.K. (Eds.), Mammendorf, Germany: pro Literatur verlag Robert Mayer-Scholz/Advanced Robotics Systems International, 583-594, 2007.

Dudita F., Diaconescu D., Optimizarea structurala a mecanismelor, Tehnica, Bucuresti, pp. 36–45, 229–254, 1987.

Fanghella P., Kinematics of spatial linkages by group algebra: a structure based approach. Mech Mach Theory 23:171-183, 1988.

Fanghella P., Galletti C., Mobility analysis of single-loop kinematic chains: an algorithmic approach based on displacement groups, Mech. Mach. Theory 29, 1187–1204, 1994.

Fanghella P., Kinematics of spatial linkages by group algebra: a structure-based approach, Mech. Mach. Theory 23, 171–183, 1988.

Fanghella P., Stability of Branches of a Kinematotropic Mechanism, in: ASME/IFToMM international conference on reconfigurable mechanisms and robots, London, UK, pp. 41–46, 2009.

Fayet M., Mécanismes multi-boucles—I: Détermination des espaces de torseurs cinématiques dans un mécanisme multi-boucles quelqonque, Mech. Mach. Theory 30, 201–217, 1995a.

Fayet M., Bonnet P., Mécanismes multi-boucles—II: Processus de détermination du rang des équations de liaison—distribution des mobilite´s, Mech. Mach. Theory 30, 219–232,1995b.

Fayet M., Mécanismes multi-boucles—III: Hyperstatisme au sens de la dynamique et au sens de la cinématique— dualite, Mech. Mach. Theory 30, 233–252,1995c.

Finistauri A.D, Xi F., Type synthesis and kinematics of a modular variable geometry truss mechanism for aircraft wing morphing. In: Proceedings of international conference on reconfigurable mechanisms and robots , pp 470–477, 2009.

Fischer R., Podhorodeski RP., Nokleby SB., Design of a reconfigurable planar Parallel manipulator. J Robotic Syst 21(12):665-675, 2004.

Firmani F., Podhorodeski RP., Force-unconstrained poses for a redundantly-actuated planar Parallel manipulator. Mech Mach Theory 39:459-476, 2004.

Freudenstein F., Alizade R., On the degree-of-freedom of mechanisms with variable general constraint, Fourth World Congress on the Theory of Machines and Mechanisms, Newcastle upon Tyne, 1975.

Galletti C., Fanghella P., Single-loop kinematotropic mechanisms, Mech. Mach. Theory 36 (6) pp. 743-761, 2001.

Gan D.M., Dai J.S., Liao Q.Z., Mobility Change in Two Types of Metamorphic Parallel Mechanisms, J. Mech. Rob., Trans. ASME 1 (4): 041007_1-9, 2009.

Gan D.M., Dai J.S., Liao Q.Z., Constraint analysis on mobility change of a novel metamorphic parallel mechanism, Mech. Mach. Theory, 45 (12): 1864-1876, 2010.

Gan D.M., Dai J.S., Caldwell D.G., Constraint-Based Limb Synthesis and Mobility-Change Aimed Mechanism Construction, J. Mech. Des. Trans. ASME 133 (5), pp. 051001_1-9, 2011.

Gan D.M., Dai J.S., Dias J., Seneviratne L.D., Reconfiguration and Actuation Scheme of 3rTPS Metamorphic Parallel Mechanisms with Parallel Constraint Screws, In Advances in Reconfigurable mechanisms and robots 1,J.S. Dai et al, (eds), Springer, pp. 259-268, 2012.

Gan D.M, Dai J.S., Geometry Constraint and Branch Motion Evolution of 3-PUP Parallel Mechanisms with Bifurcated Motion, Mech. Mach. Theory 61, pp. 35-49, 2013a.

Gan D.M., Dai J.S., Dias J., Seneviratne L.D., Unified Kinematics and Singularity Analysis of A Metamorphic Parallel Mechanism with Bifurcated Motion, J. Mech. Robot. Trans. ASME 5 (3): 041104_1-11, 2013b.

Gan D.M., Dai J.S., Dias J., Seneviratne L.D., Constraint-Plane-Based Synthesis and Topology Variation of A Class of Metamorphic Parallel Mechanisms, J. Mech. Sci. Tech., 28 (10) pp. 4179-4191, 2014.

Gogu G., Coiffet P., Mathématiques pour la robotique : Représentation des mouvements des corps solides, Edition Hermès, Paris, ISBN 2-86601-531-2, 1996.

Gogu G., Coiffet P., Barraco A., Mathématiques pour la robotique : Représentation des déplacements des robots, Edition Hermès, Paris, ISBN 2-86601-575-X, 1997.

Gogu G., Mobility of mechanisms: a critical review, Mech Mach Theory 40:pp.1068-1097, 2005a.

Gogu G., Chebychev-Grubler-Kutzbach's criterion for mobility calculation of multi-loop mechanisms revisited via theory of linear transformations. Eur H Mech A-Solids 24:pp.427-441, 2005b.

Gogu G., Fully-isotropic redundantly-actuated parallel manipulators with five degrees of Freedom. In: Husty M, Schrocker HP(eds) Proc First European Conference on Mechanism Science, Obergurgl, 2006.

Gogu G., Structural Synthesis of Parallel Robots, Part 1: Methodology, Dordrecht, Springer, 2008a

Gogu, G., Constrained singularities and the structural parameters of parallel robots. In: Lenarčič J, Wenger P. (Eds) Advances in Robot Kinematics: Analysis and Design, Springer, Dordrecht, 21-28, 2008b

Gogu G., Branching singularities in kinematotropic parallel mechanisms, in Computational Kinematics, in: Proceedings of the 5th International Workshop on Computational Kinematics, A. Kecskeméthy and A. Müller (Eds.), Springer-Verlag, Berlin Heidelberg, ISBN:978-3-642-01947-0, pp. 341-348,2009.

Gogu G., Structural synthesis of parallel robots, Part 3: Topologies with planar motion of the moving platform, Springer, Dordrecht, 2010.

Gogu G., Maximally regular T2R1- type parallel manipulators with bifurcated spatial motion, J. Mech. Robot. Trans. ASME 3 (1), pp. 011010_1-011010_8, 2011.

Gogu G., T2R1-type parallel manipulators with bifurcated planar-spatial motion, Eur J Mech/A-Solids 33, pp. 242–269, 2012.

Gosselin C., Angeles J., "Singularity analysis of closed-loop kinematic chains," *IEEE Trans. Robot. Automat.*, vol. 6, pp. 281–290, June 1990.

Gronowicz A., Identifizierungs-Methode der Zwanglaufbedingungen von kinematischen ketten, Mech. Mach. Theory 16, 127–135, 1981.

Grubler M., Allgemeine Eigenschaften der Zwanglaufigen ebenen kinematischen Ketten, Part I, Zivilingenieur 29, 167–200, 1883

Grubler M., Allgemeine Eigenschaften der Zwanglaufigen ebenen kinematischen Ketten, Part II, Verh. Ver. Bef. Gew. 64, 179–223,1885.

Grubler M., Das Kriterium der Zwanglaufigkeit der Schraubenkelten, Festschrift, O. Muhr. Zum 80, Gubertstag, Berlin, 1916.

Grubler M., Getriebelehre: Eine Theorie Des Zwanglaufes Und Der Ebenen Mechanismen, Springer, Berlin, 1917.

Hartenberg R. S., Denavit J., Kinematic synthesis of linkages, New York: Mc Graw-Hill, pp.316-319, 1964.

Hervé J.M., Analyse structurelle des me´canismes par groupe des de´placements, Mech. Mach. Theory 13, 437–450, 1978a.

Hervé J.M., Principes fondamentaux d'une théorie des mécanismes, Rev. Roum. Sci. Tech.—Me´c. Appl. 23/5, 693–709, 1978b.

Hochman K.I., Kinematics of machinery (in Russian), Odesa, 1890.

Huang Z., Kong L.F., Fang Y.F., Mechanism Theory and Control of Parallel Manipulators, China Machine Press, 2003, quoted by Z. Huang, Q.C. Li, Type synthesis of symmetrical lower-mobility parallel mechanisms using the constraint-synthesis method, Int. J. Robotics Res. 22, 59–79, 2003.

Hunt K.H., Phillips J.R., Zur Kinematic mechanischer Verbindung fu¨r ra¨umliche Bewegung, Maschinenbau. Getriebe. 14, 657–664, 1965.

Hunt K.H., Kinematic Geometry of Mechanisms, Oxford University Press, Oxford, 1978.

Hunt K.H., "Special configurations of robot-arm via screw theory (part 1)," *Robotica*, vol. 4, no. 3, pp. 171–179, 1986.

IFR, International Federation of Robotics, Industrial Robot Statistics, http://www.ifr.org/industrial-robots/statistics/, 2014.

Ionescu T.G., Terminology for mechanisms and machine science. Mech Mach Theory 38, pp. 597–901, 2003.

Jin Y., Chen IM., Yang G., Structure synthesis and singularity analysis of a parallel Manipulator based on selective actuation. Proc IEEE Conf Robotics and automation, pp 4533-4538 , 2004.

Joshi S. A., Tsai L. W., "Jacobian analysis of limited-DOF parallel manipulators," *ASME J. Mech. Des.*, vol. 124, no. 2, pp. 254–258, 2002.

Khalil W., Dombre E., Modeling, Identification and Control of Robots. Hermes Penton Science, London-Pairs, 2002.

Khalil W., Dombre E., Modeling, Identification and Control of Robots. Chapter 1: Terminology and general definitions, pp.6 , 2004.

Kim S., Operational quality analysis of parallel manipulators with actuation redundancy. In: Proc IEEE Conf Robotics and Automation, pp 2651-2656, 1997.

Kock S., Scumacher W., A parallel x-y manipulator with actuation redundancy for high Speed and active-stiffness applications. In: Proc of IEEE Conf Robotics and Automation, pp 2295-2300, 1998.

Kock S., Scumacher W., A mixed elastic and rigid-body dynamic model of an actuation Redundant parallel robot with with high-reduction gears. In:Proc IEEE Conf Robotics and Automation, pp 1918-1923, 2000.

Koenigs G., Introduction à Une Théorie Nouvelle Des Mécanismes, Librairie Scientifique A. Hermann, Paris, pp. 27–28,1905.

Kolchin I., Experiment in the construction of an expanded structural classification of mechanisms and a structural table based on it. Trans. 2nd All-Union Conf. Basic Problems of the Theory of Machines and Mechanisms (in Russian), Moscow, 1960.

Kong X., Gosselin C.M., Richard P.L., Type synthesis of parallel mechanisms with multiple operation modes, J. Mech. Des. ASME 129, pp. 595-601, 2007.

Kong X., Reconfiguration analysis of a 3-DOF parallel mechanism using Euler parameter quaternions and algebraic geometry method, Mech. Mach. Theory 74, pp. 188-201, 2014.

Krut S., Company O., Pierrot F., Velocity performance indices for parallel mechanisms With actuation redundancy. Robotica 22:129-139, 2004.

Kumar V., Gardner J. F., "Kinematics of redundantly actuated closed chains," *IEEE Trans. Robot. Automat.*, vol. 6, pp. 269–274, Apr. 1990.

Kurokawa H., Yoshida E., Tomita K., Kamimura A., Murata S., Kokaji S., Self-reconfigurable M-TRAN structures and walker generation, Journal of Robotics and Autonomous Systems**,** Volume 54, Issue 2, pp. 142-149, 2006.

Kurtz R., Hayward V., Mutiple-goal Kinematic optimisation of parallel spherical mechanisms With actuator redundancy. IEEE Trans Robot Autom 8(5): 644-651, 1992.

Kutzbach K., Mechanische Leitungsverzweigung, ihre Gesetze und Anwendungen, Maschinenbau. Betrieb. 8, 710–716, 1929.

Lee C.C., Hervé J.M., Discontinuous Mobility of One Family of Spatial 6R Mechanisms through the Group Algebraic Structure of Displacement Set, in: Proc. ASME Design Engineering Technical Conferences, September 29-October 2, DETC2002/MECH-34273, Montreal, Canada, Sep. 2002

Lee C.C., Hervé J.M., Discontinuously Movable Seven-link Mechanisms via Group-Algebraic Approach, in: Proc. IMechE, Vol.219, Part C: J. Mechanical Engineering Science, No.6, pp.577-587. (SCI), Jun. 2005

Lee C.C., Hervé J.M., Discontinuously Movable 8R Mechanisms with an Infinity of Bifurcations, 12th IFToMM World Congress, Besançon (France), June18-21, 2007.

Lee C.C., Hervé J.M., A novel discontinuously movable six-revolute mechanism, Reconfigurable Mechanisms and Robots, ReMAR, ASME/IFToMM International Conference on, pp. 58 – 62, 22-24 June 2009.

Lee C.C., Hervé J.M., A Discontinuously Movable Constant Velocity Shaft Coupling of Koenigs Joint Type, In Advances in Reconfigurable mechanisms and robots 1,J.S. Dai et al, (eds), Springer, pp : 35-43, 2012.

Lenain R., Thuilot B., Cariou C., Martinet P., Adaptive and predictive non linear control for sliding vehicle guidance : application to trajectory tracking of farm vehicles relying on a single RTK GPS. 2004 IEEE/RSJ International Conference on Intelligent Robots and Systems (IROS) (IEEE Cat. No.04CH37566), 1, 2004.

Lenain R., Contribution à la modélisation et à la commande de robots mobiles en présence de glissement. PhD thesis, Université Blaise Pascal, Clermont-Ferrand II, 2005.

Leonesio M., Bianchi G., Manara P., A general approach for self-locking analysis in closed kinematic chains, in: Proceedings of the 12th world congress in mechanism and machine theory, Besancon, pp. 141–147, 2007.

Li S., Dai J.S., Augmented adjacency matrix for topological configuration of the metamorphic mechanisms, J. Adv. Mech. Des. Syst. Manuf. 5 (3), pp. 187-198, 2011.

Li S., Dai J.S., Structure Synthesis of Single-Driven Metamorphic Mechanisms Based on Augmented Assur Group, J. Mech. Rob., Trans. ASME 4 (3): 031004, 2012.

Li S., Wang H., Dai J.S., Li X., Ren Z., Xiu S., Topological Representation and Operation of Motion Space Exchange Reconfiguration of Metamorphic Mechanisms Computational Kinematics, in: Proceedings of the 6th International Workshop on Computational Kinematics (CK2013), Barcelona , Spain, pp:31-39, 2013.

Liu G.F., Wu Y.L., Wu X.Z., Kuens Y.Y., Li Z.X., Analysis and control of redundant parallel manipulators. In: proc IEEE Conf Robotics and Automation, pp : 3748-3754, 2001.

Liu G., Lou Y., Li Z., Singularities of parallel manipulators: A geometric treatment, in IEEE transactions on robotics and automation, Vol 19, No 4, pp 579-594, August 2003.

Ma O., Angeles J., "Architecture singularities of platform manipulators," in *Proc. IEEE Int. Conf. Robotics and Automation,* 1991, pp. 1542–1547.

Malytsheff A.P., Analysis and synthesis of mechanisms with a viewpoint of their structure (in Russia), Izvestiya Tomskogo of Technological Institute, 1923.

Manolescu N., Manafu V., Sur la détermination du degré de mobilité des mécanismes, Bull. Inst. Politechnic Bucuresti 25, 45–66, 1963.

Manolescu N., For a united point of view in the study of the structural analysis of kinematic chains and mechanisms, J. Mech. 3, 149–169, 1968.

Marquet F., Krut S., Company O., Pierrot F., ARCHI: a new redundant mechanism – modeling, Control and first results. Proc IEEE International Conference on Intelligent Robots and Systems, Pp 183-188, 2001a.

Marquet F., Krut S., Company O., Pierrot F., ARCHI: a redundant mechanism for machining With unlimited rotation capacities. In: Proc IEEE International conference on Advanced Robotics, pp 683-689, 2001b.

McCarthy J.M., Geometric Design of Linkages, Springer-Verlag, New York, pp. 3–8, 2000.

Merlet J.P., Les Robots parallèles, 2nd edn, Hermès, Paris, 1997.

Merlet J.P., "Singular configurations of parallel manipulators and Grassmann geometry", *Int. J. Robot. Res.*, vol. 8, no. 5, pp. 45–56, Oct. 1989.

Merlet J.P., " Parallel robots", Kluwer Academic Publishers, 2000.

Merlet J.P., *Parallel Robots, 2nd Edition*, Springer, ISBN 978-1-4020-4132-7, 2008.

Mohamed M.G., On the redundancy of parallel manipulators. In: Proc IEEE 7th Int Conf Intelligent Engineering Systems, 2003a.

Mohamed M.G., Kinematic analysis of redundant parallel manipulators. In:Proc IEEE 7th Int Conf Intelligent Engineering Systems, 2003b.

Mohamed M.G., Gosselin C.M., Design and analysis of kinematically redundant parallel Manipulators with configurable platforms. IEEE Trans Robot Autom 21(3) : 277-287, 2005.

Moosavian A., Xi F., Design and analysis of reconfigurable parallel robots with enhanced stiffness, Mech. Mach. Theory 77, pp. 92-110, 2014.

Moroskine Y.F., General analysis of the theory of mechanisms, Akad. Nauk. SSSR, Trudy Sem. Teorii Masin I Mekhanizmov 14, 25–50, 1954, (in Russian).

Moroskine Y.F., On the geometry of complex kinematic chains, Sov. Phys.—Dokl. 3/2, 269–272, 1958.

Mukherjee S., Murlidhar S., Massively parallel binary manipulators. Trans ASME, J Mech Design 123:68-73, 2001.

Nahon M.A., Angeles J., Reducing the effect of shocks using redundant actuation, In: Proc IEEE Conf. Robotics and Automation, pp 238-243, 1991.

Nokleby N.S., Fischer R., Podhorodeski R.P., Firmani F., Force capabilities of redundantly- Actuated parallel manipulators. Mech Mach Theory 40:578-599, 2005.

Ozol O.T., On a new structural formula of mechanisms, Izv.—Vuz—ov. Maschinostroenie 2, 1963, (in Russian).

Paccot F., Andreff F., Martinet P, A review on the dynamic control of parallel kinematic machine : theory and experiments. The International Journal of Robotics Research, 28(3) :395–416. pp. 65-100, 2009.

Pagis G., Bouton N., Briot S., Martinet P., *Design of a Controller for Enlarging Parallel Robots Workspace through Type 2 Singularity Crossing*. In IEEE Intern. Conf. on Robotics and Automation (ICRA), Hong Kong, Chine, 2014.

Pagis G., Augmentation de la taille de l'espace de travail operationnel des robots paralleles en traversant les singularites de Type 2 : Generation de trajectoires optimales et commande avancee. Automatic. Ecole Centrale de Nantes, 2015.

Park F. C., Kim J. W., "Singularity analysis of closed kinematic chains," *Trans. ASME J. Mech. Des.*, vol. 121, no. 1, pp. 32–38, 1999.

Patel Y.D., George P.M., Parallel Manipulators Applications – A Survey, In Modern Mechanical Engineering, pp. 57-64, 2012

Philip A.V., Brian K., Brian S., Mechanism State Matrices for Spatial Reconfigurable Mechanisms, in Proceedings of the ASME International on Design Engineering Technical Conference and Computers and Information in Engineering Conference, 2012.

Plitea N., Lese D., Pisla D., Vaida C., Structural design and kinematics of a new parallel reconfigurable robot, J. Robot. Comp. Integ. Manuf. 23, pp. 219-235, 2013.

Propoï, A., Use of linear programming methods for synthesizing sampled-data automatic systems. Automn. Remote Control, 24(7) :pp. 837–844, 1963.

Qin Y., Dai J.S., Gogu G., Multi-furcation in a derivative queer-square mechanism, Mech. Mach. Theory 81, pp. 36–53, 2014.

Richalet, J., Industrial applications of model based predictive control. Automatica, 29 :pp. 1251–1274, 1993a.

Richalet, J., Pratique de la commande prédictive. Hermes, ISBN : 2212115539 ; 978-2212115536, 1993b.

Rico Martinez J.M., Ravani B., On mobility analysis of linkages using group theory, Trans. ASME, J. Mech.Des. 135, 70–80, 2003a.

Rico J.M., Gallardo J., Ravani B., Lie algebra and the mobility of kinematic chains, J. Robotics Syst. 20, 477–499, 2003b.

Rossner W., Zur strukturellen Ordnung der Getriebe, Wissenschaft. Tech. Univ., Dresden, vol. 10, pp. 1101–1115, 1961.

Sarkissyan Y.L., Kharatyan A.G., Egishyan K.M., Parikyan T.F., Synthesis of mechanisms with variable structure and geometry for reconfigurable manipulation systems, International Conference on Reconfigurable Mechanisms and Robots, ReMAR, pp.195 – 199, 2009.

Shumeiu Y., Shugen M., Bin L., Yuechao W., An amphibious snake-like robot with terrestrial and aquatic gaits, In IEEE International Conference on Robotics and Automation (ICRA), pp. 2960 – 2961, 2011.

Simaan N., Shoham M., "Singularity analysis of a class of composite serial in-parallel robots," *IEEE Trans. Robot. Automat.*, vol. 17, pp. 301–311, June 2001.

Somov P.I., On the degree of freedom of motion of kinematic chains, J. Phys. Chem. Soc. Russia 19 (9) , 443–477 (in Russian), 1887.

Spong M., Hutchinson S., Vidyasagar M., Robot modeling and control (Vol. 3). New York : Wiley, ISBN : 0471649902 ; 978-0471649908. pp. 65, 2006

Sylvester J.J., On recent discoveries in mechanical conversion of motion, Proc. Roy. Inst. Great Britain 7/5 (1874) 179–198.

Tlusty J., Ziegert J., Ridgeway S., Fundamental comparison of the use of serial and parallel kinematics for machine tools, Annals of the CIRP, 48(1): pp. 351-365, 1999

Tsai L.W., Robot Analysis: the Mechanics of Serial and Parallel Manipulators, John Wiley, 1999.

Valasek M., Sika Z., Bauma V., Vampola T., The innovative potential of redundantly actuated PKM. In Neugebauer R (ed) Parallel Kinematic Machines in research and practice, The 4th Chemnitz Parallel Kinematics Seminar, pp 365-383, 2004.

Voinea R., Atanasiu M., Contribution à l'étude de la structure des chaines cinématiques, Bull. Inst. Politechnic Bucuresti XXII, 29–77, 1960.

Waldron K.J., The constraint analysis of mechanisms, J. Mech. 1, 101–114, 1966.

Wang J., Masory O., "On the accuracy of a Steward platform-part I: the effect of manufacturaing tolerances" in IEEE International Conference on Robotics and Automation (ICRA'93), Atlanta, USA, pp. 114-120, 1993.

Wang J., Gosselin C.M., Kinematics analysis and design of kinematically redundant parallel Mechanisms. Transactions of the ASME, J Mech design 126:109-118, 2004.

Wang W., Zhang H., Zong G., Zhang J., Design and Realization of a Novel Reconfigurable Robot with Serial and Parallel Mechanisms, in: Proceedings of IEEE International Conference on Robotics and Biomimetics, pp.697-702, 2006.

Wei G., Dai J.S., Wang S., Luo H., Kinematic analysis and prototype of a metamorphic anthropomorphic hand with a reconfigurable palm, International Journal of Humanoid Robotics, 8 (3) 459-479, 2011.

Wei G., Dai J. S., A spatial eight-bar linkage and its association with the deployable platonic mechanism. *ASME J. of Mechanisms and Robotics*, 6, 021010-1, 2014.

Wohlhart K., Kinematotropic linkages, in: J. Lenarcic, V. Parenti-Castelli (Eds.), Advances in Robot Kinematics, Kluwer Academic, Dordrecht, The Netherlands, pp. 359–368, 1996.

Wolf A., Shoham M., Park F. C., "Investigation of singularities and self-motions of the 3-UPU robot," in *Advances in Robot Kinematics*, J. Lenaric and F. Thomas, Eds. Norwell, MA: Kluwer, pp. 165–174, 2002.

Xi F., Finistauri A.D., Reconfiguration analysis of a fully reconfigurable parallel robot, In Advances in Reconfigurable mechanisms and robots 1,J.S. Dai et al, (Eds.), Springer, pp. 295-307, 2012.

Yan H.S., Liu N.T., Finite-state-machine representations for mechanisms and chains with variable topologies, in Proceedings of ASME Design Engineering Technical Conference, Baltimore, MD, DETC2000/Mech-14054, 10-13 Sept 2000.

Yan H.S., Liu N.T., Joint-codes representations for mechanisms and chains with variable topologies, Transactions of the Canadian Society for Mechanical Engineering, 17 (1 and 2), 131-143, 2003.

Yan H.S., Kuo C.H., Topological representations and characteristics of variable kinematic joints, J. Mech. Des. ASME 128 (2), pp: 384–391, 2006.

Yan H.S., Kuo C.H., On the mobility and configuration singularity of mechanisms with variable topologies, J. Mech. Des. ASME 129 (6), pp: 617-624, 2007.

Yan H.S., Kang C.H, Configuration synthesis of mechanisms with variable topologies, Mech. Mach. Theory 44 ,896-911,2008.

Yan H.S., Kuo C.H., Structural analysis and configuration synthesis of mechanisms with variable topologies. In: Proceedings of ASME/IFToMM international conference on reconfigurable mechanisms and robots, London, pp 23-31, 22-24 June 2009.

Yao,W. Cannella F., Dai J.S., Automatic folding of cartons using reconfigurable robotic system, J. Robot. Com. Integ. Manuf., 22 (3) 604-613, 2011.

Ye W., Fang Y.F., Zhang K.T., Guo S., A new family of reconfigurable parallel mechanisms with diamond kinematotropic chain, Mech. Mach. Theory 74, pp.1-9, 2014.

Zanganach K.E., Angeles J., Instantaneous kinematics and design of a novel redundant Parallel manipulator. In: Proc IEEE Conf Robotics and Automation, pp 3043-3048, 1994a.

Zanganach K.E., Angeles J., Mobility and position analysis of a novel redundant Parallel manipulator. In: Proc IEEE Conf Robotics and Automation, pp 3049-3054, 1994b.

Zhang L., Dai J.S., Reconfiguration of Spatial Metamorphic Mechanisms, J. Mech. Rob., Trans. ASME 1(1), pp. 011012, 2008a.

Zhang L., Wang D., Dai J.S., Biological modeling and evolution based synthesis of metamorphic mechanisms, J. Mech. Des. ASME 130 (7), pp. 072303, 2008b.

Zhang K.T., Dai J.S., Fang Y.F., A new metamorphic mechanism with ability for platform orientation switch and mobility change, in: ASME/IFToMM international conference on reconfigurable mechanisms and robots, London, UK, pp. 626–632, 2009.

Zhang K.T., Dai J.S., Fang Y.F., Topology and constraint analysis of phase change in the metamorphic chain and its evolved mechanism, J. Mech. Des. ASME 132 (12), pp. 121001_1-121001_11, 2010.

Zhang K.T., Dai J.S., Fang Y.F., Zeng Q., String matrix based geometrical and topological representation of mechanisms. In: *Proc. of 13th World Congress in Mechanism and Machine Science*, Guanajuato, Mexico, A23-493, 2011a.

Zhang W., Ding X., Dai J.S., Morphological synthesis of metamorphic mechanisms based on constraint variation, IMechE, Journal of Mechanical Engineering Science, 225 (12), pp. 2297-2310, 2011b.

Zhang K.T., Dai J.S., Fang Y.F., Constraint analysis and bifurcated motion of the 3PUP parallel mechanism, Mech. Mach. Theory 47 (3), pp. 256-269, 2012a.

Zhang W., Ding X., A Method for Configuration Representation of Metamorphic Mechanisms with Information of Component Variation, In Advances in Reconfigurable mechanisms and robots 1, J.S. Dai et al, (eds), Springer, pp : 13-24, 2012b.

Zhang K., Emmanouil E., Fang Y.F., Dai J.S., Type-Changeable Kinematic Pair Evolved Reconfigurable Parallel Mechanisms, In Advances in Reconfigurable mechanisms and robots 1,J.S. Dai et al, (Eds.), Springer, pp. 309-319, 2012c.

Zhang K.T., Fang Y.F., Wei G., Dai J.S., Structural representation of reconfigurable linkage. In Advances in Reconfigurable mechanisms and robots 1, J.S. Dai et al, (eds), Springer, pp: 127-137, 2012d.

Zhang K.T., Dai J.S., Fang Y.F., Geometric constraint and mobility variation of Two 3SvPSv metamorphic parallel mechanisms, J. Mech. Des. ASME 135 (1), pp. 11001, 2013.

Zhang K.T., Dai J.S., A kirigami-inspired 8R linkage and its evolved overconstrained 6R linkages with the rotational symmetry of order two, J. Mech. Rob., Trans. ASME 6 (2):021008, 2014.

Zhao J.S., Yan Z.F., Chu F.L., A reconfigurable linkage and its application in lift mechanism, In Advances in Reconfigurable mechanisms and robots 1, J.S. Dai et al, (eds), Springer, pp. 815-829, 2012.

Zlatanov D., Bonev I.A., Gosselin C. M., "Constraint singularities of parallel mechanisms," in *Proc. IEEE Int. Conf. Robotics and Automation*, pp. 496–502, 2002.

Annex I

Geometric modeling of the eight-bar mechanism:

The expression of the homogeneous matrices defining the direct geometric model of the open chain associated with the 8-bar reconfigurable mechanism calculated using maple software are as follows,

$A_{01} = R^{z}_{01}(\emptyset_{10})$

where,

$$R01Z := \begin{bmatrix} 1 & 0 & 0 & 0 \\ 0 & c10 & -s10 & 0 \\ 0 & s10 & c10 & 0 \\ 0 & 0 & 0 & 1 \end{bmatrix}$$

$$A02 := \begin{bmatrix} 1 & 0 & 0 & 0 \\ -s10c21\,b2 & c10 & -s10c21 & s10s21 \\ c10c21\,b2 & s10 & c10c21 & -c10s21 \\ s21\,b2 & 0 & s21 & c21 \end{bmatrix}$$

$$A03 := \begin{bmatrix} 1 & 0 & 0 & 0 \\ -s10c21\,b2 & c10 & -s10c321 & s10s321 \\ c10c21\,b2 & s10 & c10c321 & -c10s321 \\ s21\,b2 & 0 & s321 & c321 \end{bmatrix}$$

$$A04 := \begin{bmatrix} 1 & 0 & 0 & 0 \\ c10s43\,b4 - s10c21\,b2 + s10c43\,b4\,s321 & c10c43 - s10s43s321 & -s10c321 & c10s43 + s10c43s321 \\ s10s43\,b4 + c10c21\,b2 - c10c43\,b4\,s321 & s10c43 + c10s43s321 & c10c321 & s10s43 - c10c43s321 \\ s21\,b2 + c321\,c43\,b4 & -s43c321 & s321 & c43c321 \end{bmatrix}$$

$$A05 := \begin{bmatrix} 1 & 0 & 0 & 0 \\ c10s43\,b4 - s10c21\,b2 + s10c43\,b4\,s321 & c10c543 - s10s321s543 & -s10c321 & s10s321c543 + c10s543 \\ s10s43\,b4 + c10c21\,b2 - c10c43\,b4\,s321 & s10c543 + c10s321s543 & c10c321 & -c10s321c543 + s10s543 \\ s21\,b2 + c321\,c43\,b4 & -c321\,s543 & s321 & c321\,c543 \end{bmatrix}$$

$A06 := [[1,0,0,0],$
$[c10s43\,b4 - s10c21\,b2 + s10c43\,b4\,s321 + (c10c543 - s10s321s543)\,c65\,b6 - s10c321\,s65\,b6, (c10c543 - s10s321s543)\,c65 - s10c321\,s65, -(c10c543 - s10s321s543)\,s65 - s10c321\,c65, s10s321c543 + c10s543],$
$[s10s43\,b4 + c10c21\,b2 - c10c43\,b4\,s321 + (s10c543 + c10s321s543)\,c65\,b6 + c10c321\,s65\,b6, (s10c543 + c10s321s543)\,c65 + c10c321\,s65, -(s10c543 + c10s321s543)\,s65 + c10c321\,c65, -c10s321c543 + s10s543],$
$[s21\,b2 + c321\,c43\,b4 - c321\,s543\,c65\,b6 + s321\,s65\,b6, -c321\,s543\,c65 + s321\,s65, c321\,s543\,s65 + s321\,c65, c321\,c543]]$

```
A07 := [[1, 0, 0, 0],
 [c10 s43 b4 − s10 c21 b2 + s10 c43 b4 s321 + (c10 c543 − s10 s321 s543) c65 b6 − s10 c321 s65 b6, ((c10 c543 − s10 s321 s543) c65 − s10 c321 s65) c76 + (−(c10 c543 − s10 s321 s543) s65
  − s10 c321 c65) s76, −((c10 c543 − s10 s321 s543) c65 − s10 c321 s65) s76 + (−(c10 c543 − s10 s321 s543) s65 − s10 c321 c65) c76, s10 s321 c543 + c10 s543],
 [s10 s43 b4 + c10 c21 b2 − c10 c43 b4 s321 + (s10 c543 + c10 s321 s543) c65 b6 + c10 c321 s65 b6, ((s10 c543 + c10 s321 s543) c65 + c10 c321 s65) c76 + (−(s10 c543 + c10 s321 s543) s65
  + c10 c321 c65) s76, −((s10 c543 + c10 s321 s543) c65 + c10 c321 s65) s76 + (−(s10 c543 + c10 s321 s543) s65 + c10 c321 c65) c76, −c10 s321 c543 + s10 s543],
 [s21 b2 + c321 c43 b4 − c321 s543 c65 b6 + s321 s65 b6, (−c321 s543 c65 + s321 s65) c76 + (c321 s543 s65 + s321 c65) s76, −(−c321 s543 c65 + s321 s65) s76 + (c321 s543 s65 + s321 c65) c76,
 c321 c543]]
```

where,
s10 = sin($\emptyset_{10}$), c10 = cos($\emptyset_{10}$),
s21 = sin($\emptyset_{21}$), c21 = cos($\emptyset_{21}$),
s32 = sin($\emptyset_{32}$), c32 = cos($\emptyset_{32}$),
s43 = sin($\emptyset_{43}$), c43 = cos($\emptyset_{43}$),
s54 = sin($\emptyset_{54}$), c54 = cos($\emptyset_{54}$),
s65 = sin($\emptyset_{65}$), c65 = cos($\emptyset_{65}$),
s76 = sin($\emptyset_{76}$), c76 = cos($\emptyset_{76}$),
s87 = sin($\emptyset_{87}$), c87 = cos($\emptyset_{87}$),
s321= sin($\emptyset_{32} + \emptyset_{21}$), c321 = cos($\emptyset_{32} + \emptyset_{21}$),
s543= sin($\emptyset_{54} + \emptyset_{43}$), c543 = cos($\emptyset_{54} + \emptyset_{43}$),

'b_i' is the distance defined on the direction of the common normal to the axes of joints (*i-1*, *i*) and (*i*, *i+1)*.

Annex II

The table below presents all possible combinations of the vector spaces of dimension 4 for each limb. Among these the ones with the minimum S_F are selected as presented in Table 2.1 in Chapter 2. The other bases are associated with various types of singularities.

Table A2.1 Possible bases for each limb

$(\boldsymbol{R_{G1}})$	$(\boldsymbol{R_{G2}})$	$(\boldsymbol{R_F})$	$\boldsymbol{S_F}$
$(v_z, \omega_x, \omega_y, \omega_z)$	$(v_z, \omega_x, \omega_y, \omega_z)$	$(v_z, \omega_x, \omega_y, \omega_z)$	4
$(v_z, \omega_x, \omega_y, \omega_z)$	$(v_y, \omega_x, \omega_y, \omega_z)$	$(\omega_x, \omega_y, \omega_z)$	3
$(v_z, \omega_x, \omega_y, \omega_z)$	$(v_y, v_z, \omega_y, \omega_z)$	$(v_z, \omega_y, \omega_z)$	3
$(v_z, \omega_x, \omega_y, \omega_z)$	$(v_y, v_z, \omega_x, \omega_z)$	$(v_z, \omega_y, \omega_z)$	3
$(v_z, \omega_x, \omega_y, \omega_z)$	$(v_y, v_z, \omega_x, \omega_y)$	$(v_z, \omega_y, \omega_y)$	3
$(v_z, \omega_x, \omega_y, \omega_z)$	$(v_x, \omega_x, \omega_y, \omega_z)$	$(\omega_x, \omega_y, \omega_z)$	3
$(v_z, \omega_x, \omega_y, \omega_z)$	$(v_x, v_z, \omega_y, \omega_z)$	$(v_z, \omega_y, \omega_z)$	3
$(v_z, \omega_x, \omega_y, \omega_z)$	$(v_x, v_z, \omega_x, \omega_z)$	$(v_z, \omega_y, \omega_z)$	3
$(v_z, \omega_x, \omega_y, \omega_z)$	$(v_x, v_z, \omega_x, \omega_y)$	$(v_z, \omega_x, \omega_y)$	3
$(v_z, \omega_x, \omega_y, \omega_z)$	$(v_x, v_y, \omega_y, \omega_z)$	(ω_y, ω_z)	2
$(v_z, \omega_x, \omega_y, \omega_z)$	$(v_x, v_y, \omega_x, \omega_z)$	(ω_x, ω_z)	2
$(v_z, \omega_x, \omega_y, \omega_z)$	$(v_x, v_y, \omega_x, \omega_y)$	(ω_x, ω_y)	2
$(v_z, \omega_x, \omega_y, \omega_z)$	$(v_x, v_y, v_z, \omega_z)$	(v_z, ω_z)	2
$(v_z, \omega_x, \omega_y, \omega_z)$	$(v_x, v_y, v_z, \omega_y)$	(v_z, ω_y)	2
$(v_z, \omega_x, \omega_y, \omega_z)$	$(v_x, v_y, v_z, \omega_x)$	(v_z, ω_x)	2
$(v_y, \omega_x, \omega_y, \omega_z)$	$(v_z, \omega_x, \omega_y, \omega_z)$	$(\omega_x, \omega_y, \omega_z)$	3
$(v_y, \omega_x, \omega_y, \omega_z)$	$(v_y, \omega_x, \omega_y, \omega_z)$	$(v_y, \omega_x, \omega_y, \omega_z)$	4
$(v_y, \omega_x, \omega_y, \omega_z)$	$(v_y, v_z, \omega_y, \omega_z)$	$(v_y, \omega_y, \omega_z)$	3
$(v_y, \omega_x, \omega_y, \omega_z)$	$(v_y, v_z, \omega_x, \omega_z)$	$(v_y, \omega_x, \omega_z)$	3
$(v_y, \omega_x, \omega_y, \omega_z)$	$(v_y, v_z, \omega_x, \omega_y)$	$(v_y, \omega_x, \omega_y)$	3
$(v_y, \omega_x, \omega_y, \omega_z)$	$(v_x, \omega_x, \omega_y, \omega_z)$	$(\omega_x, \omega_y, \omega_z)$	3
$(v_y, \omega_x, \omega_y, \omega_z)$	$(v_x, v_z, \omega_y, \omega_z)$	(ω_y, ω_z)	2
$(v_y, \omega_x, \omega_y, \omega_z)$	$(v_x, v_z, \omega_x, \omega_z)$	(ω_x, ω_z)	2
$(v_y, \omega_x, \omega_y, \omega_z)$	$(v_x, v_z, \omega_x, \omega_y)$	(ω_x, ω_y)	2
$(v_y, \omega_x, \omega_y, \omega_z)$	$(v_x, v_y, \omega_y, \omega_z)$	$(v_y, \omega_y, \omega_z)$	3
$(v_y, \omega_x, \omega_y, \omega_z)$	$(v_x, v_y, \omega_x, \omega_z)$	$(v_y, \omega_x, \omega_z)$	3
$(v_y, \omega_x, \omega_y, \omega_z)$	$(v_x, v_y, \omega_x, \omega_y)$	$(v_y, \omega_x, \omega_y)$	3
$(v_y, \omega_x, \omega_y, \omega_z)$	$(v_x, v_y, v_z, \omega_z)$	(v_y, ω_z)	2
$(v_y, \omega_x, \omega_y, \omega_z)$	$(v_x, v_y, v_z, \omega_y)$	(v_y, ω_y)	2
$(v_y, \omega_x, \omega_y, \omega_z)$	$(v_x, v_y, v_z, \omega_x)$	(v_y, ω_x)	2

$(v_y, v_z, \omega_y, \omega_z)$	$(v_z, \omega_x, \omega_y, \omega_z)$	$(v_z, \omega_y, \omega_z)$	3
$(v_y, v_z, \omega_y, \omega_z)$	$(v_y, \omega_x, \omega_y, \omega_z)$	$(v_y, \omega_y, \omega_z)$	3
$(v_y, v_z, \omega_y, \omega_z)$	$(v_y, v_z, \omega_y, \omega_z)$	$(v_y, v_z, \omega_y, \omega_z)$	4
$(v_y, v_z, \omega_y, \omega_z)$	$(v_y, v_z, \omega_x, \omega_z)$	(v_y, v_z, ω_z)	3
$(v_y, v_z, \omega_y, \omega_z)$	$(v_y, v_z, \omega_x, \omega_y)$	(v_y, v_z, ω_y)	3
$(v_y, v_z, \omega_y, \omega_z)$	$(v_x, \omega_x, \omega_y, \omega_z)$	(ω_y, ω_z)	2
$(v_y, v_z, \omega_y, \omega_z)$	$(v_x, v_z, \omega_y, \omega_z)$	$(v_z, \omega_y, \omega_z)$	3
$(v_y, v_z, \omega_y, \omega_z)$	$(v_x, v_z, \omega_x, \omega_z)$	(v_z, ω_z)	2
$(v_y, v_z, \omega_y, \omega_z)$	$(v_x, v_z, \omega_x, \omega_y)$	(v_z, ω_y)	2
$(v_y, v_z, \omega_y, \omega_z)$	$(v_x, v_y, \omega_y, \omega_z)$	$(v_y, \omega_y, \omega_z)$	3
$(v_y, v_z, \omega_y, \omega_z)$	$(v_x, v_y, \omega_x, \omega_z)$	(v_y, ω_z)	2
$(v_y, v_z, \omega_y, \omega_z)$	$(v_x, v_y, \omega_x, \omega_y)$	(v_y, ω_y)	2
$(v_y, v_z, \omega_y, \omega_z)$	$(v_x, v_y, v_z, \omega_z)$	(v_y, v_z, ω_z)	3
$(v_y, v_z, \omega_y, \omega_z)$	$(v_x, v_y, v_z, \omega_y)$	(v_y, ω_y)	2
$(v_y, v_z, \omega_y, \omega_z)$	$(v_x, v_y, v_z, \omega_x)$	(v_y, v_z)	2
$(v_y, v_z, \omega_x, \omega_z)$	$(v_z, \omega_x, \omega_y, \omega_z)$	$(v_z, \omega_x, \omega_z)$	3
$(v_y, v_z, \omega_x, \omega_z)$	$(v_y, \omega_x, \omega_y, \omega_z)$	$(v_y, \omega_x, \omega_z)$	3
$(v_y, v_z, \omega_x, \omega_z)$	$(v_y, v_z, \omega_y, \omega_z)$	(v_y, v_z, ω_z)	3
$(v_y, v_z, \omega_x, \omega_z)$	$(v_y, v_z, \omega_x, \omega_z)$	$(v_y, v_z, \omega_x, \omega_z)$	4
$(v_y, v_z, \omega_x, \omega_z)$	$(v_y, v_z, \omega_x, \omega_y)$	(v_y, v_z, ω_x)	3
$(v_y, v_z, \omega_x, \omega_z)$	$(v_x, \omega_x, \omega_y, \omega_z)$	(ω_x, ω_z)	2
$(v_y, v_z, \omega_x, \omega_z)$	$(v_x, v_z, \omega_y, \omega_z)$	(v_z, ω_z)	2
$(v_y, v_z, \omega_x, \omega_z)$	$(v_x, v_z, \omega_x, \omega_z)$	$(v_z, \omega_x, \omega_z)$	3
$(v_y, v_z, \omega_x, \omega_z)$	$(v_x, v_z, \omega_x, \omega_y)$	(v_z, ω_x)	2
$(v_y, v_z, \omega_x, \omega_z)$	$(v_x, v_y, \omega_y, \omega_z)$	(v_y, ω_z)	2
$(v_y, v_z, \omega_x, \omega_z)$	$(v_x, v_y, \omega_x, \omega_z)$	$(v_y, \omega_x, \omega_z)$	3
$(v_y, v_z, \omega_x, \omega_z)$	$(v_x, v_y, \omega_x, \omega_y)$	(v_y, ω_x)	2
$(v_y, v_z, \omega_x, \omega_z)$	$(v_x, v_y, v_z, \omega_z)$	(v_y, v_z, ω_z)	3
$(v_y, v_z, \omega_x, \omega_z)$	$(v_x, v_y, v_z, \omega_y)$	(v_y, v_z)	2
$(v_y, v_z, \omega_x, \omega_z)$	$(v_x, v_y, v_z, \omega_x)$	(v_y, v_z, ω_x)	3
$(v_y, v_z, \omega_x, \omega_y)$	$(v_z, \omega_x, \omega_y, \omega_z)$	$(v_z, \omega_x, \omega_y)$	3
$(v_y, v_z, \omega_x, \omega_y)$	$(v_y, \omega_x, \omega_y, \omega_z)$	$(v_y, \omega_x, \omega_y)$	3
$(v_y, v_z, \omega_x, \omega_y)$	$(v_y, v_z, \omega_y, \omega_z)$	(v_y, v_z, ω_y)	3
$(v_y, v_z, \omega_x, \omega_y)$	$(v_y, v_z, \omega_x, \omega_z)$	(v_y, v_z, ω_x)	3
$(v_y, v_z, \omega_x, \omega_y)$	$(v_y, v_z, \omega_x, \omega_y)$	$(v_y, v_z, \omega_x, \omega_y)$	4
$(v_y, v_z, \omega_x, \omega_y)$	$(v_x, \omega_x, \omega_y, \omega_z)$	(ω_x, ω_y)	2
$(v_y, v_z, \omega_x, \omega_y)$	$(v_x, v_z, \omega_y, \omega_z)$	(v_z, ω_y)	2
$(v_y, v_z, \omega_x, \omega_y)$	$(v_x, v_z, \omega_x, \omega_z)$	(v_z, ω_x)	2
$(v_y, v_z, \omega_x, \omega_y)$	$(v_x, v_z, \omega_x, \omega_y)$	$(v_z, \omega_x, \omega_y)$	3
$(v_y, v_z, \omega_x, \omega_y)$	$(v_x, v_y, \omega_y, \omega_z)$	(v_y, ω_y)	2
$(v_y, v_z, \omega_x, \omega_y)$	$(v_x, v_y, \omega_x, \omega_z)$	(v_y, ω_x)	2

$(v_y, v_z, \omega_x, \omega_y)$	$(v_x, v_y, \omega_x, \omega_y)$	$(v_y, \omega_x, \omega_y)$	3
$(v_y, v_z, \omega_x, \omega_y)$	$(v_x, v_y, v_z, \omega_z)$	(v_y, v_z)	2
$(v_y, v_z, \omega_x, \omega_y)$	$(v_x, v_y, v_z, \omega_y)$	(v_y, v_z, ω_y)	3
$(v_y, v_z, \omega_x, \omega_y)$	$(v_x, v_y, v_z, \omega_x)$	(v_y, v_z, ω_x)	3
$(v_x, \omega_x, \omega_y, \omega_z)$	$(v_z, \omega_x, \omega_y, \omega_z)$	$(\omega_x, \omega_y, \omega_z)$	3
$(v_x, \omega_x, \omega_y, \omega_z)$	$(v_y, \omega_x, \omega_y, \omega_z)$	$(\omega_x, \omega_y, \omega_z)$	3
$(v_x, \omega_x, \omega_y, \omega_z)$	$(v_y, v_z, \omega_y, \omega_z)$	(ω_y, ω_z)	2
$(v_x, \omega_x, \omega_y, \omega_z)$	$(v_y, v_z, \omega_x, \omega_z)$	(ω_x, ω_z)	2
$(v_x, \omega_x, \omega_y, \omega_z)$	$(v_y, v_z, \omega_x, \omega_y)$	(ω_x, ω_y)	2
$(v_x, \omega_x, \omega_y, \omega_z)$	$(v_x, \omega_x, \omega_y, \omega_z)$	$(v_x, \omega_x, \omega_y, \omega_z)$	4
$(v_x, \omega_x, \omega_y, \omega_z)$	$(v_x, v_z, \omega_y, \omega_z)$	$(v_x, \omega_y, \omega_z)$	3
$(v_x, \omega_x, \omega_y, \omega_z)$	$(v_x, v_z, \omega_x, \omega_z)$	$(v_x, \omega_x, \omega_z)$	3
$(v_x, \omega_x, \omega_y, \omega_z)$	$(v_x, v_z, \omega_x, \omega_y)$	$(v_x, \omega_x, \omega_y)$	3
$(v_x, \omega_x, \omega_y, \omega_z)$	$(v_x, v_y, \omega_y, \omega_z)$	$(v_x, \omega_y, \omega_z)$	3
$(v_x, \omega_x, \omega_y, \omega_z)$	$(v_x, v_y, \omega_x, \omega_z)$	$(v_x, \omega_x, \omega_z)$	3
$(v_x, \omega_x, \omega_y, \omega_z)$	$(v_x, v_y, \omega_x, \omega_y)$	$(v_x, \omega_x, \omega_y)$	3
$(v_x, \omega_x, \omega_y, \omega_z)$	$(v_x, v_y, v_z, \omega_z)$	(v_x, ω_z)	2
$(v_x, \omega_x, \omega_y, \omega_z)$	$(v_x, v_y, v_z, \omega_y)$	(v_x, ω_y)	2
$(v_x, \omega_x, \omega_y, \omega_z)$	$(v_x, v_y, v_z, \omega_x)$	(v_x, ω_x)	2
$(v_x, v_z, \omega_y, \omega_z)$	$(v_z, \omega_x, \omega_y, \omega_z)$	$(v_z, \omega_y, \omega_z)$	3
$(v_x, v_z, \omega_y, \omega_z)$	$(v_y, \omega_x, \omega_y, \omega_z)$	(ω_y, ω_z)	2
$(v_x, v_z, \omega_y, \omega_z)$	$(v_y, v_z, \omega_y, \omega_z)$	$(v_z, \omega_y, \omega_z)$	3
$(v_x, v_z, \omega_y, \omega_z)$	$(v_y, v_z, \omega_x, \omega_z)$	(v_z, ω_z)	2
$(v_x, v_z, \omega_y, \omega_z)$	$(v_y, v_z, \omega_x, \omega_y)$	(v_z, ω_y)	2
$(v_x, v_z, \omega_y, \omega_z)$	$(v_x, \omega_x, \omega_y, \omega_z)$	$(v_x, \omega_y, \omega_z)$	3
$(v_x, v_z, \omega_y, \omega_z)$	$(v_x, v_z, \omega_y, \omega_z)$	$(v_x, v_z, \omega_y, \omega_z)$	4
$(v_x, v_z, \omega_y, \omega_z)$	$(v_x, v_z, \omega_x, \omega_z)$	(v_x, v_z, ω_z)	3
$(v_x, v_z, \omega_y, \omega_z)$	$(v_x, v_z, \omega_x, \omega_y)$	(v_x, v_z, ω_y)	3
$(v_x, v_z, \omega_y, \omega_z)$	$(v_x, v_y, \omega_y, \omega_z)$	$(v_x, \omega_y, \omega_z)$	3
$(v_x, v_z, \omega_y, \omega_z)$	$(v_x, v_y, \omega_x, \omega_z)$	(v_x, ω_z)	2
$(v_x, v_z, \omega_y, \omega_z)$	$(v_x, v_y, \omega_x, \omega_y)$	(v_x, ω_y)	2
$(v_x, v_z, \omega_y, \omega_z)$	$(v_x, v_y, v_z, \omega_z)$	(v_x, v_z, ω_z)	3
$(v_x, v_z, \omega_y, \omega_z)$	$(v_x, v_y, v_z, \omega_y)$	(v_x, v_z, ω_y)	3
$(v_x, v_z, \omega_y, \omega_z)$	$(v_x, v_y, v_z, \omega_x)$	(v_x, v_z)	2
$(v_x, v_z, \omega_x, \omega_z)$	$(v_z, \omega_x, \omega_y, \omega_z)$	$(v_z, \omega_x, \omega_z)$	3
$(v_x, v_z, \omega_x, \omega_z)$	$(v_y, \omega_x, \omega_y, \omega_z)$	(ω_x, ω_z)	2
$(v_x, v_z, \omega_x, \omega_z)$	$(v_y, v_z, \omega_y, \omega_z)$	(v_z, ω_z)	2
$(v_x, v_z, \omega_x, \omega_z)$	$(v_y, v_z, \omega_x, \omega_z)$	$(v_z, \omega_x, \omega_z)$	3
$(v_x, v_z, \omega_x, \omega_z)$	$(v_y, v_z, \omega_x, \omega_y)$	(v_z, ω_x)	2
$(v_x, v_z, \omega_x, \omega_z)$	$(v_x, \omega_x, \omega_y, \omega_z)$	$(v_x, \omega_x, \omega_z)$	3
$(v_x, v_z, \omega_x, \omega_z)$	$(v_x, v_z, \omega_y, \omega_z)$	(v_x, v_z, ω_z)	3

$(v_x, v_z, \omega_x, \omega_z)$	$(v_x, v_z, \omega_x, \omega_z)$	$(v_x, v_z, \omega_x, \omega_z)$	4
$(v_x, v_z, \omega_x, \omega_z)$	$(v_x, v_z, \omega_x, \omega_y)$	(v_x, v_z, ω_x)	3
$(v_x, v_z, \omega_x, \omega_z)$	$(v_x, v_y, \omega_y, \omega_z)$	(v_x, ω_z)	2
$(v_x, v_z, \omega_x, \omega_z)$	$(v_x, v_y, \omega_x, \omega_z)$	$(v_x, \omega_x, \omega_z)$	3
$(v_x, v_z, \omega_x, \omega_z)$	$(v_x, v_y, \omega_x, \omega_y)$	(v_x, ω_x)	2
$(v_x, v_z, \omega_x, \omega_z)$	$(v_x, v_y, v_z, \omega_z)$	(v_x, v_z, ω_z)	3
$(v_x, v_z, \omega_x, \omega_z)$	$(v_x, v_y, v_z, \omega_y)$	(v_x, v_z)	2
$(v_x, v_z, \omega_x, \omega_z)$	$(v_x, v_y, v_z, \omega_x)$	(v_x, v_z, ω_x)	3
$(v_x, v_z, \omega_x, \omega_y)$	$(v_z, \omega_x, \omega_y, \omega_z)$	$(v_z, \omega_x, \omega_y)$	3
$(v_x, v_z, \omega_x, \omega_y)$	$(v_y, \omega_x, \omega_y, \omega_z)$	(ω_x, ω_y)	2
$(v_x, v_z, \omega_x, \omega_y)$	$(v_y, v_z, \omega_y, \omega_z)$	(v_z, ω_y)	2
$(v_x, v_z, \omega_x, \omega_y)$	$(v_y, v_z, \omega_x, \omega_z)$	(v_z, ω_x)	2
$(v_x, v_z, \omega_x, \omega_y)$	$(v_y, v_z, \omega_x, \omega_y)$	$(v_z, \omega_x, \omega_y)$	3
$(v_x, v_z, \omega_x, \omega_y)$	$(v_x, \omega_x, \omega_y, \omega_z)$	$(v_x, \omega_x, \omega_y)$	3
$(v_x, v_z, \omega_x, \omega_y)$	$(v_x, v_z, \omega_y, \omega_z)$	(v_x, v_z, ω_y)	3
$(v_x, v_z, \omega_x, \omega_y)$	$(v_x, v_z, \omega_x, \omega_z)$	(v_x, v_z, ω_x)	3
$(v_x, v_z, \omega_x, \omega_y)$	$(v_x, v_z, \omega_x, \omega_y)$	$(v_x, v_z, \omega_x, \omega_y)$	4
$(v_x, v_z, \omega_x, \omega_y)$	$(v_x, v_y, \omega_y, \omega_z)$	(v_x, ω_y)	2
$(v_x, v_z, \omega_x, \omega_y)$	$(v_x, v_y, \omega_x, \omega_z)$	(v_x, ω_x)	2
$(v_x, v_z, \omega_x, \omega_y)$	$(v_x, v_y, \omega_x, \omega_y)$	$(v_x, \omega_x, \omega_y)$	3
$(v_x, v_z, \omega_x, \omega_y)$	$(v_x, v_y, v_z, \omega_z)$	(v_x, v_z)	2
$(v_x, v_z, \omega_x, \omega_y)$	$(v_x, v_y, v_z, \omega_y)$	(v_x, v_z, ω_y)	3
$(v_x, v_z, \omega_x, \omega_y)$	$(v_x, v_y, v_z, \omega_x)$	(v_x, v_z, ω_x)	3
$(v_x, v_y, \omega_y, \omega_z)$	$(v_z, \omega_x, \omega_y, \omega_z)$	(ω_y, ω_z)	2
$(v_x, v_y, \omega_y, \omega_z)$	$(v_y, \omega_x, \omega_y, \omega_z)$	$(v_y, \omega_y, \omega_z)$	3
$(v_x, v_y, \omega_y, \omega_z)$	$(v_y, v_z, \omega_y, \omega_z)$	$(v_y, \omega_y, \omega_z)$	3
$(v_x, v_y, \omega_y, \omega_z)$	$(v_y, v_z, \omega_x, \omega_z)$	(v_y, ω_z)	2
$(v_x, v_y, \omega_y, \omega_z)$	$(v_y, v_z, \omega_x, \omega_y)$	(v_y, ω_y)	2
$(v_x, v_y, \omega_y, \omega_z)$	$(v_x, \omega_x, \omega_y, \omega_z)$	$(v_x, \omega_y, \omega_z)$	3
$(v_x, v_y, \omega_y, \omega_z)$	$(v_x, v_z, \omega_y, \omega_z)$	$(v_x, \omega_y, \omega_z)$	3
$(v_x, v_y, \omega_y, \omega_z)$	$(v_x, v_z, \omega_x, \omega_z)$	(v_x, ω_z)	2
$(v_x, v_y, \omega_y, \omega_z)$	$(v_x, v_z, \omega_x, \omega_y)$	(v_x, ω_y)	2
$(v_x, v_y, \omega_y, \omega_z)$	$(v_x, v_y, \omega_y, \omega_z)$	$(v_x, v_y, \omega_y, \omega_z)$	4
$(v_x, v_y, \omega_y, \omega_z)$	$(v_x, v_y, \omega_x, \omega_z)$	(v_x, v_y, ω_z)	3
$(v_x, v_y, \omega_y, \omega_z)$	$(v_x, v_y, \omega_x, \omega_y)$	(v_x, v_y, ω_y)	3
$(v_x, v_y, \omega_y, \omega_z)$	$(v_x, v_y, v_z, \omega_z)$	(v_x, v_y, ω_z)	3
$(v_x, v_y, \omega_y, \omega_z)$	$(v_x, v_y, v_z, \omega_y)$	(v_x, v_y, ω_y)	3
$(v_x, v_y, \omega_y, \omega_z)$	$(v_x, v_y, v_z, \omega_x)$	(v_x, v_y)	2
$(v_x, v_y, \omega_x, \omega_z)$	$(v_z, \omega_x, \omega_y, \omega_z)$	(ω_x, ω_z)	2
$(v_x, v_y, \omega_x, \omega_z)$	$(v_y, \omega_x, \omega_y, \omega_z)$	$(v_y, \omega_x, \omega_z)$	3
$(v_x, v_y, \omega_x, \omega_z)$	$(v_y, v_z, \omega_y, \omega_z)$	(v_y, ω_z)	2

$(v_x, v_y, \omega_x, \omega_z)$	$(v_y, v_z, \omega_x, \omega_z)$	$(v_y, \omega_x, \omega_z)$	3
$(v_x, v_y, \omega_x, \omega_z)$	$(v_y, v_z, \omega_x, \omega_y)$	(v_y, ω_x)	2
$(v_x, v_y, \omega_x, \omega_z)$	$(v_x, \omega_x, \omega_y, \omega_z)$	$(v_x, \omega_x, \omega_z)$	3
$(v_x, v_y, \omega_x, \omega_z)$	$(v_x, v_z, \omega_y, \omega_z)$	(v_x, ω_z)	2
$(v_x, v_y, \omega_x, \omega_z)$	$(v_x, v_z, \omega_x, \omega_z)$	$(v_x, \omega_x, \omega_z)$	3
$(v_x, v_y, \omega_x, \omega_z)$	$(v_x, v_z, \omega_x, \omega_y)$	(v_x, ω_x)	2
$(v_x, v_y, \omega_x, \omega_z)$	$(v_x, v_y, \omega_y, \omega_z)$	(v_x, v_y, ω_z)	3
$(v_x, v_y, \omega_x, \omega_z)$	$(v_x, v_y, \omega_x, \omega_z)$	$(v_x, v_y, \omega_x, \omega_z)$	4
$(v_x, v_y, \omega_x, \omega_z)$	$(v_x, v_y, \omega_x, \omega_y)$	(v_x, v_y, ω_x)	3
$(v_x, v_y, \omega_x, \omega_z)$	$(v_x, v_y, v_z, \omega_z)$	(v_x, v_y, ω_z)	3
$(v_x, v_y, \omega_x, \omega_z)$	$(v_x, v_y, v_z, \omega_y)$	(v_x, v_y)	2
$(v_x, v_y, \omega_x, \omega_z)$	$(v_x, v_y, v_z, \omega_x)$	(v_x, v_y, ω_x)	3
$(v_x, v_y, \omega_x, \omega_y)$	$(v_z, \omega_x, \omega_y, \omega_z)$	(ω_x, ω_y)	2
$(v_x, v_y, \omega_x, \omega_y)$	$(v_y, \omega_x, \omega_y, \omega_z)$	$(v_y, \omega_x, \omega_y)$	3
$(v_x, v_y, \omega_x, \omega_y)$	$(v_y, v_z, \omega_y, \omega_z)$	(v_y, ω_y)	2
$(v_x, v_y, \omega_x, \omega_y)$	$(v_y, v_z, \omega_x, \omega_z)$	(v_y, ω_x)	2
$(v_x, v_y, \omega_x, \omega_y)$	$(v_y, v_z, \omega_x, \omega_y)$	$(v_y, \omega_x, \omega_y)$	3
$(v_x, v_y, \omega_x, \omega_y)$	$(v_x, \omega_x, \omega_y, \omega_z)$	$(v_x, \omega_x, \omega_y)$	3
$(v_x, v_y, \omega_x, \omega_y)$	$(v_x, v_z, \omega_y, \omega_z)$	(v_x, ω_y)	2
$(v_x, v_y, \omega_x, \omega_y)$	$(v_x, v_z, \omega_x, \omega_z)$	(v_x, ω_x)	2
$(v_x, v_y, \omega_x, \omega_y)$	$(v_x, v_z, \omega_x, \omega_y)$	$(v_x, \omega_x, \omega_y)$	3
$(v_x, v_y, \omega_x, \omega_y)$	$(v_x, v_y, \omega_y, \omega_z)$	(v_x, v_y, ω_y)	3
$(v_x, v_y, \omega_x, \omega_y)$	$(v_x, v_y, \omega_x, \omega_z)$	(v_x, v_y, ω_x)	3
$(v_x, v_y, \omega_x, \omega_y)$	$(v_x, v_y, \omega_x, \omega_y)$	$(v_x, v_y, \omega_x, \omega_y)$	4
$(v_x, v_y, \omega_x, \omega_y)$	$(v_x, v_y, v_z, \omega_z)$	(v_x, v_y)	2
$(v_x, v_y, \omega_x, \omega_y)$	$(v_x, v_y, v_z, \omega_y)$	(v_x, v_y, ω_y)	3
$(v_x, v_y, \omega_x, \omega_y)$	$(v_x, v_y, v_z, \omega_x)$	(v_x, v_y, ω_x)	3
$(v_x, v_y, v_z, \omega_z)$	$(v_z, \omega_x, \omega_y, \omega_z)$	(v_z, ω_z)	2
$(v_x, v_y, v_z, \omega_z)$	$(v_y, \omega_x, \omega_y, \omega_z)$	(v_y, ω_z)	2
$(v_x, v_y, v_z, \omega_z)$	$(v_y, v_z, \omega_y, \omega_z)$	(v_y, ω_z)	2
$(v_x, v_y, v_z, \omega_z)$	$(v_y, v_z, \omega_x, \omega_z)$	(v_y, v_z, ω_z)	3
$(v_x, v_y, v_z, \omega_z)$	$(v_y, v_z, \omega_x, \omega_y)$	(v_y, v_z)	2
$(v_x, v_y, v_z, \omega_z)$	$(v_x, \omega_x, \omega_y, \omega_z)$	(v_x, ω_z)	2
$(v_x, v_y, v_z, \omega_z)$	$(v_x, v_z, \omega_y, \omega_z)$	(v_x, v_z, ω_z)	3
$(v_x, v_y, v_z, \omega_z)$	$(v_x, v_z, \omega_x, \omega_z)$	(v_x, v_z, ω_z)	3
$(v_x, v_y, v_z, \omega_z)$	$(v_x, v_z, \omega_x, \omega_y)$	(v_x, ω_z)	2
$(v_x, v_y, v_z, \omega_z)$	$(v_x, v_y, \omega_y, \omega_z)$	(v_x, v_y, ω_z)	3
$(v_x, v_y, v_z, \omega_z)$	$(v_x, v_y, \omega_x, \omega_z)$	(v_x, v_y, ω_z)	3
$(v_x, v_y, v_z, \omega_z)$	$(v_x, v_y, \omega_x, \omega_y)$	(v_x, v_y)	2
$(v_x, v_y, v_z, \omega_z)$	$(v_x, v_y, v_z, \omega_z)$	$(v_x, v_y, v_z, \omega_z)$	4

$(v_x, v_y, v_z, \omega_z)$	$(v_x, v_y, v_z, \omega_y)$	(v_x, v_y, v_z)	3
$(v_x, v_y, v_z, \omega_z)$	$(v_x, v_y, v_z, \omega_x)$	(v_x, v_y, v_z)	3
$(v_x, v_y, v_z, \omega_y)$	$(v_z, \omega_x, \omega_y, \omega_z)$	(v_z, ω_y)	2
$(v_x, v_y, v_z, \omega_y)$	$(v_y, \omega_x, \omega_y, \omega_z)$	(v_y, ω_y)	2
$(v_x, v_y, v_z, \omega_y)$	$(v_y, v_z, \omega_y, \omega_z)$	(v_y, ω_y)	2
$(v_x, v_y, v_z, \omega_y)$	$(v_y, v_z, \omega_x, \omega_z)$	(v_y, v_z)	2
$(v_x, v_y, v_z, \omega_y)$	$(v_y, v_z, \omega_x, \omega_y)$	(v_y, v_z, ω_y)	3
$(v_x, v_y, v_z, \omega_y)$	$(v_x, \omega_x, \omega_y, \omega_z)$	(v_x, ω_y)	2
$(v_x, v_y, v_z, \omega_y)$	$(v_x, v_z, \omega_y, \omega_z)$	(v_x, v_z, ω_y)	3
$(v_x, v_y, v_z, \omega_y)$	$(v_x, v_z, \omega_x, \omega_z)$	(v_x, v_z)	2
$(v_x, v_y, v_z, \omega_y)$	$(v_x, v_z, \omega_x, \omega_y)$	(v_x, v_z, ω_y)	3
$(v_x, v_y, v_z, \omega_y)$	$(v_x, v_y, \omega_y, \omega_z)$	(v_x, v_y, ω_y)	3
$(v_x, v_y, v_z, \omega_y)$	$(v_x, v_y, \omega_x, \omega_z)$	(v_x, v_y)	2
$(v_x, v_y, v_z, \omega_y)$	$(v_x, v_y, \omega_x, \omega_y)$	(v_x, v_y, ω_y)	3
$(v_x, v_y, v_z, \omega_y)$	$(v_x, v_y, v_z, \omega_z)$	(v_x, v_y, v_z)	3
$(v_x, v_y, v_z, \omega_y)$	$(v_x, v_y, v_z, \omega_y)$	$(v_x, v_y, v_z, \omega_y)$	4
$(v_x, v_y, v_z, \omega_y)$	$(v_x, v_y, v_z, \omega_x)$	(v_x, v_y, v_z)	3
$(v_x, v_y, v_z, \omega_x)$	$(v_z, \omega_x, \omega_y, \omega_z)$	(v_z, ω_x)	2
$(v_x, v_y, v_z, \omega_x)$	$(v_y, \omega_x, \omega_y, \omega_z)$	(v_y, ω_x)	2
$(v_x, v_y, v_z, \omega_x)$	$(v_y, v_z, \omega_y, \omega_z)$	(v_y, v_z)	2
$(v_x, v_y, v_z, \omega_x)$	$(v_y, v_z, \omega_x, \omega_z)$	(v_y, v_z, ω_x)	3
$(v_x, v_y, v_z, \omega_x)$	$(v_y, v_z, \omega_x, \omega_y)$	(v_y, v_z, ω_x)	3
$(v_x, v_y, v_z, \omega_x)$	$(v_x, \omega_x, \omega_y, \omega_z)$	(v_x, ω_x)	2
$(v_x, v_y, v_z, \omega_x)$	$(v_x, v_z, \omega_y, \omega_z)$	(v_x, v_z)	2
$(v_x, v_y, v_z, \omega_x)$	$(v_x, v_z, \omega_x, \omega_z)$	(v_x, v_z, ω_x)	3
$(v_x, v_y, v_z, \omega_x)$	$(v_x, v_z, \omega_x, \omega_y)$	(v_x, v_z, ω_x)	3
$(v_x, v_y, v_z, \omega_x)$	$(v_x, v_y, \omega_y, \omega_z)$	(v_x, v_y)	2
$(v_x, v_y, v_z, \omega_x)$	$(v_x, v_y, \omega_x, \omega_z)$	(v_x, v_y, ω_x)	3
$(v_x, v_y, v_z, \omega_x)$	$(v_x, v_y, \omega_x, \omega_y)$	(v_x, v_y, ω_x)	3
$(v_x, v_y, v_z, \omega_x)$	$(v_x, v_y, v_z, \omega_z)$	(v_x, v_y, v_z)	3
$(v_x, v_y, v_z, \omega_x)$	$(v_x, v_y, v_z, \omega_y)$	(v_x, v_y, v_z)	3
$(v_x, v_y, v_z, \omega_x)$	$(v_x, v_y, v_z, \omega_x)$	$(v_x, v_y, v_z, \omega_x)$	4

Formulating the six loop closure constraint equations while considering two independent input joints:

The **first kinematic constraint equation** corresponding to the natural coordinates as shown in figure 2.8 is obtained from the coordinates of O_5O_6 and O_7O_8.

$$\| \overrightarrow{\mathbf{O_5O_7}} \| = b \tag{1}$$

where,

O_5 is obtained from the matrix of $\mathbf{A_{05}}$, i.e the x, y and z coordinates of O_5 corresponds to $\mathbf{A_{05}}(2,1), \mathbf{A_{05}}(3,1)$ and $\mathbf{A_{05}}(4,1)$ respectively.

$O_7 = \begin{bmatrix} b \\ 0 \\ 0 \end{bmatrix}$, also $\overrightarrow{\mathbf{O_8H}} = \overrightarrow{\mathbf{O_5O_7}}$

Expanding equation (1) we get,

$$\left\| \begin{pmatrix} x_5 - b \\ y_5 - 0 \\ z_5 - 0 \end{pmatrix} \right\|^2 = b^2$$

$$\Rightarrow (x_5 - b)^2 + (y_5)^2 + (z_5)^2 = b^2$$

The values of x5, y5 and z5 are substituted in the above equation and the equation is simplified.

After solving and simplifying the above equation with the trigonometric formulae we get,

$$C_{10}S_{43} - S_{10}C_{21} + S_{10}C_{43}S_{321} = 1 \qquad (2)$$

where, $C_{ab} = Cos(\phi_{ab})$ and $S_{ab} = Sin(\phi_{ab})$

The **second kinematic equation** is obtained by various sets of equations involving parallelism and perpendicularity and thereafter making a common intersection between those equations as illustrated below. In the general configuration, $\overrightarrow{\mathbf{x_6}}$ and $\overrightarrow{\mathbf{x_7}}$ are non-collinear

$$\overrightarrow{\mathbf{x_7}} \perp \overrightarrow{\mathbf{z_7}} \qquad (3)$$

$$\overrightarrow{\mathbf{x_7}} \;//\; \overrightarrow{\mathbf{z_1}} \qquad (4)$$

$$\overrightarrow{\mathbf{z_1}} \perp \overrightarrow{\mathbf{z_7}} \qquad (5)$$

$$\overrightarrow{\mathbf{x_6}} \perp \overrightarrow{\mathbf{z_7}} \qquad (6)$$

From (5) and (6), $(\overrightarrow{\mathbf{x_6}} \times \overrightarrow{\mathbf{z_1}}) \;//\; \overrightarrow{\mathbf{z_7}}$ (7)

Also, $\overrightarrow{\mathbf{z_7}} \;//\; \overrightarrow{\mathbf{z_5}} \perp \overrightarrow{\mathbf{y_5}} \;//\; \overrightarrow{\mathbf{y_3}}$ (8)

From equation (8), $\Rightarrow \overrightarrow{\mathbf{z_7}} \perp \overrightarrow{\mathbf{y_3}}$ (9)

From (7) and (9), $(\overrightarrow{\mathbf{x_6}} \times \overrightarrow{\mathbf{z_1}}) \perp \overrightarrow{\mathbf{y_3}}$ (10)

$$\Rightarrow \overrightarrow{\mathbf{y_3}} \cdot (\overrightarrow{\mathbf{x_6}} \times \overrightarrow{\mathbf{z_1}}) = \mathbf{0} \qquad (11)$$

Where, $\overrightarrow{\mathbf{x_6}} \;//\; \overrightarrow{\mathbf{O_8H}}$

Hence, equation (11) becomes, $\overrightarrow{\mathbf{y_3}} \cdot (\overrightarrow{\mathbf{O_8H}} \times \overrightarrow{\mathbf{z_1}}) = \mathbf{0}$ (12)

$\overrightarrow{\mathbf{y_3}}$ is obtained from the matrix of $\mathbf{A_{03}}$, i.e the x, y and z coordinates of $\overrightarrow{\mathbf{y_3}}$ corresponds to $\mathbf{A_{03}}(2,3)$, $\mathbf{A_{03}}(3,3)$ and $\mathbf{A_{03}}(4,3)$ respectively.

$\overrightarrow{\mathbf{z_1}}$ is obtained from the matrix of $\mathbf{A_{01}}$, i.e the x, y and z coordinates of $\overrightarrow{\mathbf{z_1}}$ corresponds to $\mathbf{A_{01}}(2,4)$, $\mathbf{A_{01}}(3,4)$ and $\mathbf{A_{01}}(4,4)$ respectively.

After solving and simplifying the above equation with the trigonometric formulae we get,

$$[C_{32}C_{21} - S_{32}S_{21}][C_{10} - S_{43}] = 0$$

$$C(\phi_{32} + \phi_{21})(C_{10} - S_{43}) = 0 \qquad (13)$$

Solving the final simplified equations of (2) and (13), we obtain two values for $Ø_{32}$ and two values for $Ø_{43.}$ The complete schema of all the solutions is illustrated in a tabulation in the Annex II.

The **third kinematic constraint equation** is obtained as follows,

We know that, $\overrightarrow{\mathbf{x_1}} \;//\; \overrightarrow{\mathbf{z_6}}$ and $\overrightarrow{\mathbf{x_7}} \perp \overrightarrow{\mathbf{z_6}}$ (14)

From (14) we have, $\overrightarrow{\mathbf{x_1}} \perp \overrightarrow{\mathbf{x_7}}$ (15)

$\Rightarrow \overrightarrow{\mathbf{x_1}} \,.\, \overrightarrow{\mathbf{x_7}} = \mathbf{0}$ (Since $\overrightarrow{x_1}$ and $\overrightarrow{x_7}$) are orthogonal

Also, $\overrightarrow{\mathbf{x_7}} \perp \overrightarrow{\mathbf{z_6}}$ (16)

From equation (15) and (16) we get, $(\overrightarrow{\mathbf{x_1}} \times \overrightarrow{\mathbf{z_6}}) \;//\; \overrightarrow{\mathbf{x_7}}$

From figure 2.7, we can say that, $\overrightarrow{\mathbf{x_7}} \;//\; \overrightarrow{\mathbf{z_1}} \perp \overrightarrow{\mathbf{x_1}} \;//\; \overrightarrow{\mathbf{x_3}}$

$\Rightarrow \overrightarrow{\mathbf{x_7}} \perp \overrightarrow{\mathbf{x_3}}$ (17)

From equation (16) and (17) we get, $(\overrightarrow{\mathbf{x_3}} \times \overrightarrow{\mathbf{z_6}}) \perp \overrightarrow{\mathbf{x_7}}$ (18)

$\Rightarrow \overrightarrow{\mathbf{x_7}} \,.\, (\overrightarrow{\mathbf{x_3}} \times \overrightarrow{\mathbf{z_6}}) = 0$ (19)

Also from figure 2.7 we can say that, $\overrightarrow{\mathbf{x_7}} \;//\; \overrightarrow{\mathbf{z_1}}$ (20)

From equation (19) and (20) we get,

$$\overrightarrow{\mathbf{z_1}} . (\overrightarrow{\mathbf{x_3}} \times \overrightarrow{\mathbf{z_6}}) = 0 \qquad (21)$$

$\overrightarrow{\mathbf{x_3}}$ is obtained from the matirx of $\mathbf{A_{03}}$, i. e the x, y and z coordinates of $\overrightarrow{\mathbf{x_3}}$ corresponds to $\mathbf{A_{03}}(2,2)$, $\mathbf{A_{03}}(3,2)$ and $\mathbf{A_{03}}(4,2)$ respectively.

$\overrightarrow{\mathbf{z_1}}$ is obtained from the matirx of $\mathbf{A_{01}}$, i. e the x, y and z coordinates of $\overrightarrow{\mathbf{z_1}}$ corresponds to $\mathbf{A_{01}}(2,4)$, $\mathbf{A_{01}}(3,4)$ and $\mathbf{A_{01}}(4,4)$ respectively.

$\overrightarrow{\mathbf{z_6}}$ is obtained from the matirx of $\mathbf{A_{06}}$, i. e the x, y and z coordinates of $\overrightarrow{\mathbf{z_6}}$ corresponds to $\mathbf{A_{06}}(2,4)$, $\mathbf{A_{06}}(3,4)$ and $\mathbf{A_{06}}(4,4)$ respectively.

After solving and simplifying equation (21) we obtain,

$$S(\phi_{32}+\phi_{21})C(\phi_{54}+\phi_{43})=0 \tag{22}$$

Solving equation (22), we get a set a solutions for ϕ_{32} and ϕ_{54}. The complete sets of solutions are illustrated in Annex II.

The **fourth kinematic constraint** is quite simple and is directly obtained by homogeneous matrix as,

$$\overrightarrow{\mathbf{z_7}}=0 \tag{23}$$

$\overrightarrow{\mathbf{z_7}}$ is obtained from the matirx of $\mathbf{A_{07}}$, i. e the x, y and z coordinates of $\overrightarrow{\mathbf{z_7}}$ corresponds to $\mathbf{A_{07}}(2,4)$, $\mathbf{A_{07}}(3,4)$ and $\mathbf{A_{07}}(4,4)$ respectively.

There are two possible ways to obtain the joint angles for the fifth kinematic constraint equation. They are as follows,

i. From figure 2.7 we can see that, $\overrightarrow{\mathbf{x_8}} \perp \overrightarrow{\mathbf{x_1}} \Rightarrow \overrightarrow{\mathbf{x_8}}.\overrightarrow{\mathbf{x_1}}=0$ (24)

where, $\overrightarrow{\mathbf{x_1}}$ is obtained from the matrix of $\mathbf{A_{01}}$, i.e the x, y and z coordinates of $\overrightarrow{\mathbf{x_1}}$ corresponds to $\mathbf{A_{01}}(2,2)$, $\mathbf{A_{01}}(3,2)$ and $\mathbf{A_{01}}(4,2)$ respectively.

$\overrightarrow{\mathbf{x_8}}$ is obtained from the matirx of $\mathbf{A_{08}}$, i. e the x, y and z coordinates of $\overrightarrow{\mathbf{x_8}}$ corresponds to $\mathbf{A_{08}}(2,2)$, $\mathbf{A_{08}}(3,2)$ and $\mathbf{A_{08}}(4,2)$ respectively.

Substituting the values of $\overrightarrow{\mathbf{x_8}}$ and $\overrightarrow{\mathbf{x_1}}$ and simplifying the calculations we get,

$$C_{543}C_{765}=0$$

$$\Rightarrow [C(\phi_{54}+\phi_{43})][C(\phi_{76}+\phi_{65})]=0 \tag{25}$$

Solving equation (25) we obtain two solutions for ϕ_{54} and two solutions for ϕ_{76}.

ii. From figure 2.7 we can see that, $\overrightarrow{\mathbf{z_8}} \perp \overrightarrow{\mathbf{z_1}}$ and $\overrightarrow{\mathbf{z_1}} \perp \overrightarrow{\mathbf{x_1}}$

$$\Rightarrow (\overrightarrow{\mathbf{z_8}} \times \overrightarrow{\mathbf{x_1}}) // \overrightarrow{\mathbf{z_1}} \tag{26}$$

Also, $\overrightarrow{\mathbf{z_1}} // \overrightarrow{\mathbf{x_7}} \perp \overrightarrow{\mathbf{z_7}} // \overrightarrow{\mathbf{z_5}}$

$$\Rightarrow \overrightarrow{\mathbf{z_1}} \perp \overrightarrow{\mathbf{z_5}} \tag{27}$$

From equation (26) and (27) we get, $(\overrightarrow{\mathbf{z_8}} \times \overrightarrow{\mathbf{x_1}}) \perp \overrightarrow{\mathbf{z_5}}$ (28)

$$\Rightarrow \overrightarrow{\mathbf{z_5}}.(\overrightarrow{\mathbf{z_8}} \times \overrightarrow{\mathbf{x_1}}) = 0 \qquad (29)$$

where,

$\overrightarrow{\mathbf{z_5}}$ is obtained from the matirx of $\mathbf{A_{05}}$, i. e the x, y and z coordinates of $\overrightarrow{\mathbf{z_5}}$ corresponds to $\mathbf{A_{05}}(2,4)$, $\mathbf{A_{05}}(3,4)$ and $\mathbf{A_{05}}(4,4)$ respectively.

$\overrightarrow{\mathbf{z_8}}$ is obtained from the matirx of $\mathbf{A_{08}}$, i. e the x, y and z coordinates of $\overrightarrow{\mathbf{z_8}}$ corresponds to $\mathbf{A_{08}}(2,4)$, $\mathbf{A_{08}}(3,4)$ and $\mathbf{A_{08}}(4,4)$ respectively.

Solving equation (29) we obtain, $C_{543}C_{765}S_{87} = 0$

$$\Rightarrow C(\phi_{54}+\phi_{43})C(\phi_{76}+\phi_{65})S(\phi_{87}) = 0 \qquad (30)$$

By solving equation (30), we get a set of solutions for $\phi_{43}, \phi_{54}, \phi_{65}$ and ϕ_{76}.

The sixth kinematic constraint equation is obtained from figure 2.7 by equating $\overrightarrow{\mathbf{x_0}}$ and $\overrightarrow{\mathbf{y_8}}$

$$\overrightarrow{\mathbf{y_8}} = -\overrightarrow{\mathbf{x_0}} \qquad (31)$$

$\overrightarrow{\mathbf{y_8}}$ is obtained from the matirx of $\mathbf{A_{08}}$, i. e the x, y and z coordinates of $\overrightarrow{\mathbf{y_8}}$ corresponds to $\mathbf{A_{08}}(2,3)$, $\mathbf{A_{08}}(3,3)$ and $\mathbf{A_{08}}(4,3)$ respectively.

Substituting the values of $\overrightarrow{\mathbf{x_0}}$ and $\overrightarrow{\mathbf{y_8}}$ in equation (31) and after simplification we get,

$$C_{543}S_{765}S_{87} + S_{543}C_{87} = 0$$

$$\Rightarrow C(\phi_{54}+\phi_{43})S(\phi_{76}+\phi_{65})S(\phi_{87}) + S(\phi_{54}+\phi_{43})C(\phi_{87}) = 0 \qquad (32)$$

By solving equation (32), we obtain the joint angular values of the angles associated in the above equation.

Mathematical Calculation using Maple software:

#Equation 1:Distance between O5O7:

```
> x_h:= A05[2,1];
```

$$x\_h := -s10\,c21\,b + c10\,s43\,b + s10\,s321\,c43\,b$$

```
> y_h:= A05[3,1];
```

$$y\_h := c10\,c21\,b + s10\,s43\,b - c10\,s321\,c43\,b$$

```
> z_h:= A05[4,1];
```

$$z\_h := s21\,b + c321\,c43\,b$$

```
> x_7:= b;
```

$$x\_7 := b$$

```
> y_7:= 0;
```

$$y\_7 := 0$$

```
> z_7:= 0;
```

$$z\_7 := 0$$

```
> x:=expand((x_h-b)^2);
```

$$x := s10^2\,c21^2\,b^2 - 2\,s10\,c21\,b^2\,c10\,s43 - 2\,s10^2\,c21\,b^2\,s321\,c43 + 2\,s10\,c21\,b^2 + c10^2\,s43^2\,b^2 + 2\,c10\,s43\,b^2\,s10\,s321\,c43 - 2\,c10\,s43\,b^2 + s10^2\,s321^2\,c43^2\,b^2 - 2\,s10\,s321\,c43\,b^2 + b^2$$

```
> y:=expand((y_h-0)^2);
```

$$y := c10^2\,c21^2\,b^2 + 2\,s10\,c21\,b^2\,c10\,s43 - 2\,c10^2\,c21\,b^2\,s321\,c43 + s10^2\,s43^2\,b^2 - 2\,c10\,s43\,b^2\,s10\,s321\,c43 + c10^2\,s321^2\,c43^2\,b^2$$

```
> z:=expand((z_h-0)^2);
```

$$z := s21^2\,b^2 + 2\,s21\,b^2\,c321\,c43 + c321^2\,c43^2\,b^2$$

```
> d:=(x+y+z=b^2):
>
dis:=simplify(d,{c10*c10+s10*s10=1,c21*c21+s21*s21=1,c43*c43+s43*s43
=1,c321*c321+s321*s321=1});
```

$$dis := 3\,b^2 + 2\,s21\,b^2\,c321\,c43 - 2\,c10\,s43\,b^2 - 2\,s10\,s321\,c43\,b^2 + 2\,s10\,c21\,b^2 - 2\,b^2\,c21\,s321\,c43 = b^2$$

```
> #Equation  2: y3.(O5O7xz1):
> #Results: 1.)phi32:= -Pi/2-phi21, 2.)phi32:= Pi/2-phi21;
3.)phi43:= Pi/2-phi10, 4.)phi43:= phi10-Pi/2:

> #Substituting results of equation 2 in eq1:
> #For phi32:= (-Pi/2-phi21);
> solve(cos(phi10)*sin(phi43)-sin(phi10)*cos(phi43)-
sin(phi10)*cos(phi21)-cos(phi21)*cos(phi43)=1,phi43);
```

$$\phi10 + \frac{1}{2}\,\pi,\ \arctan\left(\frac{\sin(\phi21)^2\cos(\phi10)}{2\sin(\phi10)\cos(\phi21) + 2 - \sin(\phi21)^2},\ -\frac{\sin(\phi10) + 2\cos(\phi21) + \left(1 - \sin(\phi21)^2\right)\sin(\phi10)}{2\sin(\phi10)\cos(\phi21) + 2 - \sin(\phi21)^2}\right)$$

```
> #For phi32:= (Pi/2-phi21);
> solve(cos(phi10)*sin(phi43)+sin(phi10)*cos(phi43)-
sin(phi10)*cos(phi21)+cos(phi21)*cos(phi43)=1,phi43);
```

$$\frac{1}{2}\,\pi - \phi10,\ \arctan\left(\frac{\sin(\phi21)^2\cos(\phi10)}{2\sin(\phi10)\cos(\phi21) + 2 - \sin(\phi21)^2},\ \frac{\sin(\phi10) + 2\cos(\phi21) + \left(1 - \sin(\phi21)^2\right)\sin(\phi10)}{2\sin(\phi10)\cos(\phi21) + 2 - \sin(\phi21)^2}\right)$$

#Equation_3:Angle $Ø_{54}$:

```
> f:=solve(sin(phi43)+cos(phi54+phi43)*cos(phi65)=cos(phi10),phi54);
```

$$f := -\phi 43 + \pi - \arccos\left(\frac{\sin(\phi 43) - \cos(\phi 10)}{\cos(\phi 65)}\right)$$

#Equation_4:Angle $Ø_{65}$:

```
> z7:=simplify(z7,{c10*c10+s10*s10=1,c21*c21+s21*s21=1});
```

$$z7 := s21\,b - s65\,b$$

#Equation_5:Distance between (O3O5).y3 :Angle $Ø_{76}$

```
> O5:=matrix(3,1,[A05_eq5[2,1],A05_eq5[3,1],A05_eq5[4,1]]);
```

$$O5 := \begin{bmatrix} b - s76\,c87\,b \\ -s87\,s76\,b \\ c76\,b \end{bmatrix}$$

```
> O3:=matrix(3,1,[A03[2,1],A03[3,1],A03[4,1]]);
```

$$O3 := \begin{bmatrix} -s10\,c21\,b \\ c10\,c21\,b \\ s21\,b \end{bmatrix}$$

```
> x:=expand((A03[2,1]-A05_eq5[2,1])^2);
```

$$x := s10^2\,c21^2\,b^2 + 2\,s10\,c21\,b^2 - 2\,s10\,c21\,b^2\,s76\,c87 + b^2 - 2\,s76\,c87\,b^2 + s76^2\,c87^2\,b^2$$

```
> y:=expand((A03[3,1]-A05_eq5[3,1])^2);
```

$$y := c10^2\,c21^2\,b^2 + 2\,c10\,c21\,b^2\,s87\,s76 + s87^2\,s76^2\,b^2$$

```
> z:=expand((A03[4,1]-A05_eq5[4,1])^2);
```

$$z := s21^2\,b^2 - 2\,s21\,b^2\,c76 + c76^2\,b^2$$

```
> d:=(x+y+z=b^2):
dis_eq5:=simplify(d,{c10*c10+s10*s10=1,c21*c21+s21*s21=1,c87*c87+s87
*s87=1,c76*c76+s76*s76=1});
```

$$dis\_eq5 := 3\,b^2 + 2\,s10\,c21\,b^2 - 2\,s76\,c87\,b^2 - 2\,s21\,b^2\,c76 + 2\,c10\,c21\,b^2\,s87\,s76 - 2\,s10\,c21\,b^2\,s76\,c87 = b^2$$

#Equation_6: Distance between O0O3 :Angle $Ø_{87}$:

```
> x3:=A03_eq3[2,1];
```

$$x3 := b - c87\,(s76\,b - s54\,b\,s765) + c54\,s87\,b$$

```
> y3:=A03_eq3[3,1];
```

$$y3 := -s87\,(s76\,b - s54\,b\,s765) - c87\,c54\,b$$

```
> z3:=A03_eq3[4,1];
```

$$z3 := c76\,b - s54\,b\,c765$$

```
> x:=expand((0-A03_eq3[2,1])^2);
```

$$x := b^2 - 2\,s76\,c87\,b^2 + 2\,c87\,s54\,b^2\,s765 + 2\,c54\,s87\,b^2 + s76^2\,c87^2\,b^2 - 2\,s76\,c87^2\,b^2\,s54\,s765 - 2\,s76\,c87\,b^2\,c54\,s87 + c87^2\,s54^2\,b^2\,s765^2 + 2\,c87\,s54\,b^2\,s765\,c54\,s87 + c54^2\,s87^2\,b^2$$

```
> y:=expand((0-A03_eq3[3,1])^2);
```

$$y := s87^2\,s76^2\,b^2 - 2\,s87^2\,s76\,b^2\,s54\,s765 + 2\,s76\,c87\,b^2\,c54\,s87 + s87^2\,s54^2\,b^2\,s765^2 - 2\,c87\,s54\,b^2\,s765\,c54\,s87 + c87^2\,c54^2\,b^2$$

```
> z:=expand((0-A03_eq3[4,1])^2);
```

$$z := c76^2\,b^2 - 2\,c76\,b^2\,s54\,c765 + s54^2\,b^2\,c765^2$$

```
> d:=(x+y+z=b^2):
>
dis_eq3:=simplify(d,{c76*c76+s76*s76=1,c54*c54+s54*s54=1,c87*c87+s87
*s87=1,c765*c765+s765*s765=1});
```

$$dis\_eq3 := 3\,b^2 - 2\,s76\,c87\,b^2 + 2\,c54\,s87\,b^2 + 2\,c87\,s54\,b^2\,s765 - 2\,c76\,b^2\,s54\,c765 - 2\,b^2\,s76\,s54\,s765 = b^2$$

```
> # Result of phi87:
> v1:=sin(phi76)*cos(phi87)-cos(phi87)*sin(phi54)*sin(phi76+phi65)-
cos(phi54)*sin(phi87)+cos(phi76)*sin(phi54)*cos(phi76+phi65)+sin(phi
76)*sin(phi54)*sin(phi76+phi65)=1;
```

$$v1 := \sin(\phi76)\cos(\phi87) - \cos(\phi87)\sin(\phi54)\sin(\phi76 + \phi65) - \cos(\phi54)\sin(\phi87) + \cos(\phi76)\sin(\phi54)\cos(\phi76 + \phi65) + \sin(\phi76)\sin(\phi54)\sin(\phi76 + \phi65) = 1$$

```
> # Case :1
> phi76:=-Pi/2-phi21;phi65:=phi21-Pi;
```

$$\phi76 := -\frac{1}{2}\,\pi - \phi21$$

$$\phi65 := \phi21 - \pi$$

```
> v1;
```

$$-\cos(\phi21)\cos(\phi87) - \cos(\phi87)\sin(\phi54) - \cos(\phi54)\sin(\phi87) - \cos(\phi21)\sin(\phi54) = 1$$

```
> solve(v1,phi87);
```

$$-\frac{1}{2}\pi-\phi54,\ \arctan\left(\frac{\left(-1+\cos(\phi21)^2\right)\cos(\phi54)}{\cos(\phi21)^2+2\cos(\phi21)\sin(\phi54)+1},\ -\frac{\sin(\phi54)+\sin(\phi54)\cos(\phi21)^2+2\cos(\phi21)}{\cos(\phi21)^2+2\cos(\phi21)\sin(\phi54)+1}\right)$$

```
> # Case :2
> phi76:=Pi/2-phi21;phi65:=phi21-Pi;
```

$$\phi76 := \frac{1}{2}\pi-\phi21$$

$$\phi65 := \phi21-\pi$$

```
> v1;
```

$$\cos(\phi21)\cos(\phi87)+\cos(\phi87)\sin(\phi54)-\cos(\phi54)\sin(\phi87)-\cos(\phi21)\sin(\phi54)=1$$

```
> solve(v1,phi87);
```

$$\phi54-\frac{1}{2}\pi,\ \arctan\left(\frac{\left(-1+\cos(\phi21)^2\right)\cos(\phi54)}{\cos(\phi21)^2+2\cos(\phi21)\sin(\phi54)+1},\ \frac{\sin(\phi54)+\sin(\phi54)\cos(\phi21)^2+2\cos(\phi21)}{\cos(\phi21)^2+2\cos(\phi21)\sin(\phi54)+1}\right)$$

```
> # Case :3
> phi76:=Pi/2+phi21;phi65:=-phi21;
```

$$\phi76 := \frac{1}{2}\pi+\phi21$$

$$\phi65 := -\phi21$$

```
> v1;
```

$$\cos(\phi21)\cos(\phi87)-\cos(\phi87)\sin(\phi54)-\cos(\phi54)\sin(\phi87)+\cos(\phi21)\sin(\phi54)=1$$

```
> solve(v1,phi87);
```

$$-\frac{1}{2}\pi-\phi54,\ \arctan\left(\frac{\left(-1+\cos(\phi21)^2\right)\cos(\phi54)}{-2\cos(\phi21)\sin(\phi54)+1+\cos(\phi21)^2},\ -\frac{\sin(\phi54)+\sin(\phi54)\cos(\phi21)^2-2\cos(\phi21)}{-2\cos(\phi21)\sin(\phi54)+1+\cos(\phi21)^2}\right)$$

```
> # Case :4
> phi76:=phi21-Pi/2;phi65:=-phi21;
```

$$\phi76 := -\frac{1}{2}\pi+\phi21$$

$$\phi65 := -\phi21$$

```
> v1;
```

$$-\cos(\phi 21)\cos(\phi 87) + \cos(\phi 87)\sin(\phi 54) - \cos(\phi 54)\sin(\phi 87) + \cos(\phi 21)\sin(\phi 54) = 1$$

```
> solve(v1,phi87);
```

$$\phi 54 - \frac{1}{2}\pi, \arctan\left(\frac{\left(-1+\cos(\phi 21)^2\right)\cos(\phi 54)}{-2\cos(\phi 21)\sin(\phi 54)+1+\cos(\phi 21)^2}, \frac{\sin(\phi 54)+\sin(\phi 54)\cos(\phi 21)^2-2\cos(\phi 21)}{-2\cos(\phi 21)\sin(\phi 54)+1+\cos(\phi 21)^2}\right)$$

Angular values for a particular configuration of an eight-bar reconfigurable mechanism

The tabulation presented below shows the complete set of joint values for each joint angle. The solutions high lightened are a complete set of joint angular values for a particular configuration.

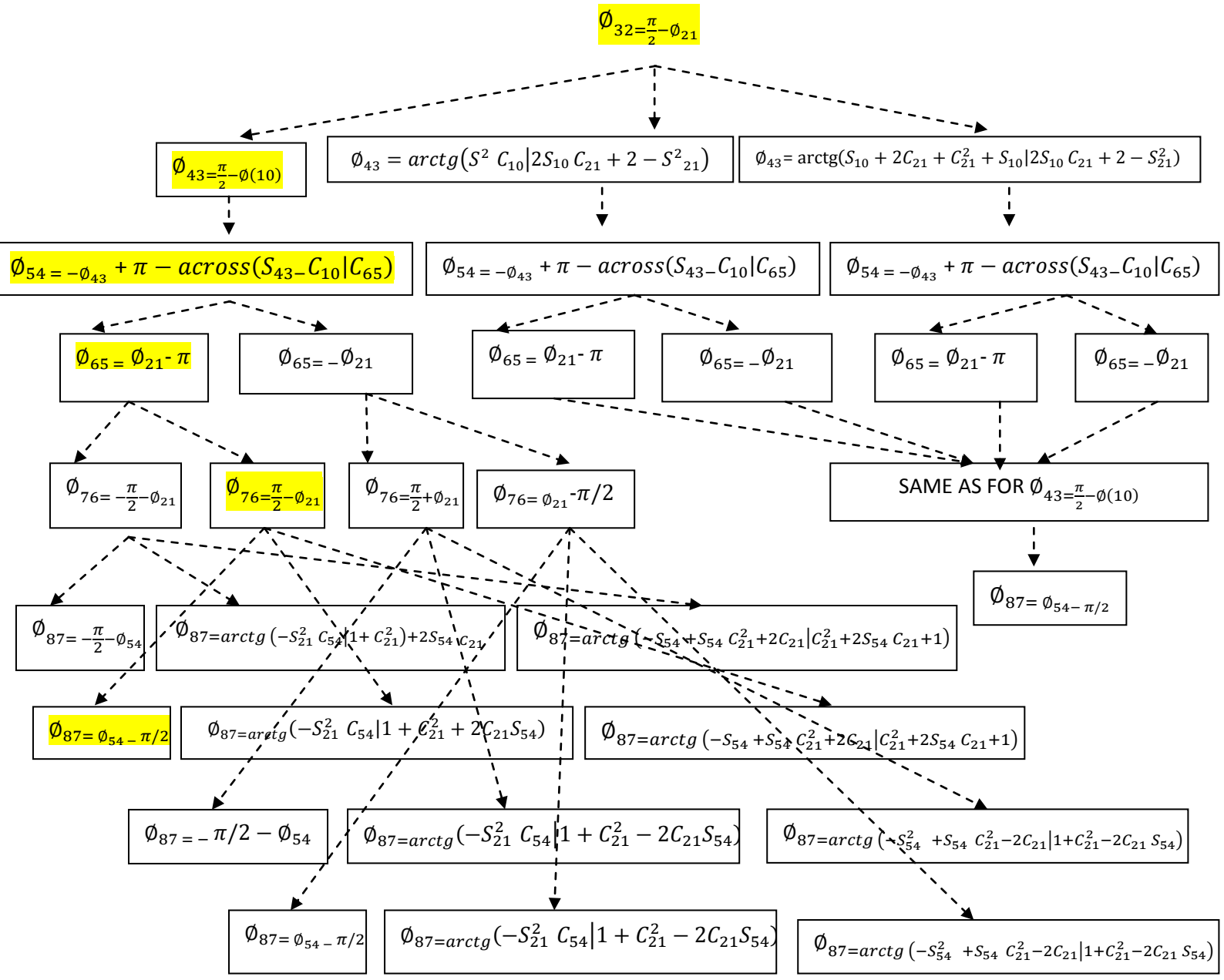

Annex III

The vector spaces associated with each limb of the mechanism presented in Figure 3.4a are illustrated below by means of calculating the Jacobian matrix of each limb.

$$J_{04}=\begin{bmatrix}0 & b & 0 & 0\\ b & 0 & 0 & b\\ 0 & -b & -b & 0\\ 0 & 0 & 0 & 0\\ 0 & 1 & 1 & 0\\ 1 & 0 & 0 & 1\end{bmatrix}, Rank(J_{04})=3$$

$$R_{G1}=(v_x,\omega_y,\omega_z),(v_z,\omega_y,\omega_z) or (v_x,v_z,\omega_z)$$

$$J_{85}=\begin{bmatrix}0 & 0 & 0 & 0\\ -b & 0 & -b & b\\ 0 & 0 & 0 & 0\\ 0 & 1 & 1 & 0\\ 0 & 0 & 0 & 0\\ 1 & 0 & 0 & -1\end{bmatrix}, Rank(J_{04})=3$$

$$R_{G2}=(v_y,\omega_x,\omega_z)$$

Table A3.1 Possible combinations of vector spaces with minimum S_F presented in Figure 3.4a

$(\boldsymbol{R_{G1}})$	$(\boldsymbol{R_{G2}})$	$(\boldsymbol{R_F})$	$\boldsymbol{S_F}$
(v_x, v_y, v_z)	$(v_y, \omega_x, \omega_z)$	(v_y)	1
(v_x, v_y, ω_y)	$(v_y, \omega_x, \omega_z)$	(v_y)	1
(v_x, v_y, ω_z)	$(v_y, \omega_x, \omega_z)$	(v_y, ω_z)	2
(v_x, v_z, ω_y)	$(v_y, \omega_x, \omega_z)$	(-)	0
(v_x, v_z, ω_z)	$(v_y, \omega_x, \omega_z)$	(ω_z)	1
$(v_x, \omega_y, \omega_z)$	$(v_y, \omega_x, \omega_z)$	(ω_z)	1
$(v_y, \omega_y, \omega_z)$	$(v_y, \omega_x, \omega_z)$	(v_y, ω_z)	2
(v_y, v_z, ω_y)	$(v_y, \omega_x, \omega_z)$	(v_y)	1
(v_y, v_z, ω_z)	$(v_y, \omega_x, \omega_z)$	(v_y, ω_z)	2
$(v_z, \omega_y, \omega_z)$	$(v_y, \omega_x, \omega_z)$	(ω_z)	1

Direct Kinematic model of Limb G_1	***Dim*$(R_{G1}) =$ *rank of JG1***	***Basis*** (R_{G1})
$\begin{bmatrix} v_x \\ v_y \\ v_z \end{bmatrix} = \begin{bmatrix} 0 & b & 0 & 0 \\ b & 0 & 0 & b \\ 0 & -b & -b & 0 \end{bmatrix} \begin{bmatrix} \dot{\varphi}_{10} \\ \dot{\phi}_{21} \\ \dot{\phi}_{32} \\ \dot{\phi}_{43} \end{bmatrix}$	3	(v_x, v_y, v_z)
$\begin{bmatrix} v_x \\ v_y \\ \omega_y \end{bmatrix} = \begin{bmatrix} 0 & b & 0 & 0 \\ b & 0 & 0 & b \\ 0 & 1 & 1 & 0 \end{bmatrix} \begin{bmatrix} \dot{\varphi}_{10} \\ \dot{\phi}_{21} \\ \dot{\phi}_{32} \\ \dot{\phi}_{43} \end{bmatrix}$	3	(v_x, v_y, ω_y)
$\begin{bmatrix} v_x \\ v_z \\ \omega_z \end{bmatrix} = \begin{bmatrix} 0 & b & 0 & 0 \\ 0 & -b & -b & 0 \\ 1 & 0 & 0 & 1 \end{bmatrix} \begin{bmatrix} \dot{\varphi}_{10} \\ \dot{\phi}_{21} \\ \dot{\phi}_{32} \\ \dot{\phi}_{43} \end{bmatrix}$	3	(v_x, v_z, ω_z)
$\begin{bmatrix} v_x \\ \omega_y \\ \omega_z \end{bmatrix} = \begin{bmatrix} 0 & b & 0 & 0 \\ 0 & 1 & 1 & 0 \\ 1 & 0 & 0 & 1 \end{bmatrix} \begin{bmatrix} \dot{\varphi}_{10} \\ \dot{\phi}_{21} \\ \dot{\phi}_{32} \\ \dot{\phi}_{43} \end{bmatrix}$	3	$(v_x, \omega_y, \omega_z)$

Direct Kinematic model of Limb G_2	***Dim*$(R_{G2}) =$ *rank of JG2***	***Basis*** (R_{G2})
$\begin{bmatrix} v_y \\ \omega_x \\ \omega_z \end{bmatrix} = \begin{bmatrix} 0 & 0 & -b & b \\ 0 & 1 & 1 & 0 \\ 1 & 0 & 0 & -1 \end{bmatrix} \begin{bmatrix} \dot{\varphi}_{87} \\ \dot{\phi}_{76} \\ \dot{\phi}_{65} \\ \dot{\phi}_{54} \end{bmatrix}$	3	$(v_y, \omega_x, \omega_z)$

In Figure 3.4b : $\phi^a_{21} = 0^\circ, \phi^a_{32} = 90^\circ, \phi^a_{43} = 0^\circ, \phi^a_{54} = 90^\circ, \phi^b_{45} = 90^\circ, \phi^b_{34} = 270^\circ, \phi^b{}_{23} = 0^\circ,\ \phi^b_{12} = 0^\circ$.

$$J_{04}=\begin{bmatrix}0&0&0&0\\b&-b&0&b\\0&0&0&0\\0&1&1&0\\0&0&0&0\\1&0&0&1\end{bmatrix}, Rank(J_{04})=3$$

$$R_{G1}=(v_y,\omega_x,\omega_z))$$

$$J_{85}=\begin{bmatrix}0&0&-b&0\\0&-b&-b&0\\b&0&0&-b\\0&0&0&0\\1&0&0&-1\\0&1&1&0\end{bmatrix}, Rank(J_{04})=3$$

$$R_{G2}=(v_x,v_z,\omega_z),(v_x,\omega_y,\omega_z),(v_z,\omega_y,\omega_z)$$

The vector spaces associated with each limb of the mechanism presented in Figure 3.4b are illustrated below by means of calculating the Jacobian matrix of each limb.

Table A3.2 Possible combinations of vector spaces with minimum S_F presented in Figure 3.4b

$(\boldsymbol{R_{G1}})$	$(\boldsymbol{R_{G2}})$	$(\boldsymbol{R_F})$	$\boldsymbol{S_F}$
(v_y,ω_x,ω_z)	(v_x,v_y,v_z)	(v_y)	1
(v_y,ω_x,ω_z)	(v_x,v_y,ω_y)	(v_y)	1
(v_y,ω_x,ω_z)	(v_x,v_y,ω_z)	(v_y,ω_z)	2
(v_y,ω_x,ω_z)	(v_x,v_z,ω_y)	(-)	0
(v_y,ω_x,ω_z)	(v_x,v_z,ω_z)	(ω_z)	1
(v_y,ω_x,ω_z)	(v_x,ω_y,ω_z)	(ω_z)	1
(v_y,ω_x,ω_z)	(v_y,ω_y,ω_z)	(v_y,ω_z)	2
(v_y,ω_x,ω_z)	(v_y,v_z,ω_y)	(v_y)	1
(v_y,ω_x,ω_z)	(v_y,v_z,ω_z)	(v_y,ω_z)	2
(v_y,ω_x,ω_z)	(v_z,ω_y,ω_z)	(ω_z)	1

Direct Kinematic model of Limb G_1	***Dim(R_{G1}) = rank of JG1***	***Basis (R_{G1})***
$\begin{bmatrix}v_y\\\omega_x\\\omega_z\end{bmatrix}=\begin{bmatrix}b&-b&0&b\\0&1&1&0\\1&0&0&1\end{bmatrix}\begin{bmatrix}\dot{\varphi}_{10}\\\dot{\phi}_{21}\\\dot{\phi}_{32}\\\dot{\phi}_{43}\end{bmatrix}$	3	(v_y,ω_x,ω_z)

Direct Kinematic model of Limb G_2	***Dim(R_{G2}) = rank of JG2***	***Basis (R_{G2})***
$\begin{bmatrix} v_x \\ v_y \\ v_z \end{bmatrix} = \begin{bmatrix} 0 & 0 & -b & 0 \\ 0 & -b & -b & 0 \\ b & 0 & 0 & -b \end{bmatrix} \begin{bmatrix} \dot{\varphi}_{87} \\ \dot{\phi}_{76} \\ \dot{\phi}_{65} \\ \dot{\phi}_{54} \end{bmatrix}$	3	(v_x, v_y, v_z)
$\begin{bmatrix} v_x \\ v_y \\ \omega_y \end{bmatrix} = \begin{bmatrix} 0 & 0 & -b & 0 \\ 0 & -b & -b & 0 \\ 1 & 0 & 0 & -1 \end{bmatrix} \begin{bmatrix} \dot{\varphi}_{87} \\ \dot{\phi}_{76} \\ \dot{\phi}_{65} \\ \dot{\phi}_{54} \end{bmatrix}$	3	(v_x, v_y, ω_y)
$\begin{bmatrix} v_x \\ v_z \\ \omega_z \end{bmatrix} = \begin{bmatrix} 0 & 0 & -b & 0 \\ b & 0 & 0 & -b \\ 0 & 1 & 1 & 0 \end{bmatrix} \begin{bmatrix} \dot{\varphi}_{87} \\ \dot{\phi}_{76} \\ \dot{\phi}_{65} \\ \dot{\phi}_{54} \end{bmatrix}$	3	(v_x, v_z, ω_z)
$\begin{bmatrix} v_x \\ \omega_y \\ \omega_z \end{bmatrix} = \begin{bmatrix} 0 & 0 & -b & 0 \\ 1 & 0 & 0 & -1 \\ 0 & 1 & 1 & 0 \end{bmatrix} \begin{bmatrix} \dot{\varphi}_{87} \\ \dot{\phi}_{76} \\ \dot{\phi}_{65} \\ \dot{\phi}_{54} \end{bmatrix}$	3	$(v_x, \omega_y, \omega_z)$

The vector spaces associated with each limb of the mechanism presented in Figure 3.4c are illustrated below by means of calculating the Jacobian matrix of each limb. In Figure 3.4c : $\phi^a_{21} = 90^\circ, \phi^a_{32} = 90^\circ, \phi^a_{43} = 0^\circ, \phi^a_{54} = 0^\circ, \phi^b_{45} = 90^\circ, \phi^b_{34} = 270^\circ, \phi^b_{23} = 0^\circ,\ \phi^b_{12} = 0^\circ$.

$$J_{04} = \begin{bmatrix} 0 & b & 0 & 0 \\ b & 0 & 0 & b \\ 0 & -b & -b & 0 \\ 0 & 0 & 0 & 0 \\ 0 & 1 & 1 & 0 \\ 1 & 0 & 0 & 1 \end{bmatrix}, Rank(J_{04}) = 3$$

$$R_{G1} = (v_x, \omega_y, \omega_z), (v_x, v_y, v_z) or\ (v_x, v_y, \omega_y)$$

$$J_{85} = \begin{bmatrix} 0 & 0 & -b & 0 \\ 0 & -b & -b & 0 \\ b & 0 & 0 & -b \\ 0 & 0 & 0 & 0 \\ 1 & 0 & 0 & -1 \\ 0 & 1 & 1 & 0 \end{bmatrix}, Rank(J_{04}) = 3$$

$$R_{G2} = (v_x, \omega_y, \omega_z)$$

Table A3.3 Possible combinations of vector spaces with minimum S_F presented in Figure 3.4c

(R_{G1})	(R_{G2})	(R_F)	S_F
(v_x, v_y, v_z)	(v_x, v_y, v_z)	(v_x, v_y, v_z)	3
(v_x, v_y, v_z)	(v_x, v_y, ω_y)	(v_x, v_y)	2
(v_x, v_y, v_z)	(v_x, v_y, ω_z)	(v_x)	1
(v_x, v_y, v_z)	(v_x, v_z, ω_y)	(v_x)	1
(v_x, v_y, v_z)	(v_x, v_z, ω_z)	(v_x, v_z)	2
(v_x, v_y, v_z)	$(v_x, \omega_y, \omega_z)$	(v_x)	1
(v_x, v_y, v_z)	$(v_y, \omega_y, \omega_z)$	(v_y)	1
(v_x, v_y, v_z)	(v_y, v_z, ω_y)	(v_y, v_z)	2
(v_x, v_y, v_z)	(v_y, v_z, ω_z)	(v_y, v_z)	2
(v_x, v_y, v_z)	$(v_z, \omega_y, \omega_z)$	(v_z)	1
(v_x, v_y, ω_y)	(v_x, v_y, v_z)	(v_x, v_y)	2
(v_x, v_y, ω_y)	(v_x, v_y, ω_y)	(v_x, v_y, ω_y)	3
(v_x, v_y, ω_y)	(v_x, v_y, ω_z)	(v_x, v_y)	2
(v_x, v_y, ω_y)	(v_x, v_z, ω_y)	(v_x, ω_y)	2
(v_x, v_y, ω_y)	(v_x, v_z, ω_z)	(v_x)	1
(v_x, v_y, ω_y)	$(v_x, \omega_y, \omega_z)$	(v_x, ω_y)	2
(v_x, v_y, ω_y)	$(v_y, \omega_y, \omega_z)$	(v_y, ω_y)	2
(v_x, v_y, ω_y)	(v_y, v_z, ω_y)	(v_y, ω_y)	2
(v_x, v_y, ω_y)	(v_y, v_z, ω_z)	(v_y)	1
(v_x, v_y, ω_y)	$(v_z, \omega_y, \omega_z)$	(ω_y)	1
(v_x, v_y, ω_z)	(v_x, v_y, v_z)	(v_x, v_y)	2
(v_x, v_y, ω_y)	(v_x, v_y, ω_z)	(v_x, v_y)	2
(v_x, v_y, ω_y)	(v_x, v_z, ω_y)	(v_x, ω_y)	2
(v_x, v_y, ω_y)	(v_x, v_z, ω_z)	(v_x)	1
(v_x, v_y, ω_y)	$(v_x, \omega_y, \omega_z)$	(v_x, ω_y)	2
(v_x, v_y, ω_y)	$(v_y, \omega_y, \omega_z)$	(v_y, ω_y)	2
(v_x, v_y, ω_y)	(v_y, v_z, ω_y)	(v_y, ω_y)	2
(v_x, v_y, ω_y)	(v_y, v_z, ω_z)	(v_y)	1
(v_x, v_y, ω_y)	$(v_z, \omega_y, \omega_z)$	(ω_y)	1
(v_x, v_z, ω_y)	(v_x, v_y, v_z)	(v_x)	1
(v_x, v_y, ω_y)	(v_x, v_y, ω_z)	(v_x, v_y)	2
(v_x, v_y, ω_y)	(v_x, v_z, ω_y)	(v_x, ω_y)	2
(v_x, v_y, ω_y)	(v_x, v_z, ω_z)	(v_x)	1
(v_x, v_y, ω_y)	$(v_x, \omega_y, \omega_z)$	(v_x, ω_y)	2
(v_x, v_y, ω_y)	$(v_y, \omega_y, \omega_z)$	(v_y, ω_y)	2
(v_x, v_y, ω_y)	(v_y, v_z, ω_y)	(v_y, ω_y)	2
(v_x, v_y, ω_y)	(v_y, v_z, ω_z)	(v_y)	1

(v_x, v_y, ω_y)	$(v_z, \omega_y, \omega_z)$	(ω_y)	1
(v_x, v_z, ω_z)	(v_x, v_y, v_z)	(v_x, v_z)	2
(v_x, v_z, ω_z)	(v_x, v_y, ω_y)	(v_x)	1
(v_x, v_z, ω_z)	(v_x, v_y, ω_z)	(v_x, ω_z)	2
(v_x, v_z, ω_z)	(v_x, v_z, ω_y)	(v_x, v_z)	2
(v_x, v_z, ω_z)	(v_x, v_z, ω_z)	(v_x, v_z, ω_z)	3
(v_x, v_z, ω_z)	$(v_x, \omega_y, \omega_z)$	(v_x, ω_z)	2
(v_x, v_z, ω_z)	$(v_y, \omega_y, \omega_z)$	(ω_z)	1
(v_x, v_z, ω_z)	(v_y, v_z, ω_y)	(v_z)	1
(v_x, v_z, ω_z)	(v_y, v_z, ω_z)	(v_z, ω_z)	2
(v_x, v_z, ω_z)	$(v_z, \omega_y, \omega_z)$	(v_z, ω_z)	2
$(v_x, \omega_y, \omega_z)$	(v_x, v_y, v_z)	(v_x)	1
$(v_x, \omega_y, \omega_z)$	(v_x, v_y, ω_y)	(v_x, ω_y)	2
$(v_x, \omega_y, \omega_z)$	(v_x, v_y, ω_z)	(v_x, ω_z)	2
$(v_x, \omega_y, \omega_z)$	(v_x, v_z, ω_y)	(v_x, ω_y)	2
$(v_x, \omega_y, \omega_z)$	(v_x, v_z, ω_z)	(v_x, ω_z)	2
$(v_x, \omega_y, \omega_z)$	$(v_x, \omega_y, \omega_z)$	$(v_x, \omega_y, \omega_z)$	3
$(v_x, \omega_y, \omega_z)$	$(v_y, \omega_y, \omega_z)$	(ω_y, ω_z)	2
$(v_x, \omega_y, \omega_z)$	(v_y, v_z, ω_y)	(ω_y)	1
$(v_x, \omega_y, \omega_z)$	(v_y, v_z, ω_z)	(ω_z)	1
$(v_x, \omega_y, \omega_z)$	$(v_z, \omega_y, \omega_z)$	(ω_y, ω_z)	2
$(v_y, \omega_y, \omega_z)$	(v_x, v_y, v_z)	(v_y)	1
$(v_y, \omega_y, \omega_z)$	(v_x, v_y, ω_y)	(v_y, ω_y)	2
$(v_y, \omega_y, \omega_z)$	(v_x, v_y, ω_z)	(v_y, ω_z)	2
$(v_y, \omega_y, \omega_z)$	(v_x, v_z, ω_y)	(ω_y)	1
$(v_y, \omega_y, \omega_z)$	(v_x, v_z, ω_z)	(ω_z)	1
$(v_y, \omega_y, \omega_z)$	$(v_x, \omega_y, \omega_z)$	(ω_y, ω_z)	2
$(v_y, \omega_y, \omega_z)$	$(v_y, \omega_y, \omega_z)$	$(v_y, \omega_y, \omega_z)$	3
$(v_y, \omega_y, \omega_z)$	(v_y, v_z, ω_y)	(v_y, ω_y)	2
$(v_y, \omega_y, \omega_z)$	(v_y, v_z, ω_z)	(v_y, ω_z)	2
$(v_y, \omega_y, \omega_z)$	$(v_z, \omega_y, \omega_z)$	(ω_y, ω_z)	2
(v_y, v_z, ω_y)	(v_x, v_y, v_z)	(v_y, v_z)	2
(v_y, v_z, ω_y)	(v_x, v_y, ω_y)	(v_y, ω_y)	2
(v_y, v_z, ω_y)	(v_x, v_y, ω_z)	(v_y)	1
(v_y, v_z, ω_y)	(v_x, v_z, ω_y)	(v_z, ω_y)	2
(v_y, v_z, ω_y)	(v_x, v_z, ω_z)	(v_z)	1
(v_y, v_z, ω_y)	$(v_x, \omega_y, \omega_z)$	(ω_y)	1
(v_y, v_z, ω_y)	$(v_y, \omega_y, \omega_z)$	(v_y, ω_y)	2
(v_y, v_z, ω_y)	(v_y, v_z, ω_y)	(v_y, v_z, ω_y)	3
(v_y, v_z, ω_y)	(v_y, v_z, ω_z)	(v_y, v_z)	2
(v_y, v_z, ω_y)	$(v_z, \omega_y, \omega_z)$	(v_z, ω_y)	2

(v_y, v_z, ω_z)	(v_x, v_y, v_z)	(v_y, v_z)	2
(v_y, v_z, ω_z)	(v_x, v_y, ω_y)	(v_y)	1
(v_y, v_z, ω_z)	(v_x, v_y, ω_z)	(v_y, ω_z)	2
(v_y, v_z, ω_z)	(v_x, v_z, ω_y)	(v_z)	1
(v_y, v_z, ω_z)	(v_x, v_z, ω_z)	(v_z, ω_z)	2
(v_y, v_z, ω_z)	$(v_x, \omega_y, \omega_z)$	(ω_z)	1
(v_y, v_z, ω_z)	$(v_y, \omega_y, \omega_z)$	(v_y, ω_z)	2
(v_y, v_z, ω_z)	(v_y, v_z, ω_y)	(v_y, v_z)	2
(v_y, v_z, ω_z)	(v_y, v_z, ω_z)	(v_y, v_z, ω_z)	3
(v_y, v_z, ω_z)	$(v_z, \omega_y, \omega_z)$	(v_z, ω_z)	2
$(v_z, \omega_y, \omega_z)$	(v_x, v_y, v_z)	(v_z)	1
$(v_z, \omega_y, \omega_z)$	(v_x, v_y, ω_y)	(ω_y)	1
$(v_z, \omega_y, \omega_z)$	(v_x, v_y, ω_z)	(ω_z)	1
$(v_z, \omega_y, \omega_z)$	(v_x, v_z, ω_y)	(v_z, ω_y)	2
$(v_z, \omega_y, \omega_z)$	(v_x, v_z, ω_z)	(v_z, ω_z)	2
$(v_z, \omega_y, \omega_z)$	$(v_x, \omega_y, \omega_z)$	(ω_y, ω_z)	2
$(v_z, \omega_y, \omega_z)$	$(v_y, \omega_y, \omega_z)$	(ω_y, ω_z)	2
$(v_z, \omega_y, \omega_z)$	(v_y, v_z, ω_y)	(v_z, ω_y)	2
$(v_z, \omega_y, \omega_z)$	(v_y, v_z, ω_z)	(v_z, ω_z)	2
$(v_z, \omega_y, \omega_z)$	$(v_z, \omega_y, \omega_z)$	$(v_z, \omega_y, \omega_z)$	3

Direct Kinematic model of Limb G_1	***Dim(R_{G1}) = rank of JG1***	***Basis (R_{G1})***
$\begin{bmatrix} v_x \\ v_y \\ v_z \end{bmatrix} = \begin{bmatrix} 0 & b & 0 & 0 \\ b & 0 & 0 & b \\ 0 & -b & -b & 0 \end{bmatrix} \begin{bmatrix} \dot{\varphi}_{10} \\ \dot{\phi}_{21} \\ \dot{\phi}_{32} \\ \dot{\phi}_{43} \end{bmatrix}$	3	(v_x, v_y, v_z)
$\begin{bmatrix} v_x \\ v_y \\ \omega_y \end{bmatrix} = \begin{bmatrix} 0 & b & 0 & 0 \\ b & 0 & 0 & b \\ 0 & 1 & 1 & 0 \end{bmatrix} \begin{bmatrix} \dot{\varphi}_{10} \\ \dot{\phi}_{21} \\ \dot{\phi}_{32} \\ \dot{\phi}_{43} \end{bmatrix}$	3	(v_x, v_y, ω_y)
$\begin{bmatrix} v_x \\ v_z \\ \omega_z \end{bmatrix} = \begin{bmatrix} 0 & b & 0 & 0 \\ 0 & -b & -b & 0 \\ 1 & 0 & 0 & 1 \end{bmatrix} \begin{bmatrix} \dot{\varphi}_{10} \\ \dot{\phi}_{21} \\ \dot{\phi}_{32} \\ \dot{\phi}_{43} \end{bmatrix}$	3	(v_x, v_z, ω_z)

$\begin{bmatrix} \mathrm{v_x} \\ \omega_\mathrm{y} \\ \omega_\mathrm{z} \end{bmatrix} = \begin{bmatrix} 0 & b & 0 & 0 \\ 0 & 1 & 1 & 0 \\ 1 & 0 & 0 & 1 \end{bmatrix} \begin{bmatrix} \dot{\varphi}_{10} \\ \dot{\phi}_{21} \\ \dot{\phi}_{32} \\ \dot{\phi}_{43} \end{bmatrix}$	3	$(v_x, \omega_y, \omega_z)$

Direct Kinematic model of Limb G_2	***Dim$(R_{G2}) =$ rank of JG2***	***Basis (R_{G2})***
$\begin{bmatrix} \mathrm{v_x} \\ v_\mathrm{y} \\ v_\mathrm{z} \end{bmatrix} = \begin{bmatrix} 0 & 0 & -b & 0 \\ 0 & -b & -b & 0 \\ b & 0 & 0 & -b \end{bmatrix} \begin{bmatrix} \dot{\varphi}_{87} \\ \dot{\phi}_{76} \\ \dot{\phi}_{65} \\ \dot{\phi}_{54} \end{bmatrix}$	3	(v_x, v_y, v_z)
$\begin{bmatrix} \mathrm{v_x} \\ \mathrm{v_y} \\ \omega_\mathrm{y} \end{bmatrix} = \begin{bmatrix} 0 & 0 & -b & 0 \\ 0 & -b & -b & 0 \\ 1 & 0 & 0 & -1 \end{bmatrix} \begin{bmatrix} \dot{\varphi}_{87} \\ \dot{\phi}_{76} \\ \dot{\phi}_{65} \\ \dot{\phi}_{54} \end{bmatrix}$	3	(v_x, v_y, ω_y)
$\begin{bmatrix} \mathrm{v_x} \\ v_\mathrm{z} \\ \omega_\mathrm{z} \end{bmatrix} = \begin{bmatrix} 0 & 0 & -b & 0 \\ b & 0 & 0 & -b \\ 0 & 1 & 1 & 0 \end{bmatrix} \begin{bmatrix} \dot{\varphi}_{87} \\ \dot{\phi}_{76} \\ \dot{\phi}_{65} \\ \dot{\phi}_{54} \end{bmatrix}$	3	(v_x, v_z, ω_z)
$\begin{bmatrix} \mathrm{v_x} \\ \omega_\mathrm{y} \\ \omega_\mathrm{z} \end{bmatrix} = \begin{bmatrix} 0 & 0 & -b & 0 \\ 1 & 0 & 0 & -1 \\ 0 & 1 & 1 & 0 \end{bmatrix} \begin{bmatrix} \dot{\varphi}_{87} \\ \dot{\phi}_{76} \\ \dot{\phi}_{65} \\ \dot{\phi}_{54} \end{bmatrix}$	3	$(v_x, \omega_y, \omega_z)$

Annex IV

Matlab code for trajectory generation

```
%       Input parameters :
%
%                   u : time
%
%  Output parameters :
%
%                   Qcurrent=[q,dq] where :
%
%                               q      : interpolated joint variables
%                               dq     : first derivative of q  (joint velocity)
 function Qcurrent=main_8bar_5T_1(u)
temps =u;
if(u<=0.5)

   % Independent angles
   q1 =0;
   q2 =0;

   % Dependent on q1 and q2
   q3 = 0;
   q4 = 0;
   q6 = 0;
   q5 = 0;
   q7 = 0;
   q8 = 0;

   qi= [0,0,0,0,0];
   qf= [0,0,0,0,0];

   kv=[1,1,1,1,1];
   ka=[1,1,1,1,1];

   % For 1st torque
   D1=qf(:,1)-qi(:,1);
   % Calculation of minimum travelling time
   tf1=max(15*abs(D1)/(8*kv(:,1)),sqrt(10*abs(D1)/(sqrt(3)*ka(:,1))));
   % Calculation of interpolation function
   if(tf1>0)
   r1=6*(temps/tf1)^5-15*(temps/tf1)^4+10*(temps/tf1)^3;
   else
      r1=0;
   end;
   % Calculation of joint variables
   q1=qi(:,1)+r1*D1;

   % For 2nd torque
   D2=qf(:,2)-qi(:,2);
   % Calculation of minimum time
   tf2=max(15*abs(D2)/(8*kv(:,2)),sqrt(10*abs(D2)/(sqrt(3)*ka(:,2))));
```

```
   % Calculation of interpolation function
   if(tf2>0)
   r2=6*(temps/tf2)^5-15*(temps/tf2)^4+10*(temps/tf2)^3;
   else
      r2=0;
   end;
   % Calculation of joint variables
   q2=qi(:,2)+r2*D2;

   % For 3nd torque
   D3=qf(:,3)-qi(:,3);
   % Calculation of minimum time
   tf3=max(15*abs(D3)/(8*kv(:,3)),sqrt(10*abs(D3)/(sqrt(3)*ka(:,3))));
   if(tf3>0)
   r3=6*(temps/tf3)^5-15*(temps/tf3)^4+10*(temps/tf3)^3;
   else
   r3=0;
   end;
   q3=qi(:,3)+r3*D3;

   % For 4th torque
   D4=qf(:,4)-qi(:,4);
   % Calculation of minimum time
   tf4=max(15*abs(D4)/(8*kv(:,4)),sqrt(10*abs(D4)/(sqrt(3)*ka(:,4))));
   % Calculation of interpolation function
   if(tf4>0)
   r4=6*(temps/tf4)^5-15*(temps/tf4)^4+10*(temps/tf4)^3;
  else
   r4=0;
  end;
   % Calculation of joint variables
   q4=qi(:,4)+r4*D4;


   % For 5th torque
   D5=qf(:,5)-qi(:,5);
   % Calculation of minimum time
   tf5=max(15*abs(D5)/(8*kv(:,5)),sqrt(10*abs(D5)/(sqrt(3)*ka(:,5))));
   % Calculation of interpolation function
   if(tf5>0)
   r5=6*(temps/tf5)^5-15*(temps/tf5)^4+10*(temps/tf5)^3;
   else
      r5=0;
   end;
   % Calculation of joint variables
   q5=qi(:,5)+r5*D5;

   Qcurrent=[q1,q2,q3,q4,q5];
end
%%%%%%%%%%%%%%%%%%%%%%%%%%%%%%%%%%%%%%%%%%%%%%%%%%%%%%%%%%%%%%%%%%%%%%%%%%%%
if(0.5<u && u<=20);
temps_recale=temps-0.5;
%
   % Independent angles
```

```
q1 = pi/2;
q2 = 0;

% Dependent on q1 and q2
q3 = 0;
q4 = 0;
q6 = 0;
q5 = 0;
q7 = 0;
q8 = -pi/2;

qi= [0,0,0,0,0];
qf= [q1,q2,q3,q7,q8];

kv=[1,1,1,1,1];
ka=[1,1,1,1,1];

% For 1st torque
D1=qf(:,1)-qi(:,1);
% Calculation of minimum travelling time
tf1=max(15*abs(D1)/(8*kv(:,1)),sqrt(10*abs(D1)/(sqrt(3)*ka(:,1))));
% Calculation of interpolation function
if(tf1>0 && temps_recale<=tf1)
r1=6*((temps_recale)/tf1)^5-15*((temps_recale)/tf1)^4+10*((temps_recale)/tf1)^3;
   elseif(temps_recale>tf1)
   r1=1;
    end;
% Calculation of joint variables
q1=qi(:,1)+r1*D1;

% For 2nd torque
D2=qf(:,2)-qi(:,2);
% Calculation of minimum time
tf2=max(15*abs(D2)/(8*kv(:,2)),sqrt(10*abs(D2)/(sqrt(3)*ka(:,2))));
% Calculation of interpolation function
if(tf2>0 && temps_recale<=tf2)
r2=6*(temps_recale/tf2)^5-15*(temps_recale/tf2)^4+10*(temps_recale/tf2)^3;
elseif (temps_recale>tf2)
   r2=1;
   end;
% Calculation of joint variables
q2=qi(:,2)+r2*D2;

% For 3nd torque
D3=qf(:,3)-qi(:,3);
% Calculation of minimum time
tf3=max(15*abs(D3)/(8*kv(:,3)),sqrt(10*abs(D3)/(sqrt(3)*ka(:,3))));
if(tf3>0 && temps_recale<=tf3)
r3=6*(temps_recale/tf3)^5-15*(temps_recale/tf3)^4+10*(temps_recale/tf3)^3;
elseif (temps_recale>tf3)
r3=1;
end;
q3=qi(:,3)+r3*D3;
```

```
    % For 4th torque
    D4=qf(:,4)-qi(:,4);
    % Calculation of minimum time
    tf4=max(15*abs(D4)/(8*kv(:,4)),sqrt(10*abs(D4)/(sqrt(3)*ka(:,4))));
    % Calculation of interpolation function
    if(tf4>0 && temps_recale<=tf4)
    r4=6*(temps_recale/tf4)^5-15*(temps_recale/tf4)^4+10*(temps_recale/tf4)^3;
    elseif (temps_recale>tf4)
    r4=1;
    end;
    % Calculation of joint variables
    q4=qi(:,4)+r4*D4;


    % For 5th torque
    D5=qf(:,5)-qi(:,5);
    % Calculation of minimum time
    tf5=max(15*abs(D5)/(8*kv(:,5)),sqrt(10*abs(D5)/(sqrt(3)*ka(:,5))));
    % Calculation of interpolation function
    if(tf5>0 && temps_recale<=tf5)
    r5=6*(temps_recale/tf5)^5-15*(temps_recale/tf5)^4+10*(temps_recale/tf5)^3;
    elseif (temps_recale>tf5)
       r5=1;
       end;
    % Calculation of joint variables
    q5=qi(:,5)+r5*D5;

    Qcurrent=[q1,q2,q3,q4,q5];
end
```

Coupling between Adams / Simulink

Once the Adams model of the 8-bar linkage is ready, it is necessary to generate the input joint torques and the output positions of the Adams block. In our case, we have 5 input torques namely $\gamma_1, \gamma_2, \gamma_3, \gamma_4$ and γ_5 with 5 output positions ($q_1, q_{2,} q_3, q_4$ and q_5). To generate these variables we do the following:

Step 1:

Go to **Build** ⟶ **System elements** ⟶ **State variables** ⟶ **New**

Now we are free to create our state variables one by one. As shown in the figure A.0.1, to create the input torques, we go to the main toolbox and select forces and click Applied Force: Torque (Single-component), then we select the action and the reaction body and define the function as : VARVAL(Torque_1). We repeat the same for the remaining torques $\gamma_2, \gamma_3, \gamma_4$ and γ_5.

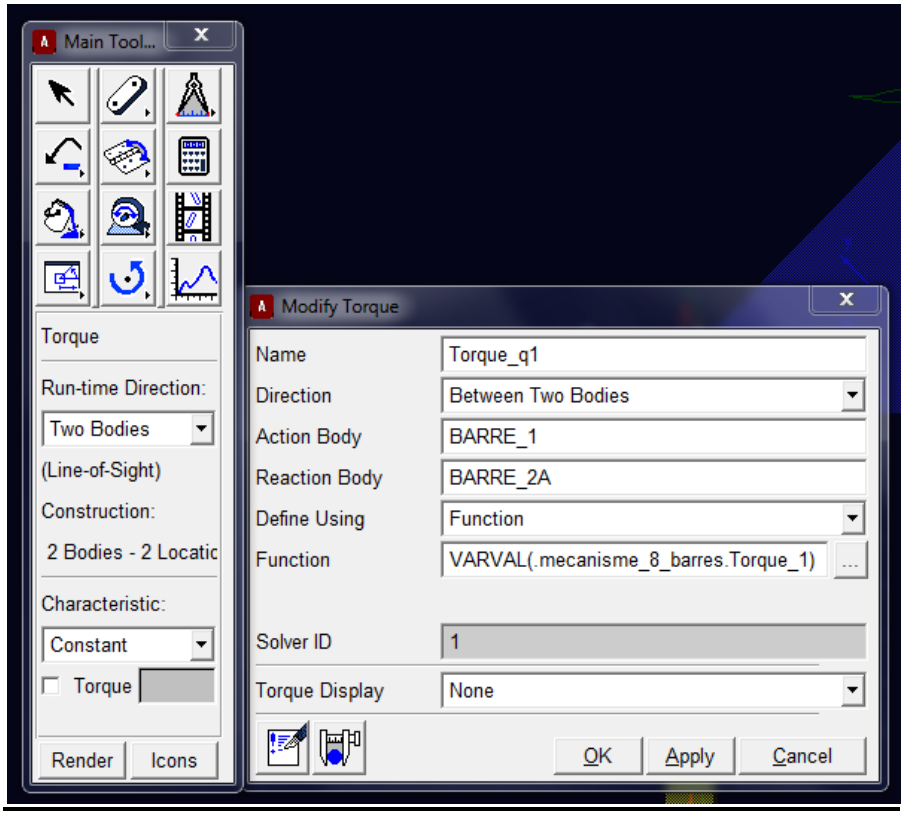

Figure A.0.1 Parameterization of the Torque_q1

By doing this, we have well-defined the input torques of the Adams model. Now we define the function for the joint variables $q_1, q_{2,} q_3, q_4$ and q_5 by clicking modify state variables. For q_1, we define its function in relation to the markers associated with joint 1 and its rotational axis 'z' as shown in figure A.0.2.

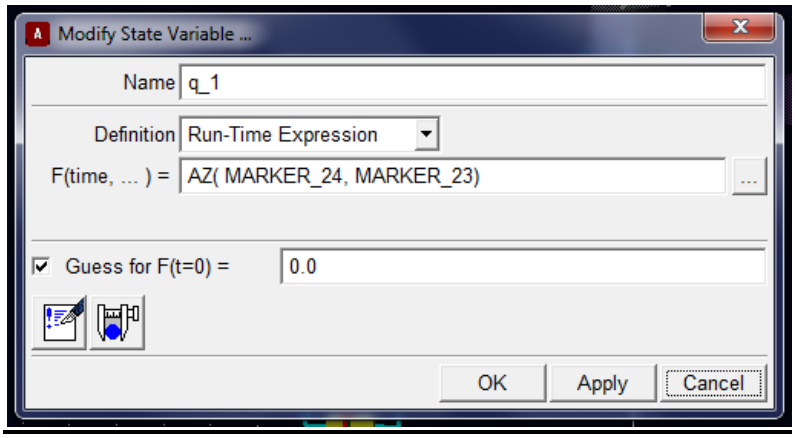

Figure A.0.2 Parameterization of the output joint variable q1

Step 2:

We now define the plant input and output for the control in Simulink. For this, we do the following:

Go to **Build** ⟶ **Data elements** ⟶ **Plants** ⟶ **Plant input** ⟶ **New**

For the plant input, we add the variable name as the Torque_1, Torque_2, Torque_3, Torque_4, Torque_5 as shown in figure A.0.3

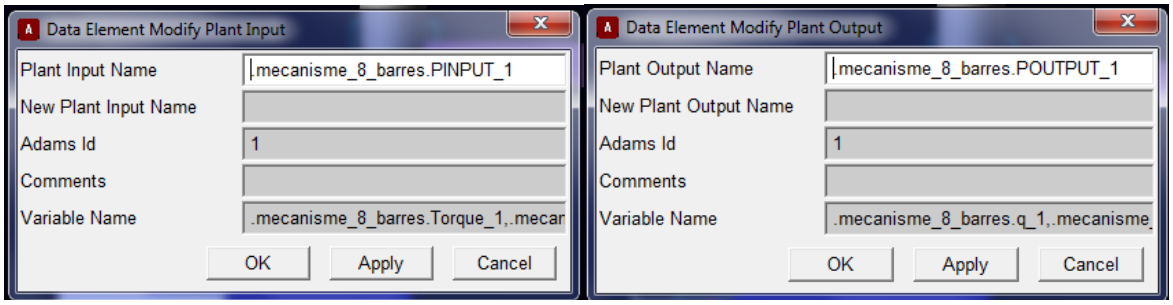

Figure A.0.3 Definition of plant input and output

To define the plant output, Go to **Build** ⟶ **Data elements** ⟶ **Plants** ⟶ **Plant output** ⟶ **New**

For the plant output, we add the variable name as the q_1, q_2, q_3, q_4, q_5 as shown in figure A.0.3.

The final step is to export the file that couples Adams with Simulink. For this we go to,

Menu controls ⟶ **Plant Export**

Once this is done, we obtain the following as shown in figure A.0.4.

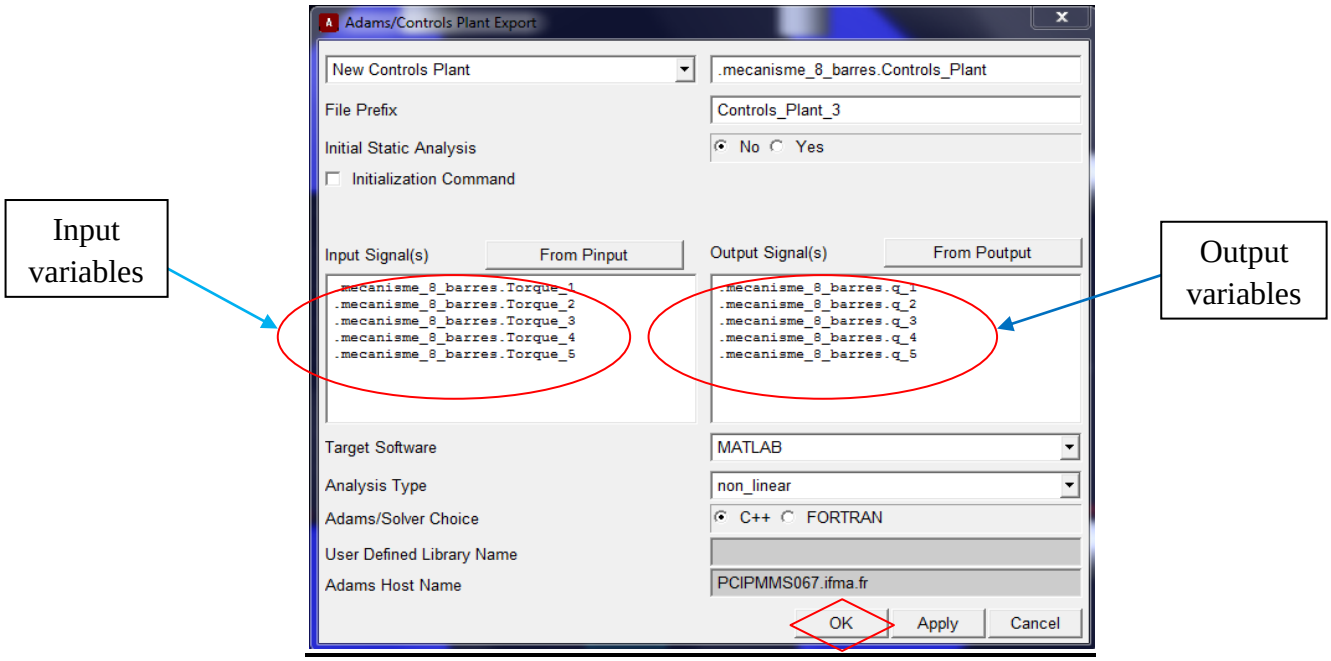

Figure A. 0.4 Generation of the control plant with input and output variables

Hence we obtain the Adams block to be connected with the PID controller in Simulink. Now to connect the block with Simulink, we need to call the file generated by Adams in the command window of Matlab. In our case, we call the function by typing, "Controls_Plant" as enumerated in figure A.0.5 and then to obtain the block, we type "adams_sys".

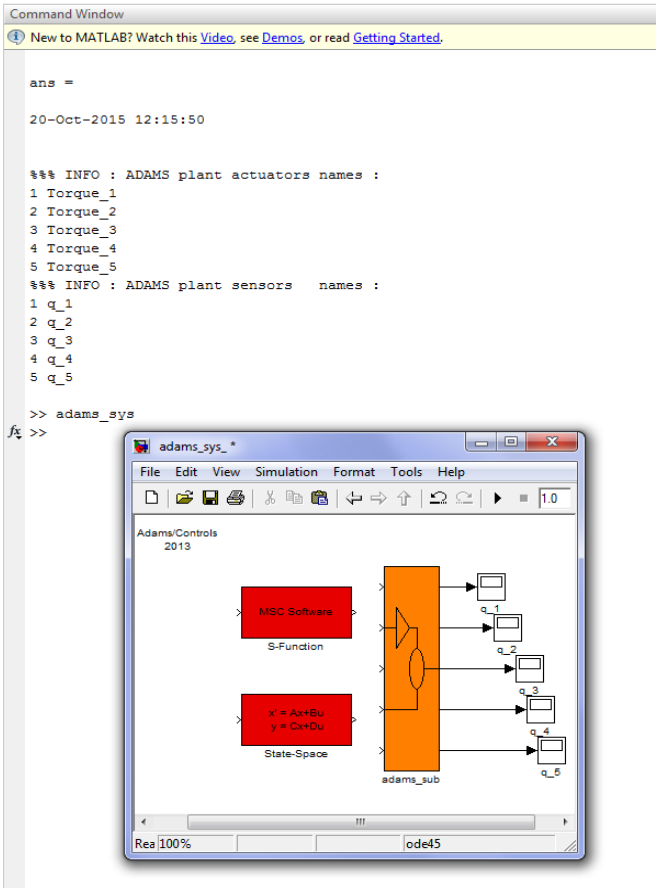

Figure A.0.5 Matlab command for obtaining the Adams block

By double clicking the red block in figure A.0.5, we obtain the sub-system as shown in figure A.0.6.

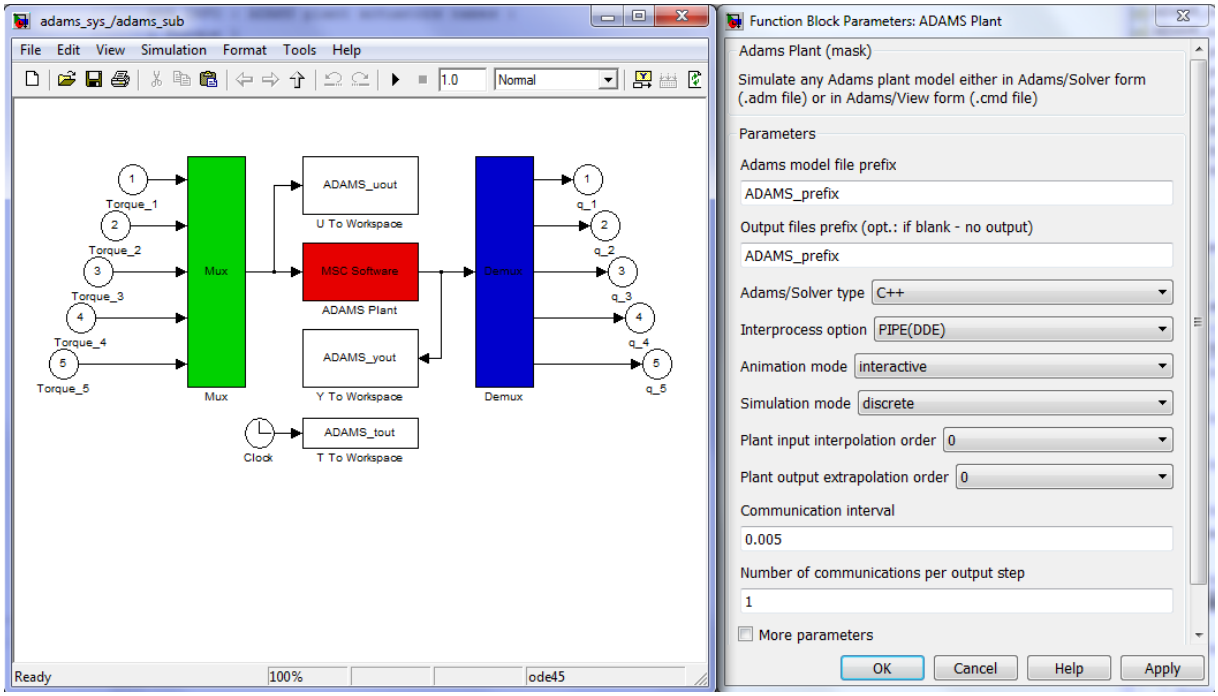

Figure A.0.6 Subsystem of the Adams block and its parameterization

Now, to parameterize the Adams plant, we click on the red block (MSC Software). By doing this, we open the function block parameters tab, we need to change the animation mode from batch to discrete so that we could see the movements of the mechanism during the simulation in Matlab Simulink.

Simulink Model for PID control

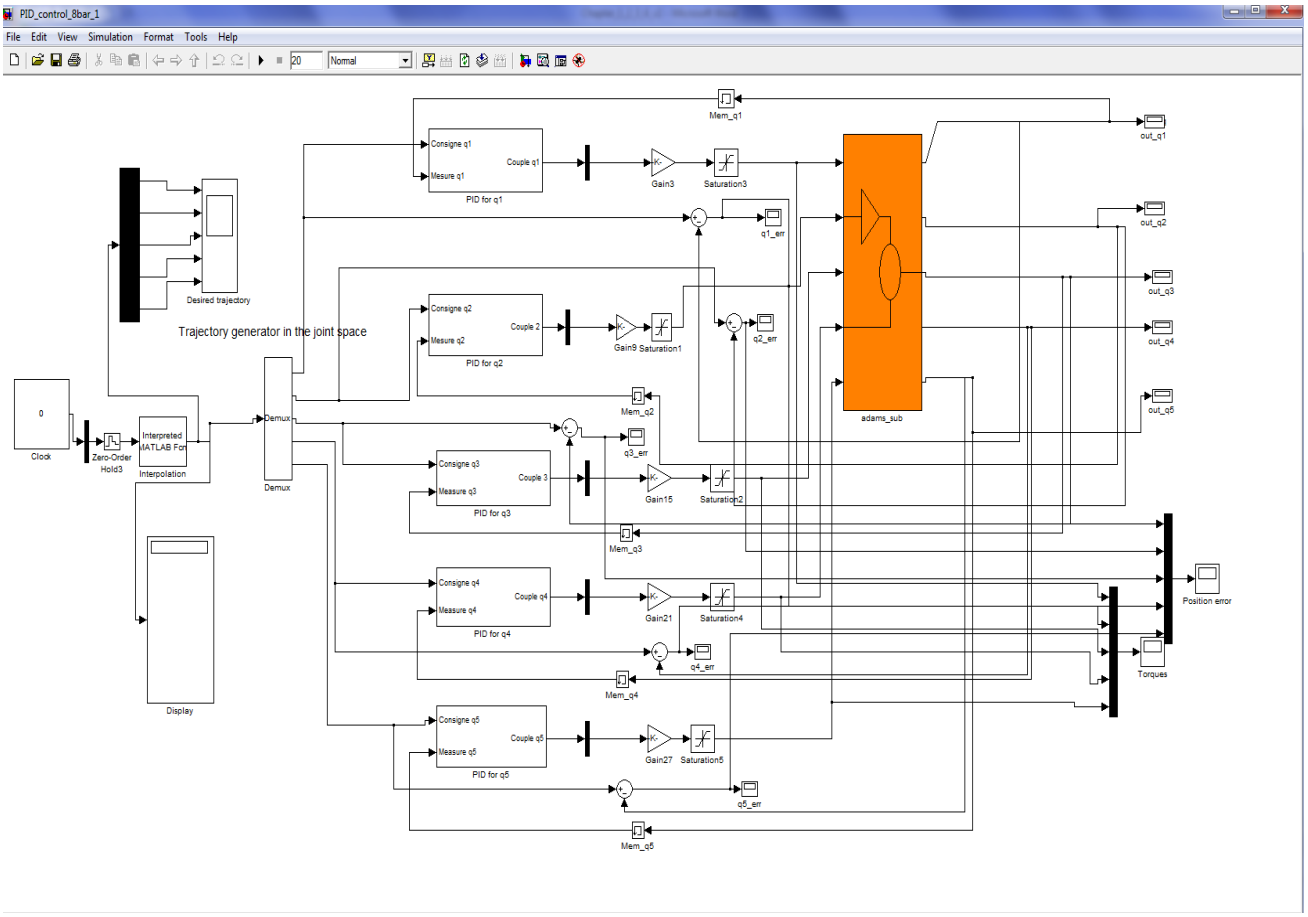

Figure A.0.7 Simulink model

Specifications of the motor

The technical specifications of the motors are [M. Lajili]:
The model of the actuators acquired is: NX210EAPR7300 below the translation of the model number:
[NX]: AC Brushless Servo NX Series Motor
[2]: Frame Size " 2 " - Pilot 40mm, 63mm PCD, Shaft Ø11x25mm
[10]: Continuous Stall Torque 1.00Nm (nominal torque 1 Nm)
[E]: Winding Series (standard)
[A]: Resolver Feedback (Standard)
[P]: 6000 RPM (230 Winding)
[R]: Standard Design
[7]: Connectors (standard)
[3]: with Brake (with brake)
[0]: IP64 Protection Class
[0]: Smooth without Keyway Shaft (Shaft without keyway)

Figure A.0.8 Servomotors PARVEX NX210EAPR7300

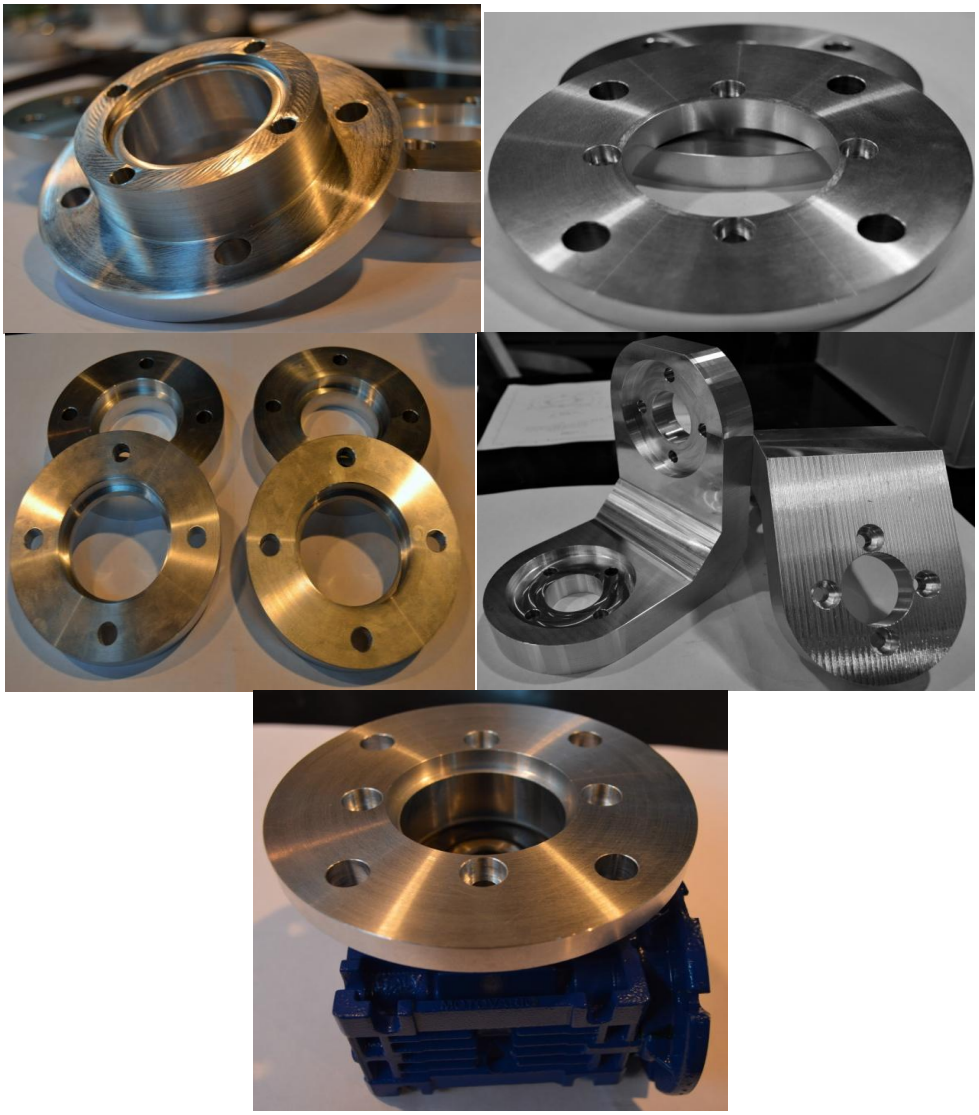

Figure A.0.9 Fabricated parts at IFMA (CTT)

Figure A.0.9 shows the fabricated parts at IFMA (CTT- Centre de Transfert de Technologie)